Durham E-Theses

The engineering behaviour of a weakly bonded artificial soil.

Malandraki, Vassiliki

How to cite:

Use policy

THE ENGINEERING BEHAVIOUR OF A WEAKLY BONDED ARTIFICIAL SOIL

A thesis submitted to the

School of Engineering and Computer Science

University of Durham

for the degree of

Doctor of Philosophy

by

Vassiliki Malandraki

June 1994

27 JUL 1994

Στην Παναγια τη Γοργοεπηκοο

και στους γονεις μου

Σπυρο και Ντινα

DECLARATION

I hereby declare that the work reported in this thesis has not been previously submitted for any degree. All material in this thesis is original except where indicated by reference to other work.

STATEMENT OF COPYRIGHT

ABSTRACT

Many natural soils have a weakly bonded structure. In order to develop a framework of behaviour for such materials, studies can be carried out on artificially bonded soils. Use of artificial soils means that difficulties due to sampling disturbance and variability of natural samples are overcome.

In this study the properties of an artificially weakly bonded sand have been examined. The effects of bonding on the soil's behaviour have been investigated using conventional drained and undrained triaxial tests. Yield of the bonds is associated with the loss in tangential stiffness. Comparisons with results from triaxial tests on destructured material, having the same nature and grading as the bonded soil, clarified the differences that the bonded structure imposed on the soil's behaviour.

The bonded soil sustained higher limiting stress ratios in the stress space and developed higher tangential stiffness values than the destructured soil due to its bonded structure. The soil's behaviour is shown to be represented by three main zones in the stress space, which are stress level dependent. In the first zone, at low mean stress, the bonds entirely control the soil's behaviour up to failure. In the third zone, at very high stresses, the effect of the bond is destroyed before failure is reached. In the transitional second zone, the bonded soil can sustain higher limiting stress ratios than those of the destructured soil due to the post yield influence of the bonds.

Triaxial drained probing tests following constant p' and constant σ_1' paths were also carried out on the bonded soil. The effects of the anticlockwise rotation of the stress path direction on the soil's behaviour were closely examined. Yield of the bonded structure was initiated at lower axial strains and higher tangential stiffness was observed as the degree of rotation of the shearing path direction increased.

Different yield loci were observed for each stress path direction. However, the bounding surface for the bonded soil was found to be unaffected by the different stress path directions.

It was found that the breakdown of bonds due to shear is not isotropic, but relates to the direction of the stress path at the point of yield. A sample which has yielded following one stress path direction may still show high stiffness if the stress path direction is changed. A further yield can occur when the stress path reaches the yield surface for the new shearing direction.

Changing the direction of the stress path during shear can affect the limiting stress ratio that the soil is able to sustain, if the change in shearing direction takes place in the second transitional zone of behaviour.

ACKNOWLEDGEMENTS

I would like to express my gratitude to my supervisor Dr. D. G. Toll for his guidance throughout the course of my studies in Durham. His friendly manner, his encouragement and support during both the good and the bad times are greatly appreciated and acknowledged.

It has been a privilege to study in Durham and to participate in the life of the Applied Mechanics Group. Thanks are especially due to Professor P. B. Attewell whose kind, congenial character combined with his expert advice were essential throughout these sometimes difficult years.

I must also express my appreciation to all the technical staff of the Soil Mechanics Laboratories, Bernard MacEleavey, Steve Richardson, Brian Scurr and Alan Swann for the unforgettable camaraderie we sheared in the Labs, which made life easier for me. Bernard's especially unselfishly willingness to help, his tolerance and support on numerous occasions are strongly acknowledged. I shall always be thankful to him and his wife Lesley for their generosity and friendship. A fellow member of the school, Andy Oliver also deserves special thanks for his consistent support, warmth and understanding.

I want to thank Andrew Farrell, Dida Chatzioannou and Panagiotis Chatzistamatiou, Dr Uahib Boulos, F. Cristofer, Paul Bidoris, Nicholas Antoniu, Dimitris Koutsohionis, Dr. Raghu Nambiar, Dimitris and Katerina Zevgoli and F. Michael for

CONTENTS

LIST OF SYMBOLS

E_{tan} Tangential stiffness

e_o Initial void ratio

ε_a Axial strain

ε_s Shear strain

ε_v Volumetric strain

μ Coefficient of friction

p' Mean effective stress $(\sigma_1'+2\sigma_3')/3$

p_o' Isotropic consolidation pressure

q Deviatoric stress $(\sigma_1'-\sigma_3')$

σ_1' Effective axial stress

σ_3' Effective radial stress

φ' Mohr-Coulomb friction angle

ABBREVIATIONS

csig3'   Constant σ_3'

cp'   Constant p'

csig1'   Constant σ_1'

cs13'   Constant σ_1' followed by constant σ_3'

p.w.p.   Pore water pressure

CHAPTER 1   INTRODUCTION

1.1 GENERAL

A large number of natural soils are structured due to weak bonds between their particles. Soft and stiff clays, granular soils and residual soils as well as weak rocks occur in various geological environments and are recognised as structured soils. Problems arise in engineering works such as foundations of buildings, stability of slopes, excavations and construction on these soils, because of their structure. They can show very brittle behaviour and often have higher permeability than might be expected.

The bonded structure of these soils may arise from a number of different reasons, such as the deposition of carbonates or hydroxides, or solution and deposition of silica at particle contacts in sands. However, such soils present similar characteristics independent of the origins of bonding.

The strength and stiffness of these soils is considerably affected by the presence of weak bonds between their particles. The soils present initially stiff behaviour followed by yield. However their engineering behaviour cannot be accounted for only by initial porosity and previous stress history and thus their behaviour does not fit into classical models of soil mechanics. Therefore, in the past these soils have been treated as special cases.

1.2 BACKGROUND AND AIMS OF THIS RESEARCH

In the last fifteen years, attempts have been made to develop a separate framework to that of the sedimentary clays that includes the effects of bonded structure on soil

behaviour. However difficulties have arisen due to sampling disturbance and variability of natural samples, as the degree and the strength of bonding often differs. The use of an artificially bonded soil was more attractive for the study of the effects of bonding on the soil's behaviour, and has been adopted by several researchers, as will be discussed later.

In this study an artificially bonded sand is examined under conventional triaxial tests and also under probing stress path triaxial tests. The main aim was to study and clarify the effects of bonding on the soil's behaviour and to present a general framework that explains the soil's behaviour under shear. However, for a better understanding of the effects of bonding it was essential to study the behaviour of destructured soil having the same nature and grading as the bonded soil.

1.3 LAYOUT OF THE THESIS

This study has mainly concentrated on the following areas:

In chapter 2, a discussion is presented of the characteristics of natural bonded soils. A literature review follows, which covers the main research presented for bonded soils in the last 40 years. Emphasis is given to research presented for artificially bonded soils although natural bonded soils are also discussed.

The methods of preparation for forming the artificially bonded soil and the destructured soil are presented in chapter 3. Some mechanical properties of the bonded soil are also studied in this chapter. The stress-path triaxial apparatus (used for the tests described in later chapters) is discussed. The basic principles of the computer control system are also presented. Finally setting up and saturation techniques for samples are presented.

In chapter 4, the effects of bonding on the soil's behaviour are examined under conventional drained shearing. Yield of the bonded structure is associated with the loss in tangential stiffness. Triaxial drained shear tests were also carried out on destructured soil and comparisons between the two are made with respect to the limiting stress ratios sustained in the stress space, the development of tangential stiffness and axial strain.

The behaviour of the bonded and the destructured soil under undrained shear is discussed in chapter 5. Bounding and yield surfaces are presented and the influences of the bonded structure on the soil's behaviour are closely examined. Comparisons between the results from drained and undrained tests are used to clarify the effects that drainage and the method of shearing control have on the soil's behaviour. Finally, a framework is presented which highlights the main characteristics of the bonded soil under drained and undrained shearing.

In chapter 6, the behaviour of the bonded soil is examined under drained probing stress path triaxial tests (constant p' and constant σ_1' paths). The effects that the anticlockwise rotation of the shearing path direction (relative to conventional drained tests) has on the soil's behaviour with respect to yield initiation, development of stiffness, axial strain and the position of the bounding surface are closely studied. Comparisons are made with results from conventional drained tests.

Results from drained probing tests carried out on bonded soil, with clockwise changes in the stress path directions during shearing (from an initial constant σ_1' path to a constant p' or to a conventional drained test) are discussed in chapter 7. A framework is presented describing the main characteristics of this soil under drained shearing with changes in stress path directions.

Finally in chapter 8, the main conclusions drawn from this study are discussed and some suggestions for further research on the artificially bonded soil are also considered.

CHAPTER 2   LITERATURE REVIEW

2.1 INTRODUCTION

At the beginning of this chapter a discussion is presented of the characteristics of natural structured soils. These soils show similar behaviour under shear in triaxial compression due to their bonded structure. A literature review follows, which covers the main research presented on natural structured soils in the last 40 years, with an emphasis given to previous work presented on artificially bonded soils.

2.2 PREVIOUS RESEARCH ON BONDED SOILS

Many naturally occurring deposits are structured due to weak bonds between their particles. Soft and stiff clays, granular and residual soils, as well as weak rocks occur in various geological environments and are recognised as structured materials. Although the structure of these soils may arise from a number of different reasons their mechanical behaviour is very similar. They have components of shear and tensile strength and stiffness which cannot be accounted for by porosity or previous stress history and are due to their bonded structure. However the initial stiff behaviour of the soil is followed by yield of its bonded structure.

Vargas (1953), discussed the characteristics of residual soils occurring in Southern Brazil. He recognised the influence of structure in residual soils and he defined a virtual pre-consolidation pressure from the behaviour of the intact soil when compared with the remoulded condition (fig. 2.1).

Sangrey (1972), presented an extensive study for cemented soils from Canada. Although there was a wide range of naturally cemented soils, they showed similar characteristics under triaxial shearing. At low confining pressures the bond predominated over the frictional resistance and after the bonds yielded the strength was due to frictional resistance. In fig. 2.2 the stress-strain curves are plotted from triaxial tests on Labrador clay. At low confining stresses (LA7) the behaviour is brittle, while at higher stress level (LA8) it changes to ductile.

A yield curve was used to describe the strength of the naturally cemented soils. In fig. 2.3 the prismatic yield curve for Labrador clay is plotted. It shows a portion which is horizontal and depends on deviatoric stress and on the right hand side of that portion, another one which is vertical and depends on the confining pressure.

Saxena and Lastrico (1978), presented a report on the static properties of lightly cemented samples from the Vincentown formation. The cementing agent was calcite. Their conclusions were similar to those previously presented by Sangrey. At low confining pressures in triaxial shearing the behaviour of the samples was brittle while at higher stresses it changed to ductile. The shear strength was variable because the deposits had variable degrees of solution of the calcite cement.

Clough et al (1981), reported on large deposits of cemented sands along the California coast. The main characteristic of these deposits was their ability to stand at steep natural slopes of 60° or steeper. Catastrophic landslides occurred due to brittle failure during seismic events. The tensile strength measured by Brazilian tests on the weakly cemented soil was about 9-10kPa. Stress-strain curves from triaxial drained tests on the weak soil from the Pacific site are presented in fig. 2.4. Again a brittle failure mode is observed at low confining pressures with a transition to ductile failure, at higher confining pressures.

Sitar (1981), used artificially cemented sands in order to test a material which simulates weakly cemented sands. He had similar results to those already presented and he emphasised that density, grain size distribution, grain shape and grain arrangement have significant effects on the behaviour of natural cemented sands.

Vaughan and Kwan (1984), presented a theory for modelling weathering as a weakening process. They emphasised that important parameters for residual soil characteristics are in-situ porosity and structure, which are a product of the weathering process, rather than in-situ stress history.

Vaughan (1985), explained the necessity for the development of a framework for describing and clarifying the engineering properties of residual soils. He suggested that bonding and porosity entirely control the properties of these soils, and that yielding of the bonds can be represented by a yield locus in stress space. He proposed that in order to study the effects of bonding on soil behaviour, a method of preparation of reproducible artificially bonded samples should be used. Thus the difficulties of variability, handling, storage and testing of natural residual soils are overcome. This is similar to the use of remoulded samples for the development of basic frameworks in soil mechanics.

Vaughan (1988), suggested three possible porosity states for a bonded soil in respect of the initial void ratio/ initial stress state, and final stress state after loading (fig. 2.5).

(1) a stable dilatant state, where large strains due to yield will not occur although dilation under shear would be observed,

(2) a stable contractive state, where again large strains due to yield are unlikely but the soil will contract under shear and

(3) a meta stable state, where yield will result in large strains as a function of how far into that stage yield occurs.

He also suggested that a comparison of the stress-void ratio states for the structured and destructured soil, helps for a better understanding of the effects of structure. In fig. 2.6 a structured soil is presented which exists in states that are not possible for the destructured soil of the same grading. Thus the abruptness of yield, the shape of the yield curve and the post-yield stiffness depend on the void ratio of the soil and the extent to which its yield point lies outside the possible states for the destructured soil.

Maccarini (1987), described a method of preparation for artificially bonded samples. He presented test results for an artificially bonded soil made up of quartz sand, a kaolin 'sand' (cfk) and a small quantity of kaolin slurry. After the samples dried they were fired in a furnace and thus the kaolin slurry formed a bond between the sand particles. The bond strength was found to be controlled by the temperature and time of firing. The kaolin 'sand' was made from a kaolin slurry, fired at higher temperatures than that used to form the bond, and then crushed and sieved to obtain sand sized particles.

Maccarini carried out triaxial compression and one-dimension consolidation tests, on loose and denser artificially bonded samples in order to clarify the role of porosity on peak shear strength.

The first and the second yield for two bonded soils at different void ratios are shown in fig. 2.7a and b. He defined first yield of the bonds at the end of the linear part at the deviatoric stress-strain curve plotted to natural scale, and second yield at the maximum point of curvature of the same graph. Thus first yield occurred at low strain values and was often muted. Second yield occurred at higher strains and was more pronounced. He found that the second yield became more difficult to define with increasing density and also that the stress increment to move from the first yield to the second, increased with decreasing porosity but decreased

8

with increasing bond strength. The two possible states for two samples in respect of their initial void ratio, the stable and the meta-stable, can be seen in fig. 2.7c.

He also presented test results from a natural residual soil derived from metamorphic gneissic rock (Brazil). He found good agreement between the behaviour of the natural and the artificially bonded soil, in respect of the peak strength and the yield characteristics of their bonded structure.

Bressani (1990), continued Maccarini's work. He examined the behaviour of a loose artificially bonded soil at different densities, at different compositions and at high confining pressures up to 3.5MPa. He defined the two yields of the bonds from the deviatoric stress-strain curve plotted to natural and log-log scale.

Results for the yield surfaces presented from four series of samples sheared under triaxial drained tests are shown in fig. 2.8a. The 100 series were samples with the same composition as the 200 and 600 series, but with a higher void ratio than those. The 600 and 200 series both had the same composition and the same void ratio, but the 600 series had a stronger bond than any other series of samples. Series 300 were samples that had fired kaolin (cfk), instead of sand. As can be seen, he found that the position of the yield surface in the stress space was influenced by the bond strength and the void ratio of samples. However a more dramatic change occurred for the samples with a different void ratio and the same composition, series 100 and 200, than those with a different bond strength. Samples in series 300 showed an earlier drop than the 200 series, for s'>1000kPa and thus a change of the mineralogy also affected the shape of the yield surface for a particular stress level.

The results for the peak shear strength envelopes from the different series of samples are presented in fig. 2.8b. The results for the 00 series of samples, that

consisted only of sand and kaolin and had approximately half the void ratio of that of the 200 series, are also presented. As can be seen, all the envelopes are very close at low stresses with higher values for the 600 series and therefore in this region bonding was the main factor that controlled the shear strength and not the mineralogy. However at higher stresses a substantial drop in the peak strength occurred for the samples that did not have quartz sand.

Bressani also compared the development of secant stiffness during shearing, for the different samples. Secant stiffness is plotted versus p' in fig. 2.8c. As can be seen he found that samples without cfk were stiffer than any other series, even than those that had a similar void ratio or a stronger bond. However the 00 samples presented a similar yield surface to the samples formed with cfk and also had the same void ratio.

Bressani also carried out triaxial tests on a marl from the Corinth Canal in Greece and a residual soil from Kenya. The marl from the canal region contained a small percentage of clay mineral <10%, large amounts of calcite and quartz and had a void ratio of $e \cong 0.6$. A series of triaxial tests were also carried out at the National Technical University in Athens, in order to investigate the peak strength envelope of the soil, sheared at low confining pressures. As can be seen in fig. 2.9a from the combined tests results, the frictional envelope for the Corinth marl presented some curvature at low s', while for s'>2250kPa the envelope followed a linear form in the stress space. The yield surface was also identified and is plotted in fig. 2.9b. As can be seen it is less centered to the isotropic axis than the yield surfaces defined for the artificial soils (fig. 2.8a). There is also some scatter between the yield points defined from the different researchers.

The soil from Kenya was selected from the site proposed for the Chemususu Dam. It was a partially saturated soil with a void ratio of e=1.47. Triaxial test results

showed some curvature for the peak strength envelope at low confining pressures, followed by a linear part at higher stresses (fig. 2.10a). The yield surface defined for this soil is plotted in fig. 2.10b. As can be seen from the two figures, sample C2 showed yield at low confining pressures and reached a peak strength at higher stresses than the frictional envelope.

Leddra et al (1990), presented test results from a research programme conducted on chalk, a weak bonded rock, from two different sites (South East England and Denmark). Large strain deformations arose under various engineering works due to the high porosity and the structure of this rock and thus an extensive study of its behaviour became very important. K_O tests are presented in fig. 2.11a for samples with different void ratios and as can be seen the yield stress increased as the void ratio decreased. Yield was associated with a change of the slope of the stress path in these tests, followed by strain softening or strain hardening. The influence of the initial void ratio on yield of the structure of the chalk can be seen in fig. 2.11b.

Two models for the chalks' behaviour were also presented and were related to the development of volume changes with the increase of p', after the occurrence of yield. A unique failure line governed the behaviour of two types of samples with different void ratios sheared at high stresses, while at lower stresses the line shows some curvature. It is interesting to see a combined graph (fig. 2.11c), that presents the K_O and the undrained triaxial test results, where the latter coincided with the initial part of yield for the K_O tests. Leddra et al also underlined that the samples in the K_O tests, during the initial part of yield are very close to the bounding surface defined for low stresses.

Leroueil and Vaughan (1990), emphasised that the concept of structure occurs in many soils such as soft clays, stiff over-consolidated clays, clay-shales, weak mudstones, sands and residual soils and presented an extensive study for the

behaviour of these soils. They underlined that although structure may arise from different causes (for example deposition of carbonates, solution and deposition of silica at particle contacts in sands) its effect on soil's behaviour is similar. Stiff behaviour, followed by yield above certain stress levels, is mainly observed in every case. They also noted that yield can occur in different ways and that three different parts of a yield curve can be identified. In fig. 2.12 the three parts are presented, where yield occurs in compression, shearing and swelling.

Little and Hataf (1990), presented test results from a series of triaxial tests on weathered undisturbed and reconstituted Keuper Marl. The two materials were at similar overconsolidation ratios but the undisturbed samples had a higher shear strength due to their bonded structure.

Anagnostopoulos et al (1991), presented an extensive study of the properties and the mechanical behaviour of the Corinth Canal marls. The Canal, although it was subjected in earthquakes on various occasions, never showed any problem in terms of stability. As was previously discussed from Bressani's study, the marls presented a bonded structure which influenced their behaviour under shear. As it can be seen in fig. 2.13, brittle behaviour with high stiffness was observed for the samples when shearing took place at low confining pressures, with higher peak shear strength values than that of the reconsolidated samples. The soils' behaviour sheared at higher stresses turned to a more ductile mode of failure and reached a similar peak shear strength with that of the reconsolidated soil. However some differences in the determination of the main yield surface are observed with that previously defined by Bressani, as can be seen in fig. 2.14.

Huang and Airey (1991), manufactured artificially cemented samples of a carbonate soil in order to overcome variability in properties of natural cemented soils and difficulties related to undisturbed sampling. An increase of the unconfined

compressive strength and the tensile strength was always observed with the increase of the cement content. They also examined samples with different cement contents under the electron microscope and they found that in samples with a low cement content, the cement formed bridges between the particles, while in samples with a higher content it formed bridges, coated the sand particles and also filled some of the voids between the particles. They had also seen that the increase of density of the cemented soil reduced the void space and increased the number of contacts between the particles and thus concluded that this probably increases the effectiveness of a given amount of cement.

In 1989, the Science and Engineering Research Council (SERC) initiated an engineering project at Bothkennar in Scotland, for an extensive study of the soft clay of the site. Hight et al (1992), presented general characterisations of the mechanical behaviour of this structured clay. The clay exhibited natural variability in structure and fabric which was reflected in its peak undrained strengths. The higher resistance of the soil due to its bonded structure was reduced progressively by shear and volumetric strains, which were initiated even by various sampling techniques.

Allman and Atkinson (1992), presented results from one-dimension consolidation and triaxial tests carried out on reconstituted Bothkennar clay. Comparisons with results from tests on intact material showed that the state boundary surface for the latter was far outside in the stress space, compared to that defined for the reconstituted soil. However at large strains the boundary surface for the intact samples moved towards the critical state for the reconstituted soil.

Smith et al (1992), presented results from triaxial stress path tests, for the yielding characteristics of the Bothkennar clay. As can be seen in fig. 2.15, two kinematic yield loci were defined within a initial bounding surface. A first elastic zone (Y_1) was located at very small strains and was difficult to map; a second zone (Y_2)

13

where the behaviour of the soil under shear was recoverable, was found at $\varepsilon_a=0.02\%$ and it was located by cyclic loading of small amplitudes. The third boundary surface (Y_3) determined the onset of large strain yielding and it was asymmetric for both the isotropic and the K_O lines. The large strain yield curve could not be normalised within the framework of the classical critical state soil mechanics and therefore a unique state boundary did not exist in the stress space. As can be seen in fig. 2.16, the water content contours collapsed inwards towards the intrinsic bounding surface of the reconstituted soil.

Clayton et al (1992), presented results from a testing programme that imposed shear and volumetric strains under triaxial stress and strain paths to high quality Bothkennar clay samples, extracted from the ground by different methods. Details for the different methods of samplings were also presented. They concluded that even high quality tube samples will suffer a significant loss of the mean effective stress and some loss of structure during sampling. They also found that the undisturbed undrained shear strength of the samples can be partially recovered by re-establishment of the initial effective stress level, depending though on the amount of destruction. However stiffness of the samples cannot be fully recovered. Clayton el al also underlined the fact that reconsolidation procedures will produce significant volumetric strains which might lead the soil close to the yield surface, with therefore a direct effect of shrinkage for the latter.

Bressani (1993), presented test results for the Corinth marl. As can be seen in fig. 2.17 the secant stiffness from triaxial drained tests did not have a direct relationship with the confining pressure, but was strongly influenced by the yield pressures associated with their bonded structure (fig. 2.9b).

Coop and Atkinson (1993), investigated the behaviour of an artificially cemented carbonate sand in triaxial shearing. They also carried out tests on uncemented

samples with the same grading as the cemented soil and compared the test results from the two. As can be seen in fig. 2.18a, yield points were identified for the cemented soil outside the state boundary surface for the uncemented material. Thereby they underlined the necessity of testing the uncemented material for the development of a general framework applicable to a cemented soil.

The framework that was developed from these tests was found to agree with the behaviour of natural calcarenite. As can be seen in fig. 2.18b, shearing at low confining pressures resulted in yield at strengths higher than those of the uncemented material, while when shearing took place at high p', yield occurred during compression and in this case the soil strength was only frictional.

One of the intriguing findings of Coop and Atkinson's research was results from a constant p' drained test carried out on a cemented sample, which showed a lower peak shear strength than that obtained from undrained tests. They also presented test results for some samples that showed yield during the initial stage of shearing but their peak strength was slightly above the frictional failure envelope, for a small stress zone in the stress space. Thus there was an indication of a post yield influence of the cementing at the transition from cohesive to frictional behaviour.

Cuccovillo and Coop (1993), presented further results from tests carried out on the same artificially soil examined by Coop and Atkinson. In their work the investigation of the behaviour of the soil was extended by examining the soil at different bond strengths. The soil reached states outside the state boundary surface defined from tests on uncemented samples, depending on its relative specific volume and on its bond strength. As can be seen in fig. 2.19, tests on two artificial soils with different bond strengths but the same specific volume revealed that the soil with the higher bond strength reached states well outside the intrinsic state boundary defined from uncemented samples, while the soil with the lower bond

strength could reach a state outside the state boundary only when shearing takes place at low confining pressures.

Results from tests on a natural calcarenite showed a very similar pattern of behaviour to that presented by the artificially bonded soil. The natural soil presented a variety of bonds strengths at any particular volume, which is strongly influenced by an increase in the degree of cementing with a decrease in the specific volume, as the void spaces filled with the bonding matrix. However only the lightly cemented samples with higher specific volumes showed the greatest influence of bonding and reached states outside the state boundary, as the decrease in specific volume had counteracting effects on the influence of the bond strength to the maximum stress ratios that were reached by the soil.

Huang and Airey (1993), presented results from triaxial tests performed on samples of an artificially cemented carbonate sand. They examined the effects of density and cement content on the samples' behaviour. An increase in cement content or the density causes the yield locus to increase in size, as it can be seen in figs. 2.20a and 2.20b respectively. However they found that as the density increased the effectiveness of the cementation decreased and caused a decrease at the shape of the yield loci for a given cement content.

Maccarini (1993), presented results from direct shear box and triaxial drained compression tests carried out on an undisturbed gneissic rock. The results for the peak shear strength defined from the two types of tests are quite similar. However the tangential stiffness for loose and medium dense samples sheared in triaxial tests was influenced from the occurrence of the first yield of the bonds (fig. 2.21), while initial stiffness defined from the direct shear box tests showed an increase with the increase of p', similar to that which occurred in sedimentary soils. Maccarini

underlined that the difference in behaviour is probably due to the different stress paths followed in the two tests.

Kavvadas et al (1993), presented results from oedometer and triaxial tests carried out on a lignite, often called 'brown coal', from Ptolemais Greece. Lignite is a soft rock that has undergone a physico-chemical alteration during geological time, which results in a bonded structure that consists of a skeleton of aliphatic carbon chains. They found that the peak shear strength of lignite was accounted for by its bonded structure.

As can be seen in fig. 2.22, yield of the bonded structure was associated with the changes of the slopes of the stress-strain curves at the points of transition from a linear domain to a plastic region, with progressively reduced stiffness. They defined an elliptic yield surface in the stress space which, as they underlined, represents an initiation of yield during shearing. The yield points agreed with the points of change of the slope of the volumetric strains versus p' curves. They had difficulties in defining the peak shear strength of lignite, as it was dependent on the in-situ moisture content. These were overcome by normalising the different results with the equivalent p_e' pressure.

Petley et al (1993), presented results from triaxial tests carried out on two different shales and various chalks. All the samples were defined as weak fine-grained rocks. Although the rocks have different origins (shales have high clay percentages in comparison with chalk), all the samples presented a higher peak strength when shearing took place at low confining pressures, than that presented under shearing at higher stresses. Yield points were observed in the stress strain curves indicating the destruction of the bonds, followed by large post-yield strains. They emphasised that the samples showed a similar behaviour due to their bonded structure and not because of their previous stress history.

Rampello et al (1993), examined the behaviour of a natural and reconstituted Vallerica clay from Italy, under triaxial shearing. Although the effective cohesion component of the peak shear strength for the reconstituted samples was found to be due to dilatancy, the micro-structure of the natural clay was the main contributing factor for the non zero intercept of the failure line of the intact material.

2.3 DISCUSSION

The study of various soils in the last 40 years clarified the fact that many different soils present similar characteristics due to their weakly bonded structure and not because of their previous stress history. Research was carried out on residual soils, on cemented sands, on marls, on chalks, on soft clays, on lignite and on clay shales and it has been appreciated that although the structure of these soils has arisen from different reasons their mechanical properties are very similar.

Hard soils or soft rocks, as they were recently addressed in the International Conference in Athens, present initially stiff behaviour under shearing, followed by yield at higher stresses. Yield of the bonds was represented in the stress space by a yield curve. Some of the researchers presented one initial yield surface, followed by a final yield surface at higher stresses, close to the bounding surface. When sheared at low confining stresses the soils' behaviour is entirely controlled by their bonded structure and thus the soils present higher strength values. At higher stresses the bonds are destroyed and they do not contribute to the soils strength which is now only due to frictional resistance.

Many researchers (Sitar, 1981, Maccarini, 1987, Bressani 1990, Coop' and Atkinson 1993, Huang and Airey, 1993), studied the behaviour of artificially bonded soils which simulates the structure of natural soils. The bond strength and the void ratio of artificially bonded soil can be changed and thus its properties are more easily

studied. This has proved to be very helpful, as it clarifies the effects of bonding on the soils' strength and stiffness. Very good agreement was found between the behaviour of artificial and natural bonded soils in respect to yield and peak shear strength.

Also the study of destructured material at the same grading and at the same void ratio as the bonded soil, by a lot of researchers (Allman and Atkinson 1982, Coop and Atkinson 1993, Cuccovillo and Coop, 1993, Rampello et al, 1993), has proved to be very helpful in providing a better understanding of the effects of bonding on the soils' behaviour, in respect of the peak shear strength and stiffness.

Some questions of significant importance arise. from the research previously presented, such as of the effect that the direction of the stress path has, as well as the level of the confining pressure on the peak shear strength of the bonded soils, and of the role that the drainage condition plays on the soils' behaviour under shearing. Furthermore the effects that a post yield influence has on the peak shear strength of the bonded soil, and therefore of the existence of a transitional area from cohesive to frictional resistance under shearing need further study. Some of the work carried out in this study answers these questions and clarifies the behaviour of an artificially bonded soil under drained and undrained shearing.
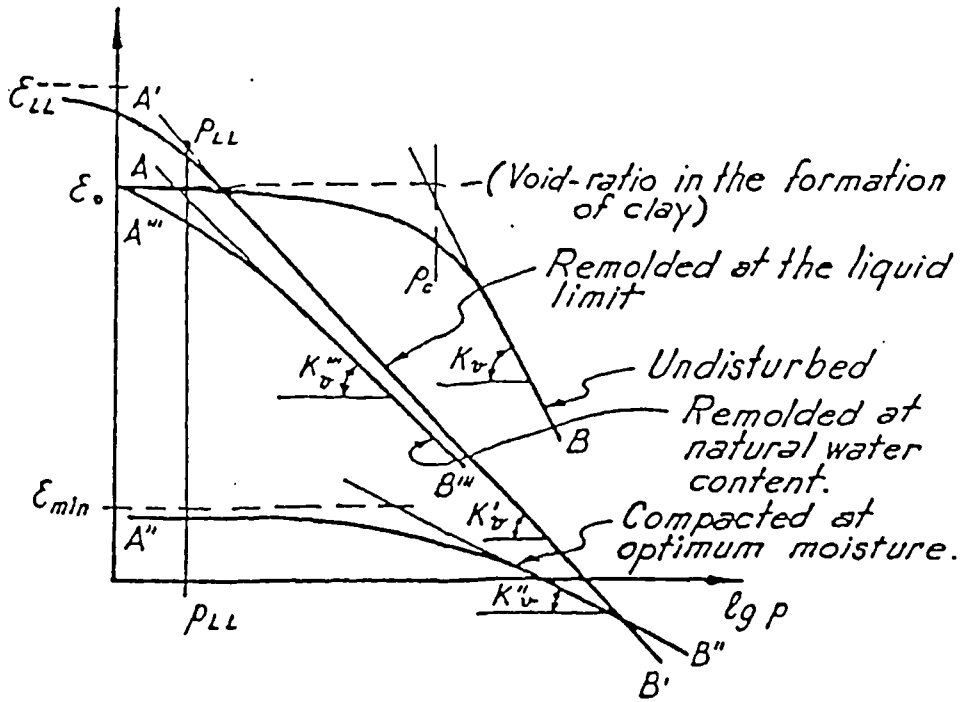
Fig. 2.1 One-dimensional compression test results on residual soils (after Vargas, 1953)
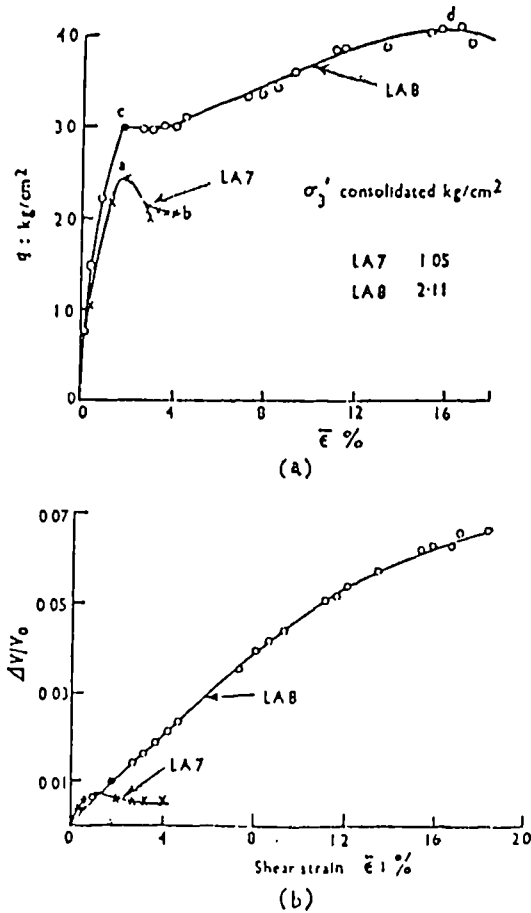
Fig. 2.2 Stress-strain curves for Labrador clay (after Sangrey, 1972)

20
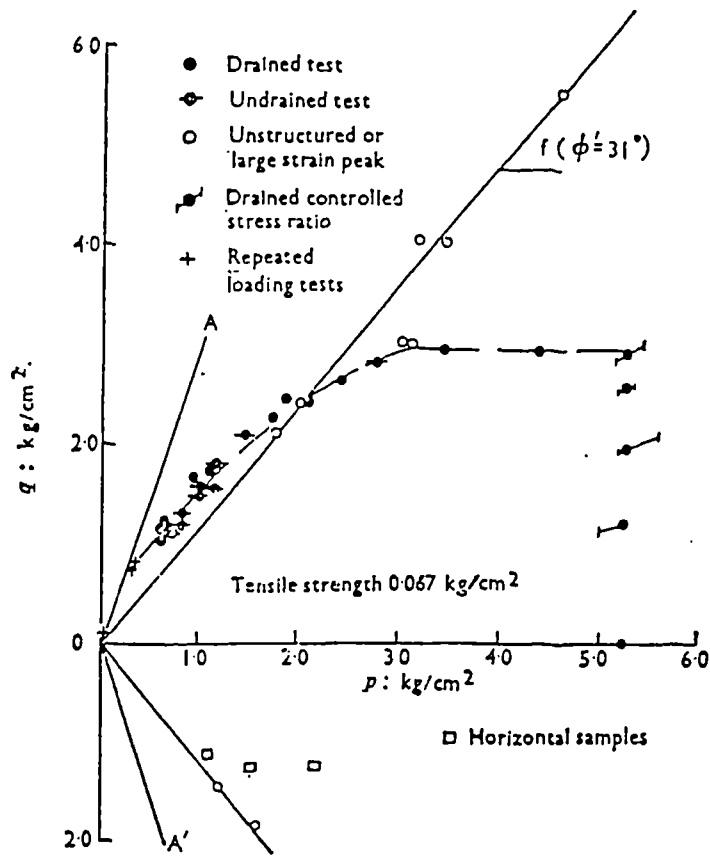
Fig. 2.3 Yield curve for Labrador clay (after Sangrey, 1972)
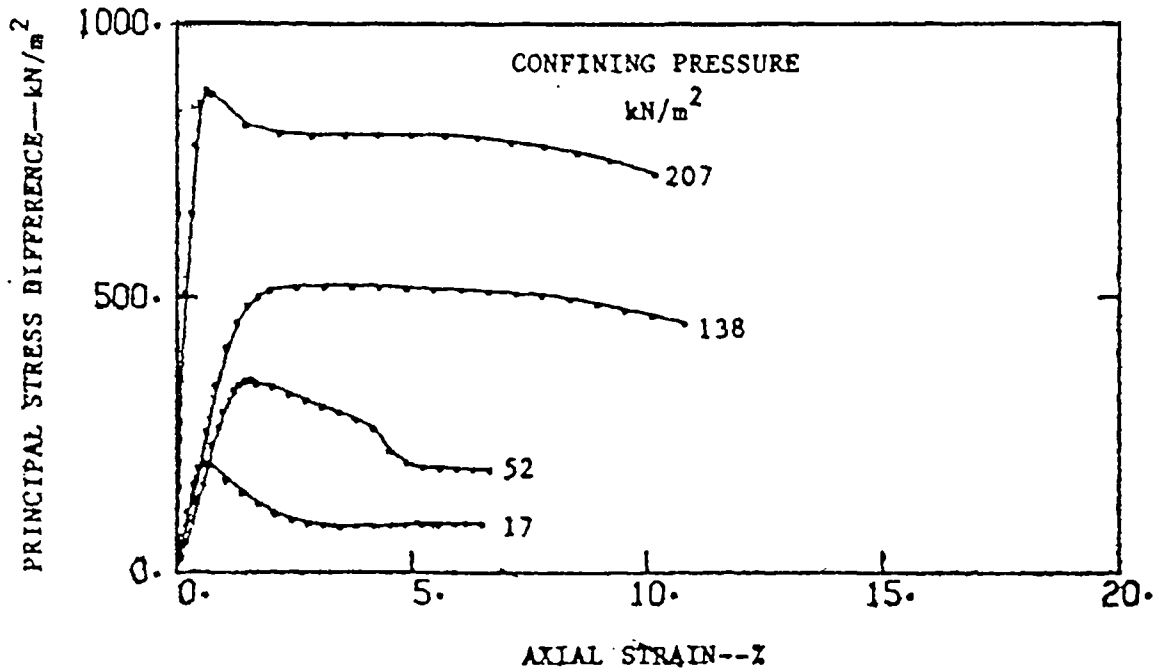
Fig. 2.4 Stress-strain curves for a weak soil from the Pacific site
(after Clough et al., 1981)
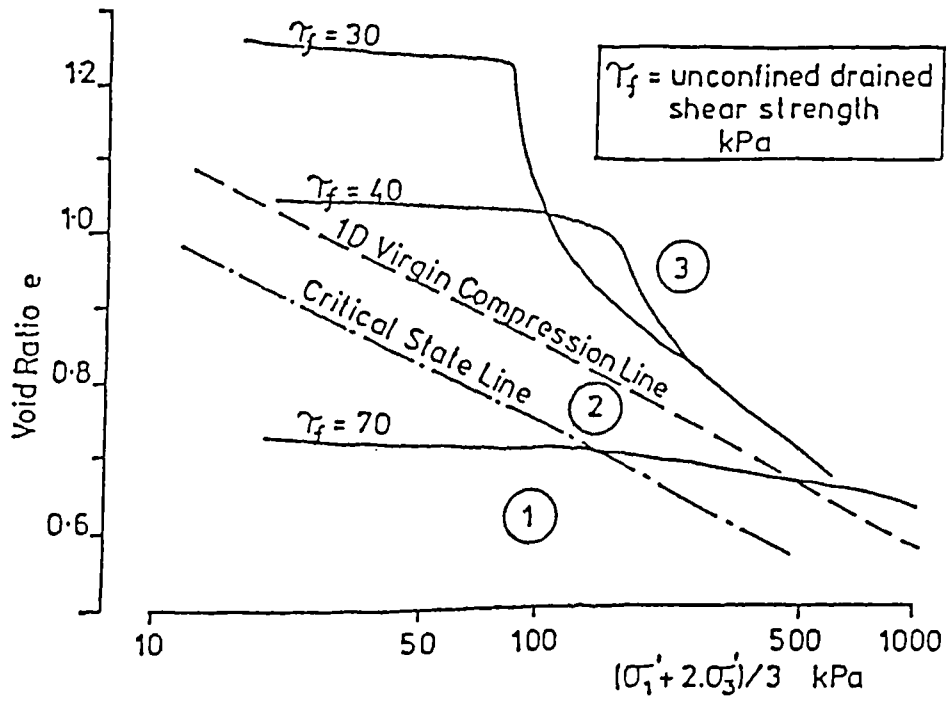
Fig. 2.5 The three porosity states for an artificial bonded soil
(after Vaughan, 1988)
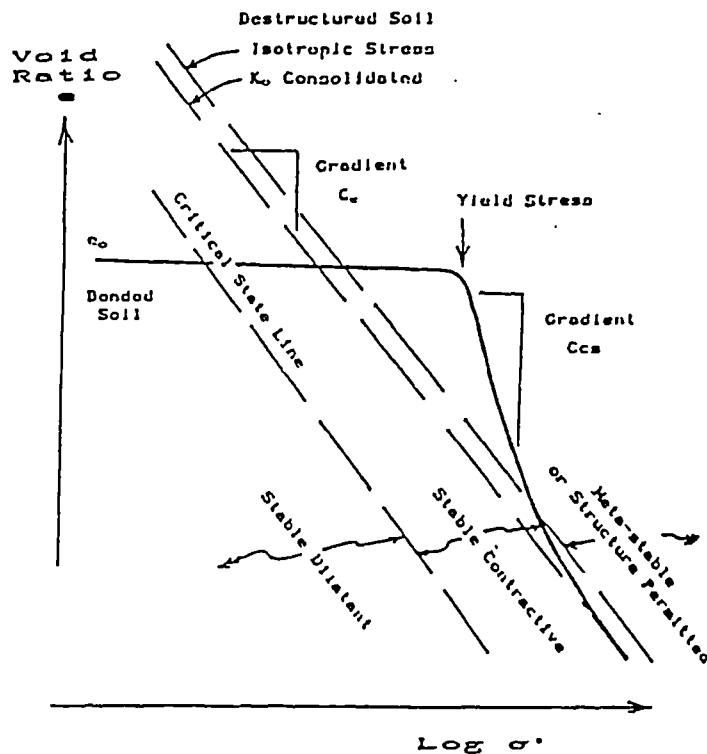
Fig. 2.6 One-dimensional compression for a bonded and a destructured soil
(after Vaughan, 1988)

22
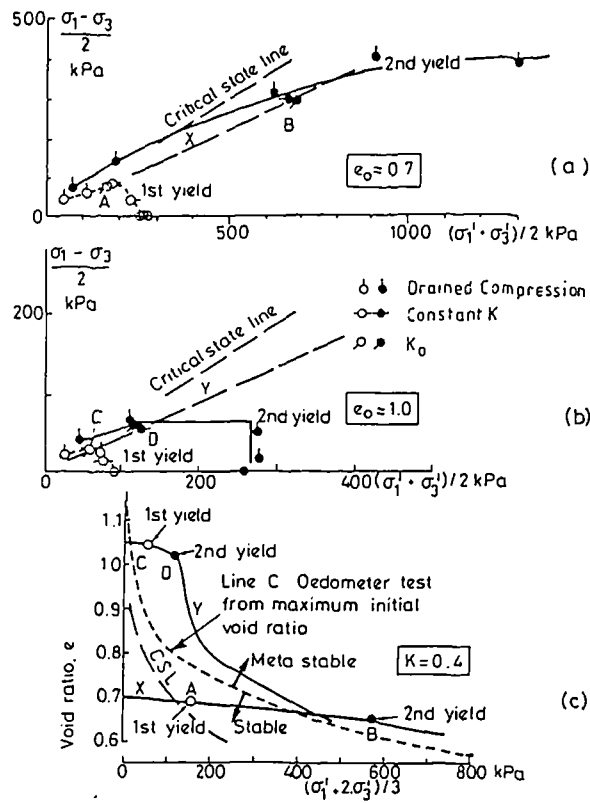
Fig. 2.7 First and second yield for an artificially bonded soil
(after Maccarini, 1987)
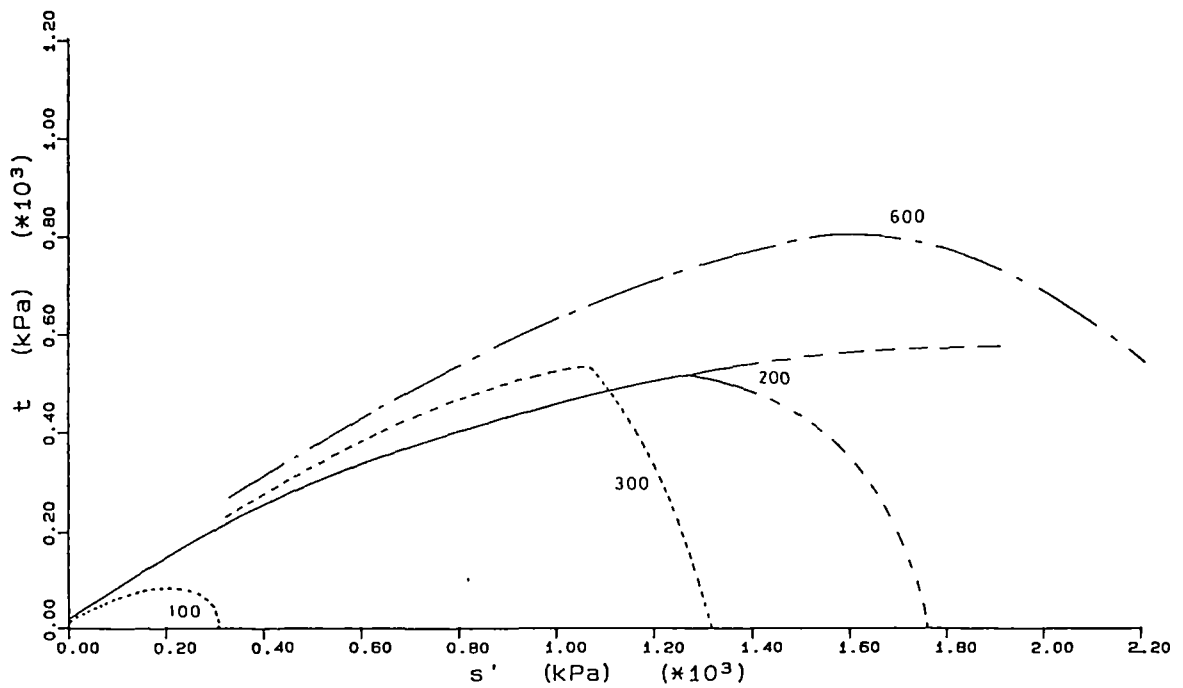
Fig. 2.8a Yield surfaces for four different artificially bonded soils
(after Bressani, 1990)
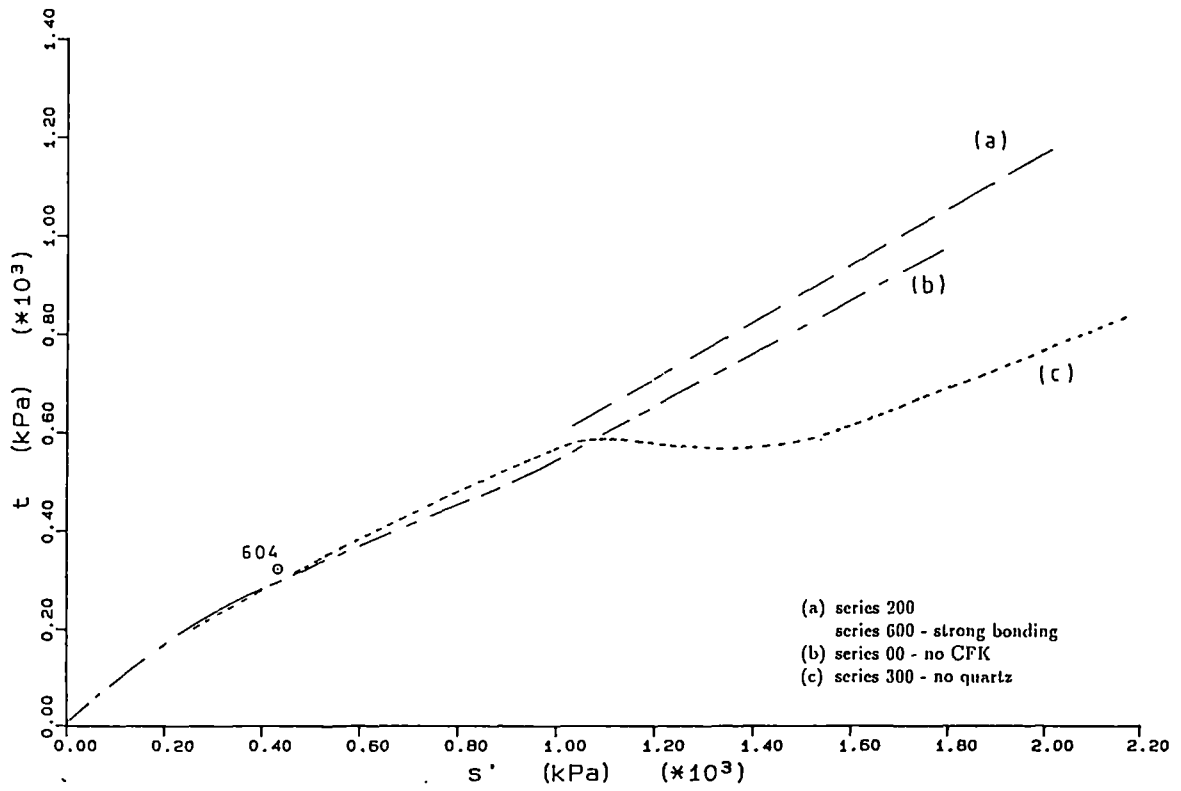
Fig. 2.8b Peak shear strength envelopes for the artificial soil series
(after Bressani, 1990)
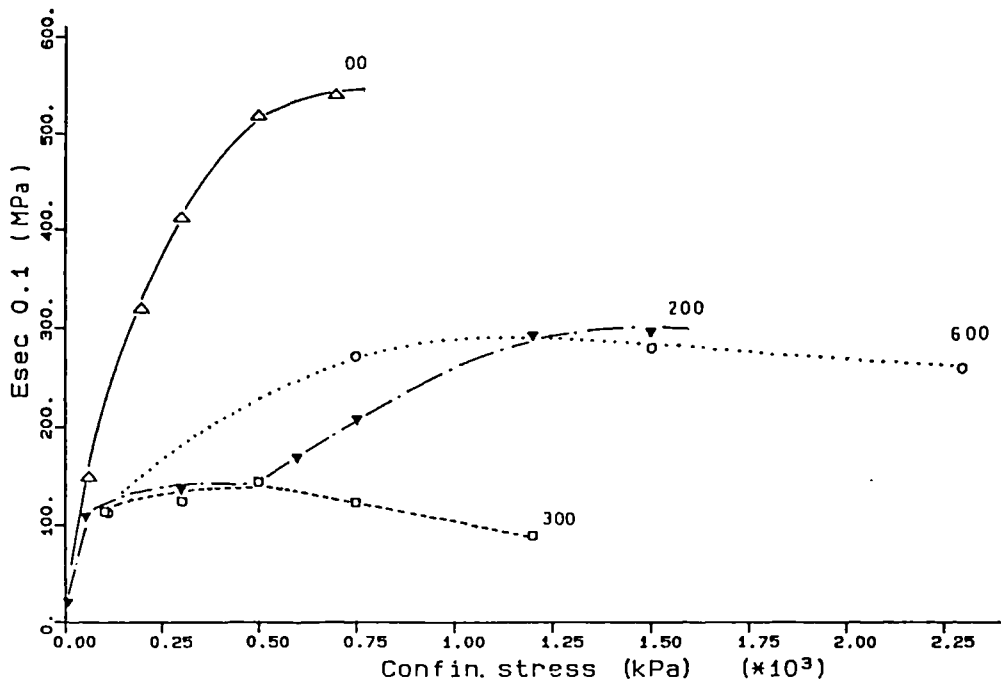
Fig. 2.8c Secant stiffness versus confining pressure for the artificial soil
series (after Bressani, 1990)
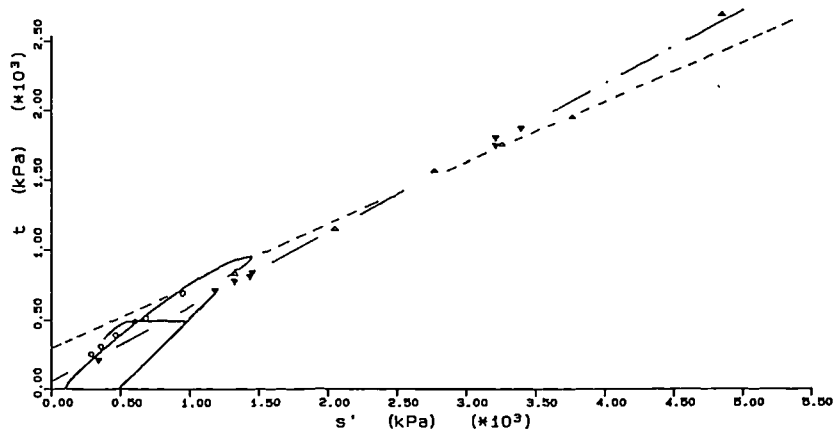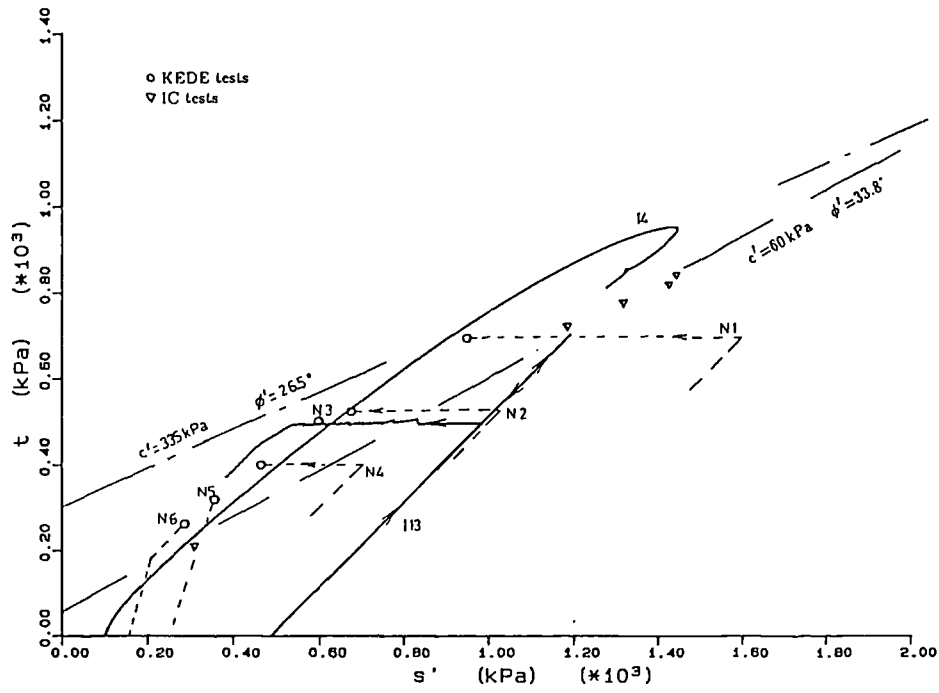
Fig. 2.9a Peak strength envelope for the Corinth Canal marl
(after Bressani, 1990)
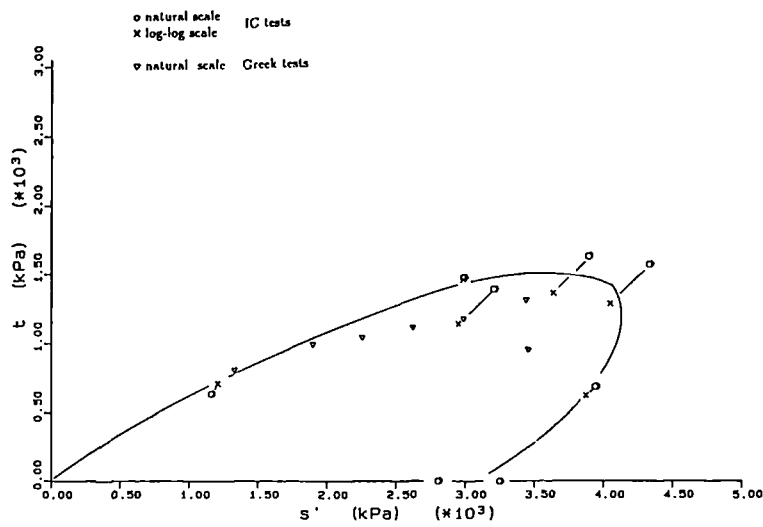
Fig. 2.9b Yield surface for the Corinth Canal marl
(after Bressani, 1990)
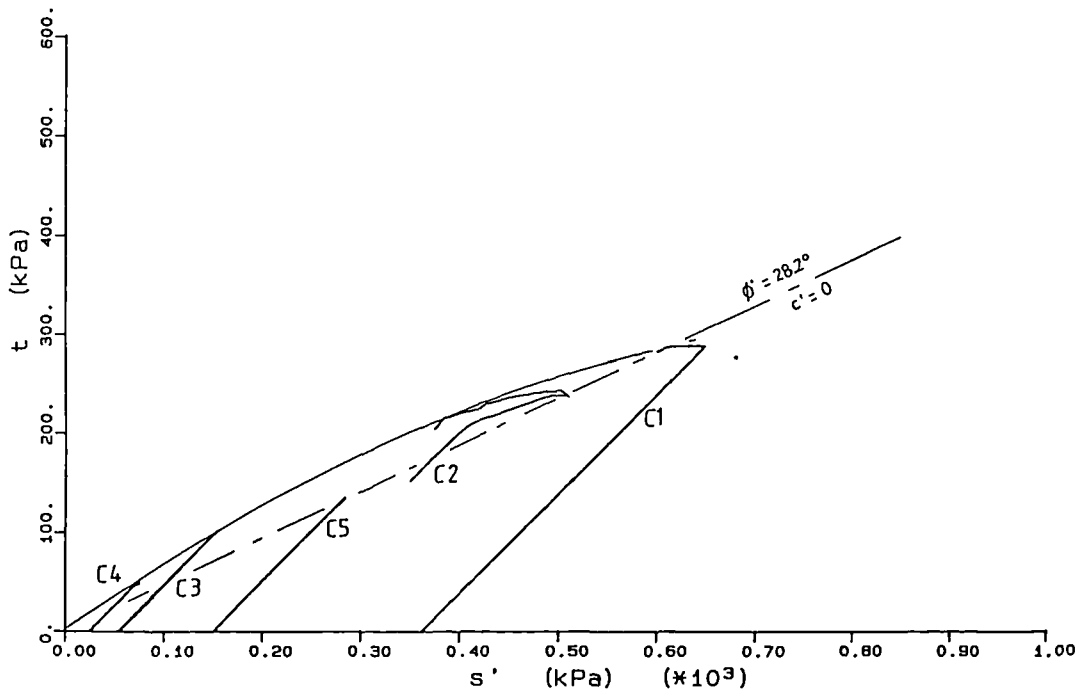
Fig. 2.10a Peak strength envelope for a soil from Chemususu Dam, Kenya
(after Bressani, 1990)
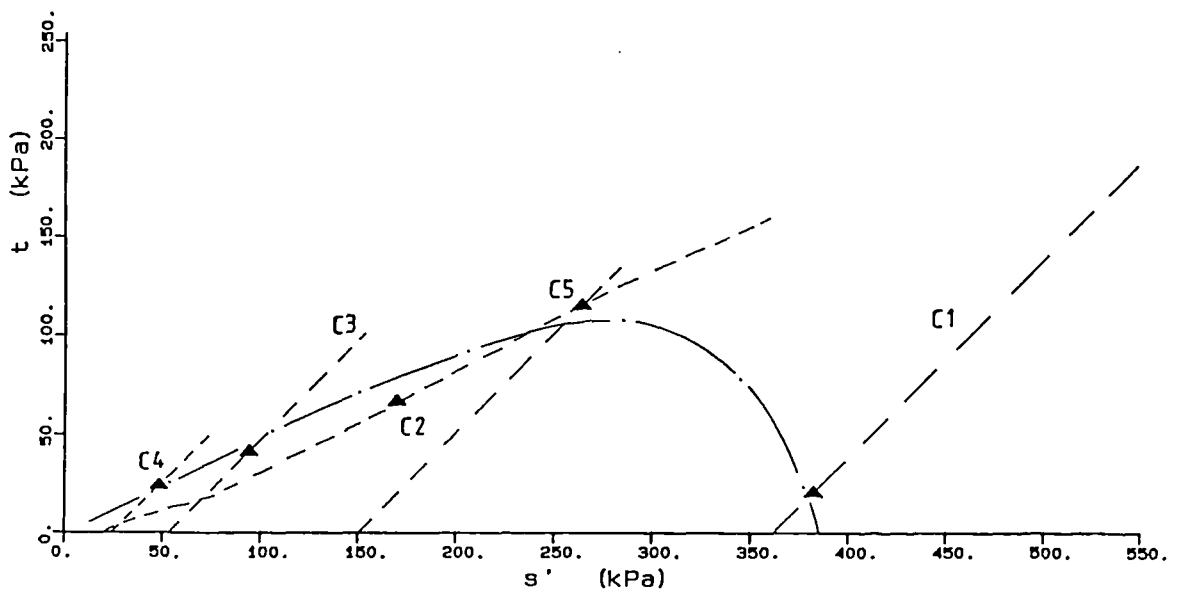
Fig. 2.10b Yield surface for the Chemususu Dam soil
(after Bressani, 1990)

26
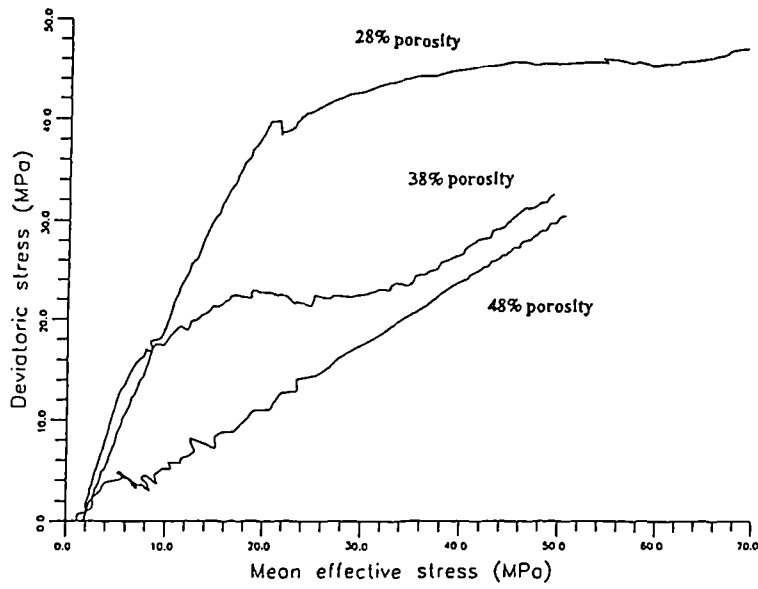
Fig. 2.11a K_0 tests on chalk (after Leddra, 1990)
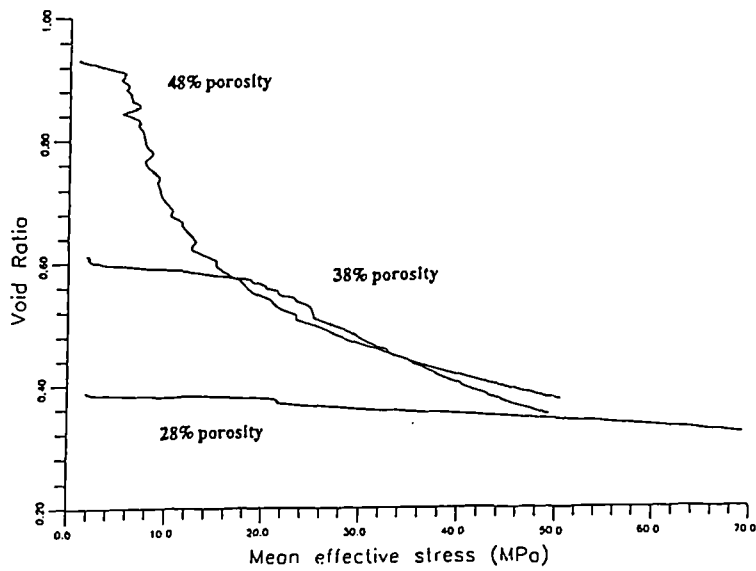
Fig. 2.11b One-dimensional compression tests on chalk (after Leddra, 1990)
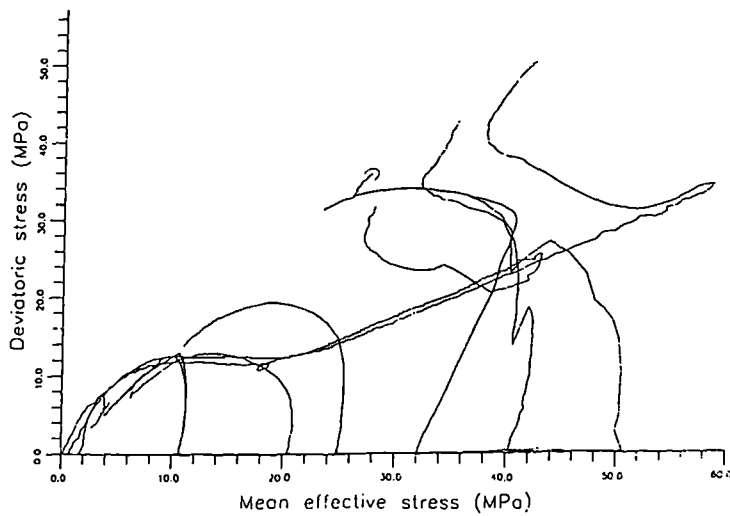
Fig. 2.11c K_0 and undrained triaxial tests on chalk (after Leddra, 1990)

27
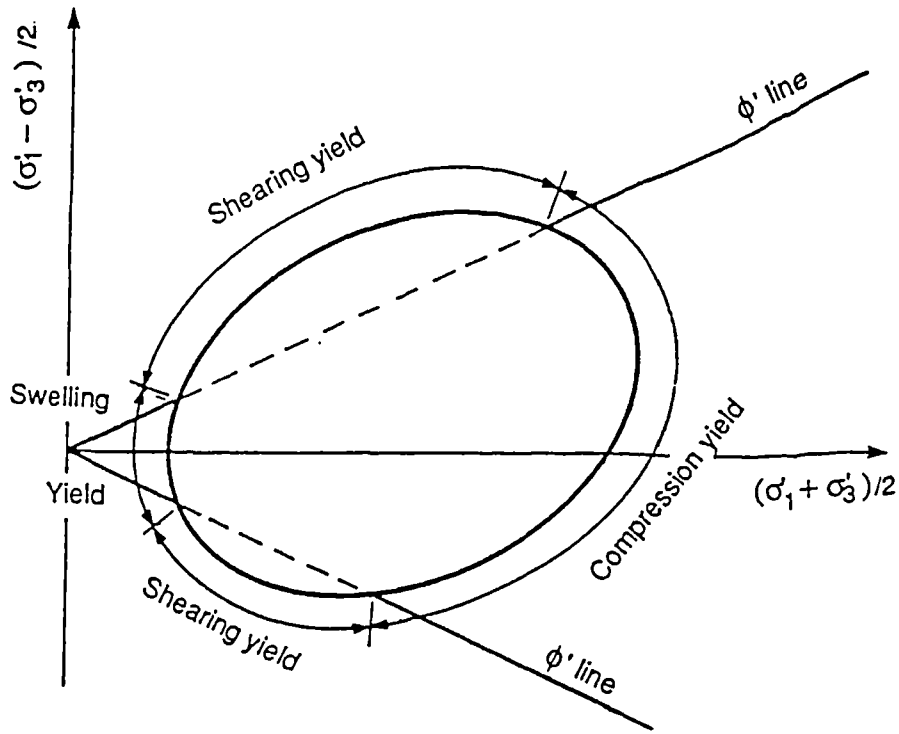
Fig. 2.12 Different types of yield in the stress space
(after Leroueil and Vaughan, 1990)
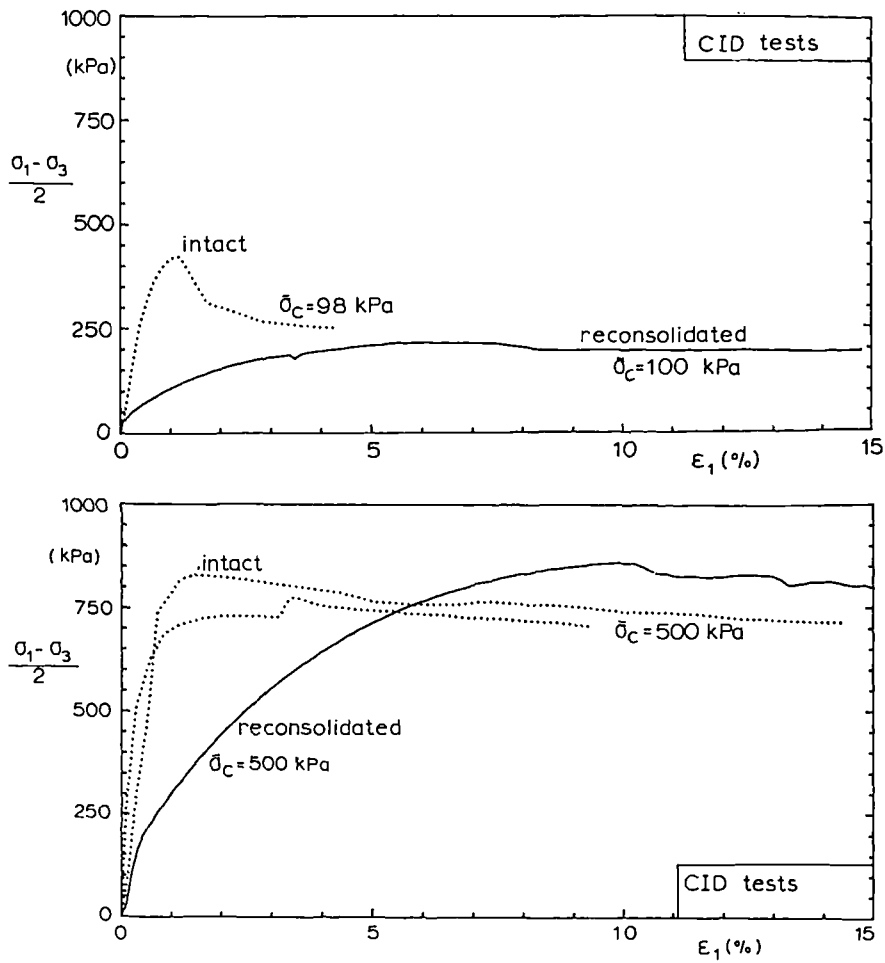
Fig. 2.13 Drained triaxial tests on intact and reconsolidated Corinth Canal
marls (after Anagnostopoulos et al, 1991)

28
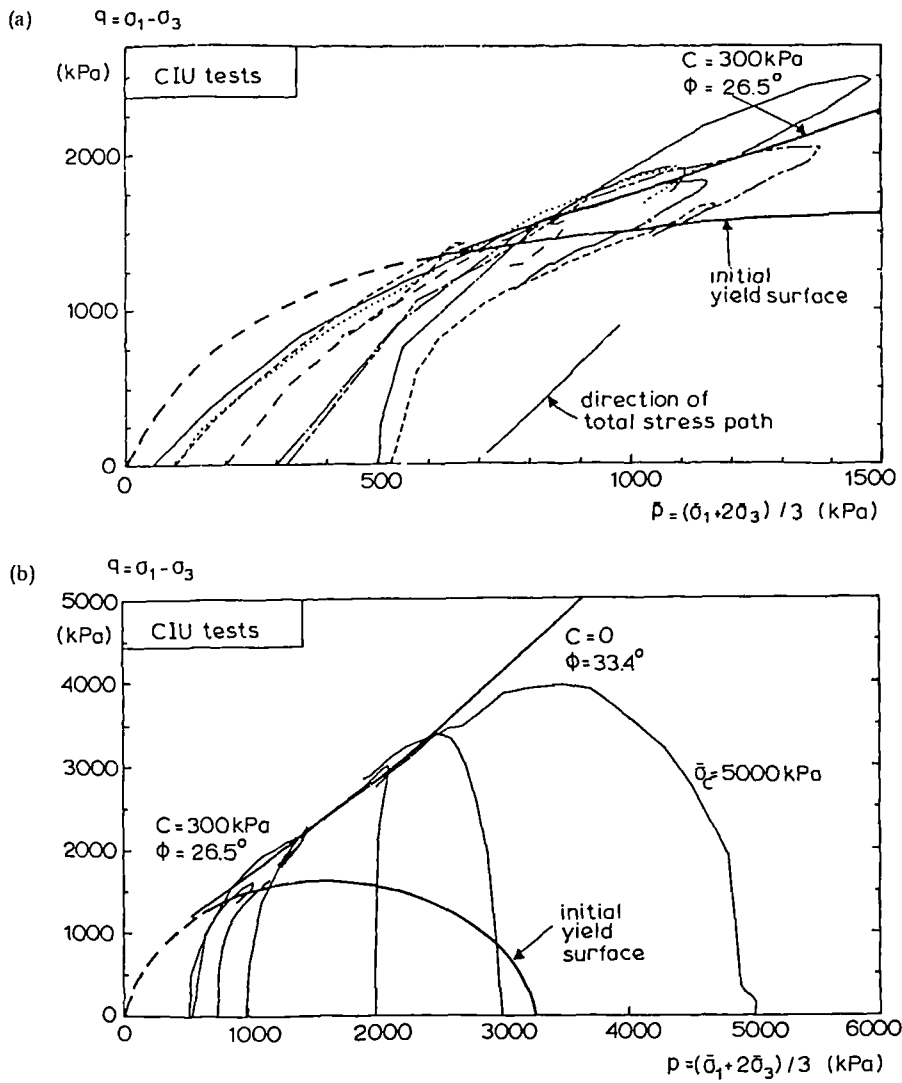
Fig. 2.14 Yield surface for the Corinth Canal marl
(after Anagnostopoulos et al, 1991)
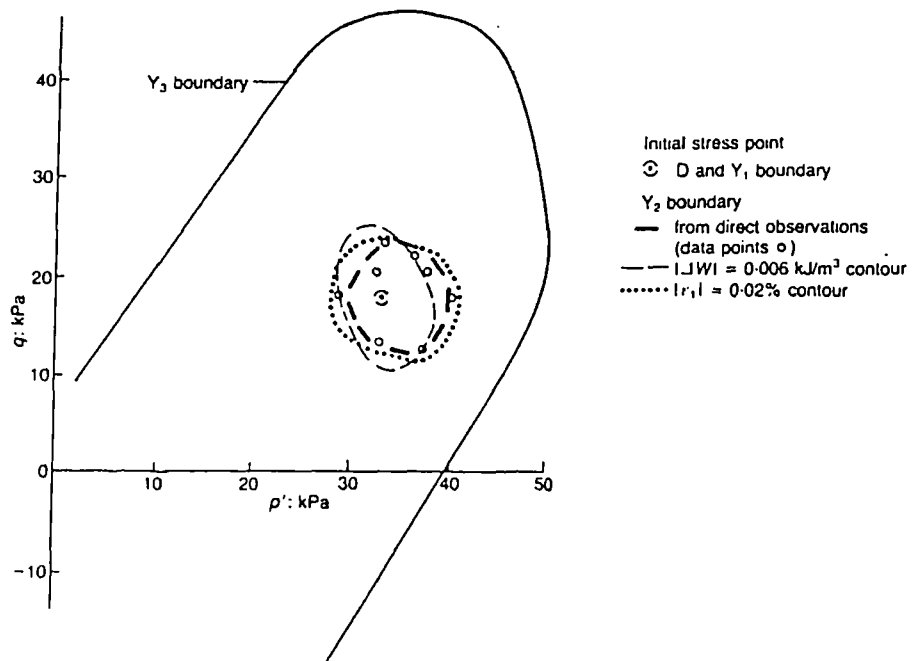
Fig. 2.15 Yield loci for the Bothkennar clay (after Smith et al, 1992)

29
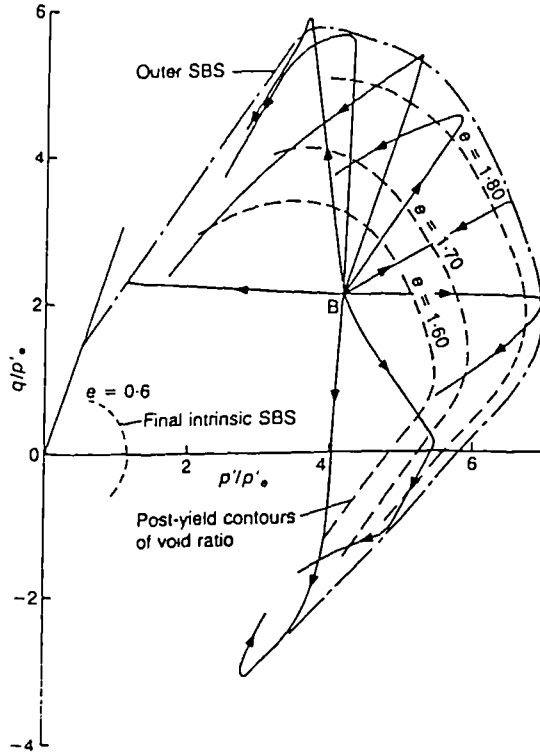
Fig. 2.16 Normalised yield loci for the Bothkennar clay
(after Smith et al, 1992)
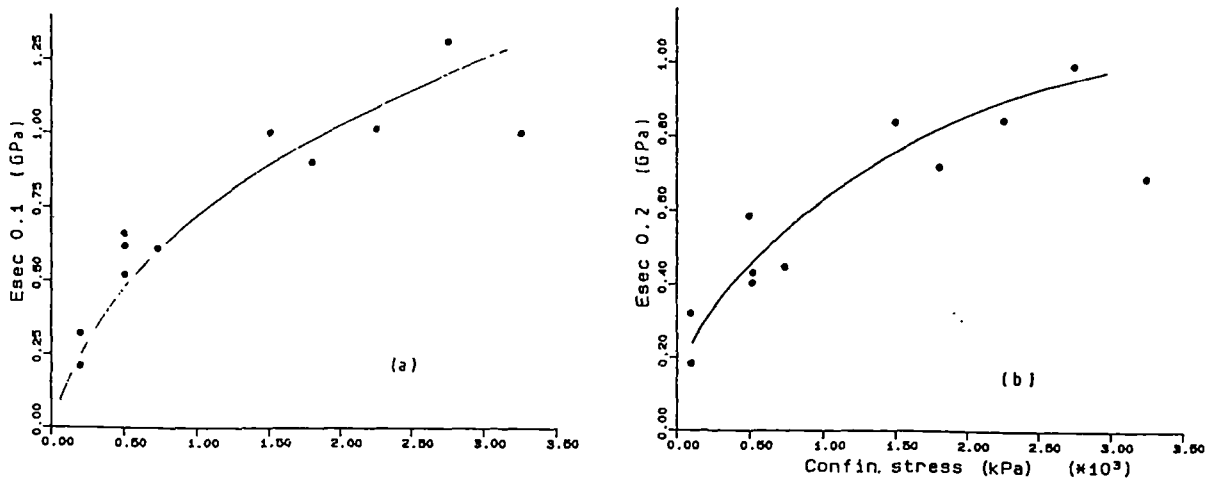
Fig. 2.17 Secant stiffness versus p' for the Corinth marl
(after Bressani, 1993)

30
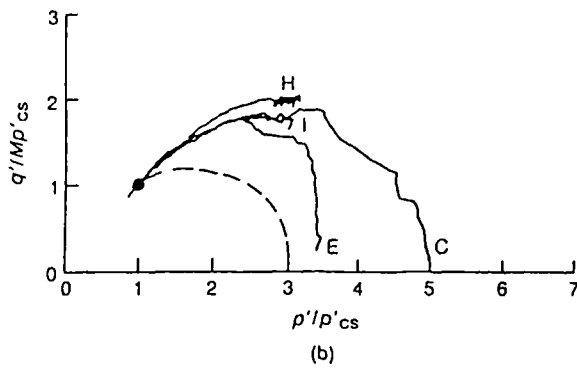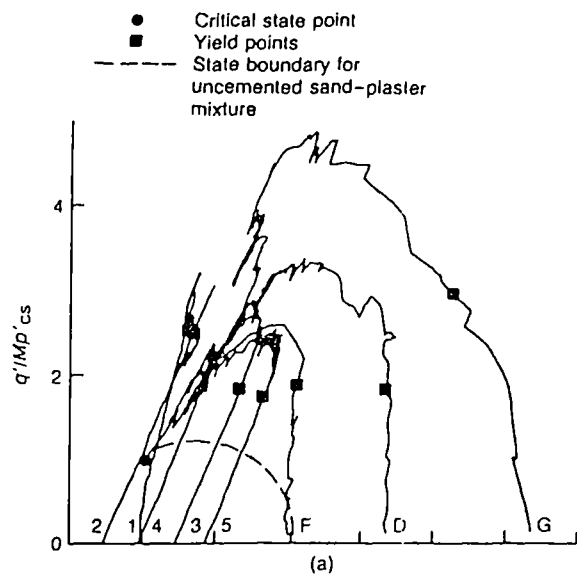
Fig. 2.18a State paths for artificially cemented samples
(after Coop and Atkinson, 1993)
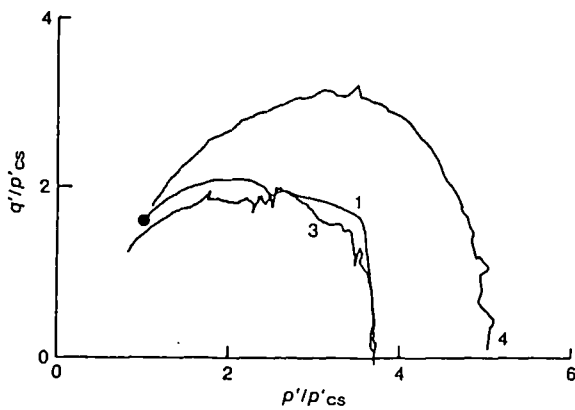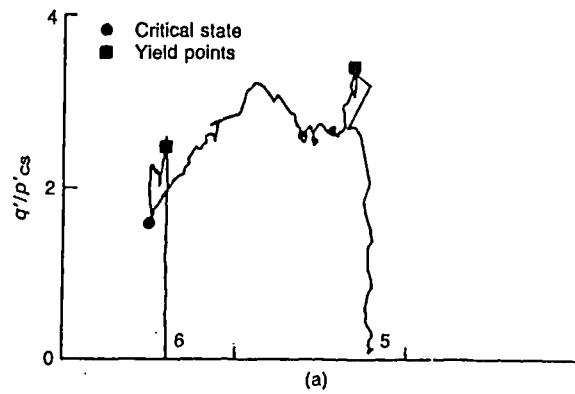
Fig. 2.18b State paths for natural calcarenite soil
(after Coop and Atkinson, 1993)

(a) Uncemented

(b) Weakly Cemented

(c) Strongly Cemented
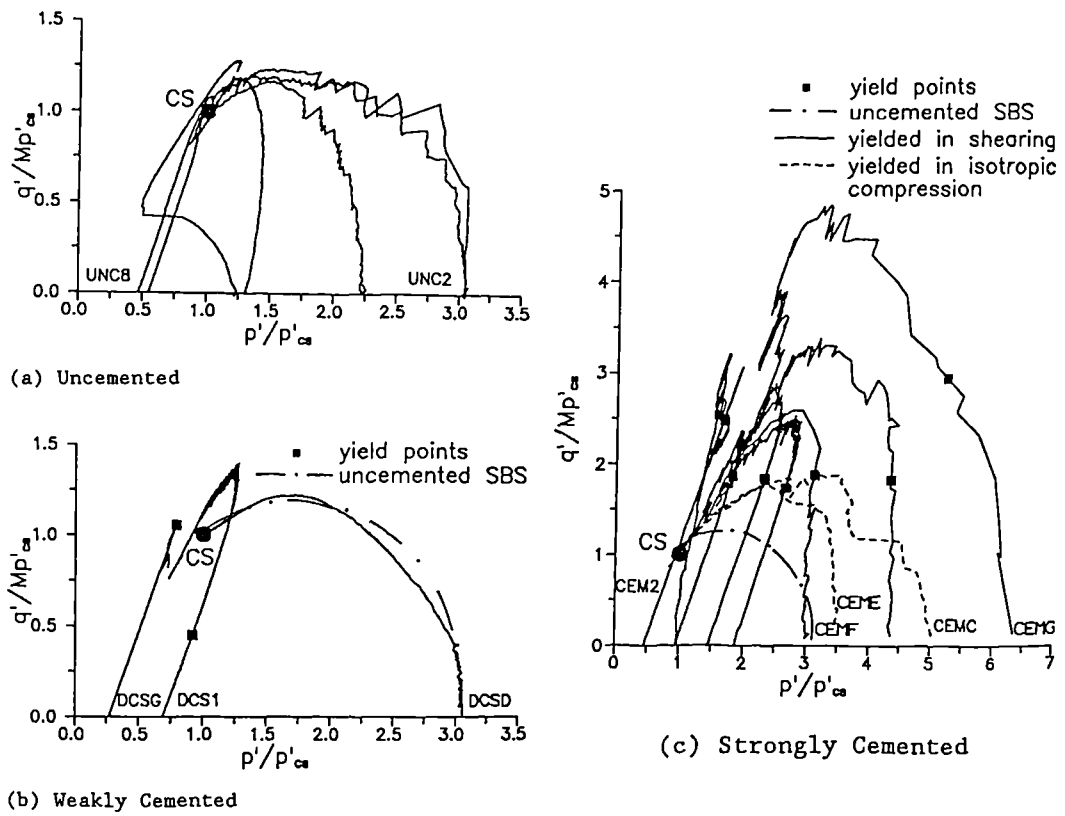
Fig. 2.19 State paths for an artificially cemented soil with different bond strengths (after Cuccovillo and Coop, 1993)
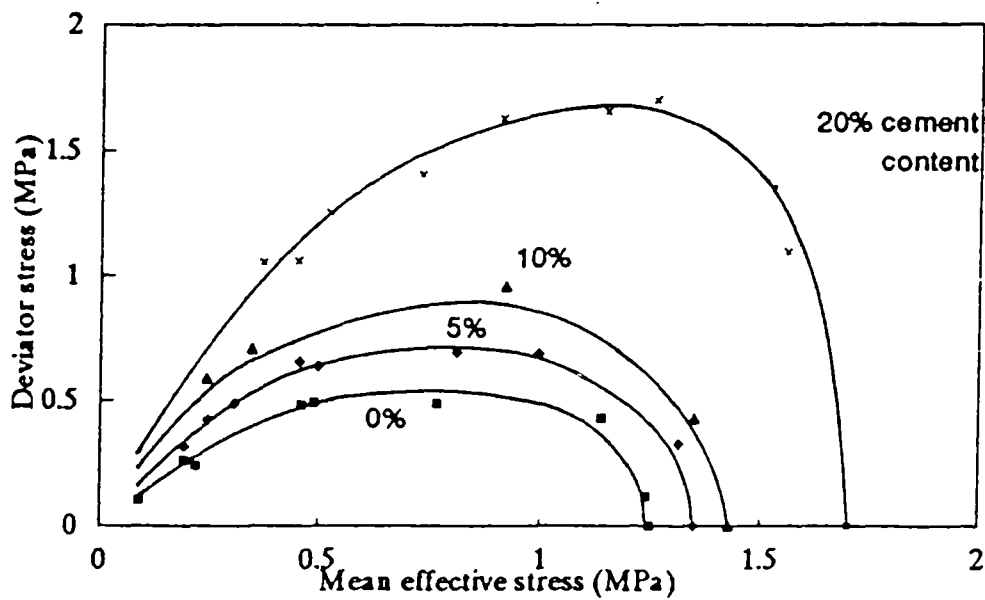
Fig. 2.20a Effect of the cement content on the size of the yield loci (after Huang and Airey, 1993)
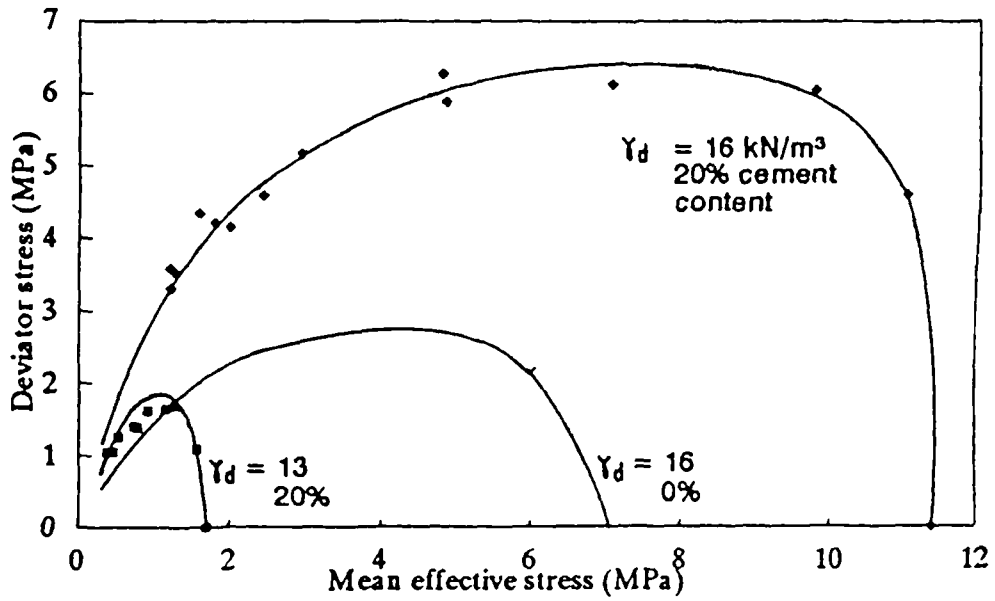
Fig. 2.20b   Effect of density on the size of the yield loci
(after Huang and Airey, 1993)
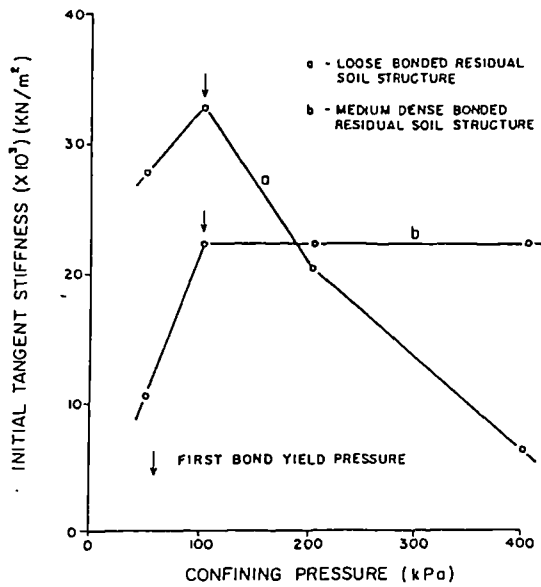
Fig. 2.21   Initial tangential stiffness versus p' for loose and medium dense
residual soils (after Maccarini, 1993)

33
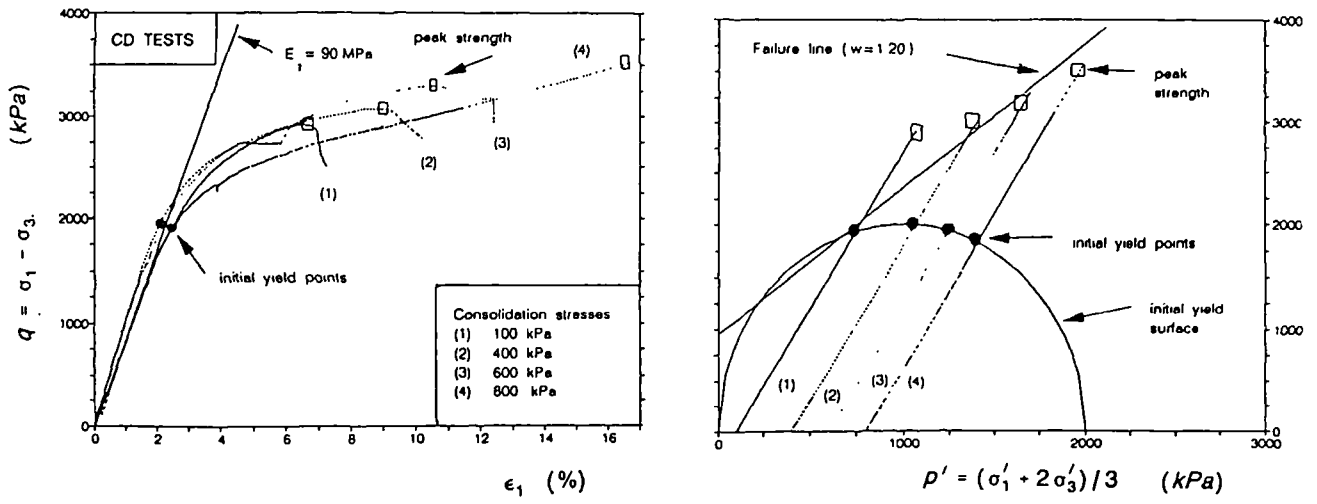
Fig. 2.22 Peak strength and yield envelope for lignite
(after Kavvadas et al, 1993)

CHAPTER 3   ARTIFICIALLY BONDED SOIL

3.1 INTRODUCTION

In this chapter the method of preparation for forming the artificially bonded soil is presented and some mechanical properties of this soil are also studied. The methods of preparation for the destructured and the sand-kaolin mixtures are also presented. The experiments were carried out in a stress-path triaxial apparatus with a computer control system. The system controls the pressures of the triaxial cell and so a complex stress path can be followed easily and with great accuracy. The basic principles of the control system are presented. Setting up and saturation of the samples is finally presented.

3.2 ARTIFICIALLY WEAKLY BONDED SAMPLES

In this section two techniques investigated for forming artificially bonded samples are presented. The technique of firing kaolin was adopted. A study of the mechanical behaviour of the soil and the effects of firing and different kaolin contents on the samples' bond strength is also included. Previous microscopic examination of the structure of the bonded soil by Bressani (1990), is also presented and clarifies the way that the fired kaolin bonds the sand particles together.

3.2.1 Preparation of artificially bonded samples with a phenolic resin and quartz sand

At the beginning of this work a method was investigated in order to produce weak bonds between sand particles with different types of glue. A wide range of glues are available in industry and some of them are waterproof. However most of them

are designed to produce a rather strong bond between the particles. It thus proved difficult to find a glue that is waterproof and produces a weak bond. A phenolic resin manufactured by BP (J2027L) was eventually tried. The resin was combined with a catalyst (Phencat 10) which caused hardening.

At the beginning, the masses of resin and catalyst were mixed at a ratio of 100:6. A small quantity of the mixture was added to quartz sand. The sand was mixed with a spatula until all the grains were coated with resin. Afterwards the sand-resin mixture was carefully spooned into the standard 38mm diameter and 76mm high moulds. In order to activate the catalyst and produce a bond between the particles the samples were put in the oven at 70°C, for an hour. Afterwards they were taken out and left to cool for 3hrs. However the resin produced a strong bond between the sand particles.

Less amount of the resin mixture was then tried in order to produce a weaker bond. Difficulties however arise as the new mixture did not provide homogeneous samples. Not all the sand grains were coated with the resin mixture. It was then decided to change the ratio of the resin and the catalyst that is added to the sand in order to produce a thinner mixture. However the thinner mixture did not produce sufficient bond between the sand particles and so the degree of temperature was increased.

Meanwhile, though, a change in the mechanical properties of the first batch of the samples was observed. The samples were becoming stronger with time. Such a change was not described in the company specifications for the two materials. The company was asked for further information, but they could not provide any further scientific background for the mechanical behaviour of the mixture. They were not worried that the resin was becoming stronger with time, as that is regarded as an advantage of the phenolic resin in the market.

Further attempts were made to control the samples behaviour but the final result was that the amount of resin and catalyst that was added in sand in order to have homogeneous samples, produced very strong bonded samples. However the interest of this work is the study of a weakly bonded artificial soil and therefore this method proved to be unsuitable to produce the desired structure. Thus the method of preparation of bonded samples previously developed by Maccarini (1987) was examined.

3.2.2 Mechanical properties of the artificially bonded samples developed by Maccarini (1987)

Maccarini (1987), developed an artificially bonded sample made up of quartz sand, a kaolin 'sand' and a small amount of kaolin slurry. The samples were fired at 500°C and a bond between the particles was produced by the fired kaolin slurry. As was previously discussed, the natural structured soils under shear present a stiff behaviour at the beginning, followed by yield at higher stresses. The bond, that yields above certain stress levels, contributes to the initial high values of stiffness and also to the peak shear strength of the sample. In this work the bond was produced artificially by the firing of kaolin at high temperatures. However the temperature, the time of firing and the percentage of kaolin have an influence on the bond yield stress of the samples.

Reproducible samples with the same properties such as bond yield stress and density were essential for this work. Maccarini (1987), did preliminary studies to investigate the effects of firing and kaolin content on the samples' behaviour. For these tests he used samples which had kaolin and sand at 13% and 87% respectively (designated 13/0/87). With this technique he produced samples with a void ratio up to 0.75. For a more porous structure he added a wax sand which was burnt off at high temperatures. He also added a kaolin 'sand', kaolin fired at

1000°C for 3 hours, crushed and sieved to achieve the same particle distribution as the quartz sand.

He found that the bond yield stress is stable for firing temperatures in the range of 500°C and for a duration of 300 minutes (fig. 3.1). He also showed that an increase of kaolin content up to 10%, causes a remarkably rapid increase in the yield stress, as can be seen in fig. 3.2, while a further increase has a more gradual effect on the stress. Thus kaolin up to 10% is sufficient to bond the contacts between the particles but further increase produces fired material in the voids between the sand particles.

Cuccovillo and Coop (1993), had also observed the same behaviour in a natural carbonate soft rock, where an increase in the degree of cementing filled the void spaces with an apparent decrease in the specific volume. In this case the influence of the bond on the peak shear strength is not so pronounced; only the lightly cemented samples showed the greatest influence because of bonding.

Maccarini investigated also the tensile strength of the bonded soil. This increased with the increase of firing temperature, time of firing, and void ratio. The tensile strength of dry samples was found to be more than twice that of saturated samples. Tests on samples with and without the fired kaolin 'sand' showed that the yield stress and the tensile strength were unaffected from the presence of the kaolin sand up to 30% of dry weight.

Maccarini also investigated the effect of time on the soil's behaviour and he did not find any significant difference between samples with different storage times. Bressani (1990), investigated the rate effects on the yield stress of the bonded soil under drained shear. Two samples sheared at the same confining stress and at different strain rates, at 5%/hr and at 0.03%/hr, showed a slight difference on the yield

stress and a more significant difference between the peak shear strengths, that indicated some influence of creep. However Bressani concluded that this influence is negligible when it is compared with much stronger effects of stress non-uniformity and isotropic cyclic loading before shearing.

3.2.3 The structure of the bonded soil

In a sand-kaolin mixture with a clay percentage greater than 5%, the kaolin coats the sand particles and also forms bridges between the particles. After firing of the samples these bridges form a bond between the sand particles. This form of the soils' preparation tends to produce a quite uniform structure.

Georgiannou (1988), examined a 7% kaolin-sand mixture under an optical microscope. The clay was concentrated at the sand grain contacts and it also formed bridges between the grain particles. Georgiannou also underlined the fact that the wet tamping method for the preparation of sand/kaolin mixtures (similar to that used by Maccarini and Bressani for forming the artificial bonded samples) produced fairly isotropic and uniform structured samples, compared with sedimented samples that have a more anisotropic structure.

Bressani (1990), presented microphotographs of a loose bonded sample with 13% kaolin, taken using a scanning electron microscope. All the particle surfaces of the sand were coated by bridges of the bonding kaolin, fired at 500°C. A study of a denser sample showed fewer voids between the particles than the loose one.

3.2.4 Preparation of the artificially bonded samples used in this work

It was finally decided for this study to adopt a similar method of preparation of artificially bonded samples to that developed by Maccarini (1987). The main advantage of using this soil was that all the preliminary studies for the soil's

properties had already been done, and thus further research could be carried out for the investigation of the soil's behaviour under probing triaxial stress path tests.

A medium grained quartz sand (Leighton Buzzard) with a uniform grading between 0.6 and 1.2mm was mixed with kaolin clay. The quartz sand has a particle density of 2.68 whereas kaolin has G_s=2.61. The particle size distribution curves for the sand used by Maccarini for his tests and for the sand used in this work are plotted in fig. 3.3. The two sands are medium grained but the sand used in this work has a greater amount of fine material than that used by Maccarini.

The partial percentages by dry weight used for the preparation of the samples were 87% of sand and 13% of kaolin and were the same as those used by Maccarini and Bressani. The required components of sand and kaolin were first mixed dry; then distilled water was added to produce the water content needed to form a sample with a required void ratio. The wet mixture was then placed into a filter paper tube within a brass supported mould, 38mm diameter and 76mm high. In order to avoid air being trapped inside the sample the tube was inclined and the wet mixture slid down the side with the help of a spatula. The samples were allowed to air dry within the moulds for 72 hours. During that period the samples shrank, with a reduction of the void ratio by 0.3. Afterwards they were removed from the moulds for further drying. The samples were then transferred to a kiln and fired at 500°C for five hours. After firing the samples were left to cool down overnight.

At 500°C an endothermic reaction takes place in the kaolin, with a change in behaviour from expansion to contraction followed by a 12% loss in weight. The kaolin forms a weak bond between the sand particles. The initial stage of drying and firing afterwards, had a considerable shrinkage effect on the samples; also the amount of water added to the initial mixture affected their final density. By

experimentation the initial void ratio required to produce the needed void ratio after firing was determined, so that samples would be produced with the desired density.

The loosest structured state achieved were samples with e_0=0.72 and the densest had e_0=0.55. Previous work on artificially bonded samples was concentrated on the study of relatively loose samples with $1.1<e_0<2$. In this study it was decided to investigate the behaviour of a denser soil with e_0=0.6.

3.3 DESTRUCTURED SOIL AND SAND-KAOLIN MIXTURES.

In this section the methods of preparation of destructured soil and sand-kaolin mixtures are presented. It has been emphasised (Vaughan, 1988), that in order to understand the behaviour of bonded soils it is essential to study a destructured soil, which is formed with the same material, the same grading and the same density as that of the bonded material. Then comparisons can be made between the behaviour of the two soils, and the influence of the bond on the peak strength and stiffness of the bonded samples can be clarified.

In this work triaxial tests have also been carried out on sand-kaolin samples (not subjected to firing and destruction) at the same void ratio as that of the bonded and destructured samples in order to make comparisons between the behaviour presented from the different soils.

3.3.1 Preparation of the destructured samples

The destructured samples were prepared from the breakdown of the weakly bonded samples. After firing, the samples were broken down by hand to destroy the bonds. In that way the composition and grading of the destructured material is as close as possible to that of the bonded samples.

41

That material was then mixed with distilled water and placed in a filter paper tube in order to form a sample at the same void ratio as the bonded samples. The sample was left to dry, to a stage when it was not too wet, so that it could be moved and placed in the triaxial cell, but was not so dry that it would crumble and fall to pieces. Only one sample was prepared for testing at a time. The specific gravity of the kaolin changed from 2.61 to 2.51 after firing, and that was taken into account in calculating the void ratio.

3.3.2 Preparation of the sand-kaolin mixtures

The same method of preparation used for the bonded samples was used for the sand-kaolin mixtures. The sand and kaolin were mixed dry and then distilled water was added. The mixture was placed into the moulds and the samples were left to dry for 72 hours. The amount of water used for the samples' preparation was different from that used for the bonded samples, as the final part of firing did not take place.

3.4 TESTING EQUIPMENT

A stress-path triaxial apparatus (Bishop and Wesley, 1975) was used with a computer control system (TRIAX) for the experimental work. The use of this apparatus allows for tests to be carried out in the entire triaxial stress space. The computer system controls the stress path cell and so a complex stress path can be followed with accuracy and without great difficulty (Toll, 1993).

The software of the system runs on a IBM compatible PC and provides data acquisition and calibration functions. The user specifies control parameters in terms of control equations and thus high flexibility of the system is achieved.

A test can be divided up into 100 stages, and control is passing from stage to stage by a series of alarms (Toll, 1993). A screen dump of the parameters defined for a stage is presented in fig. 3.4. Through this stage the system controls a constant p' drained triaxial test. Box number 1 controls the back pressure and tries to maintain it constant at a value of 300kPa; box number 2 controls the mean effective stress p' and ensures that this is maintained constant at 100kPa and box number 3 controls the deviatoric stress and increases it at a constant rate of stress of 10kPa/hr. The test will stop when a strain percentage of more than 20 has been developed (Alarm 1).

Stepper motor driven air valves are used for controlling the cell, back, and ram pressures. They are able to be controlled in increments of 0.1kPa, in the range of 10-800kPa. A constant rate of strain pump was also connected to the system. It is a stepper motor driven piston pump, which was used for the constant rate of strain tests. A Measurement System Ltd Datascan 7020 is used for data logging, which provides a resolution of 0.6μV, and it can handle up to 16 transducers, on different channels.

The cell, back, and ram pressures were measured by pressure transducers with a maximum capacity of 1000kPa. These transducers were carefully de-aired during installation, and a Budenberg dead weight tester was used for their calibration. The axial strain was measured by an external vertical displacement transducer. The range of this device was 25mm, and it was bench-calibrated using a vernier micrometer. The volume change during drained loading was measured by a volume gauge having 50cm³ capacity. The volume gauge was calibrated using a 25cm³ burette.

Calibration data for each transducer were stored in calibration data files on the computer. Polynomial regression curves (up to 2nd order) were fitted to these data

and the regression coefficients were stored and used to convert from voltages to engineering units.

3.5 SET-UP AND SATURATION OF THE SAMPLES

The bonded samples were placed dry in the triaxial cell. The cell was filled with water, and the samples were saturated by flushing through with deaired water under a small pressure gradient for three hours. Afterwards the cell and the back pressures were increased simultaneously using a rate of 20kPa/hr. The effective stress of the sample was always maintained constant at a value of 2kPa. Thus the damage to the soil structure that the saturation technique often implies is eliminated.

A back pressure of 300kPa was then applied for twenty four hours, before testing the B value. For the determination of the B value an increase of the cell pressure of 100kPa was applied. The back pressure was maintained until a value of at least 0.98 was obtained. Normally a back pressure of 300kPa was used, but because of stress limitations of the system a back pressure of 150kPa was applied to samples that were isotropically consolidated at stresses higher than 400kPa. In this case the bonded samples achieved saturation after six days, while only two days were needed to achieve a B value of 0.98 when a back pressure of 300kPa was applied. The destructured samples and the sand-kaolin mixtures needed five days of saturation when a back pressure of 300kPa was applied.
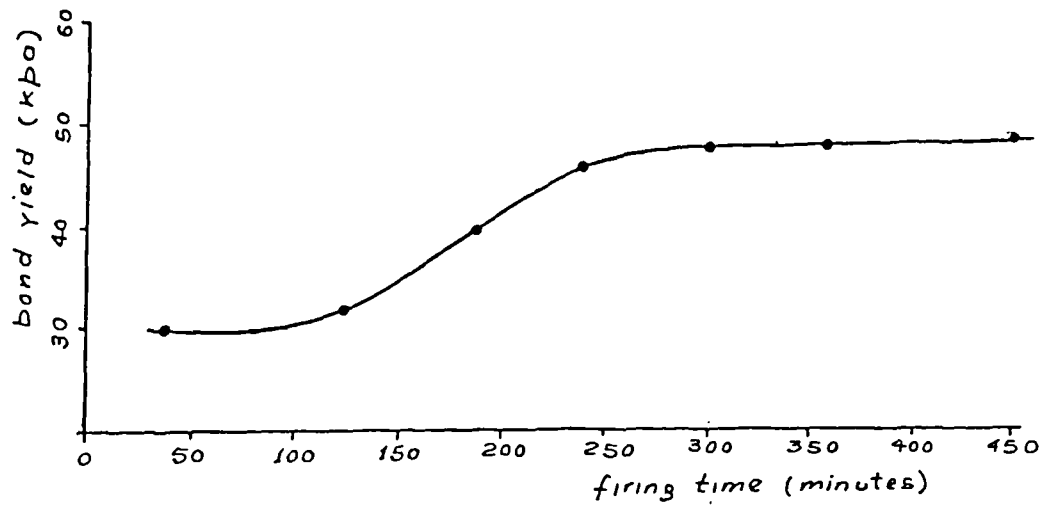
Fig. 3.1 Effect of time of firing on the bond yield stress
(after Maccarini, 1987)
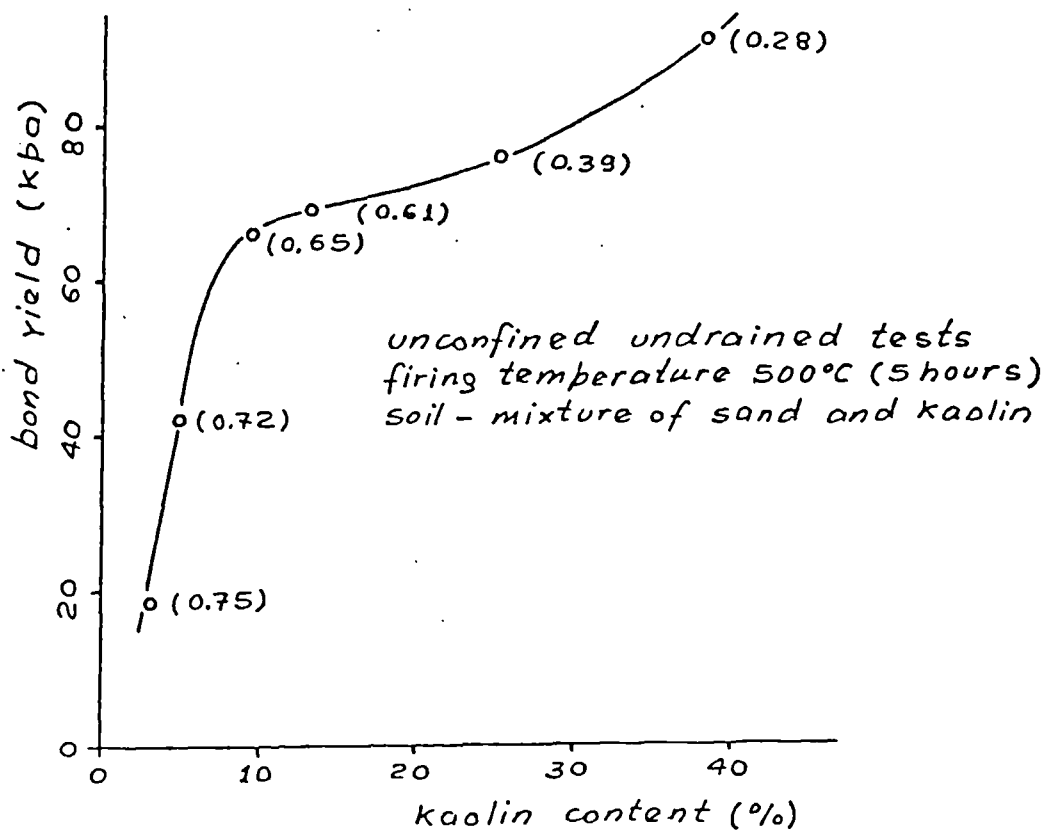
Fig. 3.2 Effect of kaolin content on the bond strength of the soil
(after Maccarini, 1987)

45
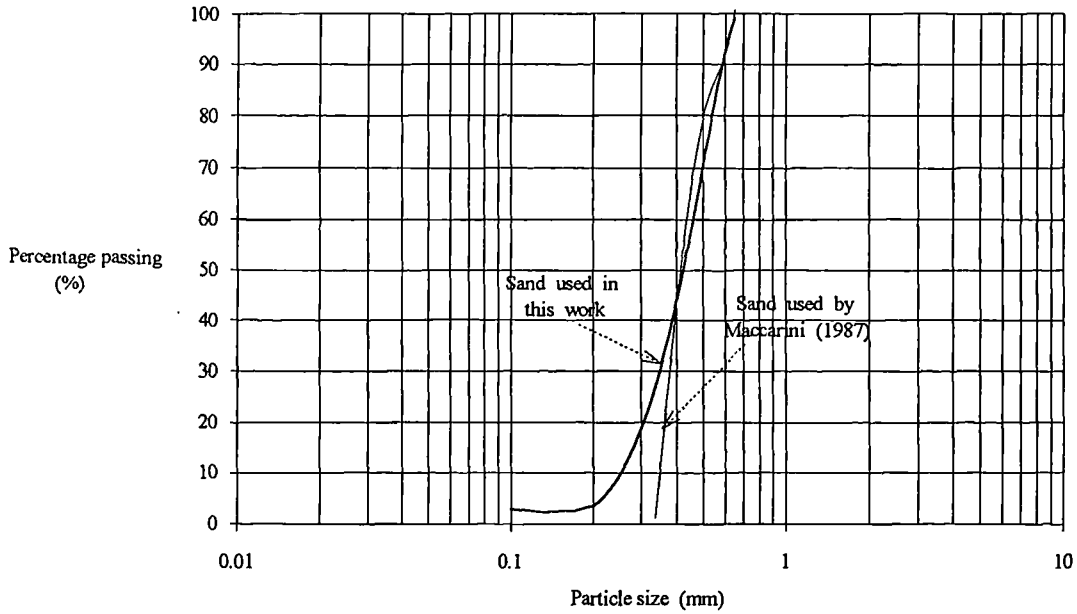
Fig. 3.3 Particle size distributions curves for the two sands

STAGE 1
Stage description: CONSTANT p'

No trigger for Stage 1 ·

Box	1 BACK	2 CELL	3 RAM	4 CRSP
Status	ON	ON	ON	OFF
Control equation	back	p'	q	Undefined
Hold value	300	100	current	Undefined
Tolerance	0.5	0.5	0.5	0.5
Increment	0	0	10	0
Maximum pulses	10	20	10	10

	Condition	Action
Alarm 1	strain>20	STOP
Alarm 2	Undefined	Undefined
Alarm 3	Undefined	Undefined
Alarm 4	Undefined	Undefined
Alarm 5	Undefined	Undefined

Use Arrowed Cursor keys to move, Continue key to leave (f10)

Fig. 3.4 A stage for controlling a constant p' drained test

46

CHAPTER 4   DRAINED TRIAXIAL TESTS ON BONDED

AND DESTRUCTURED SAMPLES

4.1 INTRODUCTION

In this chapter the behaviour of bonded and destructured soil is studied under drained shear in triaxial compression. All samples were prepared having a void ratio of 0.6. The main aim is to establish a general framework that explains the behaviour of bonded material in a shearing test. Therefore the bounding surface, and the first and second yield surfaces are identified for this soil. The study of the behaviour of the destructured soil sets the basic framework for this material in the unbonded state and thus allows for comparisons to be made between the two soils. The influence of the bond strength on the maximum q/p' stress ratios that the soil sustains in the stress space, on the initial values of stiffness and furthermore on the shape of the first and the second yield surfaces is clarified.

4.2 DRAINED TRIAXIAL TESTS ON BONDED SAMPLES

The behaviour of the bonded samples under drained shear in triaxial compression is presented in this section. The bounding surface and the position of the first and second yield surfaces in stress space are presented. Stiffness measurements at different percentages of strain clarify the positions of the two yields during shearing, at low and higher stresses. The development of strain is also studied and strain contours are presented in the stress space.

4.2.1 Testing details

A total of eleven drained triaxial tests were carried out on bonded samples. The samples were first isotropically consolidated to a range of confining pressures, in order to study the behaviour of the bonded samples at different stress levels, and

then sheared under drained conditions. Nine samples were sheared under a constant rate of strain of 1.5%/hr and two samples were sheared under a constant rate of stress of 50kPa/hr. Transducer readings were taken every two minutes, during the initial stage of the test, and after 2% of strain they were taken every six minutes. The name of the test, the void ratio of the samples, and the confining pressure at which they were consolidated prior to shear are shown in table 4.1.

The first letter of the name indicates the type of test (drained or undrained), the second letter indicates the type of sample, bonded or destructured and the third letter is used only for the stress controlled tests. The number after the two letters is the value of confining stress to which the sample was consolidated prior to shear. For example test db35, indicates a drained test on a bonded sample consolidated to 35kPa and sheared under a constant rate of strain and dbs35 indicates a drained test consolidated to 35kPa and sheared under a constant rate of stress.

4.2.2 Stress strain behaviour in drained shearing

The deviatoric stress (q)-axial strain curves for all the drained triaxial tests are shown in fig. 4.1. The tests were carried out up to 30% of strain in order to study the behaviour of the samples towards the critical state.

At low confining pressures (tests db5-200) the samples reached a peak state at low strains between 1.5%-2.5%, which was followed by rapid strain softening as shear surfaces formed in the samples. The axial strain at the peak state increased with an increase of confining pressure, indicating a gradual transition from brittle behaviour to a more ductile mode of failure during shearing. Tests dbs430 and db550 reached peak values at about 4% of strain and showed a drop in q at higher strains because of strain localisation.

The volumetric strain versus axial strain curves for all the tests are plotted in fig. 4.2. The samples showed compression at the beginning of the test and dilation

48

afterwards. Sample db5 showed initially little compression, followed by a change in behaviour at a low axial strain less than 0.5%, and an accompanying development of a high rate of dilation. Test db35 showed a higher degree of compression than that of db5 and a change in behaviour at a higher percentage of strain than that of the latter. The amount of compression that a sample developed and the percentage of strain at which the behaviour changed from compression to dilation increased with the increase of confining pressure at the first part of the test prior to shear; this behaviour is closely followed by both the stress and the strain controlled tests. The samples were dense and dilation occurred even when shearing took place at $p_0'=550kPa$ of confining pressure. The maximum positive values of volume change indicate a change in behaviour (from compression to dilation). The points at which this occurs can be plotted in the stress space and thus they define the phase transformation line (fig. 4.3).

Shearing took place under constant volume at the end of tests db100, db250, db350 dbs430 and db550, suggesting that the samples are very close to the critical state. However this is true only for test db350 because a drop in q is observed for the rest of the samples (fig. 4.1).

4.2.3 Maximum shear strength of the bonded samples

Taylor (1948), suggested that the maximum shear strength of a specimen in the shearing process is partially due to the friction between the particles and due to interlocking. Schofield and Wroth (1968), expanded his theory and presented the following equation $\tau/\sigma'=\mu+(\delta\upsilon/\delta u)$ where τ is the shear stress, σ' is the normal stress, μ is the coefficient of friction, $\delta\upsilon$ is a small increment in vertical movement and δu is a small increment in horizontal movement.

This is equivalent to $q/p'=M-(\delta\varepsilon_v/\delta\varepsilon_s)$ where M is the slope of critical state line when it is projected on to a constant volume plane, $\delta\varepsilon_v$ is a small increment

in volumetric strain and $\delta\varepsilon_s$ is a small increment in shear strain. A negative volumetric increment of $\delta\varepsilon_v$ in this equation indicates expansion (Atkinson and Bransby, 1978). This equation suggests that the q/p' ratio depends on the frictional constant M as well as on the rate at which a sample dilates during the shearing process, with higher values of q/p' produced by higher values of rate of dilation. A dense sand, when sheared at low confining pressures, demonstrates brittle behaviour and therefore the maximum shear strength coincides with the maximum rate of dilation. Taylor's model is quite simplistic in this generalised form, but it was adopted for this work since it is used only for a qualitative study.

In order to study the effects of rate of dilation, the position of the maximum rate of dilation for the tests carried out on bonded samples was defined from a $d\varepsilon_v/d\varepsilon_a$ graph plotted against ε_a. The ratio was defined in terms of axial strains rather than shear strains because the latter were subject to greater errors, since they were calculated using conventional volumetric strain readings. An example is plotted in fig. 4.4 for test db35.

The points corresponding to maximum values for the q/p' ratio and the maximum rate of dilation are marked on the stress-strain curves in fig. 4.5a. The maximum q/p' ratio always occurs before the point of the maximum rate of dilation. However for tests db350, dbs430 and db550 carried out at higher confining pressures the two points occur at similar values of deviator stress.

In fig. 4.5b the results for tests db5, db11, db35, dbs35, db100, and db150 are plotted separately. The samples sheared at low confining pressures show brittle behaviour and the maximum rate of dilation comes after the maximum q/p' ratio. The fact that the maximum rate of dilation does not coincide with the max q/p' ratio suggests that the peak strength of the bonded soil at low confining stresses is

mainly governed by the bond strength and dilation plays a secondary role. Test results for db200 are plotted in the previous figure and show similar behaviour.

For tests db350, dbs430 and db550 (fig. 4.5a) carried out at higher confining pressures the behaviour of the samples becomes more ductile and the position of the maximum q/p' ratio and the maximum rate of dilation is at the same stress level. Thus, when shearing at stresses higher than 250kPa, the close coincidence of the maximum rate of dilation and the max q/p' ratio suggests that dilation is playing the major role in governing the peak shear strength of the samples and the bond strength is less important.

For test db250 plotted on the same figure, the position of the maximum rate of dilation is close to the maximum q/p' ratio in respect of axial strain, but at a slightly lower stress level. Thus the sample is sheared at a confining stress where its peak shear strength is controlled partially by the bond strength and partially by dilation. The picture of the samples' behaviour under shearing in respect of maximum shear strength will become clearer later on, when yield of the bonds at certain stress levels will also be taken into account.

The stress paths and the maximum q/p' ratio values for all the tests, are presented in fig. 4.6 and 4.7 respectively. It is evident that the bounding surface shows some curvature at this stress level and so a curve is plotted passing through the maximum q/p' points. In this way the bounding surface for the bonded samples is best represented in the stress space. Using a conventional linear interpretation of the failure envelope, tests db5, db11 and db35 and dbs35, define a line with a high value for the equivalent angle of friction $\varphi'=48°$ and an equivalent cohesion intercept c'=34kPa. The slope of the failure line drops to a lower value ($\varphi'=35°$) with a corresponding higher value of cohesion (c'=120kPa), for the q/p' values obtained from tests db100, db150, db200 and db250. At stresses p'>600kPa the max q/p' ratio drops to 1.31 (equivalent angle of friction $\varphi'=33°$), while c'=48kPa.

The decrease of the slope of the bounding surface indicates the loss of the bond strength of the samples at failure, with the increase of p_o'. The bounding surface governs the behaviour of both strain and stress controlled tests.

It is interesting to notice that the points that define the phase transformation line, plotted in fig. 4.3 also show some curvature at low confining pressures. A curve passing through the points is plotted in the stress space. Therefore the bonded structure has also an influence to the point at which the behaviour of the samples turns from compression to dilation.

4.2.4 Definitions for the first and second yield of the bonds

When shearing a bonded soil in a triaxial test some of the stress applied to the sample is carried by the bonds and some by the interparticle contacts (Vaughan 1988). There is an initial stage, before any bond breakdown, when the soil is very stiff. With the increase of axial strain some of the bonds start to break and at this point, first yield occurs. With a further increase of the bond stress more bonds breakdown and the contribution from the bond strength decreases progressively. After a certain point the bonded structure becomes insufficient to carry the increasing stress and second yield takes place which causes a dramatic loss of the strength and stiffness in the sample.

Maccarini (1987), defined the first yield of the bonds as the end of the linear part of the stress strain curve from the triaxial test (plotted at natural scale) and the second yield as the point of maximum curvature of the same curve. He noted though that this technique is efficient for defining the two yields only for loose samples, because with the increase of density the yields become more muted and it is more difficult to identify them.

Bressani (1990) used the previous method but also continued further, based on Vaughan's idea (Vaughan 1988), and defined the two yields from the stress strain

curve plotted in log-log scale. An example of this method is shown in fig. 4.8. He defined the first yield at the end of the linear part of the curve and the second at the end of a smooth part, followed by a linear portion at higher axial strains. He found generally good agreement between the values obtained from the two different methods.

These two methods for defining the first and second yield of the bonds can be compared as follows. Two examples are presented for tests db5 and db150 carried out at low and higher stresses respectively. The axial strain measurements were determined by external readings and thus were subject to errors to some extent. However these readings are suitable for a qualitative study. The bedding error effects also made the identification of the first yield at small strains difficult in some of the tests.

In fig. 4.9a the stress strain curve for test db5 is plotted in natural scale. The point for second yield is at the maximum value of q. The same graph is plotted in log-log scale in fig. 4.9b. There is a difference in behaviour from a linear part to a smooth curve that can be identified as the first yield at q=9kPa and there is another change from the smooth curve to a linear part at q=80kPa that defines the second yield. The values obtained from the two methods are almost the same.

In figs. 4.10a and b the stress strain curve for test db150 is plotted in natural and log-log scale respectively. The second yield in the first graph is at q=445kPa, lower than the maximum q. In fig. 4.10b there is a change in behaviour at the stress strain curve at q=34kPa, that defines the first yield and a second one at q=460kPa, that gives a slightly higher value than that obtained from the natural scale graph.

Generally there is good agreement between the values obtained from the two different methods for the two tests carried out at low and higher stresses and that was also the picture for the rest of the tests. However yield of the bonds is related to a loss in stiffness and therefore a further investigation of the tangential stiffness

during shearing is considered to be essential for a general definition of the first and second yield of the bonds.

In fig. 4.11 E_{tan} is plotted with strain in log-log scale for test db5. A first drop in stiffness at 0.21% of strain indicates a first yield at q=9kPa, while a major loss at 1.5% of strain at q=81kPa indicates the second yield. The points for the first and second yield are almost the same as these obtained by Bressani's method.

Tangential stiffness for test db150 is plotted with axial strain in fig. 4.12. A first loss in stiffness occurred at ε_a=0.29% with a value of q=98kPa and a major loss was initiated at ε_a=1.12%, where q=327kPa. The bonds are breaking down progressively and accordingly stiffness decreases with the increase of strain. There is a difference in the position of the two yields obtained from this and the previous methods. A higher position for the first yield and a lower position for the second yield is obtained by the latter method.

It is possible though that the difference in the positions of the two yields obtained from the two methods is influenced by the increase of the confining pressure prior to shear. Consider the sample's behaviour for test db550. In fig. 4.13a the stress-strain curve is plotted in log-log scale. There is a change in behaviour at ε_a=0.071% with q=49kPa and another one for the second yield at ε_a=2.65%, with q=1200kPa. In fig. 4.13b E_{tan} is plotted with strain in a log-log scale. There is a loss in stiffness at ε_a=0.082% with q=53kPa and a major loss that was initiated at ε_a=1.2% with q=771kPa. Although the position of the first yield defined from the two methods is very close, there is a difference in the position of the second yield of q=429kPa.

It can also be seen, from fig. 4.11 and 4.12-4.13b that there is also a difference in the decrease in E_{tan}, when the soil is sheared at low and high p'. The second loss in E_{tan} occurred rapidly in the first case, at a stress level where the soil also

reaches its max q/p' ratio, while when the soil was sheared at higher p' the second loss in E_{tan} took place progressively with the increase of axial strain.

Compared with the definition of yield from stiffness observations, the method that Bressani used gave lower values for the position of the first yield for samples sheared at intermediate stresses $35 < p_o' < 400 kPa$ and higher values for the position of the second yield when $p_o' > 35 kPa$. The difference in the position obtained from the two methods increased with the increase of confining pressure.

The position of the second yield obtained from Bressani's method for the samples sheared at high stresses is very close to the max q/p' ratio and at a percentage of strain where almost all of the samples' stiffness had already been lost. For test db150 the position of the second yield is at $\varepsilon_a = 2.4\%$, where referring to fig. 4.12 the value of stiffness is at a very low level. For test db550 that was carried out at higher stresses, yield is defined at $\varepsilon_a = 2.65\%$ where, referring to fig. 4.13b, stiffness is very low in comparison with the initial value. It should be noted that a similar method to that presented by Bressani was also used by other researchers in the last 7 years. They defined a final yield of the bonds at large strains, very close to the bounding surface of the bonded soils and at a stress level where stiffness was very low or even negative (Smith et al, 1992, Coop and Atkinson, 1993).

However a total loss in tangential stiffness is a result of an almost complete destruction of the bonds and a large decrease in the bond strength. Vaughan initially (1988), had pointed out that second yield causes a dramatic loss in stiffness and does not coincide with the complete destruction of the bond strength that occurs at large strains. Therefore based on these grounds it is felt that the changes in E_{tan} give a clearer and more objective definition of the yield points. Thus the behaviour of the samples in respect of stiffness was investigated for the rest of the tests and the first and second yield were also identified by this method.

The first and second yield points for all the tests are plotted in the stress space in fig. 4.14, and the stress paths are also included. The yield points form consistent yield surfaces in the stress space, for both the strain and the stress controlled tests. The first yield surface increases up to p'=200kPa, but for higher stresses it levels off parallel to the isotropic axis and after p'>400kPa it curves down towards the latter. The second yield surface occurs at higher stresses than the first yield surface and also increases in q with an increase of p'. Tests were not carried out at higher stress levels due to stress limitations of the system. However undrained triaxial tests were carried out up to p'=650kPa and up to ε_a=2%, in order to clarify the shape of the second yield surface in that area. The test results are presented in the next chapter.

The position of the second yield surface at a lower stress level than the bounding surface does not contradict the idea of a final yield surface that represents the total destruction of the bonds at high axial strains and at a level where the soil has already lost all of its stiffness, as a result of the breakdown of the bonds. Maccarini (1987), and Bressani (1990), defined this state as second yield. However it is clear from the results previously presented that this represents what is called here, the final yield of the soil's bonded structure.

It is believed that the significance of the second yield surface which is associated with the loss in E_{tan} is greater than that of the final yield surface and thus this study has concentrated on the effects of second yield on the soil's behaviour. Some further study of the final yield of the bonds follows in the next section.

4.2.5 Study of the position of the second yield and the maximum q/p' ratio

The position of the second yield with respect to the maximum q/p' ratio on the stress-strain curve was also investigated. The stress strain curves for tests db5-150 are plotted in fig. 4.15a. The position of the second yield and the maximum q/p' ratios are marked on each curve. For tests db5 and db11, carried out at very low confining pressures,

second yield of the bonds almost coincides with the max q/p' ratio. When shearing took place at higher stresses the behaviour of the samples is still brittle (tests db35, dbs35, db100 and db150) but second yield occurs at lower stresses than the max q/p' ratio.

The results for tests carried out at high stresses are plotted in fig. 4.15b. The samples' behaviour for test db200 is also brittle and second yield occurs at lower percentages of strain than the max q/p' ratio. When shearing took place at confining stresses higher than 200kPa, the behaviour of the samples becomes more ductile and the difference between the position of the second yield and the max q/p' ratio also increases.

For tests db5 and db11, carried out at low confining pressures, the samples' behaviour is brittle and the point of the second yield coincides with the max q/p' ratio. Also referring to fig. 4.5a, the maximum rate of dilation is after the latter. This suggests that the bond entirely controls the peak shear strength of the samples and dilation is playing a secondary role. For tests db35-200 the samples' behaviour is still brittle but yield of the bonds does not coincide with the max q/p' ratio and the maximum rate of dilation is after the latter. The bond strength at failure is lower at this stress level, but still contributes to the maximum strength of the samples and its effect is greater than the contribution from dilation.

For tests db350, dbs430 and db550 the behaviour of the samples is ductile, the difference between the position of the second yield and the max q/p' ratio has increased substantially and the position of the maximum rate of dilation is close to the latter. This would suggest that at this high stress level the bonds yield at low stresses and so they contribute less to the samples' peak shear strength which is now mainly due to frictional resistance.

The results for test db250 lie between the test results from the last two groups. The most significant effect in passing from one group to the other is the decrease

of the bond strength at failure, as the confining stress increases and hence a lower contribution to the samples' maximum shear strength. Test db250 carried out at this intermediate stress level, possibly represents the case where the bonds still contribute some strength to the peak shear strength of a sample. After that the peak shear strength is probably mainly due to frictional resistance.

In fig. 4.16a the bounding surface and the two yield surfaces for the bonded samples are plotted in stress space. At low confining pressures the bounding surface coincides with the second yield surface. At higher stresses the second yield surface diverts towards the isotropic axis and the difference in the position between the two increases with the increase of confining pressure. The first yield surface is below the other two surfaces and at stresses higher than 400kPa curves down and meets the isotropic axis. The second yield surface is expected to have similar behaviour at very high stresses.

The final yield points for the strain controlled tests are defined as the maximum points of curvature on the deviatoric stress versus axial strain curves. These points define the final yield surface which is plotted in the stress space in fig. 4.16b. The bounding surface and the first and second yield surfaces are also included. As was expected the final yield surface almost coincides with the bounding surface for $p'<600kPa$. There is also a large difference between the position of the final and the second yield surface.

4.2.6 Stiffness measurements at 0.1%-2% of strain

The behaviour of the bonded soil under shearing is studied in respect of tangential stiffness at different percentages of strain and at a range of mean effective stress up to 1000kPa. At the beginning stiffness is plotted versus p', at particular strain percentages in fig. 4.17a, b, c. The name for each test is also included. In fig. 4.18

stiffness is plotted versus p' for all the strain contours presented in the previous figures, in order to study the loss in E_{tan} with the increase of axial strain.

In fig. 4.17a stiffness is plotted versus p' at 0.1% and 0.2% of strain for all the tests. The values of stiffness at 0.1% of strain increase rapidly for tests db5-100 while the slope of the curve changes for tests db200-550, sheared at higher stresses. The loss in stiffness from the 0.1% to 0.2% strain contour is more pronounced at mean effective stresses higher than 50kPa. The 0.2% contour increases up to p'=110kPa for tests db5-150 while the slope of the curve changes for the rest of the samples sheared at higher stresses.

In fig. 4.17b stiffness is plotted for 0.3% and 0.5% of strain. There is a small loss in stiffness from 0.3% to 0.5% of strain for tests db5-150, which becomes more substantial for tests db200-550 carried out at higher stresses. There is a rapid increase of stiffness with the increase of p' for the two curves till 200kPa, followed by a change in the slope at higher stresses.

In fig. 4.17c stiffness is plotted at 1% and 2% of strain. There is a large loss of the remaining stiffness for all the tests after 1% of strain and that coincides with the initiation of the second yield of the bonds that occurred at a similar strain level. The loss in E_{tan} from the one contour to the other decreased progressively, as the bonds breakdown progressively with the increase of stress and strain. A rapid increase in stiffness occurred at 1% strain for tests db5-150 up to 200kPa, followed by a change on the slope of the curve for tests db200-250 at higher stresses. The values of stiffness at higher stresses for tests db350-550, tend to level off parallel to the p' axis. Tests db11-100 carried out at low confining pressures have lost almost all of their stiffness at 2% of strain and only samples tested at higher stresses, tests db150-550, have stiffness values larger than 10MPa. Test db5 has no stiffness at 2% of strain.

A rapid increase in stiffness with the increase of p' occurs for all the contours up to 1% strain, referring to fig. 4.18, and up to a certain stress level followed by a change of the slope of the curves at higher stresses. There is a larger loss in stiffness from 0.1% to 0.2% of strain than any other change till 1% of strain. This coincides with the first yield of the bonds that occurred at this strain level (0.1%-0.2%). The loss of stiffness from one contour to the other up to 1% of strain is quite small at low stresses and it becomes more pronounced after p'>150kPa. The curves at ε_a>0.3% tend to level off for p'>500kPa, but this is more apparent after 1% of strain. All the contours are consistent for both the stress and the strain controlled tests.

It is interesting to see that the loss in stiffness from 0.5% to 1% of strain is quite small, in difference with the loss in E_{tan} from 0.1% to 0.5% of strain. Furthermore in another 1% of strain the soil lost almost all of the remaining stiffness, which is slightly less than the decrease of E_{tan} from 0.1% to 1% of strain.

In fig. 4.19a the 0.1%-0.5% strain contours are plotted in the stress space. In order to avoid complicating this plot the names of the tests are not included. The tests can be easily identified from the stress paths that are previously plotted in the stress space. An example is given for test db100.

There is an immediate increase in q with the increase of p' for tests db5 and db11 and for all the strain contours. For p'>50kPa the slope of the curves changes in the stress space and after test db350 the contours level off and turn parallel to the isotropic axis. The 1% and 2% strain contours and the bounding surface for the bonded soils are plotted in fig. 4.19b. The 1% contour lies between the 0.5% contour and the bounding surface and after p'>500kPa turns towards the isotropic axis. The 2% contour coincides with the bounding surface at low stress levels up to p'=300kPa and at higher stresses occurs at lower stresses but still close to it. All the strain contours are consistent for both the stress and the strain controlled tests.

It can be seen from the previous two figures that the direction of the strain contours change with the increase of strain percentage. The contours at low axial strains up to 0.5%, are positioned closer to the isotropic axis. However after 0.5% of strain they show a tendency for a change in direction from the p' axis towards to the bounding surface. This is more pronounced after the second yield at about 1% of strain, as the contours change in direction from the isotropic axis to mirror the shape of the bounding surface more closely.

4.3 DRAINED TRIAXIAL TESTS ON DESTRUCTURED SAMPLES

The behaviour of the destructured soil under drained shearing is presented in this section. The bounding surface for this soil is presented in the stress space. Stiffness values at different percentages of strain are determined and strain contours are presented in the stress space, allowing further comparisons to be made with the bonded soil.

4.3.1 Testing details

Seven drained triaxial tests were carried out on destructured samples at a range of confining pressures. The samples were formed with the same void ratio (0.6) as the bonded samples. They were sheared at a constant rate of strain of 1.5%/hr, the same as that used for the previous tests on the bonded samples. The main aim was to investigate the behaviour of the destructured soil, formed at the same void ratio as the bonded soil, and to compare the behaviour of the two in respect of strain development, stiffness, and the max stress ratios sustained in the stress space. The name of test, the void ratio of the samples and the confining pressure at which consolidation took place before shearing are shown in table 4.2. Test ddes400 for example, indicates a drained test on a destructured sample consolidated at 400kPa.

4.3.2 Stress-strain behaviour under shearing

The stress strain curves for the seven tests are plotted in fig 4.20. Tests ddes11, ddes35 and ddes100 that were carried out at low confining pressures reached a

peak value of q at axial strains higher than 5%. With a further increase in strain there is only a slight decrease in stress. The rest of the tests ddes200-500 that were carried out at higher confining pressures, show a clear peak in q and an accompanying drop with a further increase of strain. Shear surfaces were formed in the samples during the later tests because of non uniformities of strain and therefore q still decreased at the end of shearing and a critical state was not reached.

In fig. 4.21 the volumetric strain with axial strain curves are presented. The samples contracted initially and then strongly dilated. The amount of compression as well as the percentage of strain at which the behaviour of the samples turned from contraction to dilation increased, with the increase of confining pressure. Tests ddes100, ddes200 and ddes500 are very close to representing a critical state at the end of shearing, at least in respect of the volume change. However only test ddes100 could be said to achieve it as q is also constant at the end of the test, while for the other two tests q is still decreasing.

The stress strain curves for all the tests are plotted again in fig. 4.22 and the maximum q/p' ratios and the points at which the maximum rate of dilation occurred are marked on each curve. The two points are very close and almost coincide for some of the tests. This is in agreement with Atkinson and Bransby's idea for triaxial shearing of dense sands (Atkinson and Bransby 1978), that higher values of max q/p' ratios are associated with higher values of rate of dilation and these occur at the same strain percentage. Therefore the behaviour of the destructured soil under shearing is similar to the behaviour expected of a dense sand.

4.3.3 Bounding surface for the destructured soil

The maximum q/p' ratios and the stress paths for the drained tests are plotted in fig. 4.23 and 4.24 respectively. The maximum stress ratio values define a line with equivalent values of c'=29kPa and φ'=33°, (q/p'=1.32). The behaviour of these

samples under shearing in respect of the ultimate q/p' ratios is similar to the behaviour of a dense sand. The Roscoe surface is not relevant for these samples and a state boundary surface similar to the Hvorslev surface exists as a limit in the stress space. Higher values of q/p' are associated with higher densities and lower confining pressures. Samples sheared at low confining pressures achieve higher max q/p' ratios than those defined by the critical state line, because of dilation.

The behaviour of a sample consolidated at a very high stress will be similar to that of a loose sand, with an ultimate point on the critical state line. However tests were not carried out at very high confining pressures, because of stress limitations of the system. Therefore the ultimate points from the previous tests do not define the critical state line, as the high rates of dilation that occurred during shearing result in the higher max q/p' ratios. However these stress ratios are essential for the study of the destructured soil at the same void ratio as the bonded material and for comparisons to be made between the two soils.

The phase transformation line for the destructured samples is also plotted in fig. 4.23 which goes through the origin with a slope of q/p'=1.24. This line is almost parallel to the bounding surface that lies above it.

4.3.4 Stiffness measurements at different percentage of strain

The tangential stiffness has been calculated for all tests. In fig. 4.25 stiffness is plotted against mean effective stress for 0.1% to 2% of strain. There is an almost linear relationship between stiffness and p'. E_{tan} increases with the increase of p' for all the strain contours. Tests ddes11 and ddes35 carried out at low confining stresses show low values of stiffness, less than 10MPa at 0.1% of strain. The values of stiffness increase to higher levels for tests ddes100-500.

There is a drop in stiffness with the increase of strain percentage and this loss is more apparent for p'>100kPa. The loss in E_{tan} from one contour to the other is almost constant, with higher values at higher stresses and up to 0.5% of strain. The samples reached the maximum shear strength at strains >5%, and at that point all of the remaining stiffness is lost.

The 0.1%-2% strain contours and the bounding surface for the destructured samples are plotted in fig. 4.26. The test results for a specific strain percentage define straight lines which start from values higher than the origin. These higher values of q are a direct effect of the samples' density. At low strains, where the behaviour of the samples is stiffer, the 0.1%-0.2% contours are almost parallel to the isotropic axis. The contours gradually turn closer to the bounding surface with the increase of axial strain.

4.4 COMPARISONS BETWEEN THE RESULTS OF THE BONDED AND THE DESTRUCTURED SOIL

Comparisons between the behaviour of the bonded and the destructured samples are presented in this section. The behaviour of the destructured soil in respect of the max q/p' ratio and the development of stiffness, consists of a basic framework for the behaviour of this material in the unbonded state. All the differences that the bonded structure applies to the samples' behaviour are studied by referring to the framework for the destructured soil. Therefore the influence of the bond strength on the max q/p' ratio and on the stiffness of the bonded samples, sheared at a range of confining pressures, is clarified.

4.4.1 Comparisons between the maximum q/p' ratios of the bonded and the destructured soil

The development of the q/p' ratio during shearing is studied for the two soils at low, intermediate and very high p_0' stresses. In fig. 4.27a and b, the q/p' ratio is

plotted versus axial strain for bonded and destructured samples sheared at $p_0'=11kPa$ and $p_0'=200kPa$ respectively. The results plotted in fig. 4.27c are for a bonded sample that was sheared at 550kPa and for a destructured one that was sheared at 500kPa. The point at which second yield of the bond occurred for the bonded samples is also marked on each curve.

It can be seen in fig. 4.27a that the bonded sample db11, that was sheared at a low confining pressure has a higher maximum stress ratio than that of the destructured sample and this is developed at a lower percentage of strain. The position of the second yield of the bonds is very close to the maximum q/p' ratio, and thus the bonded structure results in a substantially higher stress ratio for this sample than that of the destructured material. The two tests end at almost the same stress ratio.

The max q/p' ratio for the bonded sample (db200) plotted in fig. 4.27b has decreased substantially in comparison with that of db11 and is getting closer to that of ddes200. However the position of the max stress ratio for the latter, occurs at a higher axial strain than that of the bonded sample. Second yield for test db200 occurs at a lower strains than the max q/p' ratio of the sample, but the bonds still contribute to a higher stress ratio. Shear surfaces were initiated in both tests with the increase of strain and so the q/p' ratios are decreasing at the end of shearing.

The max q/p' ratio for test db550 plotted in fig. 4.27c is very close to that of the destructured material. Although the two values are almost the same, the development of the max q/p' for the bonded sample is at a lower strain percentage than that of the destructured sample. Second yield of the bonds occurs much earlier than the max q/p' ratio and thus the bonded structure of the sample at failure is destroyed at this stress level and does not contribute to a higher stress ratio than that of the destructured material.

The behaviour of the bonded soil in respect of max q/p' ratio is different at the three stress levels. At the first level when shearing took place at a low stress, the max q/p' ratio of the sample depends totally on the bonded structure and thus it has a higher value than that of the destructured soil. At the second level when shearing took place at higher stresses, second yield of the bonds occurs earlier and thus the max q/p' ratio is decreasing towards the value of the destructured soil. At the third level where shearing took place at very high stresses, the bonded structure does not contribute to the max stress ratio which is now equal to that of the destructured soil. The soil's behaviour in respect of the different stress levels will be studied for the rest of the tests in the next paragraph.

4.4.2 Bounding surfaces for the two soils

The bounding surfaces for the bonded and the destructured soil are plotted in the stress space in fig. 4.28. The bounding surface for the bonded samples shows some curvature at low stresses and exists at higher stresses than that of the destructured samples for a specific range of stresses. The effect of bonding allows the samples to sustain higher stress ratios than the destructured samples at p' up to 800kPa. For p'>800kPa the two lines coincide in the stress space. Similar test results for structured soils were presented by Leroueil, Magnan and Tavenas (1990).

At low stresses for p'<100kPa, the bounding surface for the destructured soil is close to that of the bonded, because of the development of the high rates of dilation of the destructured samples during shearing at this stress level. Tests db35-250 sheared at higher stresses sustained higher max q/p' ratios compared to those of the destructured soil, sheared at the same range of stresses. The bounding surface for the bonded soil turns towards to that of the destructured soil after test db250.

The phase transformation lines for the two soils are plotted in fig. 4.29. The line for the bonded soil shows some curvature at low stresses and exists at higher

stresses in the stress space than that of the destructured soil. However for p'>600kPa it turns towards the latter, at a similar stress level to that at which the bounding surface of the bonded soil turns towards to that of the destructured material.

The two yield surfaces, the bounding surface for the bonded soil and the bounding surface for the destructured soil are plotted in fig. 4.30. The bounding surface of the destructured soil is the limit in the stress space for this material, at a void ratio of 0.6. The higher stress ratios developed by the bonded samples are due to their bonded structure. The effect of bonding in respect of the max q/p' ratios values is more pronounced for tests db5-35 at p'<100kPa (fig. 4.27), at a stress level where the second yield surface almost coincides with the bounding surface (fig. 4.30).

Although second yield for tests db100-250 (p'>200kPa) occurs below the maximum q/p' ratio, the bonded samples still sustain higher max stress ratios than that of the destructured samples. Only at very high stresses for p'>700kPa, where the second yield for tests db350-550 occurs at lower deviatoric stresses, does the limiting stress ratios of the bonded samples approach that of the destructured.

However it is very interesting to notice that the shape of the first, second yield and the bounding surface are in close relationship in the stress space. Referring to fig. 4.30 the first yield surface increases in shape up to test db35. The second yield surface and the bounding surface for these tests almost coincides in the stress space. Till that point the max q/p' ratio of the samples is at its highest level. For p'>100kPa the first yield surface reaches its maximum value and turns parallel to the isotropic axis up to 400kPa, for test db350. The second yield surface at this stress level, diverts from the bounding surface and turns towards the isotropic axis. However because the bonds are breaking down progressively, they are still

contributing to a higher q/p' ratio for the bonded samples than that of the destructured material at the same stress level.

The first yield surface decreases in shape after test db350 and turns down to the isotropic axis. At this stress level the second yield surface reaches possibly its highest q value in the stress space (this will be further investigated in the next chapter) and the bounding surface turns down to the bounding surface of the destructured samples. The bonds at this stress level are destroyed at lower stresses and do not contribute to the limiting stress ratios of the samples, which now coincide with those of the destructured soil.

4.4.3 Comparison between the tangential stiffness measurements for the two soils

In fig. 4.31 the tangential stiffness for the bonded and the destructured soil is plotted versus p' for 0.1%, 0.2%, 1% and 2% of strain. These curves only are plotted, in order to present a clearer picture. There is a large difference between the stiffness values of the two soils for strains up to 1%. The higher values of stiffness for the bonded soil are due to their bonded structure. The largest difference between the two is at 0.1% of strain, when yield of the bonds has not yet occurred. Stiffness progressively decreases with the increase of strain percentage and at 2% of strain the two soils have almost the same values for the whole range of the p'.

At 0.1% of strain, stiffness for the bonded soil increases rapidly up to p'=100kPa. At this point the difference compared to the destructured soil is at its maximum level. The slope of the curve changes at a lower level at higher p' and the difference between the two decreases and reaches a more or less constant value. Stiffness at 0.2% of strain increases rapidly for the bonded soil up to p'=150kPa, followed by a change in direction towards the isotropic axis and a decrease in the difference with the corresponding contour for the destructured soil. The values for

the bonded soil decrease after 1% of strain and at 2% the two soils show similar levels of stiffness. Second yield of the bonded soil occurred at about 1% of strain and so the major destruction of the bonds led to a soil structure very close to that of the destructured soil, at the same level of strain.

The development of the initial tangential stiffness $(E_{0.1\%})$ presented in fig. 4.31 shows some stress level dependency. Referring to fig. 4.30, the bonds control the behaviour of the samples up to $p'=120kPa$, with high maximum q/p' ratios sustained at this stress level. However the initial stiffness at 0.1% of strain, increases rapidly with the increase of p' for $p'<120kPa$. When shearing took place at higher stresses where the bonds partially control the behaviour of the samples, with lower q/p' ratios sustained, the initial stiffness is directly affected with an immediate decrease in the slope of the curve and a change in direction towards the isotropic axis. The development of E_{tan} for $p'>600kPa$ will be further investigated in the next chapter.

In fig. 4.32 the 0.1%, 0.2%, 0.5%, 1% and 2% strain contours are plotted for the bonded and the destructured samples in the stress space. The strain contours defined for the two soils, are curves for the bonded soil and straight lines for the destructured soil. The strain contours for the bonded soil occur at higher stresses in the stress space, in comparison with those of the destructured. The difference between the contours increases with the increase of strain percentage and has the largest value at 2% of strain.

The 0.1%-0.5% strain contours for the bonded soil level off parallel to the isotropic axis for $p'>500kPa$ and at $p'\cong600kPa$ they meet the contours of the destructured soil. The behaviour of the 1% strain contour of the bonded soil is similar to the previous ones and would probably meet that of the destructured soil at higher stresses. After the second yield of the bonds that takes place at 1% of strain, the strain contours of the bonded soil turns towards the bounding surface and the 2%

strain contour lies very close to that (fig. 4.19b). The strain contours for the destructured samples turn also towards their bounding surface with the increase of strain percentage. The difference between the two contours has its highest value at 2% of strain, but it is quite likely that the contours meet at higher stresses. Undrained shear tests were carried out at this stress level and thus a clarified picture will be presented in the next chapter.

The 2% strain contour for the bonded soil occurs at a higher stress level than that of the destructured soil, but referring to fig. 4.31 they both have the same tangential stiffness throughout the whole range of stresses. Thus even though the structure of the bonded soil is quite destroyed and is similar to that of the destructured material at ε_a=2%, the development of strain in respect of the stress paths is still affected by the initial structure of the soil.

The development of strain in respect of the stress paths for the bonded samples occurs always at higher stresses than that of the destructured. The behaviour of the samples is clearly influenced by their bonded structure. For p'<400kPa where the bonds mainly control the soil's behaviour, the samples achieve a higher stress level than that of the destructured soil at the same strain level. However for p'>500kPa where the soil's behaviour is almost frictional, the development of strains gradually becomes closer to that of the destructured soil with the increase of p'.

4.4.4 Final remarks

In this chapter the behaviour of the bonded and destructured soil was examined under drained shear in triaxial compression. The bonded soil sustained higher max q/p' ratios than the destructured soil for a specific range of p', due to its bonded structure (fig. 4.28). However the bond strength of the soil at failure decreased to lower levels as the bonds yielded with the increase of stress and strain. Yield was

associated with a loss in tangential stiffness (fig. 4.11-4.13b) and two yield surfaces were defined in the stress space (fig. 4.16a-4.30).

The decrease of the bond strength of the soil had an immediate effect on the maximum q/p' ratios that the soil sustained in the stress space. Thus, at low p' the soil's behaviour was entirely controlled by its bonded structure and high max q/p' ratios were reached. At intermediate stresses the bonds yielded at low stresses but still contribute to higher stress ratios. At very high stresses the bonds are almost destroyed by the time failure is reached and the soil's behaviour is similar to that of the destructured soil (fig. 4.27a, b, c). The decrease of the max q/p' ratio with the increase of p_0' is also reflected to the position of the bounding surface plotted in the stress space, which turned closer to that of the destructured soil with the increase of p' (fig. 4.30).

The bonded soil also presented higher tangential stiffness values than that of the destructured soil (fig. 4.31) due to its bonded structure. However after the initiation of the second major yield of the bonds at $\varepsilon_a \cong 1\%$ the structure of the bonded soil is gradually destroyed and thus at 2% of axial strain the two soils presented similar values of E_{tan}.

The development of axial strain for the bonded soil is also influenced by its bonded structure and the strain contours are positioned at higher stresses in the stress space than those developed for the destructured soil (fig. 4.32).

Strain Controlled Tests

Test	Initial void ratio e_0	Consolidation pressure (kPa)
db5	0.598	5
db11	0.597	11
db35	0.598	35
db100	0.602	100
db150	0.596	150
db200	0.600	200
db250	0.598	250
db350	0.603	350
db550	0.600	550

Stress Controlled Tests

Test	Initial void ratio	Consolidation pressure
dbs35	0.601	35
dbs430	0.602	430

Table 4.1 Details for the drained triaxial tests on bonded samples

Test	Initial void ratio e_0	Consolidation pressure (kPa)
ddes11	0.596	11
ddes35	0.600	35
ddes100	0.603	100
ddes200	0.600	200
ddes320	0.597	320
ddes350	0.600	350
ddes500	0.596	500

Table 4.2 Details for the drained triaxial tests on destructured samples
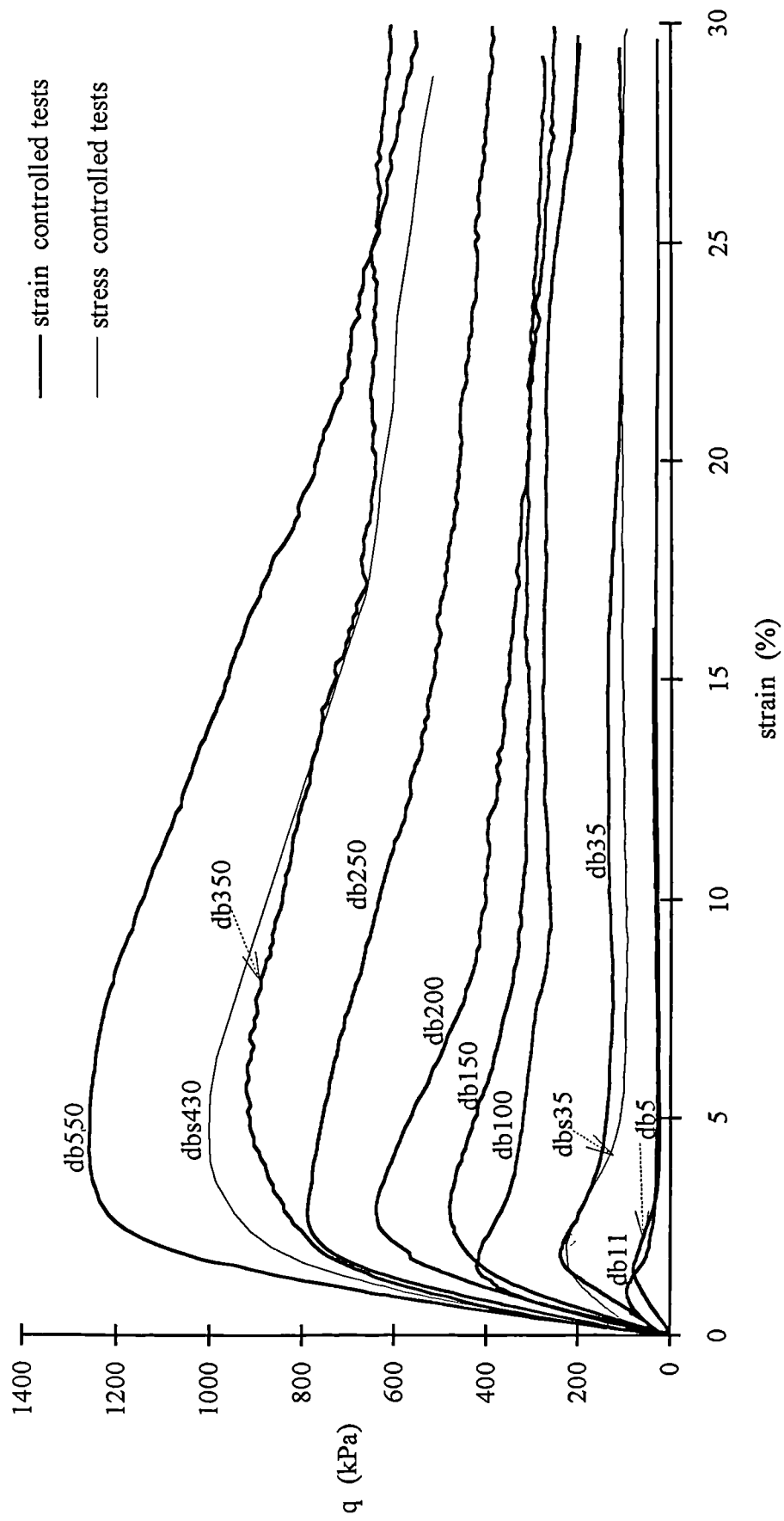
Fig. 4.1 Stress-strain curves for the triaxial drained tests on the bonded samples

74
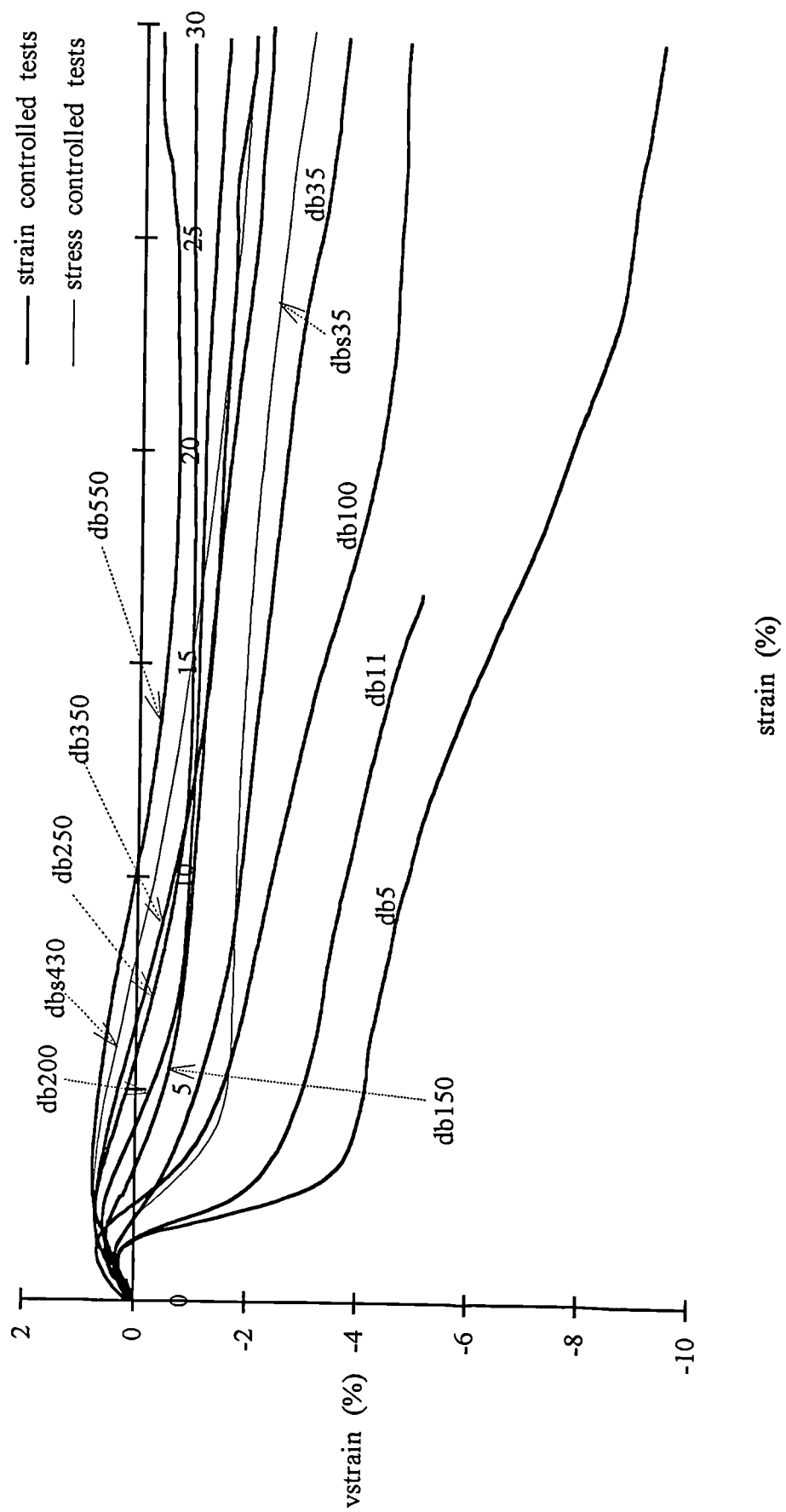
Fig. 4.2 Volumetric strain versus axial strain curves for the triaxial drained tests on the bonded soil

75
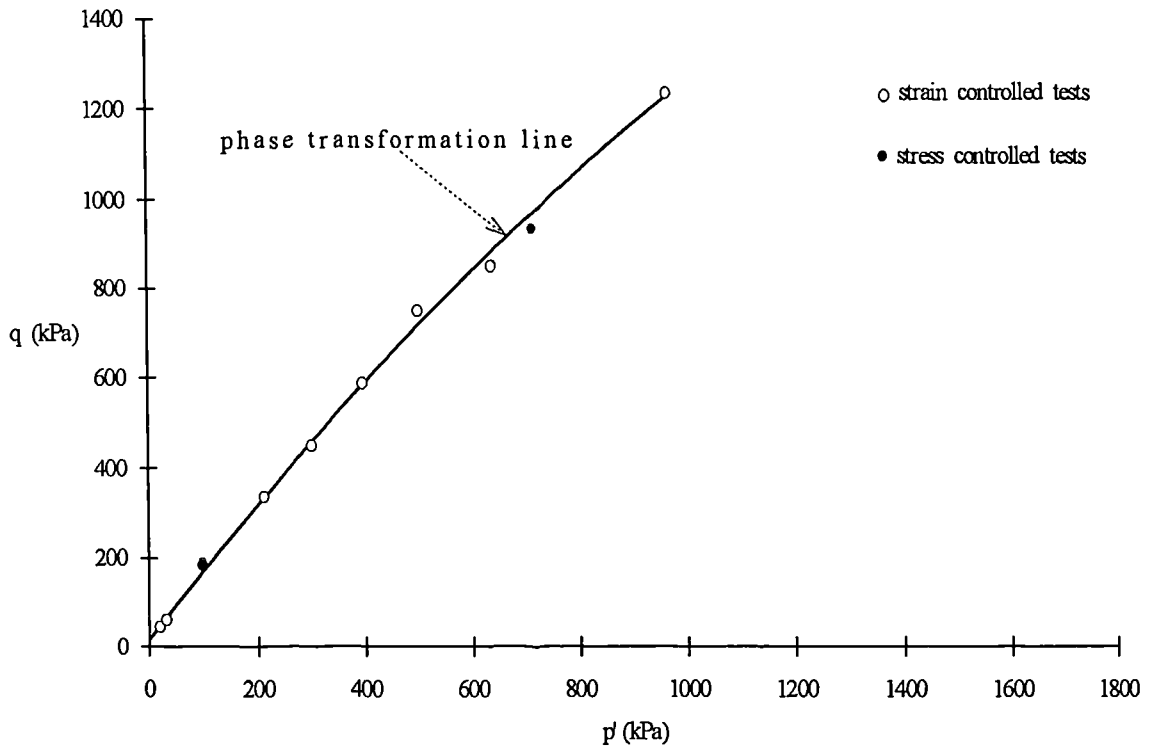
Fig. 4.3 Phase transformation line for the drained tests on bonded samples
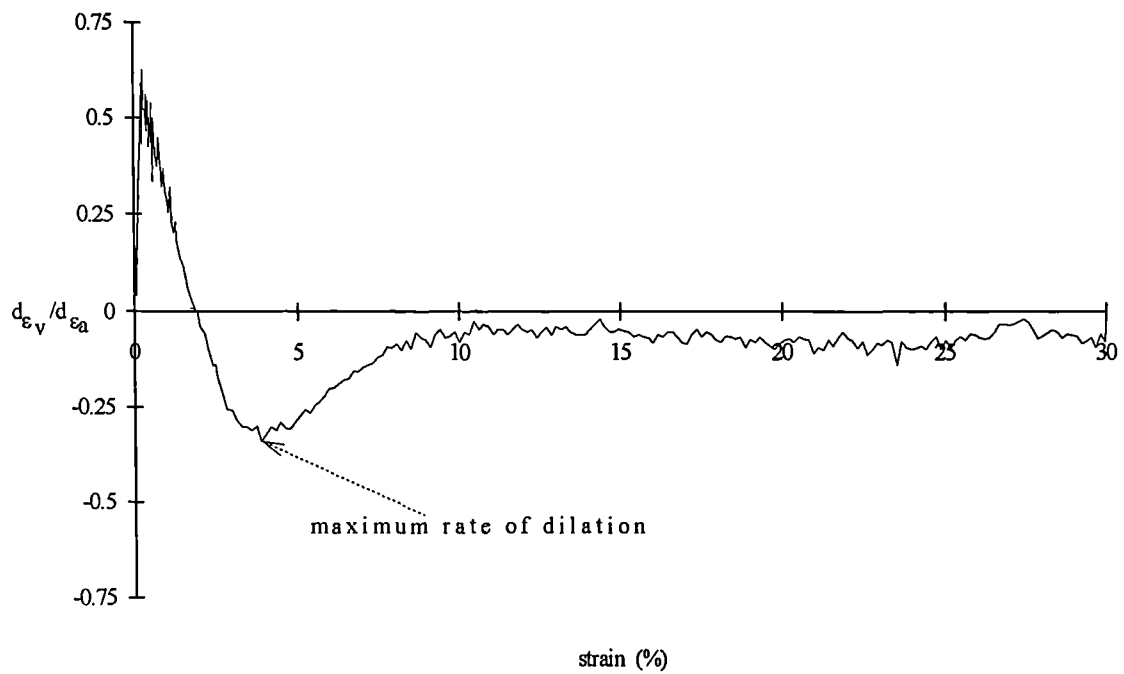
Fig. 4.4 Definition of the maximum rate of dilation for test db35

76
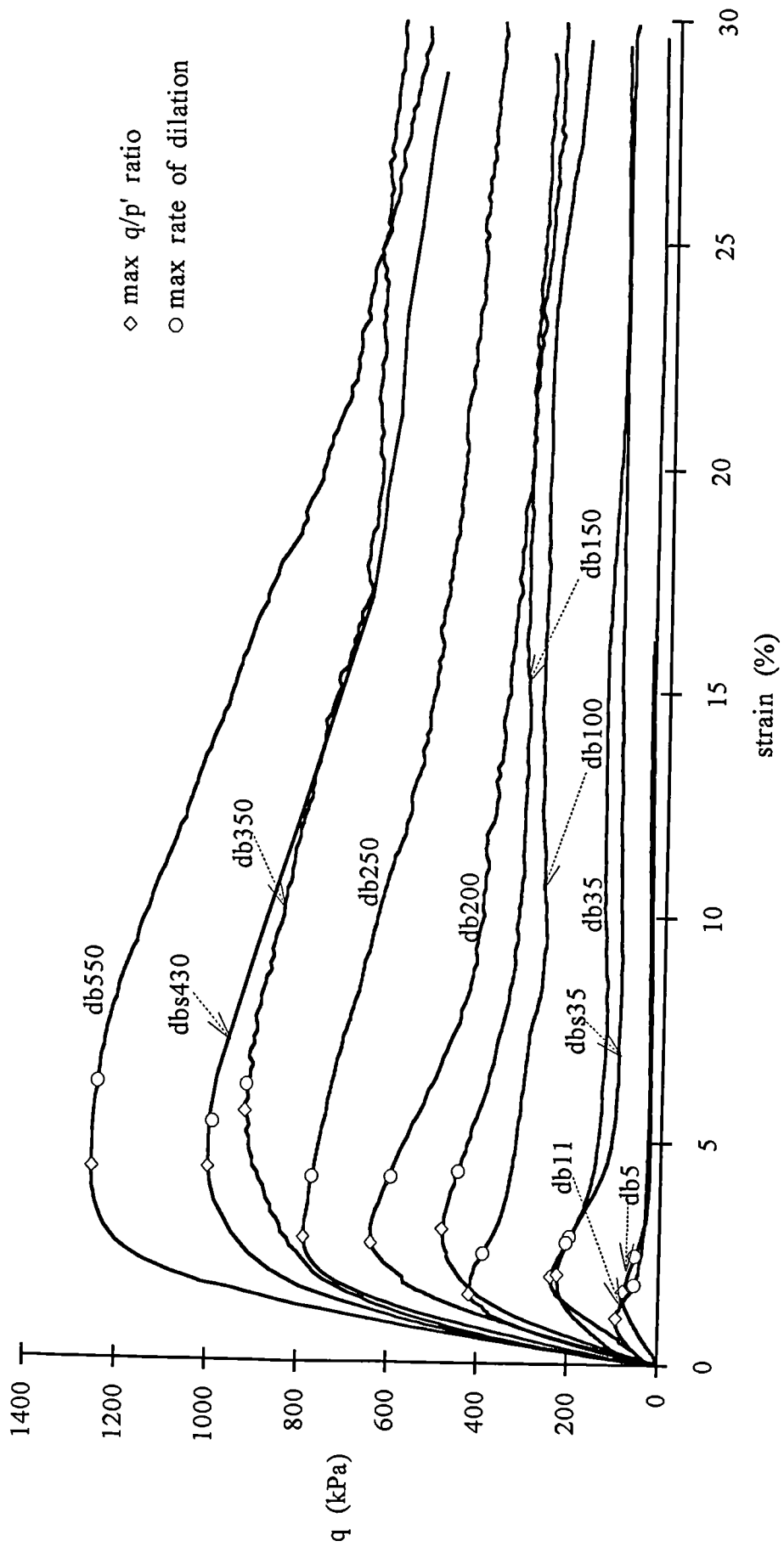
Fig. 4.5a Maximum values for q/p' ratio and maximum rate of dilation for all the tests

77
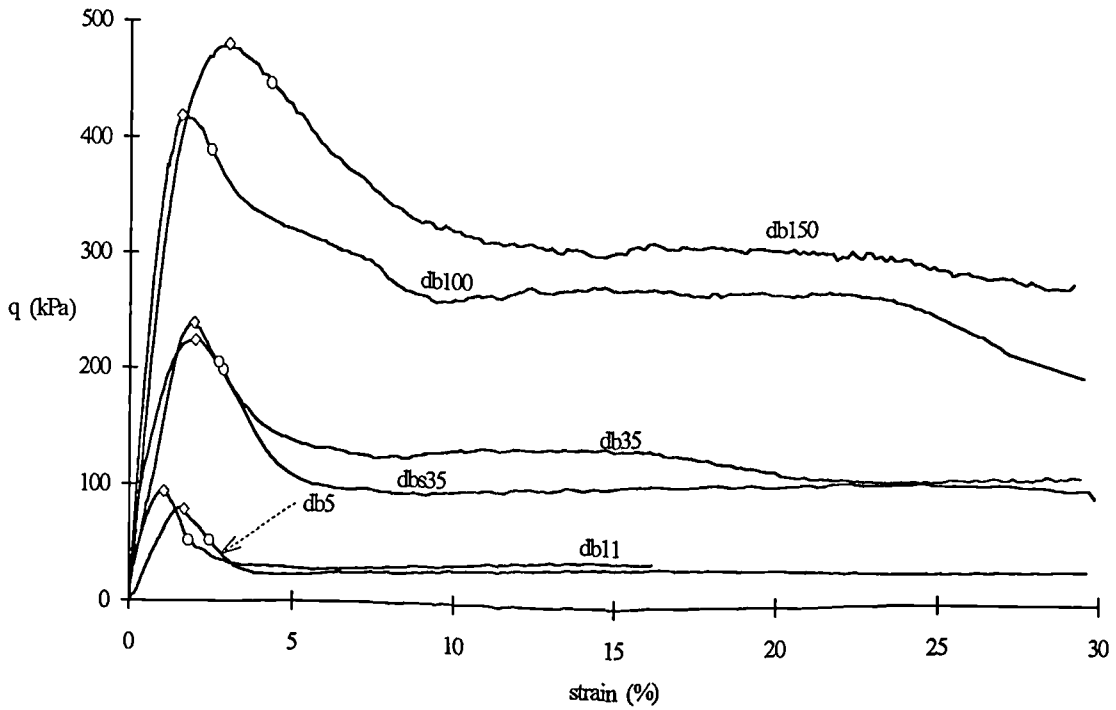
Fig. 4.5b   Maximum q/p' ratio and maximum rate of dilation for tests db5-150
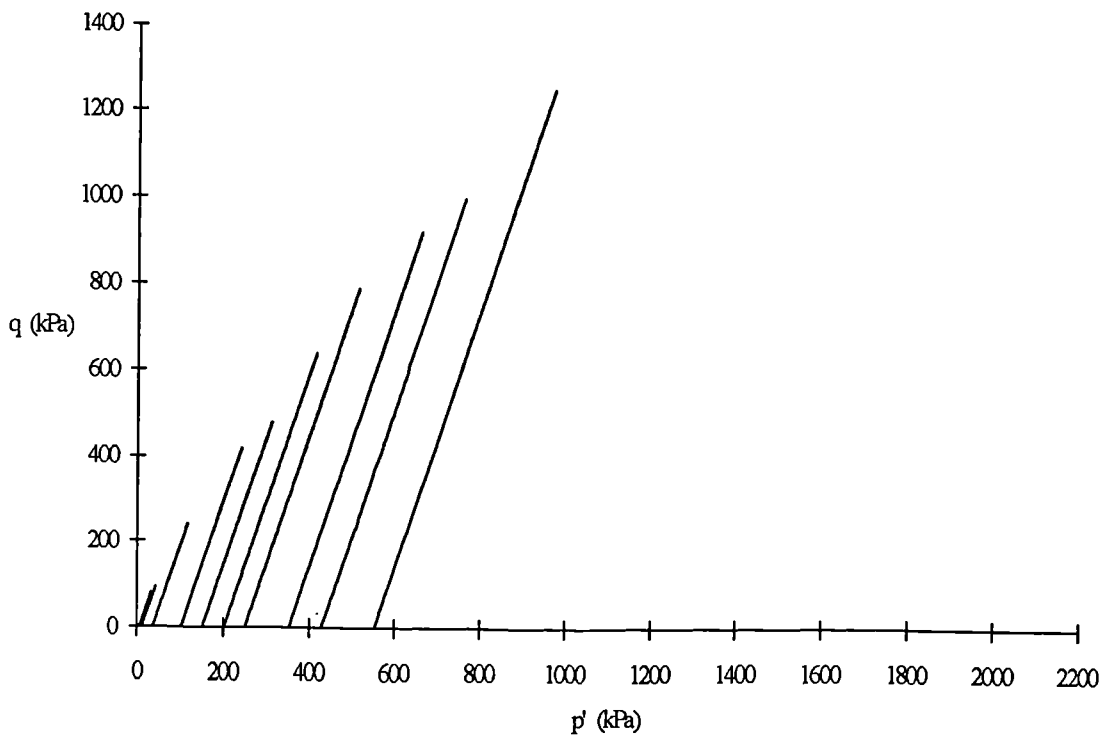
Fig. 4.6   Effective stress paths for the triaxial drained tests

on the bonded samples
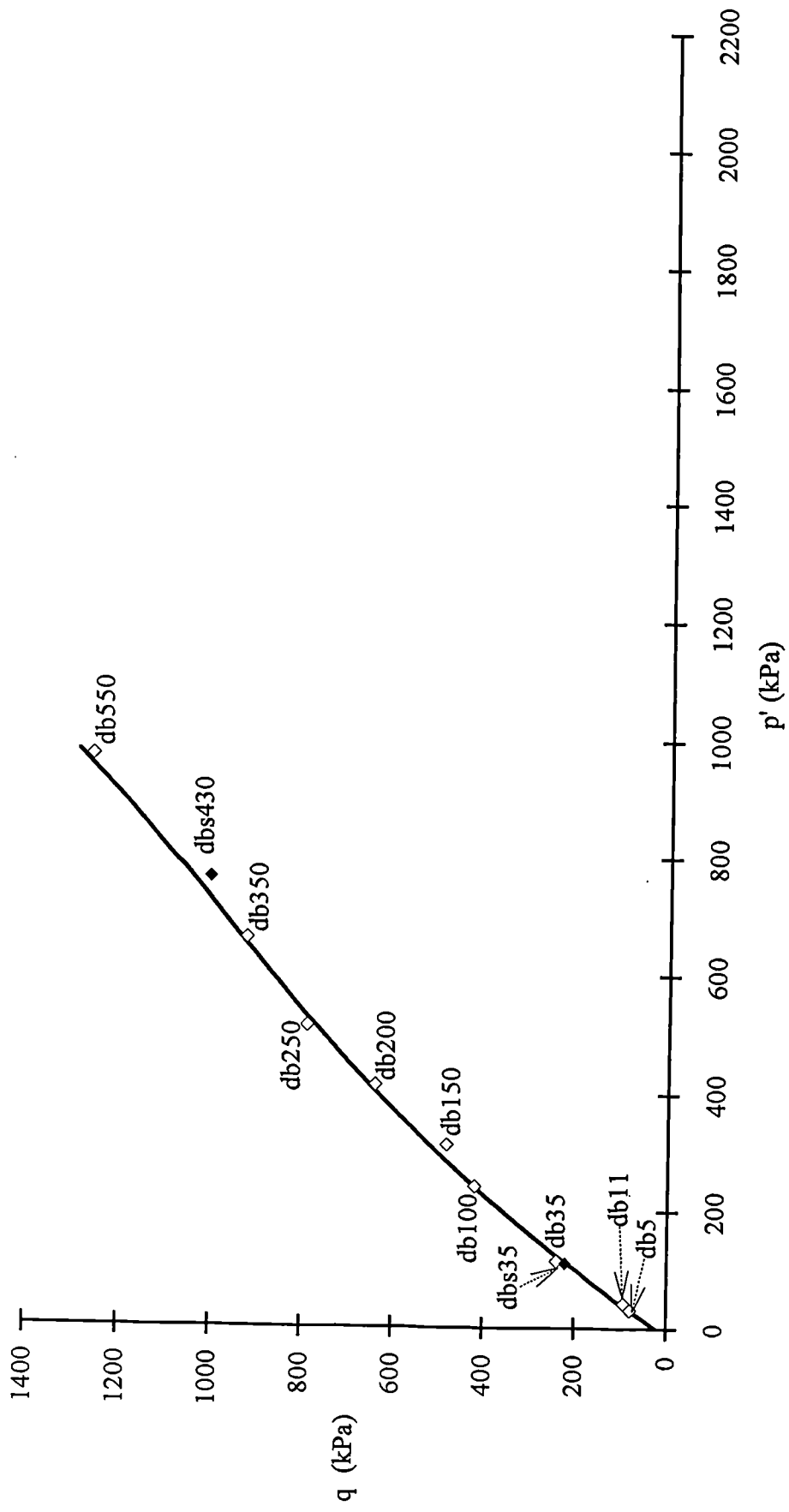
Fig. 4.7 Bounding surface for the bonded samples plotted in the stress space
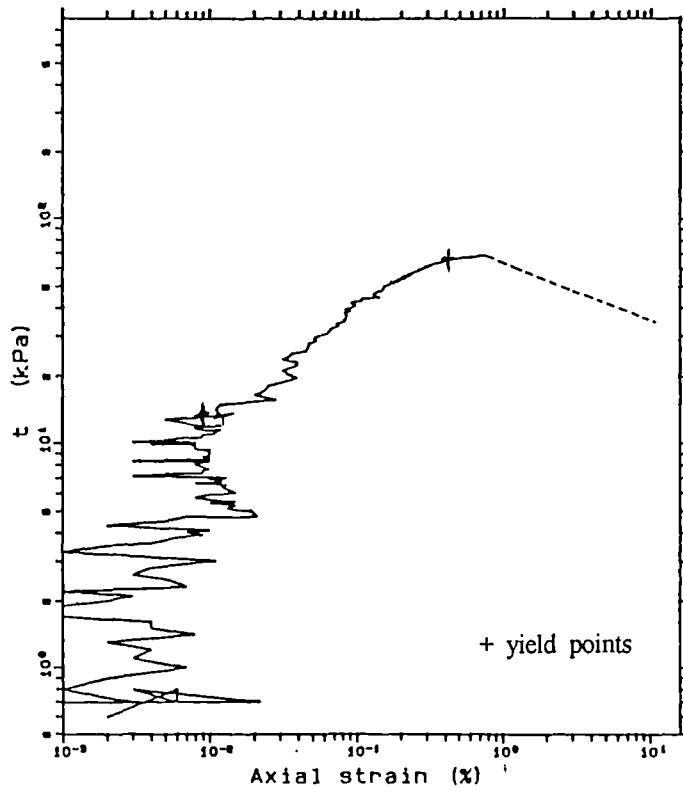
Fig. 4.8 Definition of the two yields (after Bressani 1990)
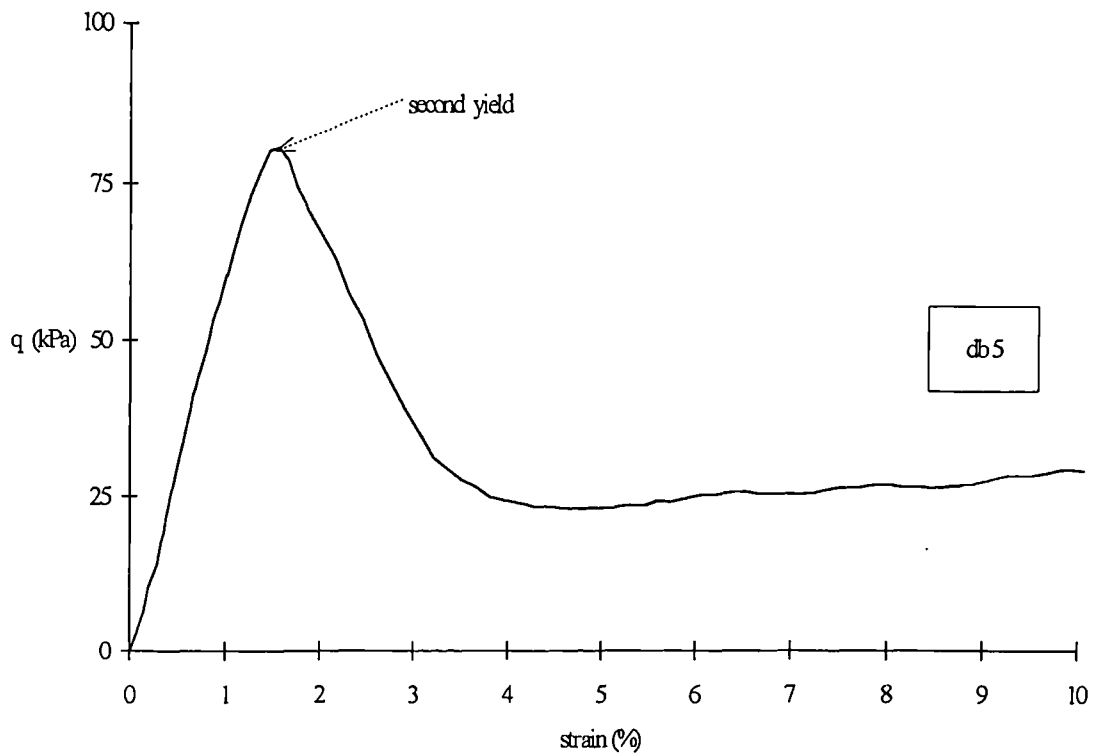
Fig. 4.9a Definition of the second yield for test db5 from the natural
scale graph
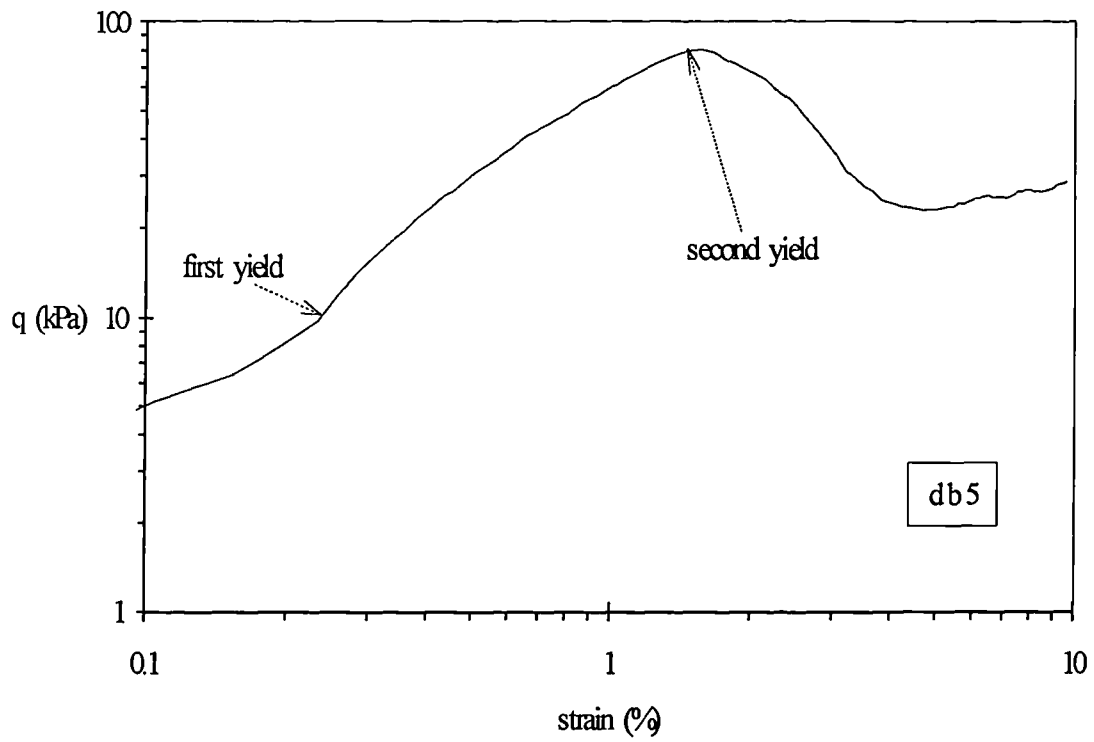
Fig. 4.9b First and second yield for test db5 from the log-log plot
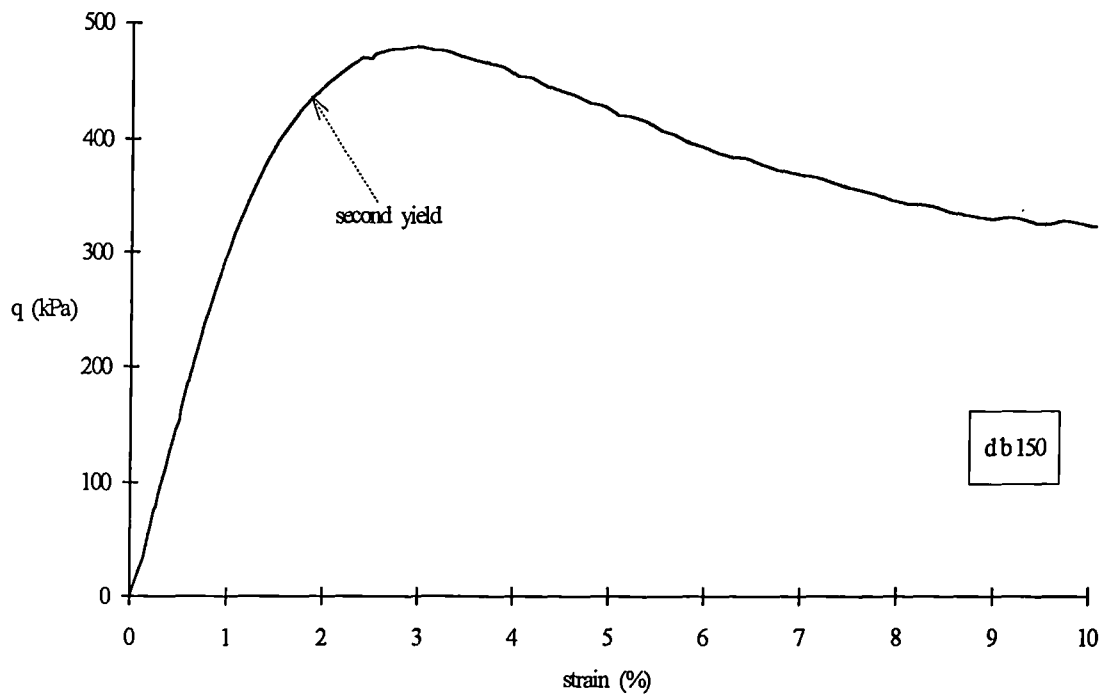
Fig. 4.10a Second yield for test db150 from the natural scale plot
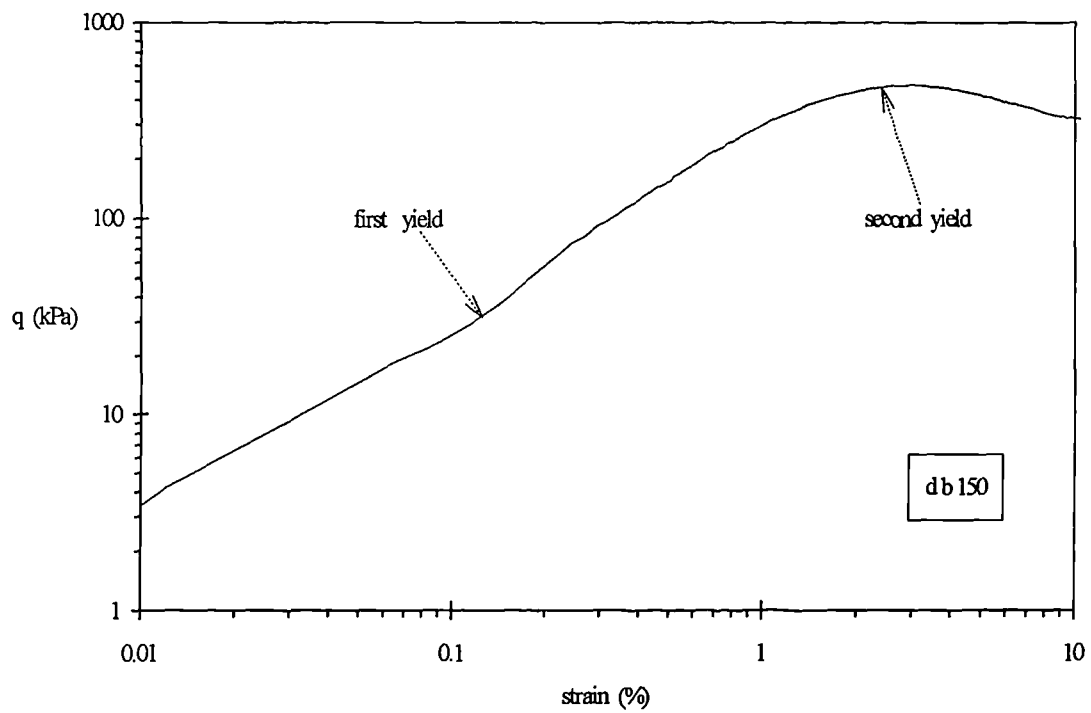
Fig. 4.10b First and second yield for test db150 from the log-log plot
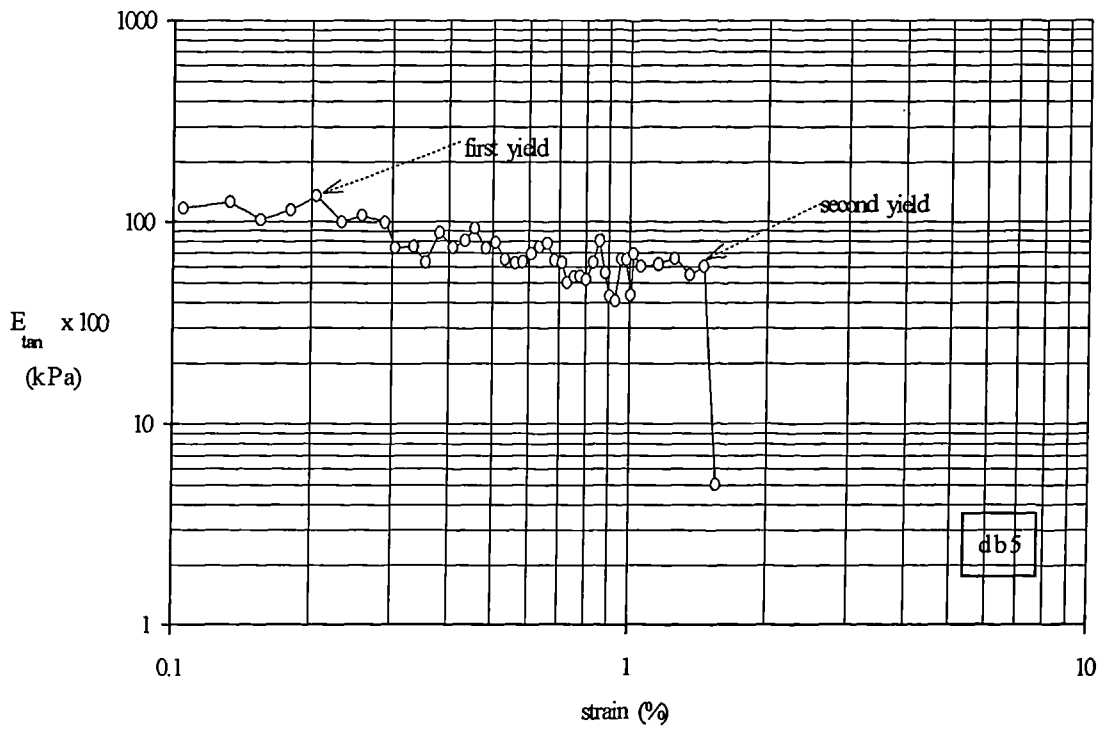
Fig. 4.11 First and second yield for db5 defined from the stiffness graph
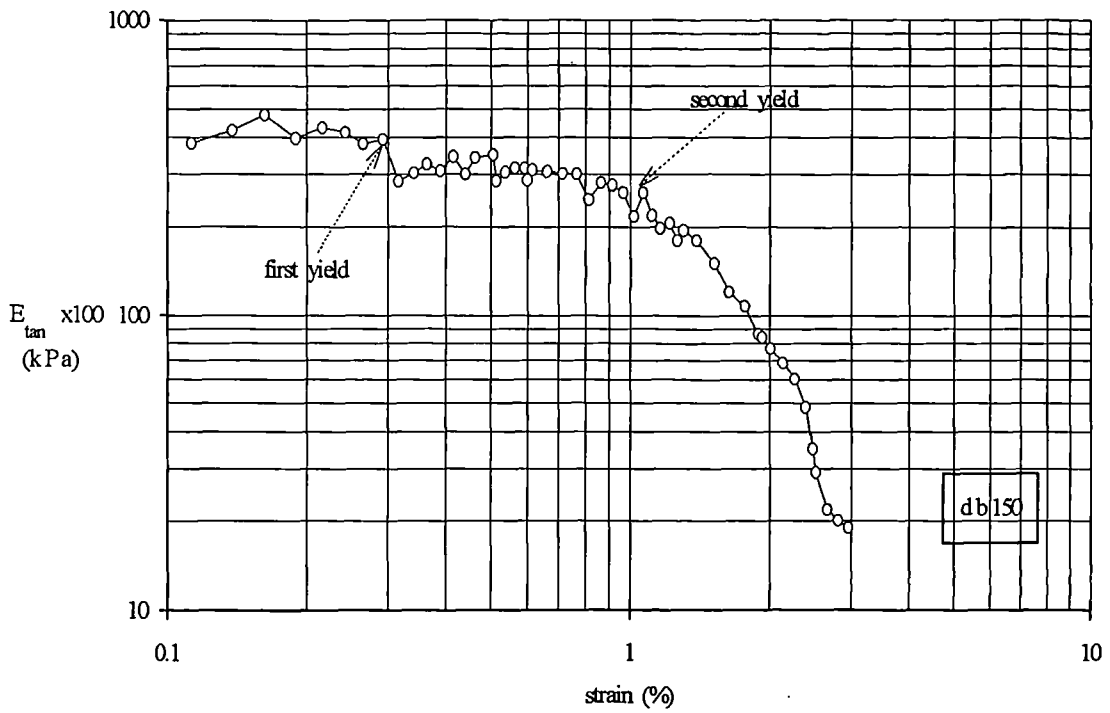
Fig. 4.12 First and second yield for test db150
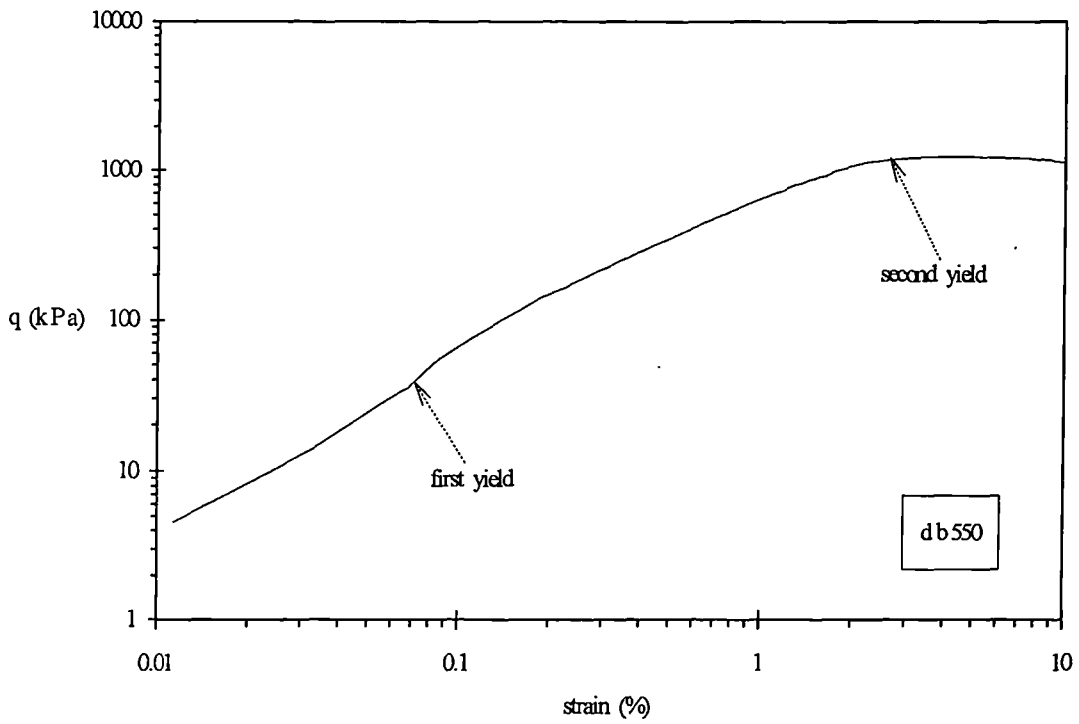
Fig. 4.13a First and second yield for db550 defined from the stress

strain curve
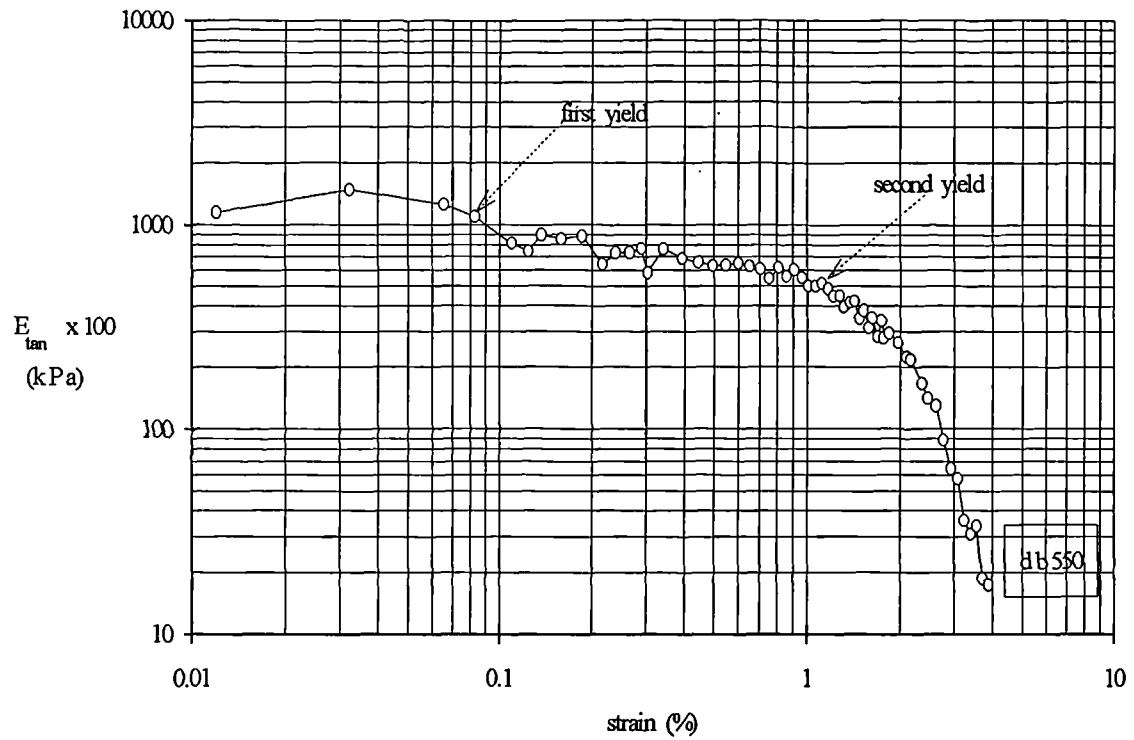
Fig. 4.13b First and second yield for db550 defined from the stiffness graph
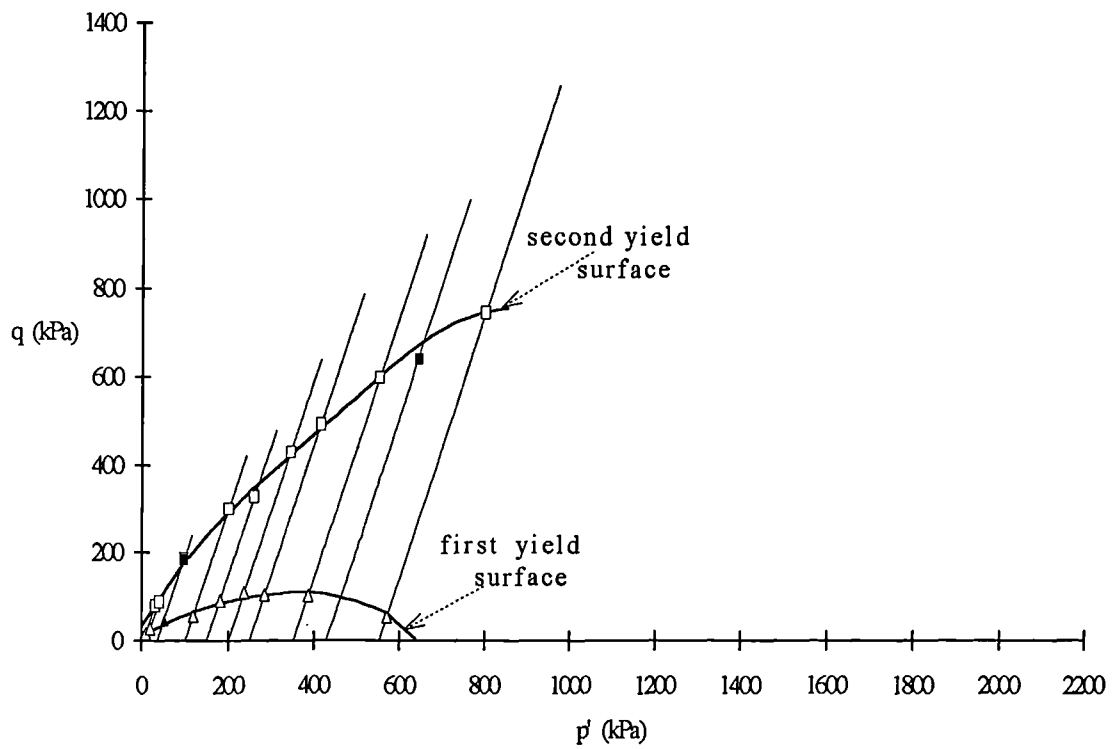
Fig. 4.14 First and second yield surfaces plotted in the stress space
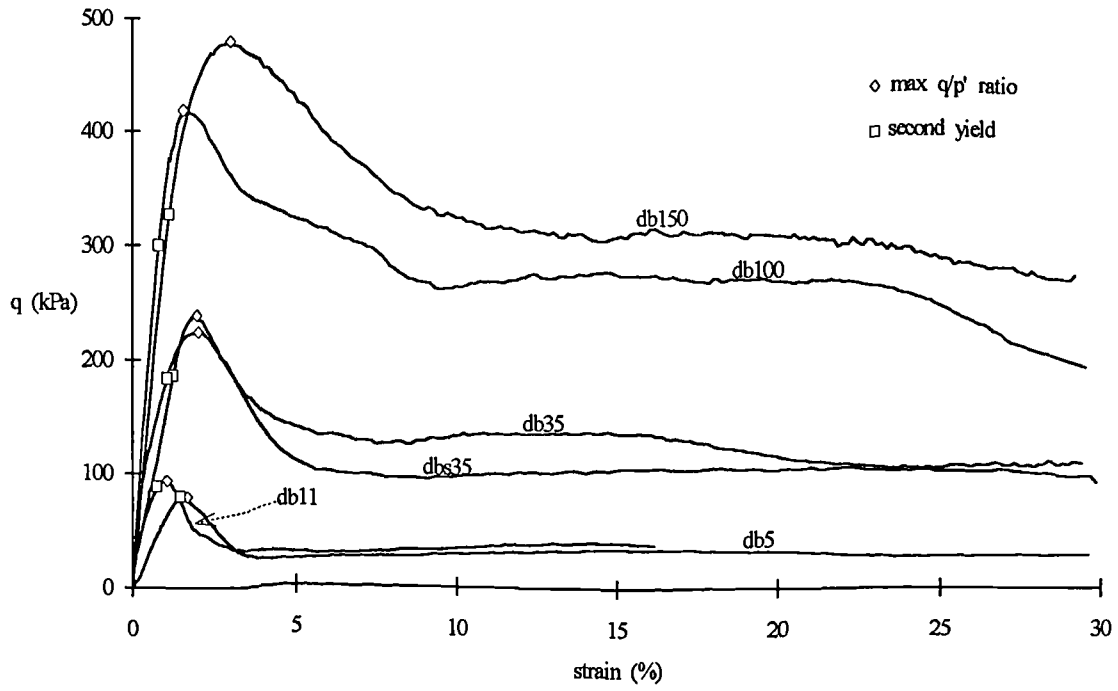
Fig. 4.15a Second yield and maximum q/p' ratio for the samples

sheared at low confining pressures
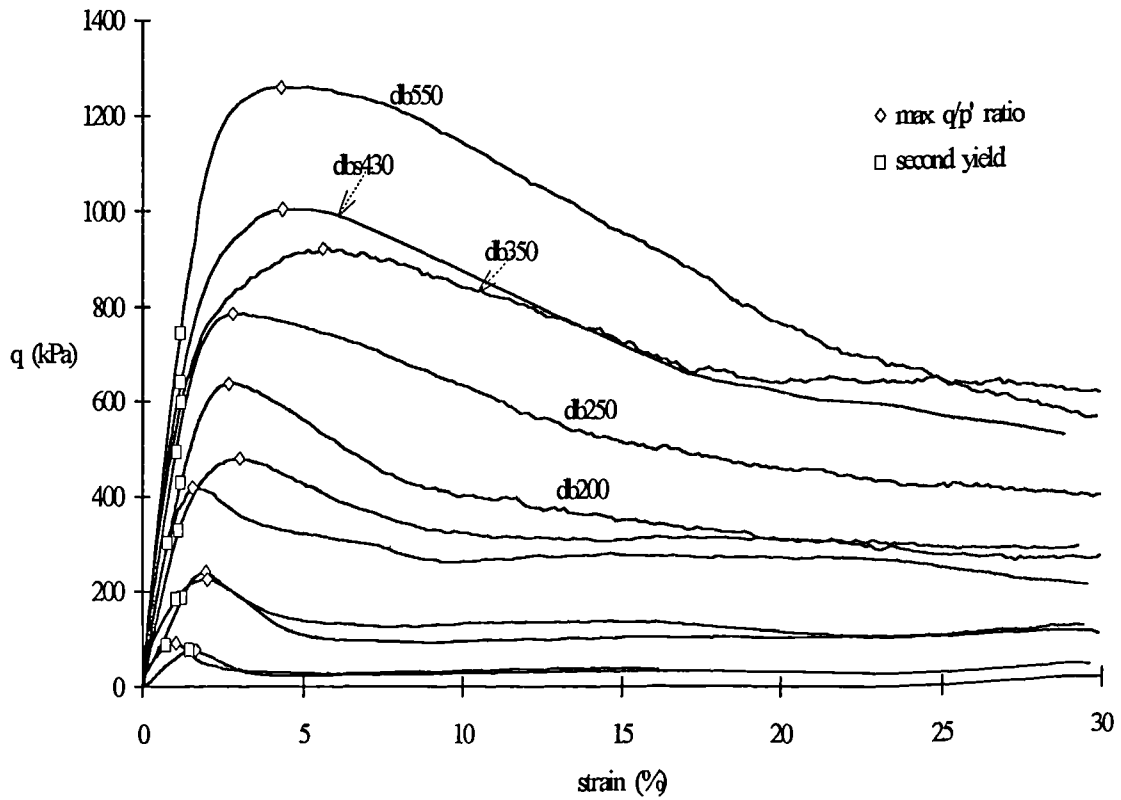
Fig. 4.15b Second yield and maximum q/p' ratio for all the samples
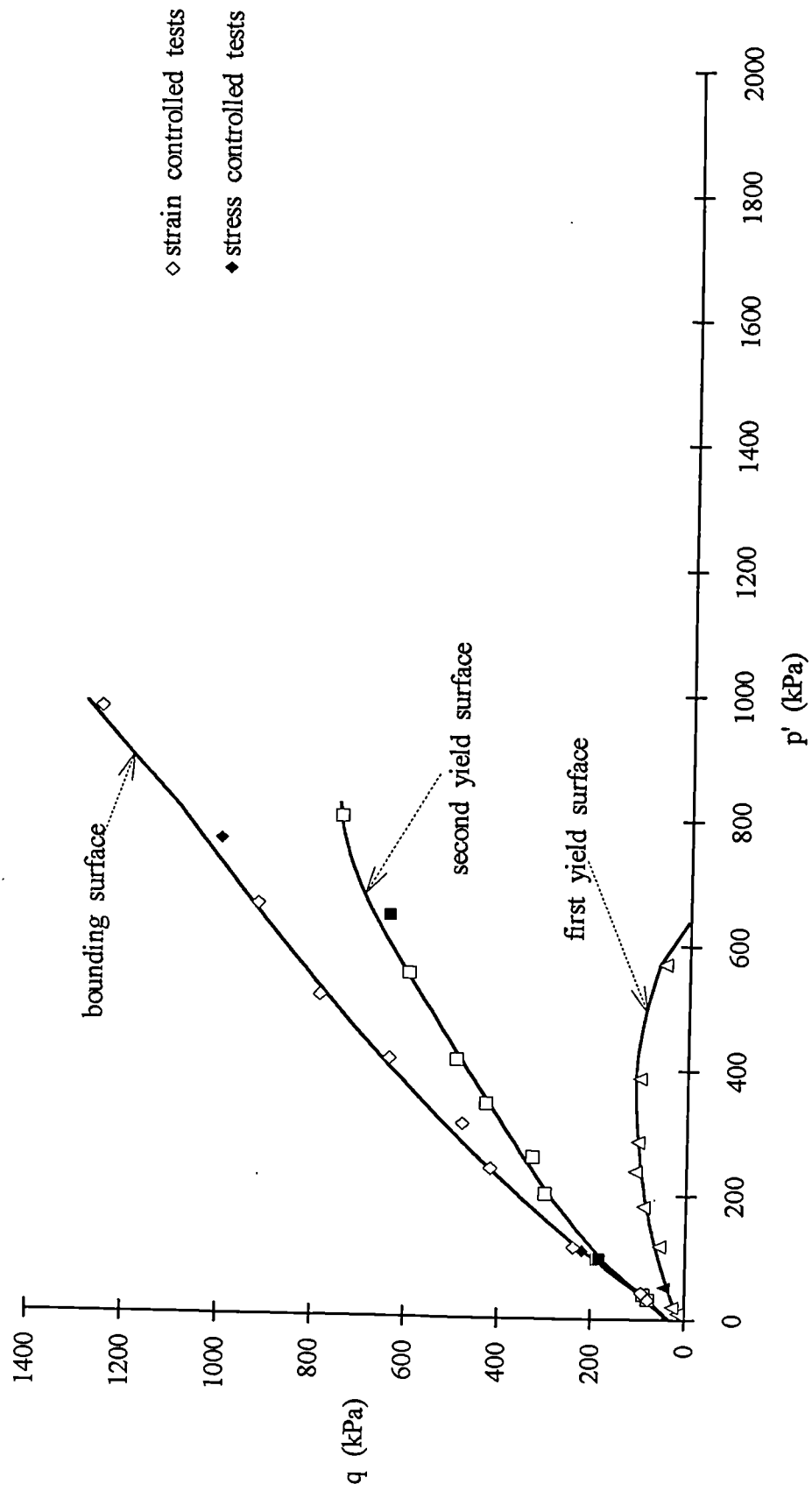
Fig. 4.16a Bounding surface and first and second yield surfaces for the bonded soil

86
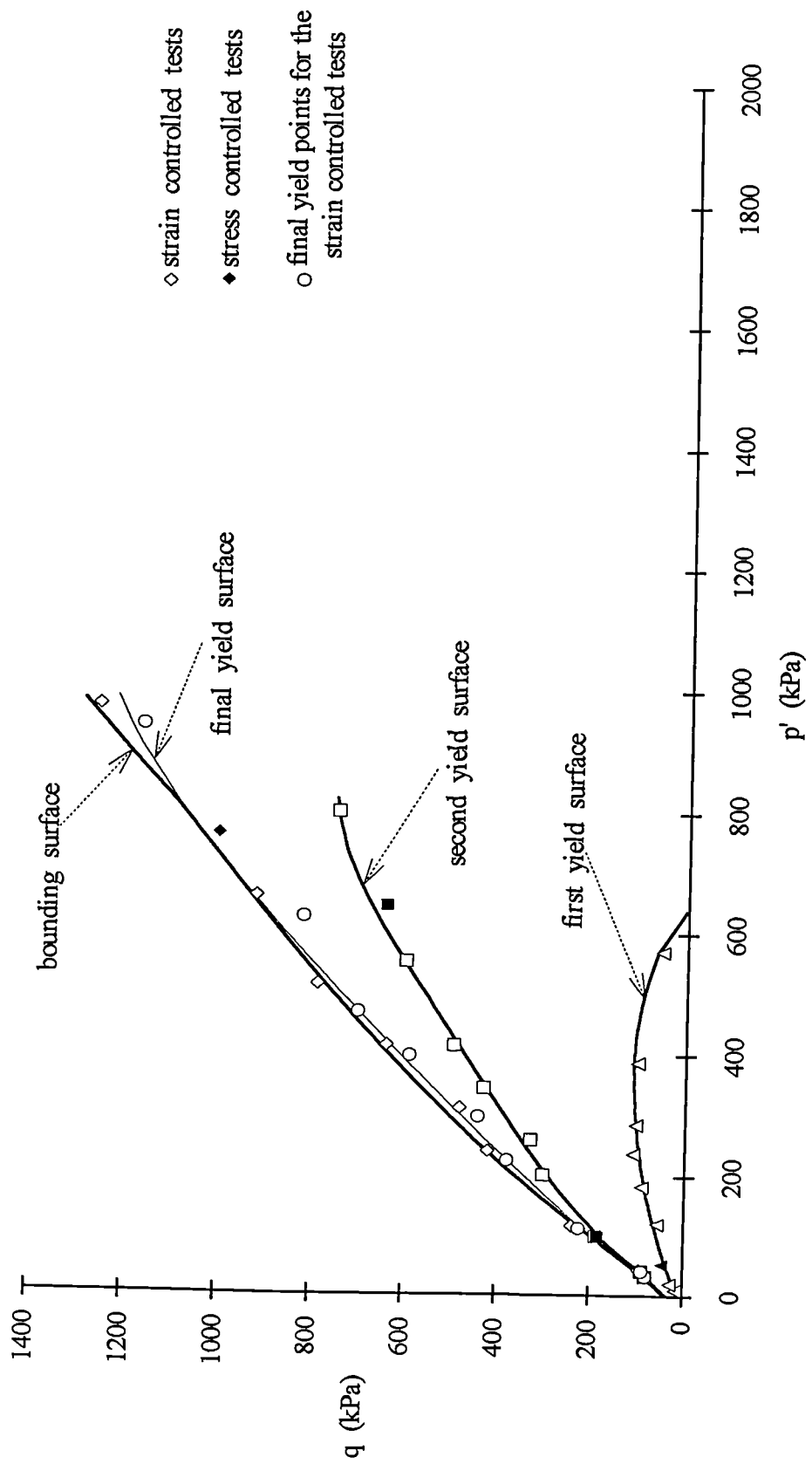
Fig. 4.16b Bounding surface and yield surfaces for the bonded soil

87
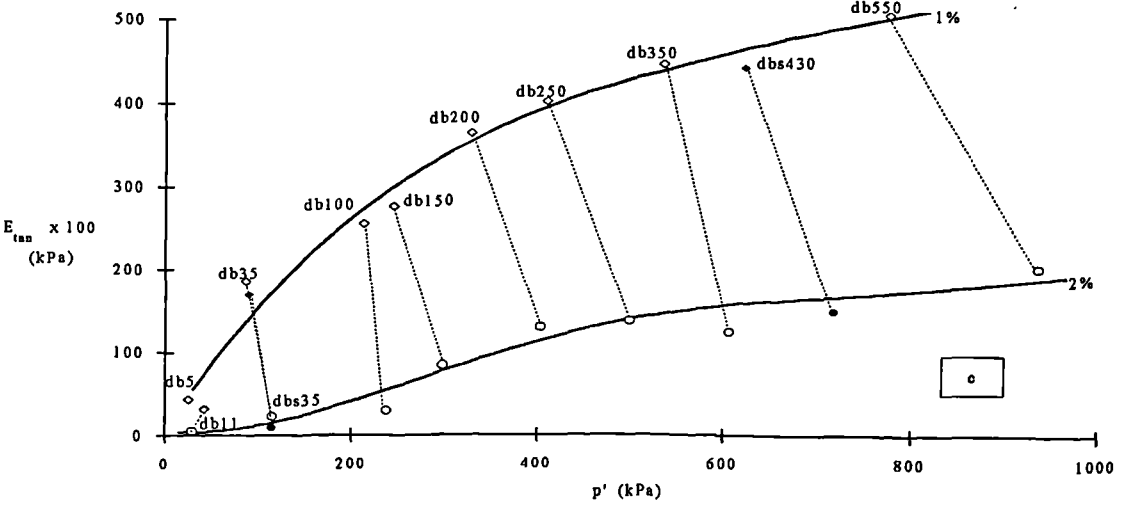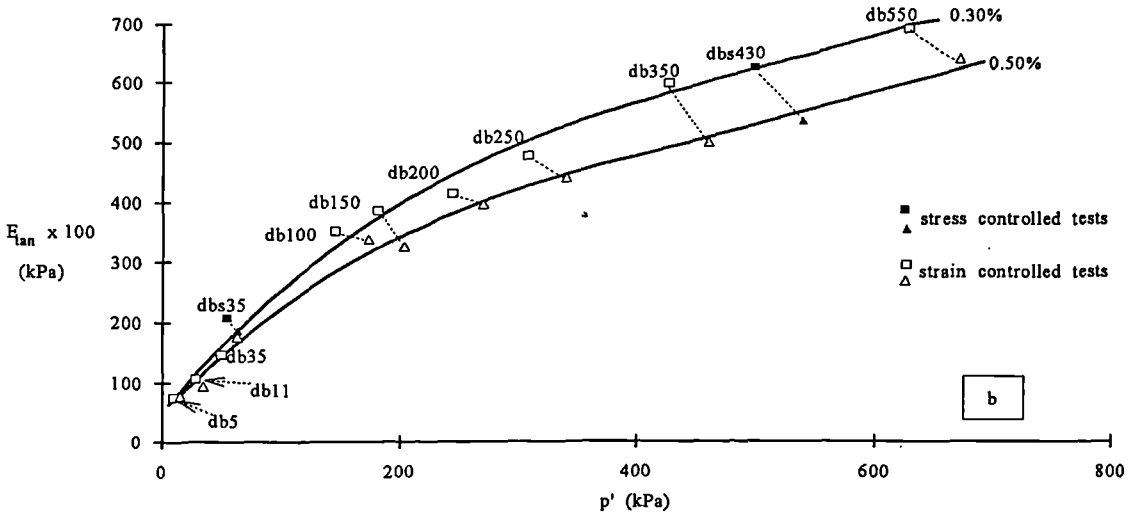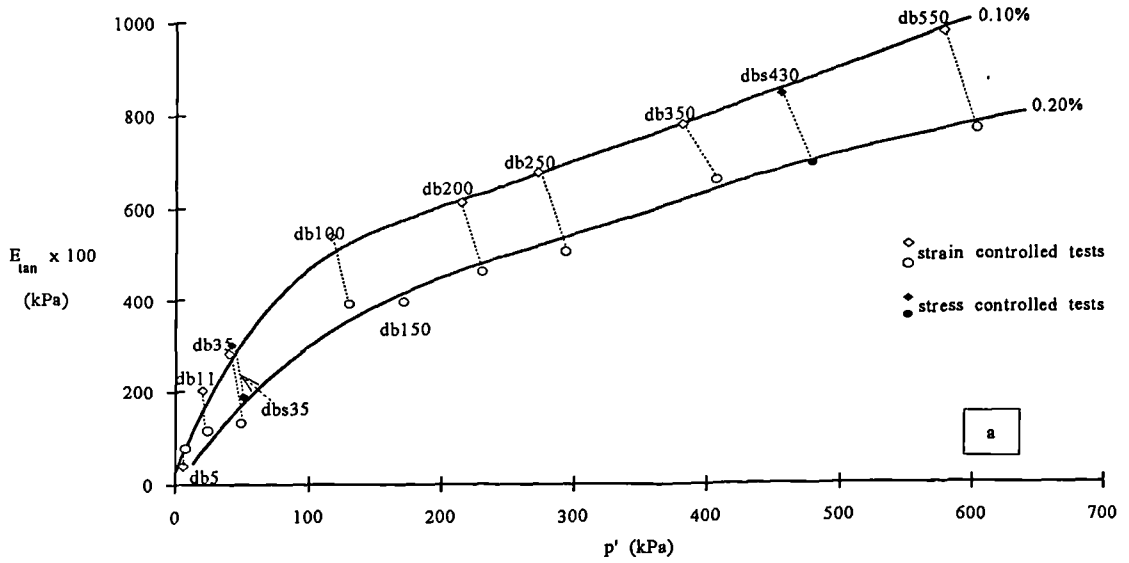
Fig. 4.17a,b,c   Tangential stiffness plotted versus mean effective stress at
different percentage of strain

strain controlled tests

stress controlled tests

0.10%

0.20%

0.30%

0.50%

1%

2%

1200

1000

800

600

400

200

0

E_{tan} x 100 (kPa)

0   200   400   600   800   1000

p' (kPa)
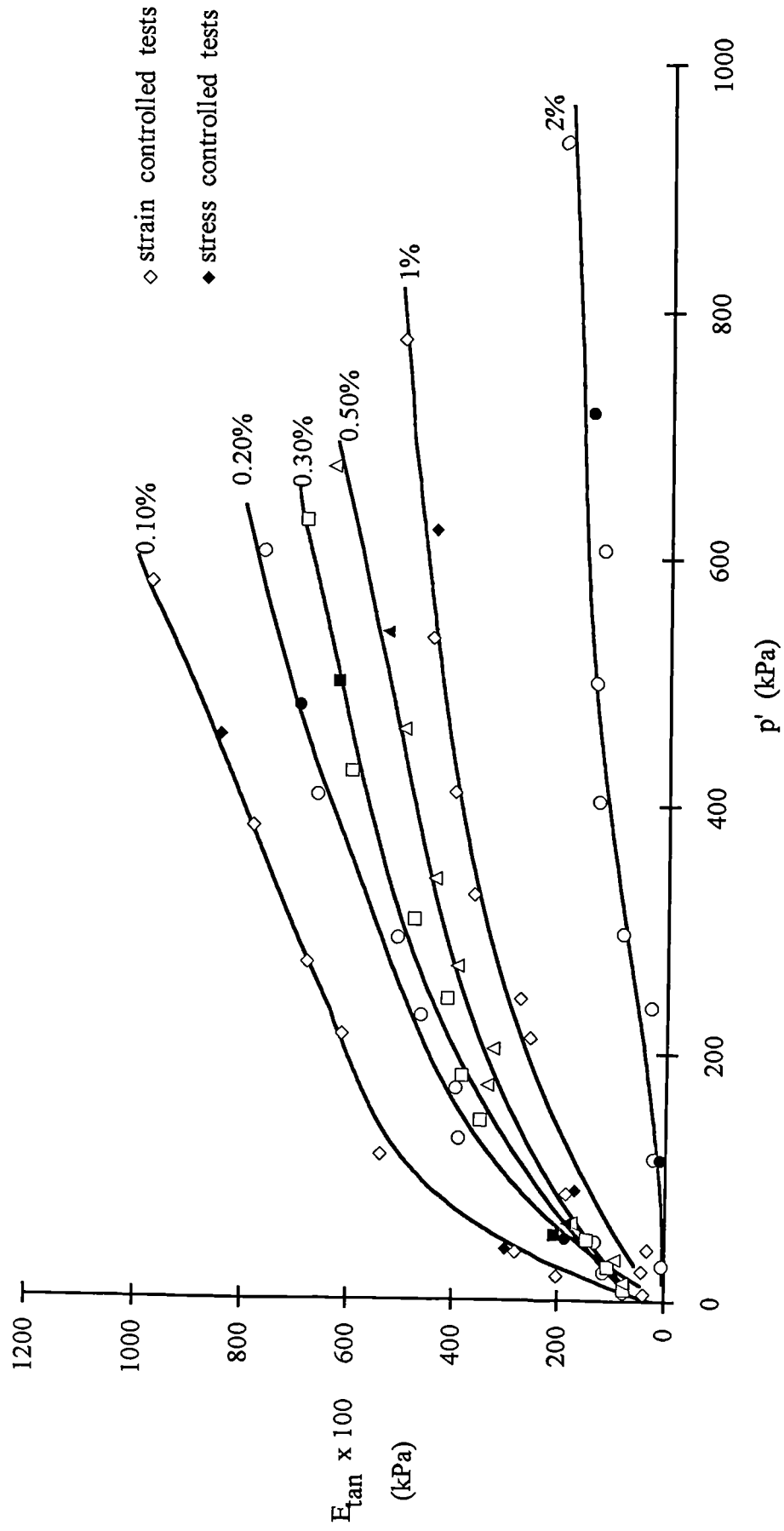
Fig. 4.18 Loss in stiffness with the increase of strain for the bonded samples

89
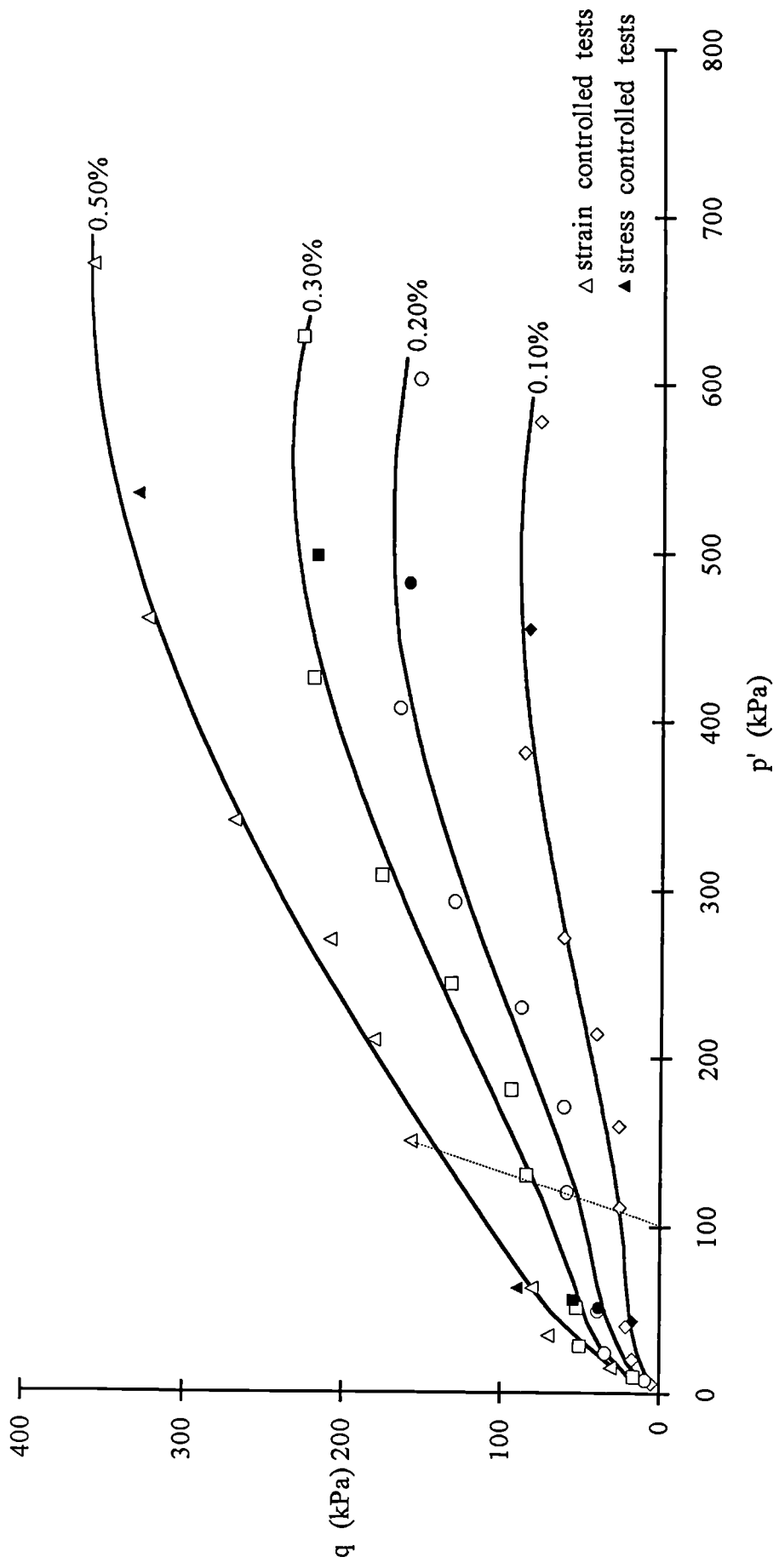
Fig. 4.19a 0.1%-0.5% strain contours plotted in the stress space for the bonded soil

90
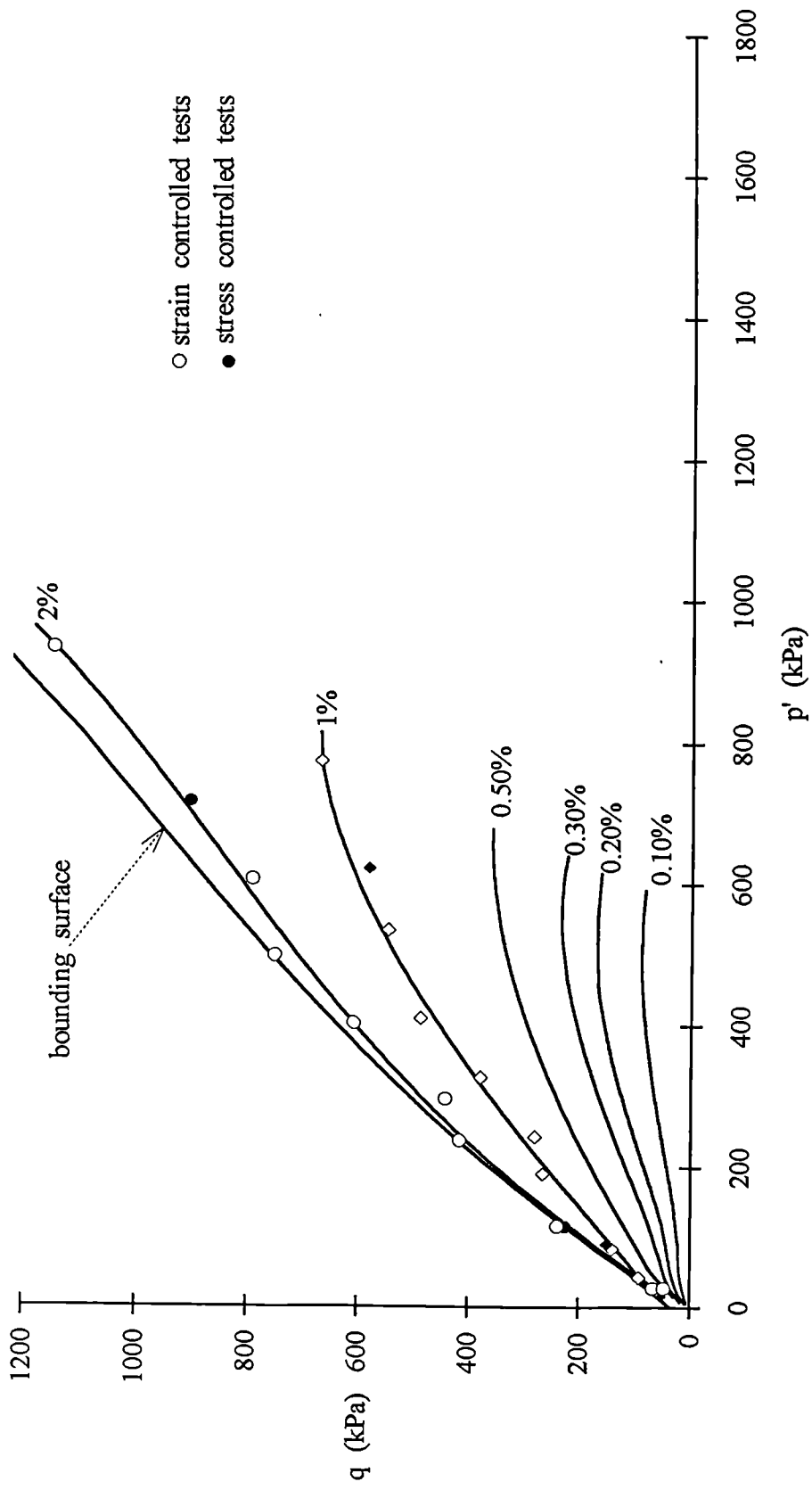
Fig. 4.19b Bounding surface and strain contours for the bonded samples
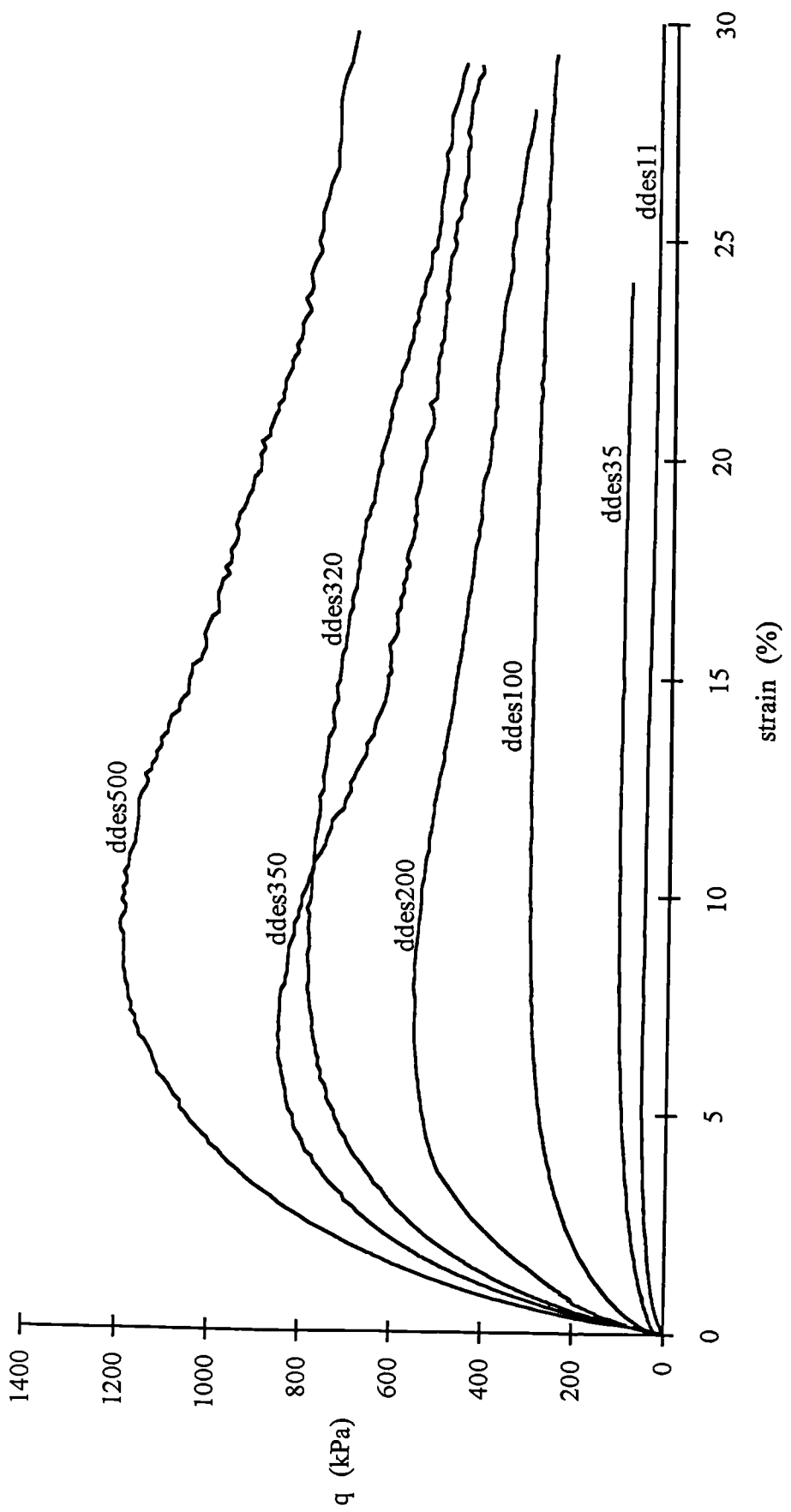
Fig. 4.20 Stress-strain curves from triaxial drained tests on the destructured samples

92
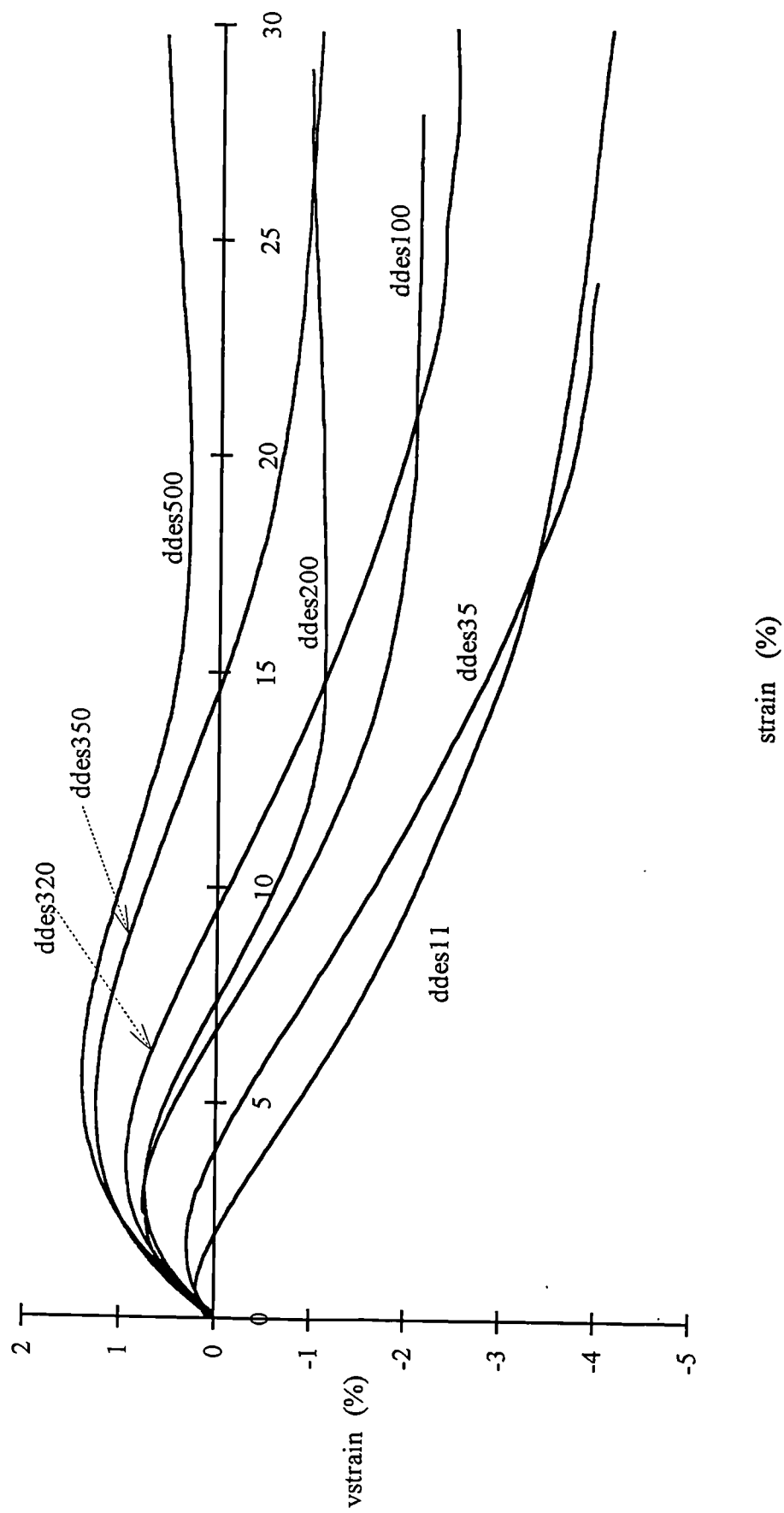
Fig. 4.21 Volumetric strain curves for the drained triaxial tests on the destructured samples

93
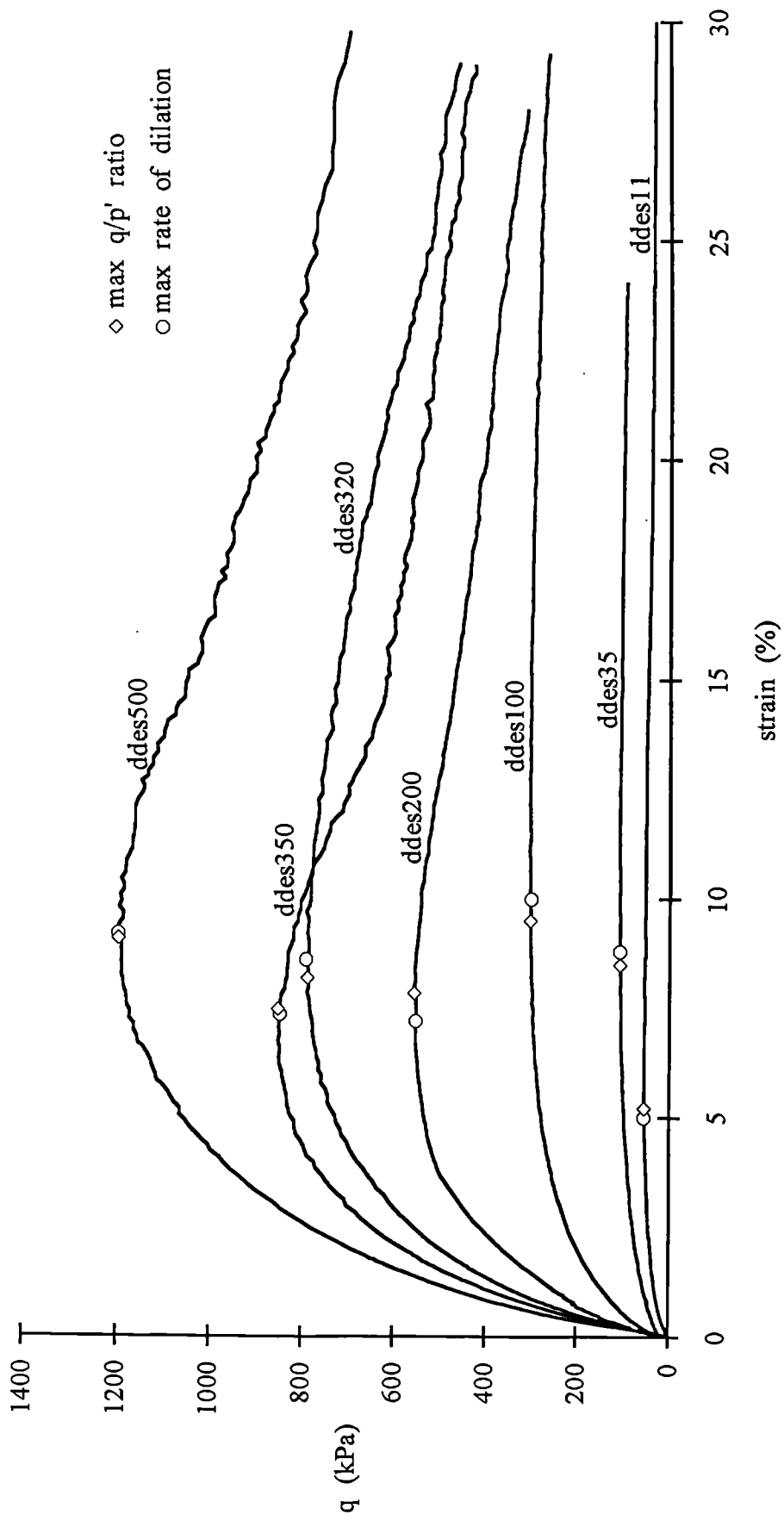
Fig. 4.22 Maximum q/p' ratio and maximum rate of dilation for the destructured samples

94
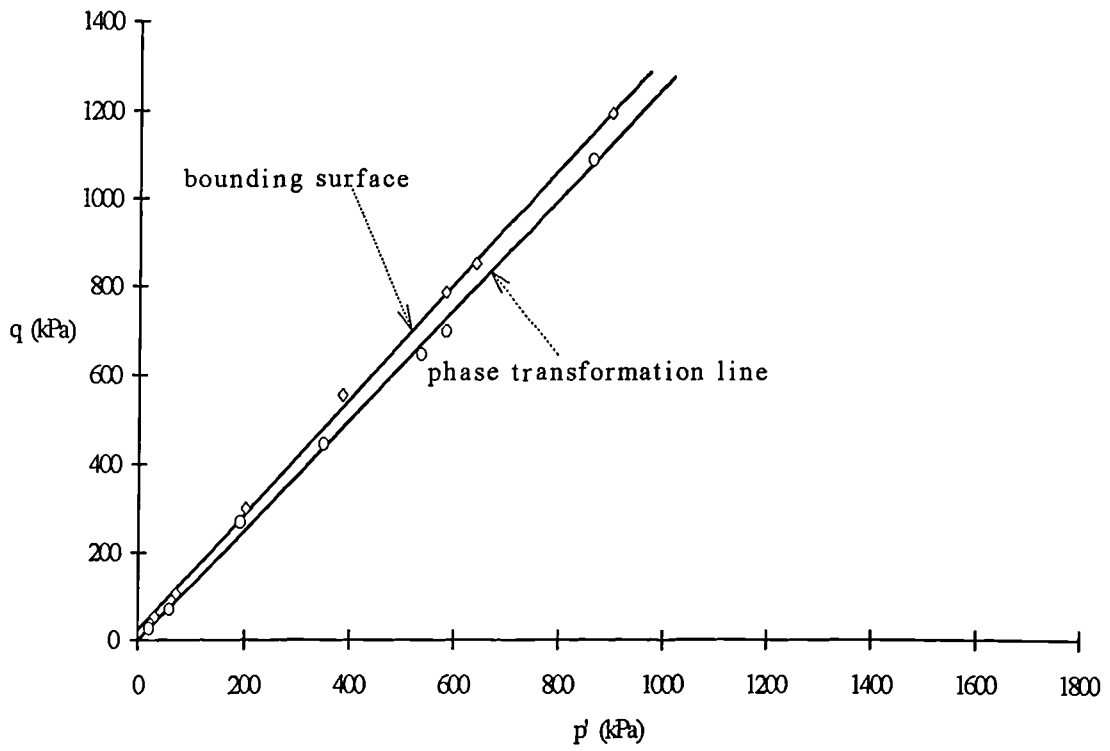
Fig. 4.23 Bounding surface and phase transformation line for the destructured samples
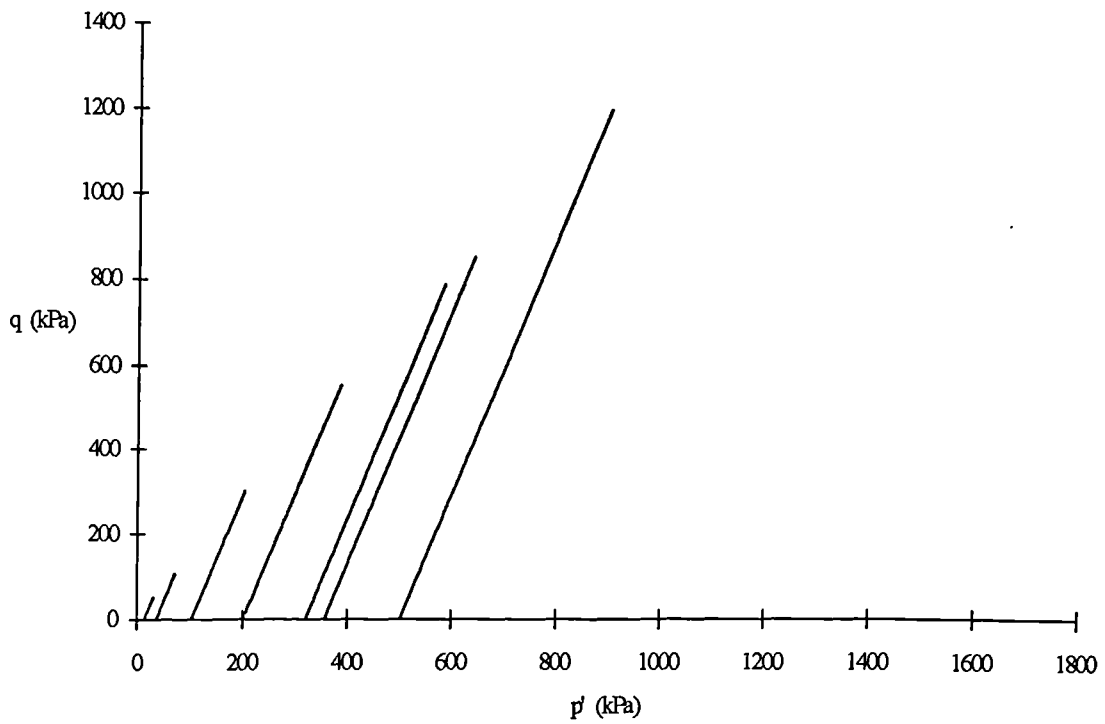
Fig. 4.24 Stress paths for the destructured samples
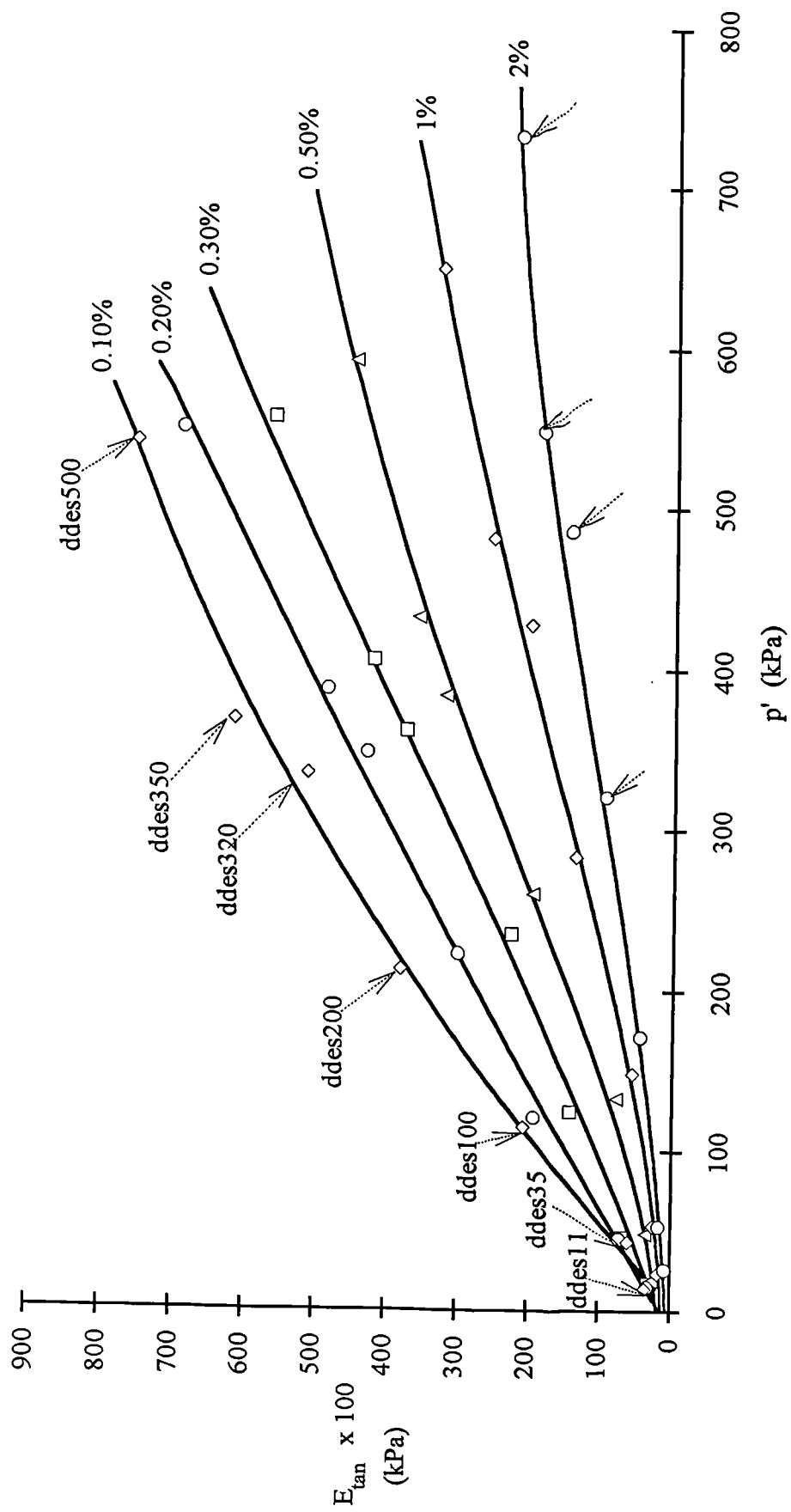
Fig. 4.25 Tangential stiffness versus mean effective stress for the destructured samples
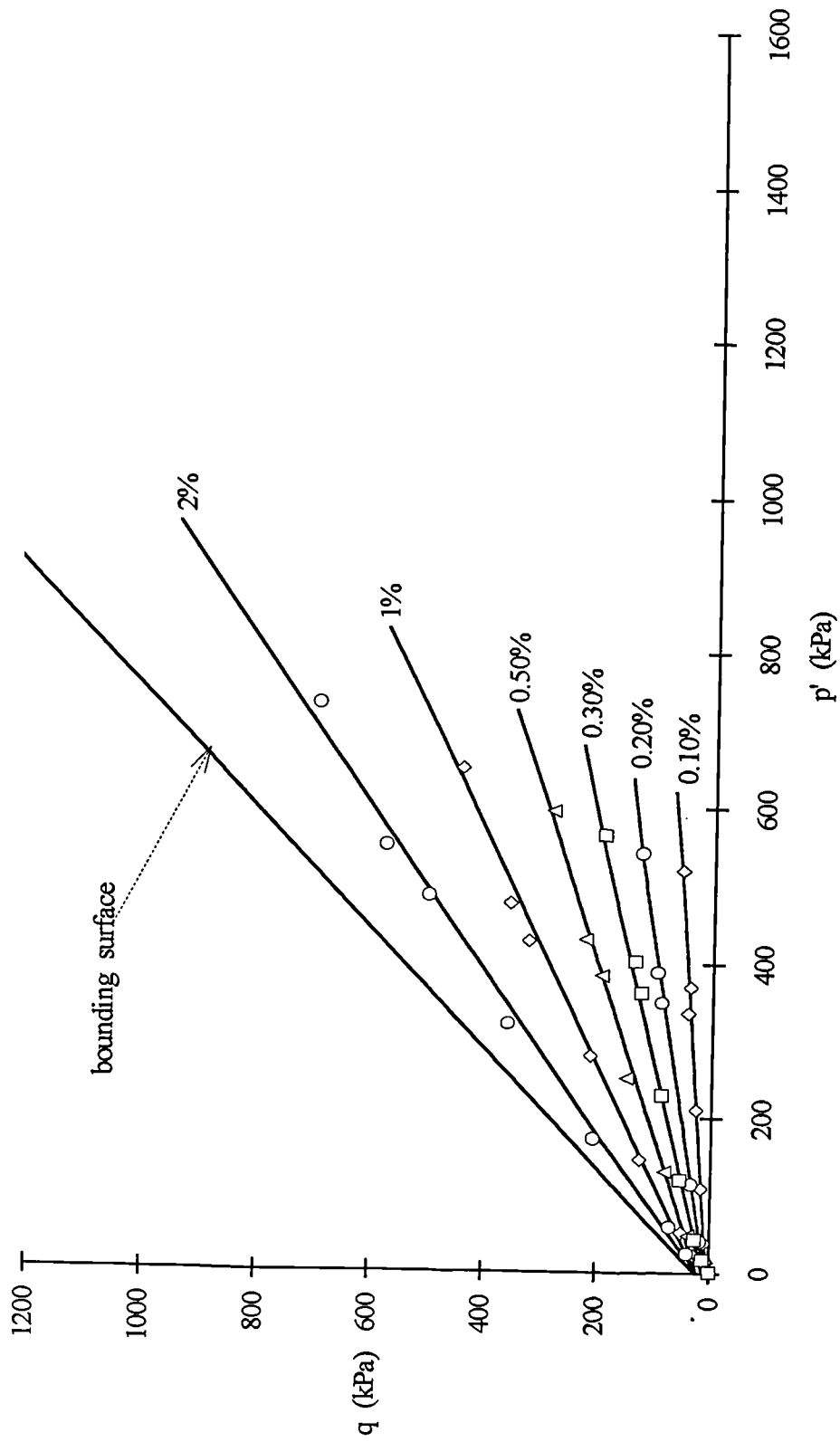
Fig. 4.26 Bounding surface and strain contours for the destructured samples

97
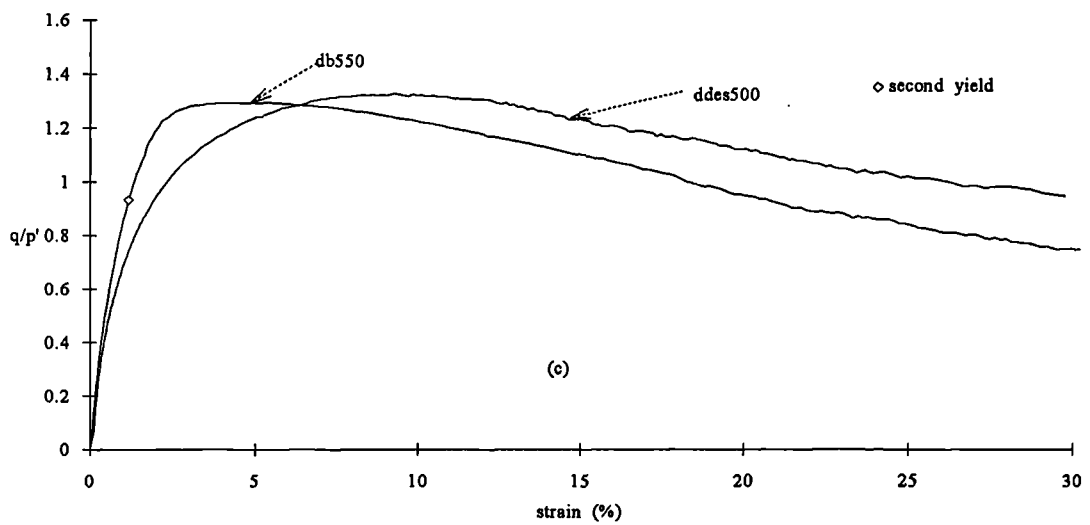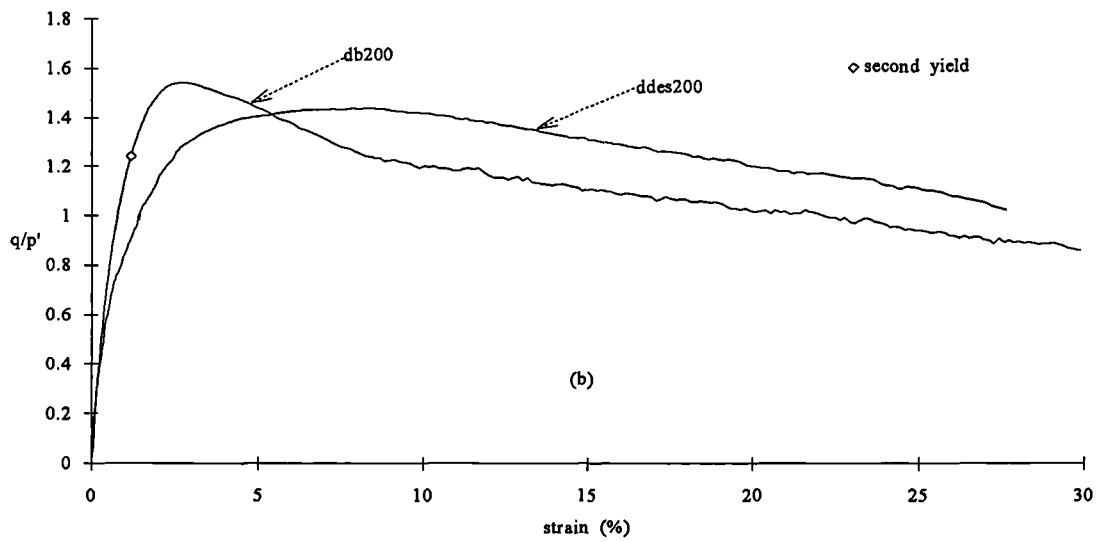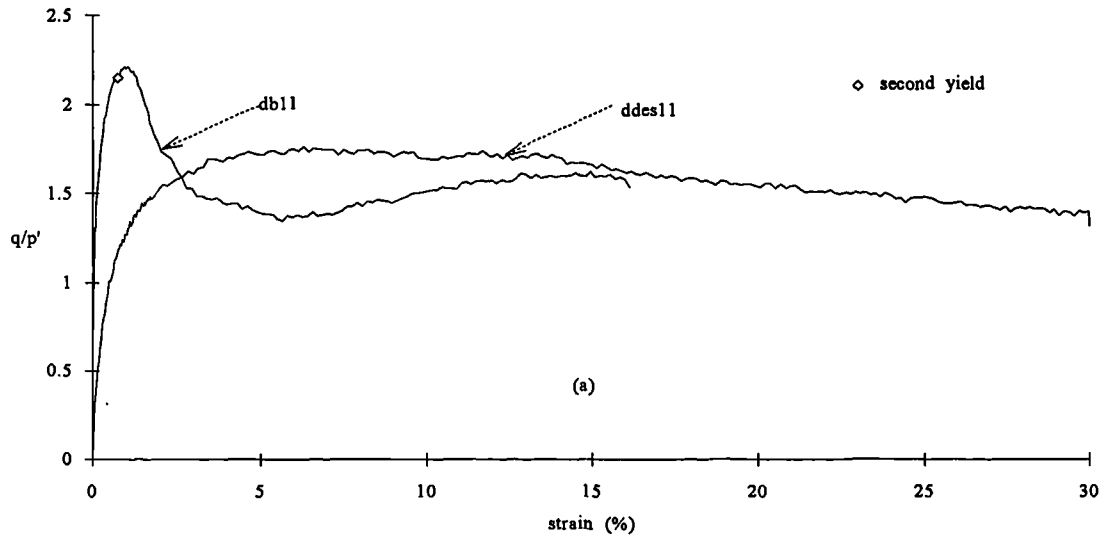
Fig. 4.27a,b,c The development of max q/p' ratio for bonded and
destructured samples at different confining pressures
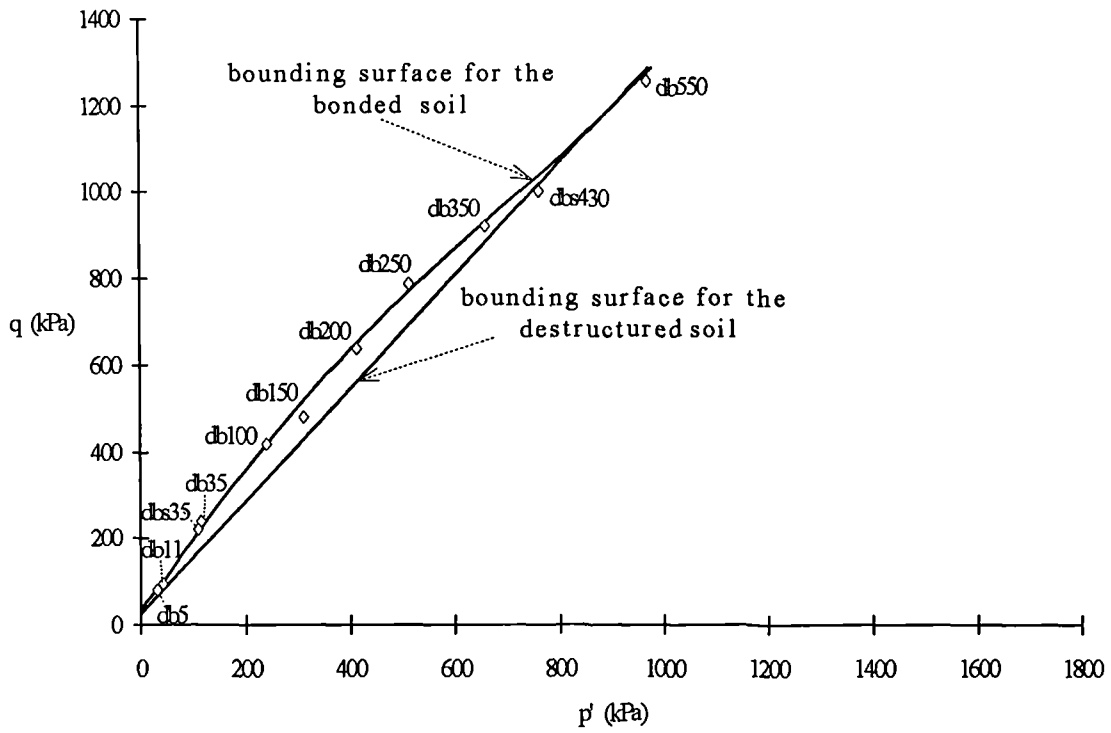
Fig. 4.28 Bounding surfaces for the bonded and the destructured soil
after drained triaxial tests
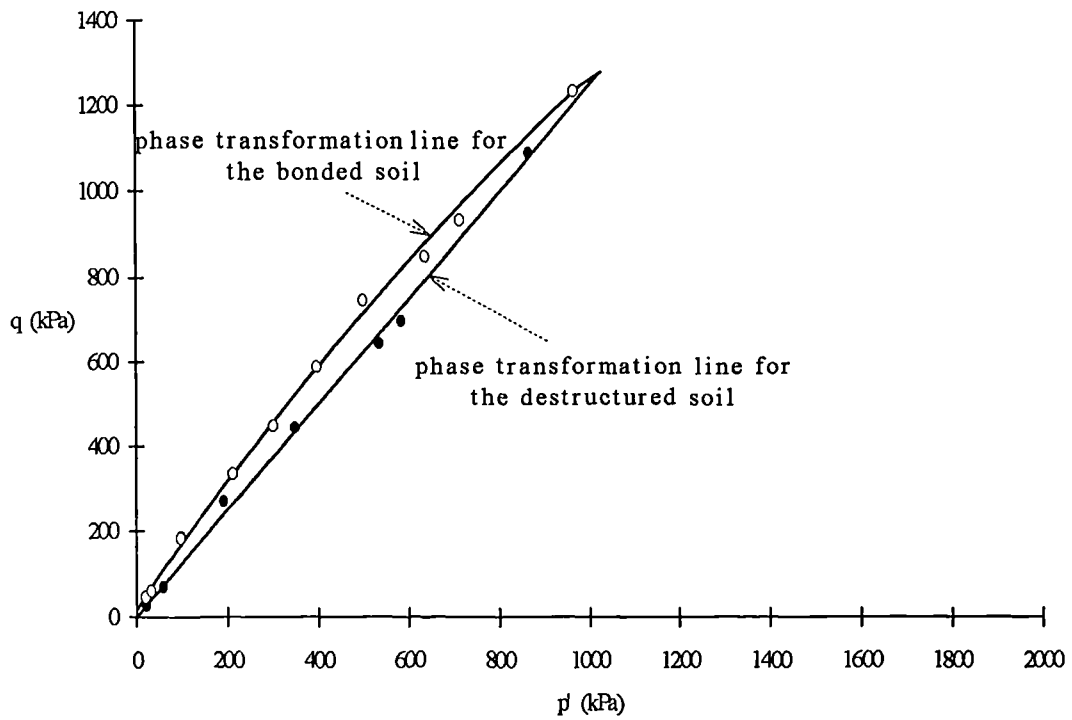
Fig. 4.29 Phase transformation lines for the bonded and the destructured soil
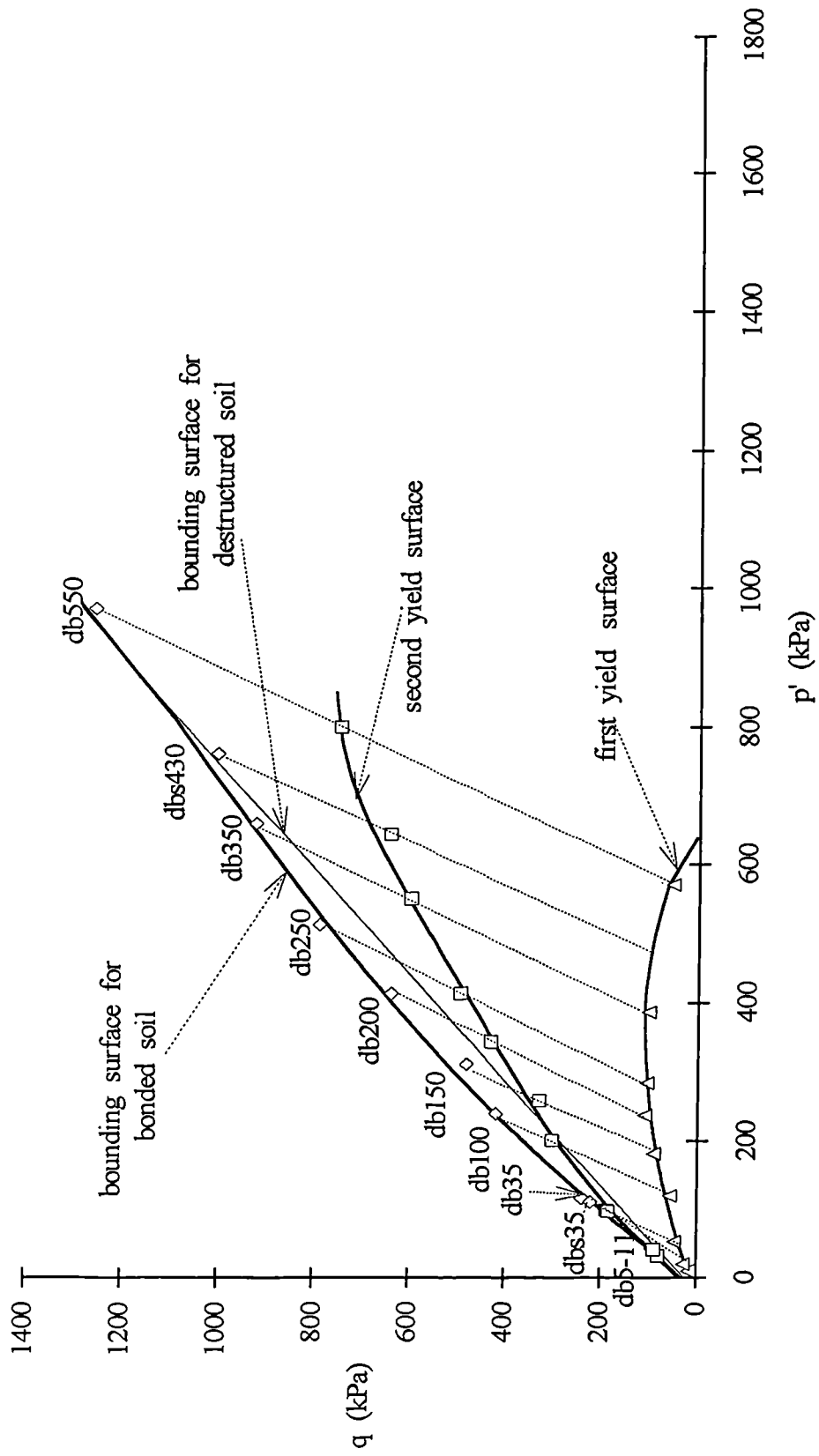
Fig. 4.30 First and second yield surfaces plotted with the bounding surfaces for the two soils
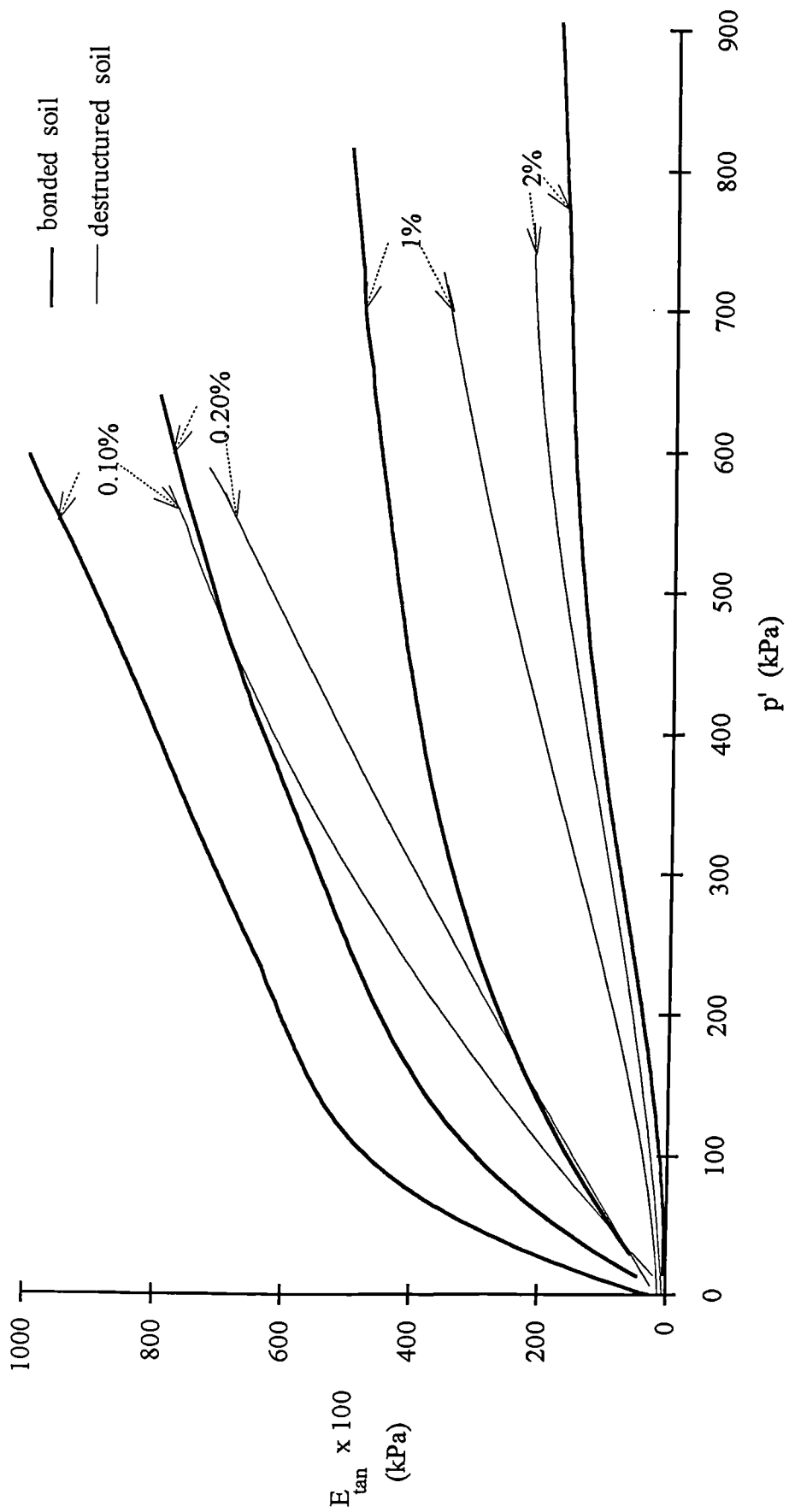
Fig. 4.31 Tangential stiffness versus mean effective stress for the two soils

101
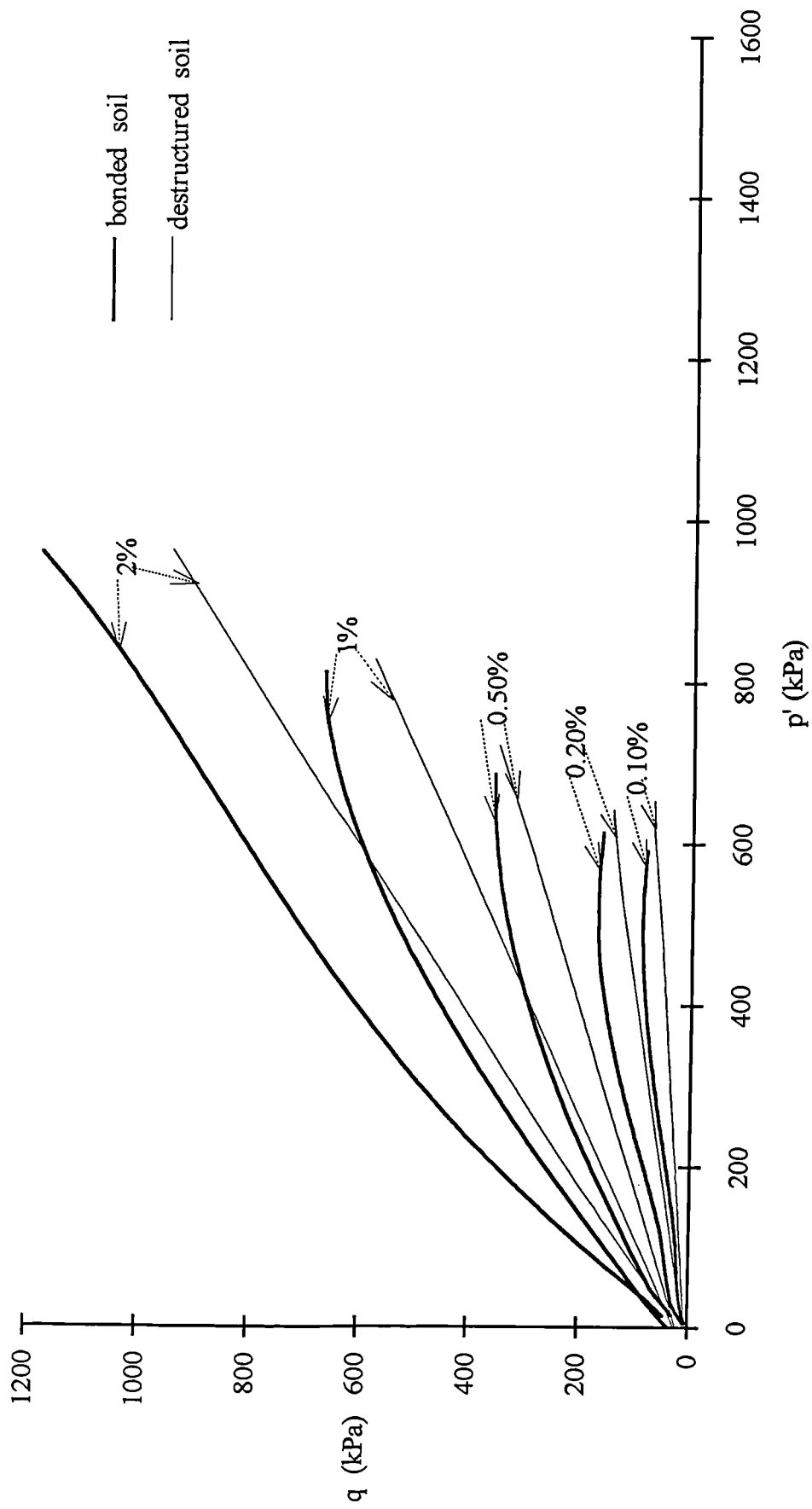
Fig. 4.32 Strain contours plotted in the stress space for the bonded and the destructured soil

102

CHAPTER 5   UNDRAINED TRIAXIAL TESTS ON BONDED AND DESTRUCTURED SAMPLES

5.1 INTRODUCTION

In this chapter the behaviour of the bonded and the destructured soil is studied under undrained shear in triaxial compression. Samples having the same void ratio (e_o=0.6) as those tested in drained triaxial tests were investigated. The limiting stress ratios that the two soils achieve in the stress space, the tangential stiffness and the development of the stress paths in respect of strain are closely studied. The understanding of the behaviour of the destructured soil, formed at the same void ratio as the bonded soil, allows for comparisons to be made between the two and therefore helps to clarify the effects that the bonded structure impose on the soil's behaviour.

Some initial tests on sand-kaolin samples (not fired) are also presented and the differences in behaviour between this soil and the destructured material are studied. Comparisons between the results from the drained and the undrained triaxial tests for the bonded and the destructured soil are also presented, and therefore the influences of the type of drainage and the method of shearing on the soil's behaviour are clarified. Finally the main characteristics of a framework for the behaviour of the bonded soil are presented.

5.2 UNDRAINED TRIAXIAL TESTS ON BONDED SAMPLES

The behaviour of the bonded soil under undrained shear in triaxial compression is discussed in this section. The bounding surface of the soil and the position of the

yield surfaces in the stress space are presented. Yield of the bonds is associated with the loss of tangential stiffness with an increase in strain, during shearing. The loss in tangential stiffness with an increase in mean effective stress is also studied. Strain contours are plotted in the stress space and therefore the development of axial strain in respect of the stress paths is clarified.

5.2.1 Testing details

A total of eighteen undrained tests were carried out on bonded samples. The samples were consolidated at a range of confining pressures from 2 up to 650kPa before shearing. Ten samples were sheared under a constant rate of strain of 1.5%/hr (the same as that used for the drained tests) and eight samples were sheared under a constant rate of deviator stress of 50kPa/hr. Transducer readings during shearing were taken every two minutes at the beginning of the test, and every six minutes at strains higher than 2%. The name of each test, the void ratio of the samples, the confining pressure that they were consolidated to prior to shearing and the method of shearing control are shown in table 5.1.

The first two letters indicate the way that shearing took place (undrained), the third letter indicates the type of sample (bonded or destructured) and a fourth letter is used only for a stress controlled test consolidated at the same confining stress as a strain controlled test (unbs100). The number after the letters is the value of confining stress at which the samples were consolidated prior to shear. Thus for example, test unb400 indicates an undrained test on a bonded sample consolidated at 400kPa and sheared under a constant rate of strain.

5.2.2 Stress strain behaviour of the bonded samples

The deviatoric stress strain curves for the stress and strain controlled tests are plotted in fig. 5.1a and b respectively. The position of the maximum q/p' ratio and the maximum rate of change of the excess pore water pressure ($\Delta u/\Delta \varepsilon_a$) are

on each curve. The maximum rate of the pore water pressure (p.w.p.) change in an undrained test is equivalent to the maximum rate of dilation in a drained test (see section 4.2.3).

The p.w.p. changes versus axial strain for the stress and strain controlled tests are plotted in fig. 5.2a and b respectively. The amount of generation of initial positive pore water pressure increases with an increase in confining pressure prior to shear. The p.w.p. continues to change at the end of shearing for all the tests and so the samples did not reach an ultimate point (critical state).

It can be seen from fig. 5.1a, b, that the maximum q/p' ratio for all the tests is developed at low strains, while q continues to increase to higher values with the increase of axial strain. For the stress and strain controlled tests, unb5-100, the maximum rate of p.w.p change is generated well after the maximum q/p' ratio and that indicates, as was discussed in the previous chapter, that the peak strength of the soil is entirely due to bonding. With an increase of p_o' the two points get closer and at very high stresses, tests unb250-600, they almost coincide. This is also reflected in the development of the stress paths in the stress space.

5.2.3 Stress paths and bounding surface plotted in the stress space

The effective stress paths for the stress and strain controlled tests are plotted in fig. 5.3a and b respectively. The position of the maximum q/p' ratio and the maximum rate of the p.w.p change is also marked. As can be seen, before failure the stress paths define almost straight lines, therefore indicating that only small changes take place in pore water pressure. For tests unb2-100 that were carried out at low stresses, the stress paths reached the max q/p' ratio and then continue, with a change in direction to higher stresses. Although there is a decrease in the max q/p' ratio, q continues to increase in the stress space. For these tests, the max rate of p.w.p. change is at higher deviator stresses than the max q/p' ratio.

At higher stresses, tests unb150-250, the maximum q/p' ratio is getting closer to the maximum rate of p.w.p, and the stress paths after they reach the max q/p' ratio continue shearing under a lower stress ratio. At $p'_0 > 250kPa$, tests unb300-600, the samples reach the max q/p' ratio and shearing continues along an almost constant stress ratio line. When q reaches a maximum value the samples then show brittle behaviour due to the development of shear surfaces. At this stress level the two points coincide and that suggests that the bonds are destroyed at failure by the increase of p' and at this stress level the samples' strength is mainly due to the development of the high negative p.w.p. during shearing.

The max q/p' ratios for the stress and strain controlled tests define the bounding surface in the stress space for the bonded soil, which is plotted in fig. 5.4. As can be seen, the bounding surface governs both the stress and strain controlled tests and shows some curvature up to $p'=800kPa$, which is more apparent at lower stresses. This suggests that the decrease of the slope of the bounding surface indicates the loss of the bond strength of the samples at failure. Although stress controlled tests were not carried out at higher stresses, above 650kPa, due to stress limitations of the system, it is unlikely that different behaviour in respect of the maximum q/p' ratio would be observed at a higher stress level.

The phase transformation line defined from the peak positive values of the p.w.p changes, is plotted in the same graph. The line is consistent for both the stress and strain controlled tests and shows some curvature up to $p'=800kPa$. This suggests that the bonds influence the samples' behaviour in respect of the generation of the excess p.w.p. up to a stress level, as for $p'>800kPa$ the line shows a tendency to follow a linear path.

5.2.4 First and second yield of the samples

The first and second yields of the samples under undrained shearing were defined from the loss in tangential stiffness when plotted against axial strain, the same method used for the drained tests (see section 4.2.4). The position of the second yield is marked on the stress strain curves for the stress and strain controlled tests in fig. 5.5a and b respectively and on the stress paths in fig 5.6a and b.

Second yield of the bonds for tests unb2-11, sheared at low confining stresses, occurs very close to the maximum rate of p.w.p. change, while the maximum q/p' ratio is developed at lower strains. This suggests that the bond strength entirely controls the limiting stress ratio of the samples at this stress level. For tests unb35-70, second yield coincides with the maximum q/p' ratio and the maximum p.w.p. occurs at higher stresses. This indicates that the bonds start to be destroyed at failure, at this stress level, but are still contributing to higher stress ratios.

With a further increase of confining pressure, second yield occurs at lower strain levels than the maximum q/p' ratio and quite far away from the maximum rate of p.w.p. change. For the two tests sheared at $p_0'=100kPa$, the maximum q/p' ratio occurs between the position of the second yield and the maximum rate of p.w.p. change. At this stress level the bond strength has substantially decreased at failure but is still contributing to a higher stress ratio. The distance between the position of the second yield and the maximum q/p' ratio increases with the increase of confining pressure.

At very high stresses $p'>400kPa$, second yield occurs at low q values relative to the maximum q/p' ratio which now coincides with the maximum rate of p.w.p. change. This suggests that the bonds are destroyed at lower stresses and they do not contribute to the peak shear strength of the samples which is now mainly due to frictional resistance.

The development of the q/p' ratio during shearing is plotted versus axial strain in fig. 5.7 for tests unb11, unbs100 and unb500-600. The positions of second yield of the bonds, maximum rate of p.w.p. change and maximum q/p' ratio are also marked. It is interesting to see how the bond strength influences the value of the maximum q/p' ratio of the samples.

Test unb11 sheared at low confining pressures reaches a high value for the maximum stress ratio, q/p'=2.4. Second yield occurs at a high strain percentage, ε_a=2.8% and its position coincides with the maximum rate of p.w.p. change. With an increase in confining pressure, test unbs100, the bond strength has decreased at failure since the second yield occurs at lower strains ε_a=1.2% and the maximum q/p' ratio is directly affected and decreases to a lower value (q/p'=1.8), relative to that of test unb11. However the maximum rate of p.w.p. still occurs at a higher strain percentage than that of the max q/p' ratio.

For tests unb500 and unb600 that were sheared at very high stresses, second yield of the bonds takes place at low strains. Thus the bonds are very much destroyed at failure and do not contribute to the peak stress ratio of the samples, which has therefore substantially decreased (q/p'=1.35). The maximum q/p' ratio now occurs close to the point at which the maximum rate of p.w.p. change takes place. All the tests that were carried out at this stress level presented similar behaviour.

5.2.5 Bounding and yield surfaces plotted in the stress space

The bounding surface and the two yield surfaces are plotted in the stress space in fig. 5.8a. The bounding surface and the second yield surface coincide for p'<115kPa (tests unb2-70). The first yield surface for these tests occurs at lower stresses and increases in shape in the stress space, up to p'=200kPa. The bonds are not destroyed before failure at this stress level and totally contribute to high stress ratio values. For p'<600kPa, tests unb100-400, the second yield surface diverts from the

bounding surface and turns towards the isotropic axis. The bond strength decreases at failure, as the bonds are destroyed at lower deviatoric stresses, and this is reflected by the slope of the bounding surface that decreases to a lower value. For these tests the first yield surface has its maximum values in the stress space and levels off parallel to the isotropic axis.

The difference between the position of the bounding surface and the second yield has its highest value for p'>600kPa. At this stress level the second yield surface reaches its maximum point in the stress space and levels off parallel to the isotropic axis and the bounding surface reaches a linear part in the stress space. The first yield surface turns down and meets the isotropic axis.

Final yield of the bonds is also defined for the samples under undrained strain controlled tests, as the maximum point of curvature on the deviatoric stress versus axial strain curves, for comparisons to be made between the different yield points. In fig. 5.8b the bounding surface and the three yield surfaces are plotted in the stress space. As can be seen the final yield surface is positioned at higher stresses than the second yield surface and almost coincides with the bounding surface. However for p'>600kPa it diverts from the latter.

5.2.6 Stiffness measurements at 0.1%-2% of strain

The behaviour of the bonded soil under undrained shearing will be studied in respect of tangential stiffness, at different percentage of strains. In fig. 5.9a tangential stiffness is plotted as individual contours for 0.1%, 0.2% and 0.5% of strain. Fig. 5.9b shows contours for 1% and 2% and fig. 5.9c shows both sets of results together. For tests unb2-155, fig. 5.9a, there is a rapid increase in E_{tan} with p' for all the contours. The slope of the curves changes for tests unb200-500 and the loss in E_{tan} from one contour to the other becomes more pronounced. At higher stresses p'>600kPa, the contours turn parallel to the isotropic axis. The

samples have lost almost all of the remaining stiffness after 1% of strain (fig. 5.9b) and at 2% of strain only tests unb500-650 presented values higher than 20MPa.

In fig. 5.9c E_{tan} is plotted versus mean effective stress at 0.1%-2% of strain, for all the tests. There is an immediate increase in stiffness with p' up to 115kPa, for the 0.1%-1% contours. For p'>115kPa, the slope of the curves changes for the 0.1%-0.5% contours and at p'>600kPa they level off parallel to the isotropic axis. The initial loss in E_{tan} from 0.1% to 0.2% of strain coincides with the first yield of the bonds. The loss in stiffness from 0.1% to 0.5% of strain is quite substantial in comparison with the loss from 0.5% to 1% of strain, which is quite small throughout the whole range of p'. The loss of the remaining stiffness after 1% of strain coincides with the second yield of the bonds, which was initiated at this strain level. Thus at 2% of strain, stiffness drops to very low levels. The contours are consistent for both the stress and the strain controlled tests.

Strain contours for 0.1% - 0.5% strain and the bounding surface of the bonded samples are plotted in the stress space in fig. 5.10a. It can be seen that there is a linear relationship between q and p' for the 0.1% - 0.3% strain contours, up to p'=115kPa. For higher stresses the slope of the curves decreases and the contours continue to increase under almost a constant stress ratio up to test unb300. For higher stresses the contours turn parallel to the isotropic axis and after unb500 they show a drop in q. The 0.5% contour shows similar behaviour up to p'<115kPa, while for higher stresses it is positioned closer to the bounding surface than to the isotropic axis.

The 0.1% - 2% strain contours and the bounding surface for all the samples are plotted in fig. 5.10b. For tests unb2-11, the 1% contour is very close to the bounding surface and well separated from the 0.5% strain contour. The maximum q/p' ratio for these tests sheared at low confining stresses occurred around 1% of

strain, before the second yield of the bonds took place at 2% of strain. The contour then diverges from the bounding surface at higher stresses up to p'<600kPa, test unb500. For p'>600kPa, tests unb600-650, it turns towards to the isotropic axis.

The 2% strain contour for p'<600kPa is very close to the bounding surface. For p'>600kPa, tests unb500-650, the contour diverges from the bounding surface (which is now only reached at ε_a>3.5%) and turns towards to the isotropic axis. It can be seen from fig. 5.10a and b that the strain contours are the same for both the stress and strain controlled tests. Therefore the development of axial strain in respect of the stress paths is similar for all the tests. Up to 0.3% of strain where the behaviour of the soil is stiffer, the strain contours are closer to the isotropic axis. However the strain contours gradually change direction towards the bounding surface with an increase in strain.

5.3 UNDRAINED TRIAXIAL TESTS ON DESTRUCTURED SAMPLES

The behaviour of the destructured soil under undrained shear in triaxial compression is presented in this section. The bounding surface and the phase transformation line for this soil are plotted in the stress space. Tangential stiffness is studied during shearing and the loss in E_{tan} is presented versus p' for different percentages of strain. The strain contours are presented in the stress space and thus the development of the stress paths during shearing is clarified.

5.3.1 Testing details

A total of ten undrained triaxial tests were carried out on destructured samples. The samples were consolidated at a range of confining pressures from 5 to 650kPa. Samples were prepared at a void ratio of 0.6, the same as the bonded samples. Shearing took place under a constant rate of strain of 1.5%/hr, the same as that

used for the drained tests. The name for each test, the void ratio of the samples and the confining pressure to which consolidation took place prior to shear are shown in table 5.2. The first two letters of the name indicate the type of shearing, the third letter indicates the type of sample and the number after the letters is the value of confining pressure at which the sample was consolidated prior to shear. Thus for example test und500, indicates an undrained test on a destructured sample consolidated at 500kPa.

5.3.2 Stress strain behaviour of the destructured samples

The stress strain curves and the change of the pore water pressures are plotted for all the tests in fig. 5.11a, b respectively. The samples reach peak shear strength values at more than $\varepsilon_a=10\%$ and failure occurred with the initiation of shear surfaces.

Tests und5-70 generated low values of positive pore water pressures at the beginning of shearing, with high negative values observed at higher axial strains. The amount of initial development of positive pore water pressures increased with the increase of confining pressure. The sample sheared in test und400 generated a higher positive excess p.w.p. than the rest due its slightly higher initial void ratio (Georgiannou, 1988). All the samples showed negative values of p.w.p. at failure. The values are still changing at the end of the tests and therefore the samples have not reached a critical state at the end of shearing.

The deviatoric stress-strain curves are plotted again in fig. 5.12 and the points at which the maximum q/p' ratios and the maximum rate of change of the excess pore water pressures occurred, are marked on each curve. The two points are very close for all the tests. This suggests that the maximum shear strength of the samples is due to the development of the high negative p.w.p. during shearing. After the maximum q/p' ratio is reached the samples continue to shear at higher q values up

to the point of failure. Shear surfaces were then initiated with a substantial drop of the maximum q/p' ratio.

5.3.3 Bounding surface for the destructured samples

The effective stress paths for all the tests are plotted in fig. 5.13. After the initial increase of the positive p.w.p., the stress paths turn towards the bounding surface. The samples reach a maximum q/p' ratio and continue shearing up to failure, where shear surfaces initiated with an accompanied drop in the q/p' ratio. The stress path for unb650 is not included, as the sample was not sheared to failure.

The bounding surface for the destructured samples is plotted in fig. 5.14. The test results define a straight line which is positioned at higher stresses than the origin with q/p'=1.26. This is equivalent to a line with a cohesion intercept of c'=28kPa and an angle of friction of φ'=31.5°. The phase transformation line is also plotted on the graph. The line passes through the origin and has a slope equivalent to φ'=29°. The two lines are quite close and almost parallel for p'<200kPa and divert at higher stresses.

5.3.4 Stiffness measurements for the destructured soil

Tangential stiffness during shearing has been calculated for all the tests. In fig. 5.15 E_{tan} is plotted versus mean effective stress, for 0.1%-2% of strain. There is an almost linear relationship between stiffness and p', for all strains up to p'<450kPa. The slope of the curves changes at higher stresses and after test und500, stiffness turns parallel to the isotropic axis. However the lines for E_{tan} at 0.1%-0.5% of strain tend to decrease for p'>700kPa. Tests could not be carried out at higher stresses and so the soil's behaviour is not clarified at this area.

There is a loss in stiffness with the increase of strain, which is more substantial up to 0.5% of strain. With a further increase of axial strain the soil gradually looses

all of the remaining stiffness. At 2% of strain, the samples have not yet reached their peak shear strength values, but have lost almost all of their stiffness. Only tests und500-650 presented values higher than 15MPa.

Strain contours for 0.1%-2% strain contours and the bounding surface for the destructured samples are plotted in fig. 5.16. The tests results for specific strain percentages define straight lines, which are initiated from higher values than the origin. At p'<200kPa the contours are close to one another, followed by an increase in distance between them, at higher mean effective stresses. They also gradually turn in direction with the increase of strain from the isotropic axis towards the bounding surface.

5.4 COMPARISONS BETWEEN THE BEHAVIOUR OF THE BONDED AND THE DESTRUCTURED SOIL UNDER UNDRAINED SHEARING

Comparisons between the behaviour of the two soils are presented in this section. The position of the bounding surfaces, the stiffness measurements and the strain contours for the two soils are closely studied. The behaviour of the destructured soil sets a basic framework for the soil's behaviour in the unbonded state. Therefore the effects that the bonded structure has on the maximum stress ratio and the stiffness of the bonded soil are clarified.

5.4.1 Bounding surfaces for the two soils plotted in the stress space

The bounding surfaces for the bonded and the destructured soil are plotted in fig. 5.17. The bounding surface for the bonded samples exists at higher stresses than that for the destructured samples. It also shows some curvature up to p'<800kPa, which is more pronounced at lower stresses. For p'>800kPa, the two lines coincide. The higher limiting stress ratios that the bonded soil sustained in the

stress space compared to those reached by the destructured soil (for a specific range of stresses) are due to the effect of bonding.

For p'<115kPa, the destructured samples reach high stress ratios, close to that of the bonded soil due to the development of high negative p.w.p. during shearing at this stress level. At higher stresses the bonded samples exhibit higher limiting stress ratios than the destructured soil. However the bond strength of the samples at failure decreases with the increase of mean effective stress and for p'>600kPa the bounding surface turns close to that of the destructured soil.

The phase transformation lines for the bonded and the destructured soil are plotted in fig. 5.18. The line for the bonded soil exists at higher stresses than that of the destructured material and shows some curvature for p'<800kPa. However after test unb500, it shows a tendency to turn close to that of the destructured soil. This suggests that the bonded structure influences the generation of the p.w.p. of the samples during shearing, with the development of positive p.w.p. occurring at higher stress ratios than those of the destructured soil.

The bounding surfaces for the two soils and the first and second yield surfaces for the bonded soil are plotted in fig. 5.19. For p'<115kPa, the bounding surface and the second yield surface for the bonded samples coincide and exist at higher stresses than that of the destructured soil. This suggests that at this stress level the bonds contribute totally to the higher stress ratios that the samples exhibit. Accordingly the first yield surface increases in shape in the stress space.

For p'>115kPa, second yield of the bonds occurs at lower q stresses than the maximum q/p' ratio of the samples. Thus the second yield surface crosses the bounding surface of the destructured samples. The first yield surface reaches its maximum point in the stress space. Although the bond strength of the samples

starts to decrease, the bonds still contribute to the higher stress ratios that the bonded samples exhibit in comparison with those of the destructured soil.

For $p'>300kPa$, the second yield surface has diverted well away from the bounding surface of the bonded samples. The slope of the latter decreases further and thus the two bounding surfaces get closer in the stress space with the increase of p'. This suggests that at this stress level the bonds are destroyed at lower deviatoric stresses and they contribute substantially less to the maximum q/p' ratio of the samples. It is interesting to notice that although the position of the maximum q/p' ratios coincides with that of the maximum rate of the p.w.p. changes for $p'_0>400kPa$, the samples still exhibit higher stress ratios than those of the destructured soil up to $p'<800kPa$.

The first yield surface is parallel to the isotropic axis for $100<p'<500kPa$. It turns towards to the latter with the increase of p' and meets the axis for $p'>600kPa$. At this stress level the second yield surface achieves its maximum shape in the stress space and turns parallel to the isotropic axis and the maximum q/p' ratios of the bonded samples coincide with those of the destructured soil. This suggests that the bonds are totally destroyed at lower stresses and the limiting q/p' ratios of the bonded samples are now only due to the development of high negative p.w.p. and thus become equal to those of the destructured material.

5.4.2 Comparisons between the tangential stiffness measurements for the two soils

The tangential stiffness for the two soils is plotted versus p' for 0.1%, 0.3%, 1% and 2% of strain, in fig. 5.20. There is a large difference between the stiffness values of the two soils, for strains up to 1%. The difference has its maximum value at 0.1% of strain where yield of the bonds has not yet occurred. The differences between the two soils decrease with the increase of strain. At 2% the two soils have similar stiffness values for the whole range of the mean effective stresses.

Stiffness for the bonded soil at 0.1% of strain increases rapidly up to p'=115kPa. At higher stresses the slope of the curve changes towards that of the destructured soil and becomes almost parallel to the latter and for p'>600kPa it levels off. However for p'>600kPa, stiffness for the destructured soil decreases. After 1% strain, second yield of the bonds takes place and the stiffness of the bonded samples drops to a similar level to that of the destructured material. Therefore, this suggests that after the occurrence of the second yield of the bonds, the structure of the bonded samples becomes similar to that of destructured soil sheared to the same strain level.

The 0.1%, 0.2%, 0.5%, 1% and 2% axial strain contours for the two soils are plotted in the stress space in fig. 5.21. The strain contours define curves for the bonded soil and straight lines for the destructured. There is a difference in the position between the contours for the two soils and this increases with the increase of strain. The contours are closer to the isotropic axis at low strains and gradually turn towards their corresponded bounding surfaces at higher stresses (fig. 5.10b and 5.16).

The strain contours for the bonded soil increase rapidly in the stress space with an increase of p', up to p'<115kPa. The difference between the contours of the two soils quickly achieves a high value at this stress level. For 115<p'<600kPa the slope of the curves for the bonded soil decreases to a lower value and the contours continue to increase almost linearly in the stress space. At this stress level the difference between the two contours has its maximum value.

For higher stresses the contours of the bonded soil change direction and turn parallel to the isotropic axis. The difference between the two contours has substantially decreased at this stress level. However for p'>600kPa, the contours of the bonded soil decrease in respect of q and turn down and cross the

corresponding contours of the destructured soil. This does not occur for the 2% contour, but is very likely that it will happen at higher p'.

The development of strain in respect of the stress paths for the bonded soil occurs at higher deviator stresses than that of the destructured soil, for a specific range of mean effective stresses. The bonded structure clearly influences the strain development of that soil. At low p', where the bonds entirely control the soil's behaviour, the samples develop axial strains at higher stress levels than that of the destructured soil. For p'>115kPa, where the bonds only partially control the soil's behaviour, the slopes of the contours for the bonded soil change in direction.

However the difference between the two continues to increase up to p'<500kPa. For p'>500kPa, where the bonds do not contribute to the maximum q/p' ratios of the samples, the contours decrease in shape and cross that of the destructured soil. It is expected that the contours will meet the isotropic axis at higher stresses. Similar behaviour is presented from triaxial tests on the artificially bonded soil by Maccarini (1987), and from triaxial tests carried out on chalk samples, by Loe et al (1992).

5.5 UNDRAINED TRIAXIAL TESTS ON SAND AND KAOLIN MIXTURES

The behaviour of the sand/kaolin soil under undrained shear in triaxial compression is studied in this section. The samples were formed at a void ratio of 0.6 and tested in the triaxial apparatus, without the final step of firing. The bounding surface and the phase transformation line for this soil are presented in the stress space. Tangential stiffness measurements are calculated and E_{tan} is plotted versus p', with the increase of axial strain during shearing. The development of strain in respect of the stress paths is also studied. Therefore a basic framework for the soil's behaviour is presented and allows for further comparisons to be made with the destructured soil formed at the same void ratio.

5.5.1 Testing details

A total of eight triaxial undrained tests were carried out on sand/kaolin samples. The samples were first isotropically consolidated at confining pressures from 5 to 500kPa. Shearing took place under a constant rate of strain of 1.5%/hr, the same as that used for the rest of the strain controlled tests. The name of each test, the void ratio of the samples and the confining pressure at which the samples were consolidated prior to shear are presented in table 5.3. These tests are labelled unsk, in order to indicate an undrained test on sand/kaolin samples.

5.5.2 Stress strain behaviour in undrained shearing

The stress strain curves and the p.w.p. changes for all the tests are plotted in fig. 5.22a, b respectively. The samples reached peak shear strength values at high strains, followed by a decrease in q with the initiation of shear surfaces. Tests unsk5-100 sheared at low confining pressures, show low values of positive p.w.p. followed by a change in behaviour at higher strains and development of high negative values. Higher values of positive p.w.p. are generated with the increase of confining pressure and negative values of p.w.p. develop at higher strains.

The stress strain curves are replotted in fig. 5.23 and the point at which the maximum q/p' ratio and the maximum rate of the p.w.p. change occurred are also marked. The two points are close for all the tests and this suggests that the peak shear strength of the samples is due to the development of high negative p.w.p. during shearing.

5.5.3 Stress paths and bounding surface for the sand-kaolin samples

The stress paths for all the tests are plotted in fig. 5.24. After the initial pore water pressure generation the samples reach the bounding surface and shearing continues under an almost constant stress ratio up to the point where shear surfaces were initiated with an accompanied large drop in the q/p' ratio.

The maximum q/p' ratios and the points at which the samples generated maximum positive p.w.p. changes are plotted in fig. 5.25. The bounding surface for the sand-kaolin samples is a straight line with c'=7kPa and $\varphi'=29.4°$ (q/p'=1.18). The phase transformation line passes through the origin and has a q/p'=1.0. It is positioned at an angle of 3.7° lower than the bounding surface.

5.5.4 Stiffness measurements for the sand-kaolin samples

The tangential stiffness during shearing has been calculated for all the samples. E_{tan} is plotted in fig. 5.26 against mean effective stress for 0.1% to 2% of strain. There is a linear relationship between stiffness and p' and E_{tan} increases with the increase of the p' for all strains.

Tests unsk5-100 show very low initial values of E_{tan}, less than 10MPa. There is loss in E_{tan} with the increase of strain percentage, which is more pronounced for p'>200kPa, after test unsk250, and is more substantial up to 0.5% of strain. However tests unsk5-40 have lost almost all of their stiffness at 0.3% of strain. The samples reached the peak shear strength at axial strains >10% and at that point they had lost all of their stiffness.

The 0.1%-2% strain contours and the bounding surface for the sand-kaolin samples are plotted in fig. 5.27. The stress values at a specific strain percentage, define straight lines in the stress space which pass through the origin. t 0.1% and 0.2% of strain where the soil's behaviour is quite stiff, the contours are closer to the isotropic axis and gradually with the increase of strain they change direction towards the bounding surface.

5.6 COMPARISONS BETWEEN THE BEHAVIOUR OF DESTRUCTURED SAMPLES AND SAND-KAOLIN MIXTURES

Comparisons between the behaviour of the two soils are presented in this section. The bounding surfaces, the stiffness measurements and the strain contours for the two soils are closely studied. The differences that are postulated between the behaviour of the two are suggested to be due to the change in the nature of the fired kaolin which apparently has a strong influence on the soil's behaviour in the destructured state.

5.6.1 Bounding surfaces for the two soils

The bounding surfaces for the destructured soil and the sand-kaolin samples are plotted in the stress space, in fig. 5.28. The bounding surface for the destructured soil lies at higher stresses and at a higher stress ratio by $q/p'=0.08$ than that of the sand-kaolin mixture.

The phase transformation lines for the two soils are plotted in fig. 5.29. The two lines pass through the origin and almost coincide for $p'<100kPa$. However they divert from one another at higher stresses and the line for the sand-kaolin samples occurs at a stress ratio lower by $q/p'=0.16$ than that of the destructured material.

5.6.2 Comparisons between the stiffness readings for the two soils

The tangential stiffness for the two soils at different percentages of strain are plotted in fig. 5.30. The behaviour of the destructured soil is generally stiffer than the sand-kaolin mixtures. The difference in E_{tan} for the two soils is more pronounced at 0.1%-0.5% of strain and for high p' values.

The fired kaolin particles of the destructured samples possibly account for the higher stiffness values that this soil exhibits, in comparison with those of the sand-

kaolin mixture. The fired kaolin particles of the destructured samples had lost 12% of their water content, during the time of firing at 500°C and thus the nature of kaolin changes. After breaking down of the bonded samples, the kaolin particles had possibly become very similar to the 'sand' particles in terms of water absorption and particle angularity. The samples are thus formed with a more random structure than that of the sand-kaolin soil, (in which the kaolin coats the sand particles and forms bridges between them, Georgiannou, 1988) and thus possibly present a similar behaviour to that of a sand sample, formed at the same void ratio. This structure possibly explains why higher stiffness values would be exhibited by the destructured samples compared to the values of the sand-kaolin mixture, formed with the same kaolin content and at the same void ratio.

The higher limiting stress ratio values that the destructured soil exhibits in comparison to that of the sand-kaolin mixtures, are also possibly due to the different nature of the fired kaolin particles of the destructured soil, which causes a higher degree of interlocking between the particles.

The 0.1%-2% strain contours for the two soils are plotted in the stress space in fig. 5.31. The strain contours for the two soils almost coincide for $p'>200kPa$ and up to 1% of strain and therefore the development of axial strain in respect of the stress paths is similar for the two. However the strain contours for the sand-kaolin mixtures pass from the origin, compared to those of the destructured soil which showed higher initial q values. This suggests that the fired kaolin particles of the destructured soil also influence the development of axial strain at higher deviator stresses, for low mean stresses, in comparison with those of the sand/kaolin mixtures.

These results stress the importance of testing true destructured materials, which have the same nature and grading as the bonded material. Similar conclusions have been reported by Vaughan et al, (1987), and Coop and Atkinson (1993).

5.7 COMPARISONS BETWEEN THE RESULTS FROM DRAINED AND UNDRAINED TESTS FOR BONDED AND DESTRUCTURED SOILS

Comparisons between the results obtained from the drained and undrained tests for the bonded and the destructured soil are presented in this section. It is essential, before further study of the bonded soil under unconventional stress paths, to examine first the influence that drainage and the method of shearing control have on the soil's behaviour.

5.7.1 Comparisons between the results from drained and undrained tests on the bonded samples

The bounding surfaces for the bonded samples obtained from the drained and the undrained triaxial tests and the individual test results are plotted in fig. 5.32a. There is good agreement between the test results for the whole range of mean effective stress. Therefore the bounding surface of the bonded samples is not affected by either the type of drainage or the method of shearing control for the particular rates of stress and strain used.

The phase transformation lines for the bonded samples obtained from the two types of triaxial tests are plotted in fig. 5.32b. There is generally good agreement between the test results and the differences between the two lines are possibly due to the limited number of drained tests that were carried out.

The first and second yield points obtained from the drained and undrained tests on the bonded samples, are plotted in the stress space in fig. 5.33. There is quite good agreement for the yield surfaces, with slightly higher q values for the first yield surface obtained from the undrained tests. However, the differences are not large and within the range of experimental variations. Therefore the results suggests

that yielding of the bonds is unaffected by the type of drainage and the method of shearing control.

Tangential stiffness curves at different percentages of strain obtained from the drained and undrained tests are plotted in fig. 5.34a. There is good agreement between the test results and the curves coincide for specific strain percentages. The differences between the 0.1%-0.5% contours for p'>200kPa, are probably due to the limited number of drained tests that were carried out. The undrained tests carried out at p'>600kPa, clarify the behaviour of stiffness at this stress level.

The 0.1%-2% strain contours obtained from the drained and the undrained triaxial tests are plotted in the stress space, in fig. 5.34b. There is generally good agreement between the two, with slightly higher values for the 0.2% and 0.3% contours obtained from the undrained tests, for p'<400kPa. The difference between the two is higher for the 0.5% contour. As only one drained test was carried out at p'>450kPa, the contours defined from the undrained tests are more representative for the strain development of the soil, at this stress level. Axial strain generally developed in a similar way in respect of the stress paths, under both drained and undrained shearing.

5.7.2 Comparisons between test results for the destructured samples

The bounding surface for the destructured samples obtained from the drained and the undrained tests and the individual test results are plotted in fig. 5.35a. There is good agreement between the test results, and the two surfaces coincide.

The phase transformation lines defined from the drained and undrained triaxial test results are plotted in fig. 5.35b. The two lines pass through the origin and for p'<400kPa are very close in the stress space. However at higher stresses, the line defined from the drained tests lies at a q/p' ratio 0.06 higher than that defined from

the undrained tests. This is probably due to the limited number of results, from drained tests that were carried out at this stress level.

Comparisons between the tangential stiffness curves defined from the drained and the undrained test results are plotted versus p', in fig. 5.36a, at different percentages of strain. There is generally good agreement for the 0.2%-2% contours and for p'<400kPa. However tangential stiffness for the drained tests occurs at higher levels than that of the undrained tests, for p'>400kPa. Only one drained test was carried out at this stress level and therefore the behaviour of the soil is better clarified from the undrained tests.

The 0.1%-2% strain contours defined from the drained and undrained test results are plotted in the stress space in fig. 5.36b. The contours for the two types of tests coincide at different percentages of strain and for the whole range of mean effective stresses. Gradually with the increase of q they turn close to the unique bounding surface. Therefore the type of drainage during shearing does not affect the soil's development of axial strain, in respect of the stress paths.

5.8 FRAMEWORK FOR THE BONDED SOIL UNDER DRAINED AND UNDRAINED TRIAXIAL COMPRESSION

The results obtained from the drained and undrained triaxial tests on the bonded soil set a basic framework that explains the behaviour of this soil under triaxial compression. The principle characteristics of the soil's behaviour are presented in this section.

5.8.1 The effects of bonded structure on the soil's behaviour

The behaviour of the bonded soil has so far been examined under drained and undrained triaxial compression tests. The soil exhibits a bounding surface which is positioned at a higher stress level than that of the destructured soil in the stress

space (fig. 5.17), and is unique for both the drained and the undrained tests. The higher q/p' ratios that the soil presents are due to its bonded structure. The behaviour of the bonded soil in respect of the maximum q/p' ratio coincides with that of the destructured soil, after p'>800kPa. Therefore the bonds contribute less to the max q/p' ratios of the soil with the increase of p'. This is discussed by Toll and Malandraki (1993).

The soil exhibits a first yield of the bonds that occurs at 0.1%-0.3% of strain and a second yield that takes place at about 1% of strain. Yield is associated with a drop in tangential stiffness. The yield points form two yield surfaces in the stress space (fig. 5.8a), which are unique for both the drained and undrained triaxial tests. The first yield surface increases in shape with the increase of p' and for higher stresses turns down towards the isotropic axis. The second yield surface exists at higher stresses than the first yield surface. For p'<115kPa, it coincides with the bounding surface and diverts from the latter at higher stresses. For p'>800kPa it levels off parallel to the isotropic axis.

The bonded structure of the soils also affects the development of the volumetric strains and the p.w.p. changes during shearing, with a result that the phase transformation line lies at a higher stress level than that of the destructured material (fig. 5.18).

The bonded soil also exhibits higher tangential stiffness values than those of the destructured material due to its bonded structure. The bonded soil, (referring to fig. 5.20), is stiffer than the destructured soil up to 1% of strain, followed by second yield of the bonds which destroyed its structure and thus at 2% strain the two soils exhibit similar stiffness values for the whole range of p'. The bonded structure of the soil directly affects the strain contours of the samples plotted in the stress space. The contours (fig. 5.21) exist at higher stresses than that of the

destructured soil. Therefore yielding of the bonds directly affects the strain development of the bonded soil in respect of the stress paths which is different to that of the destructured material. At low axial strains where the behaviour of the soil is quite stiff the contours are closer to the isotropic axis; after the second yield of the bonds takes place they turn towards the bounding surface.

5.8.2 Three main zones associated with the loss of the bond strength define the soil's behaviour under drained and undrained triaxial compression

The behaviour of the bonded soil under drained and undrained triaxial compression can be represented by three main zones based on stress level. The three zones are shown in an idealised form in fig. 5.37. The importance of these zones is characterised by the behaviour of the bonded structure of the soil, with the increase of mean effective stress. The bonds are shown to contribute less to the max q/p' ratios of the soil with an increase of p' and therefore the three zones are defined by similar characteristics of the samples sheared at a specific range of mean effective stresses. This is discussed by Malandraki and Toll (1994).

In the first zone (for $p'_0 < 70kPa$), the second yield surface coincides with the bounding surface. At this stress level the bonds are not destroyed and entirely control the behaviour of the soil up to failure. Thus higher limiting stress ratios are sustained than those of the destructured soil. The behaviour of the soil is very stiff and E_{tan}, referring to fig. 5.9c, increases rapidly with the increase of p', up to 1% of strain. There is a linear relationship for all the strain contours plotted in the stress space, which increases rapidly with the increase of p' (fig. 5.10b).

In the second zone (for $70 < p'_0 < 600kPa$), second yield of the bonds is reached first, followed by the maximum stress ratio which occurs at higher stresses. The difference between the bounding surface and the second yield surface increases with the increase of p'. Although the bonds start to get destroyed at failure the bounding surface

of the samples occurs at higher stresses than that of the destructured soil. This suggests that a significant degree of the bonded structure remains after the second yield of the bonds, and partially controls the samples' behaviour at failure. However the limiting stress ratios of the samples are lower than those achieved in the first zone and decrease further with the increase of p', from the one end of the zone to the other. The bonds are thus destroyed progressively and contribute less to the samples' maximum stress ratios.

In this zone, the second yield surface diverts from the bounding surface of the bonded soil and crosses the bounding surface of the destructured samples with the increase of p'. Up to that point the first yield surface increases in shape, while at higher stresses it levels off parallel to the isotropic axis. However for p'>500kPa it turns down towards the latter.

Shearing in the second zone of behaviour has an immediate effect on the tangential stiffness of the samples and the development of strain in respect of the stress paths. At this stress level the slope of the curves of E_{tan} versus p', (fig. 5.9c) decreases to lower values; this is quite distinctive for $E_{0.1\%}$. The slope of the strain contours also decreases to a lower value and the contours then continue to increase in the stress space under an almost constant stress ratio up to p'=500kPa (fig. 5.10b).

In the third zone (for p'_0>600kPa) second yield of the samples occurs at low deviatoric stress compared to failure and the bounding surface is very close to that of the destructured soil. This suggests that by the time that the soil reaches the bounding surface, sufficient straining has already occurred which has destroyed its bonded structure. At this stress level, the first yield surface meets the isotropic axis and the second yield surface reaches its maximum point in the stress space and levels off parallel to the latter.

At this stress level, E_{tan} (up to 0.5% strain) levels off almost parallel to the isotropic axis with the increase of p'. The strain contours also change direction and turn down to the isotropic axis.

Shearing at $p'_o > 700kPa$, the limiting stress ratio of a bonded sample will be governed by the destructured condition, the first yield will occur in isotropic consolidation and the second yield will occur under a constant deviator stress. The second yield surface is however expected to turn down and meet the isotropic axis at a higher stress level (p'). This stress level would define the upper limit for the third zone. For higher stresses a fourth zone will govern the soil's behaviour, where first and second yield of the bonds will occur in isotropic consolidation and the soil will sustain the same limiting stress ratios as those of the destructured soil sheared at the same stress level.

5.8.3 Final and second yield surfaces for the bonded soil

The last graph is replotted in fig. 5.38 and the final yield surface defined for the drained and undrained strain controlled tests is also included. The results for the position of the final yield surface close to the bounding surface agrees with previous test results on bonded soils, presented by Maccarini (1987), Bressani (1990) and Smith (1992). However it is interesting to see that zone 2, which is a transitional zone of behaviour, is masked when only the final yield of the bonds is determined and thus is regarded to have the same characteristics as those of the first zone of behaviour. However the importance of this zone is quite significant as the soil's behaviour at failure is only partially controlled by its bonded structure, unlike zone 1 where the soil's behaviour is entirely controlled by the bonds. As was previously discussed, the slope of the bounding surface in this zone decreases to a lower value and turns closer to that of the destructured soil, with an increase of p'. Thus if the second yield surface is not defined, the behaviour of the bonded soil

can be overestimated, as the post yield influence of the bonded structure to the samples strength might not be clarified.

It should also be noted, that test results from various natural bonded soils indicated a transitional zone of behaviour (see fig. 2.10a and b and 2.14) even when only the final yield surface was defined. However, this zone has not been addressed in the literature. Only Atkinson and Coop (1990) presented test results on natural and reconstituted calcarenite samples and pointed out the fact that this zone also might exist.

Therefore the method of determining the second yield surface is shown to be quite essential for the better understanding of the bonded soil's behaviour under shear.

5.8.4 Final remarks

In this chapter the behaviour of the bonded and destructured soil was examined under undrained shear in triaxial compression. The bonded soil presented higher maximum q/p' ratios, higher values of stiffness, higher development of axial strain in respect of the stress paths, in comparison to those of the destructured material due to its bonded structure (see fig. 5.19, 5.20 and 5.21 respectively). However the bond strength decreased progressively at failure with the increase of mean effective stress, as the bonds yielded at lower deviatoric stress. Thus the behaviour of the bonded soil under drained and undrained shearing was represented by three zones in the stress space, based on the stress level (fig. 5.37).

The max q/p' ratios, the development of stiffness and axial strain of the bonded soil were directly related to the zone of behaviour in which shearing takes place. Thus the max q/p' ratios (fig. 5.37) and the slopes of the initial E_{tan} versus p' (fig. 5.9c) and the strain contours (fig. 5.10b) decreased to lower levels by passing from one zone to the other. For $p'>800kPa$, the soil's behaviour became similar to that of

the destructured soil, in respect of the limiting stress ratios that can be sustained in the stress space.

The second yield, determined from the second major loss in E_{tan}, was shown to be more efficient for the better understanding of the bonded soil's behaviour than the final yield of the bonds, defined close to the bounding surface. The position of the second yield surface clarified the transitional zone of behaviour (zone 2), where some post yield influence of the bonds dominates the soil's behaviour at failure (fig. 5.38).

The behaviour of the bonded and destructured soil was unaffected by the type of drainage and the method of shearing control for the particular stress and strain rates used. Good agreement was found between the results obtained from drained and undrained tests carried out on bonded samples, in respect of the bounding surface (fig. 5.32a), of the phase transformation line (fig. 5.32b) and of the first and second yield surfaces (fig. 5.33).

Tests results for sand/kaolin mixtures stressed the importance of testing the true destructured material at the same grading and with the same nature as the bonded soil, in order to clarify the effects of bonding to the latter.

Strain Controlled Tests

Test	Initial void ratio e_0	Consolidation pressure (kPa)
unb35	0.596	35
unb70	0.598	70
unb100	0.597	100
unb150	0.598	150
unb250	0.597	250
unb300	0.603	300
unb400	0.600	400
unb500	0.602	500 ·
unb600	0.600	600
unb650	0.603	650

Stress Controlled Tests

Test	Initial void ratio e_0	Consolidation pressure (kPa)
unb2	0.600	2
unb5	0.598	5
unb11	0.598	11
unb57	0.602	57
unbs100	0.603	100
unb155	0.603	155
unb205	0.602	205
unb260	0.600	260

Table 5.1 Details for the undrained triaxial tests on bonded samples

Test	Initial void ratio e_0	Consolidation pressure (kPa)
und5	0.596	5
und35	0.598	35
und70	0.599	70
und100	0.600	100
und200	0.597	200
und300	0.602	300
und400	0.604	400 .
und500	0.596	500
und600	0.601	600
und650	0.602	650

Table 5.2 Details for the undrained triaxial tests on destructured sample

Test	Initial void ratio e_0	Consolidation pressure (kPa)
unsk5	0.597	5
unsk40	0.601	40
unsk58	0.601	58
unsk100	0.598	100
unsk250	0.606	250
unsk300	0.597	300
unsk400	0.602	400
unsk500	0.596	500

Table 5.3 Details for the undrained triaxial tests on sand-kaolin samples
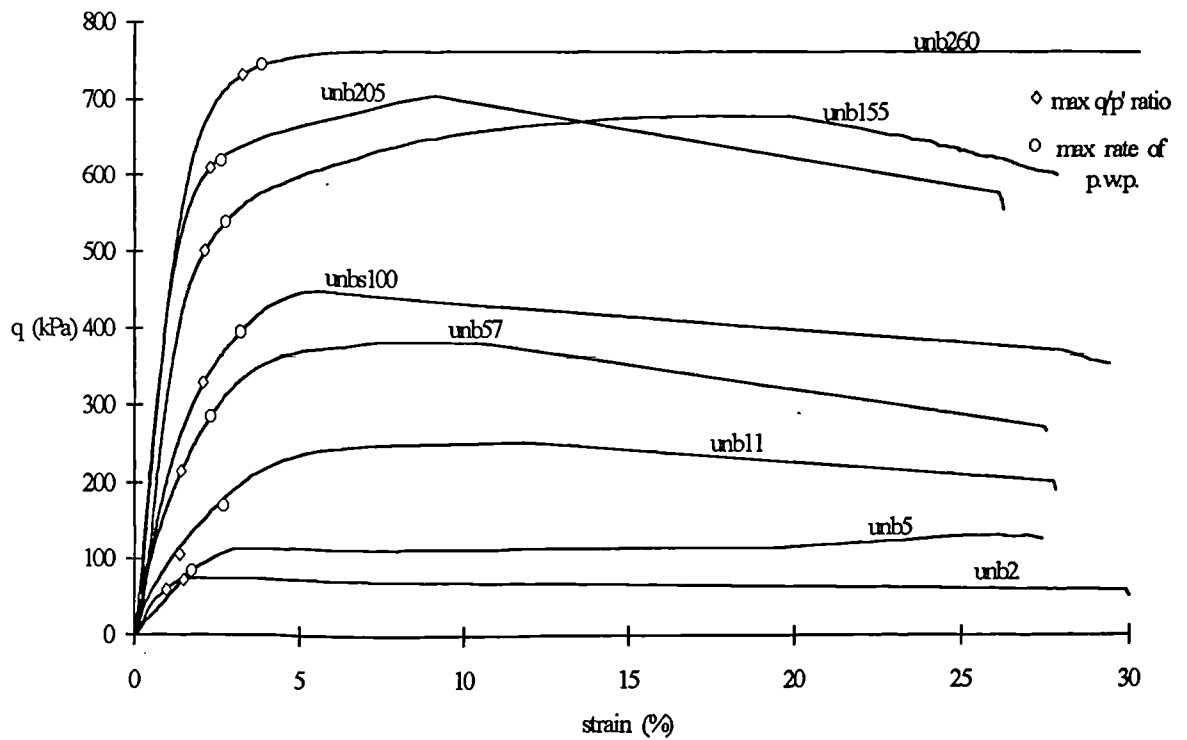
Fig. 5.1a   Maximum q/p' ratio and maximum rate of change of p.w.p. for the stress controlled tests
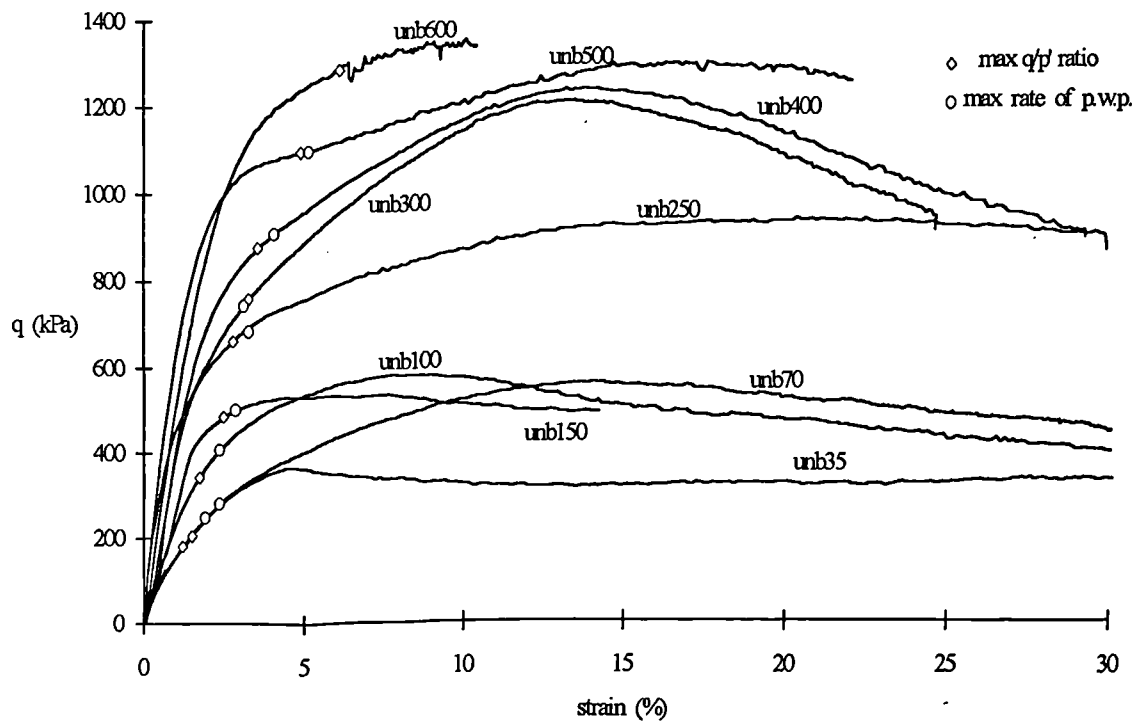
Fig. 5.1b   Maximum q/p' ratio and maximum rate of change of p.w.p. for the strain controlled tests
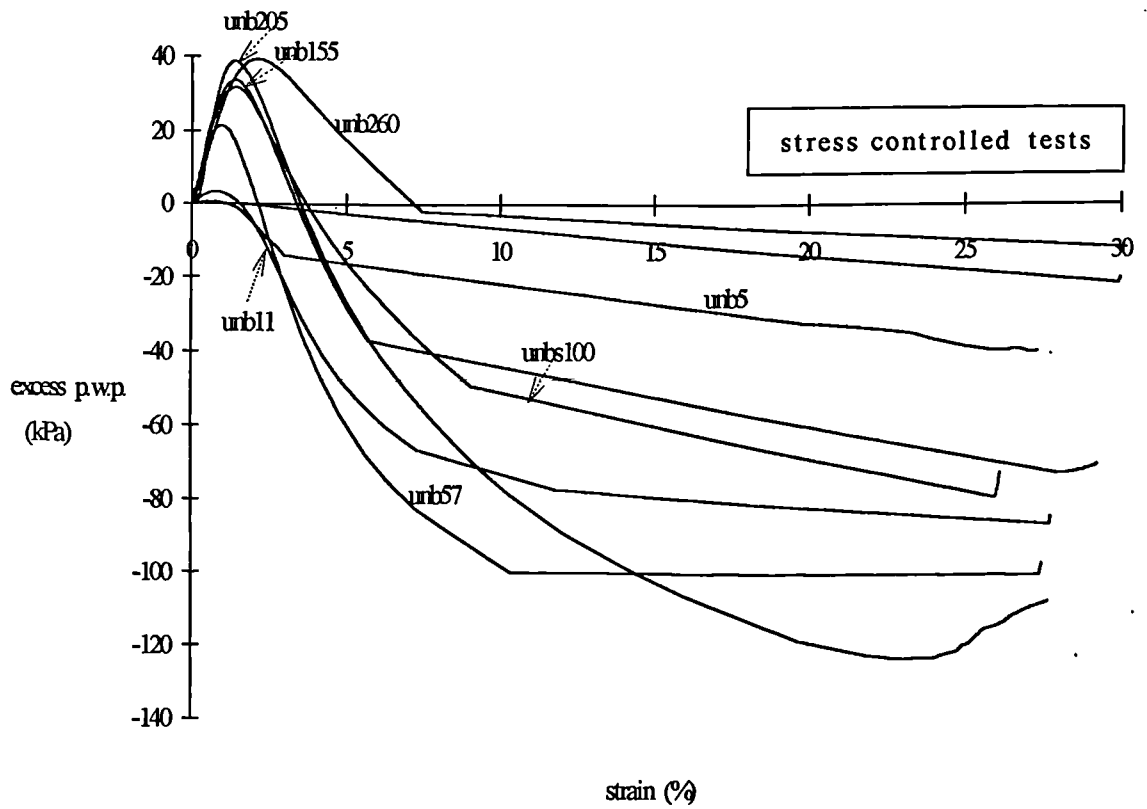
Fig. 5.2a Excess p.w.p. versus axial strain for the stress controlled tests
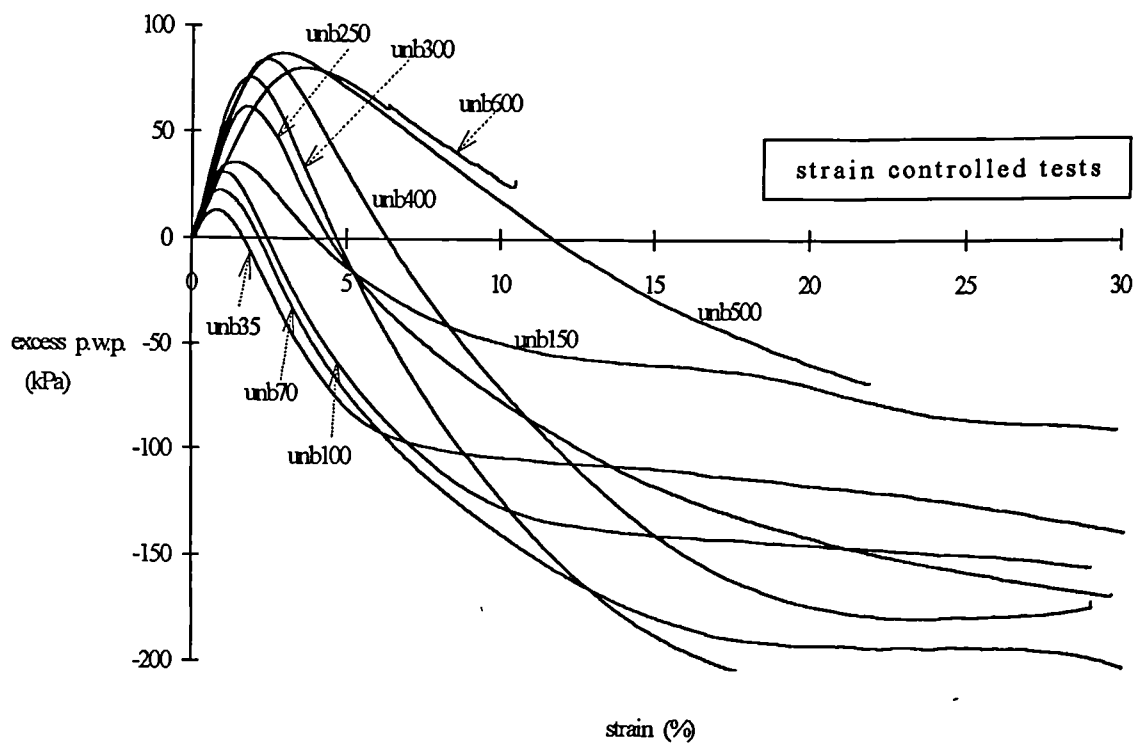
Fig. 5.2b Excess p.w.p. versus axial strain for the strain controlled tests
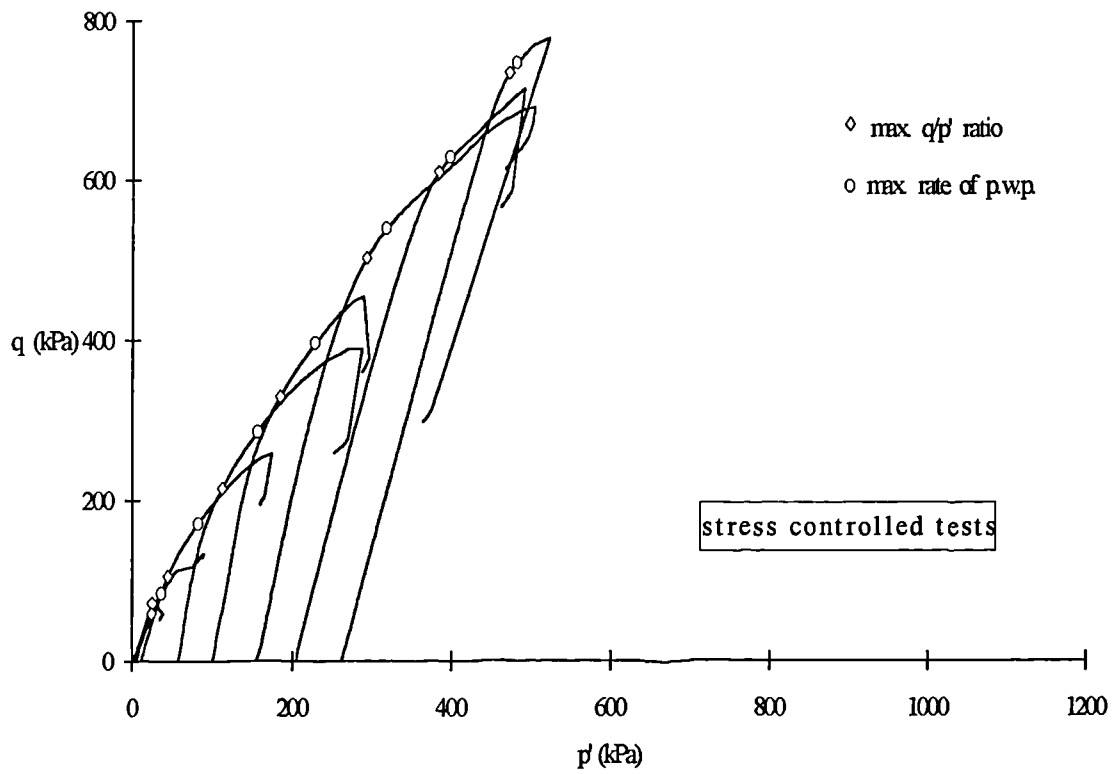
Fig. 5.3a Maximum q/p' ratio and rate of change of p.w.p.
for the stress controlled tests
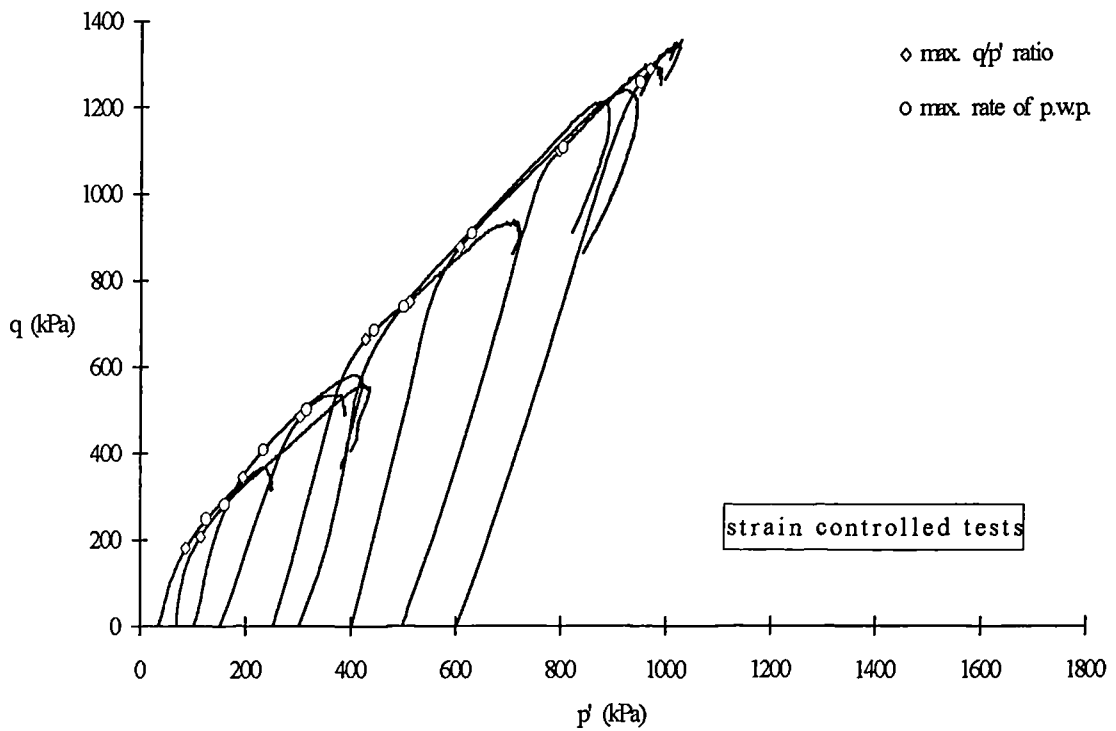
Fig. 5.3b Maximum q/p' ratio and rate of change of p.w.p.
for the strain controlled tests

136
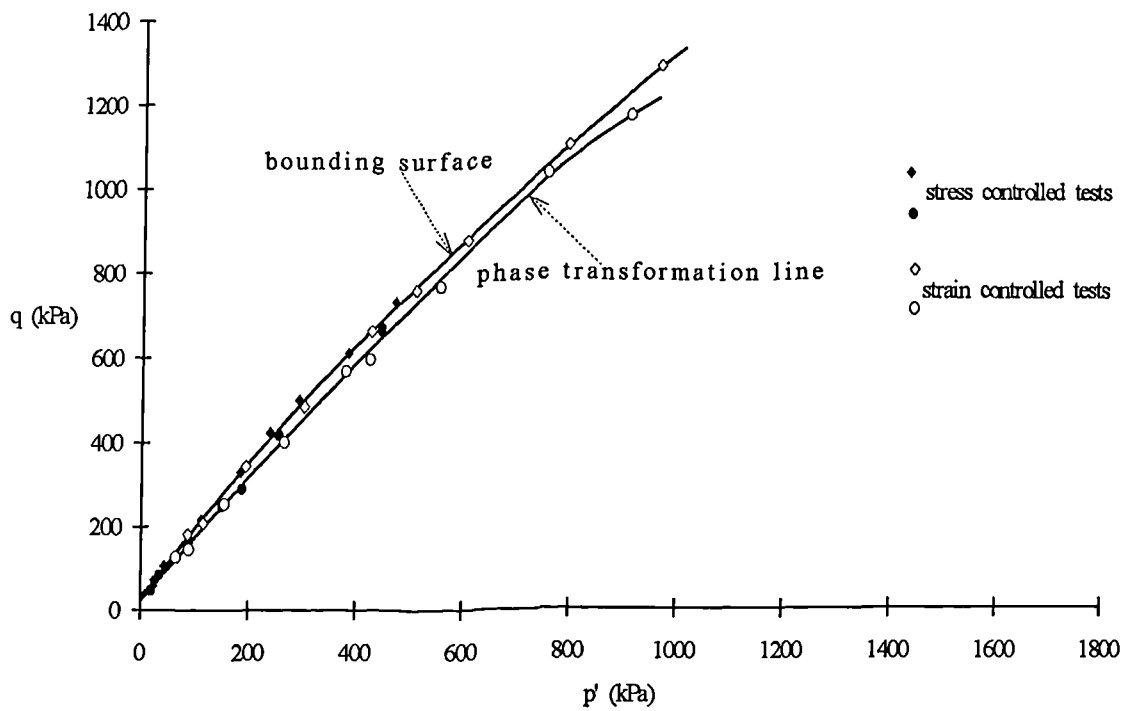
Fig. 5.4 Bounding surface and phase transformation line for the bonded soil
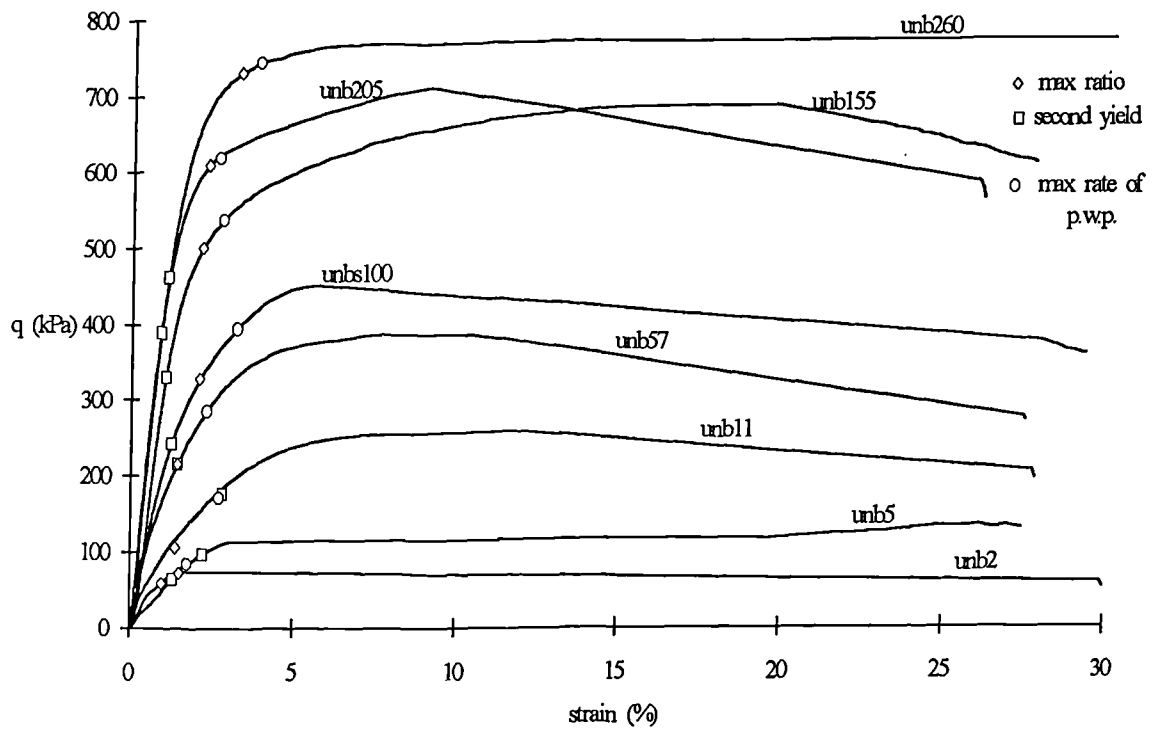
Fig. 5.5a Stress-strain curves showing second yield, max q/p' ratio and rate of change of p.w.p. for the stress controlled tests

137
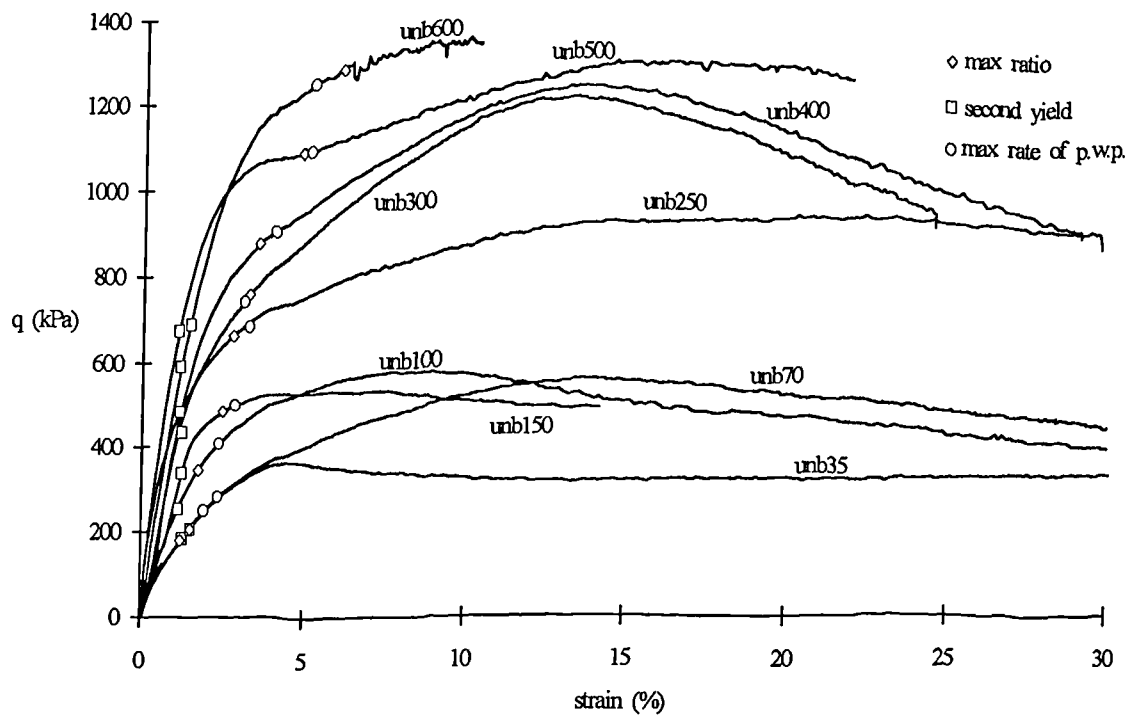
Fig. 5.5b   Stress-strain curves showing second yield, max q/p' ratio and rate
of change of p.w.p. for the strain controlled tests
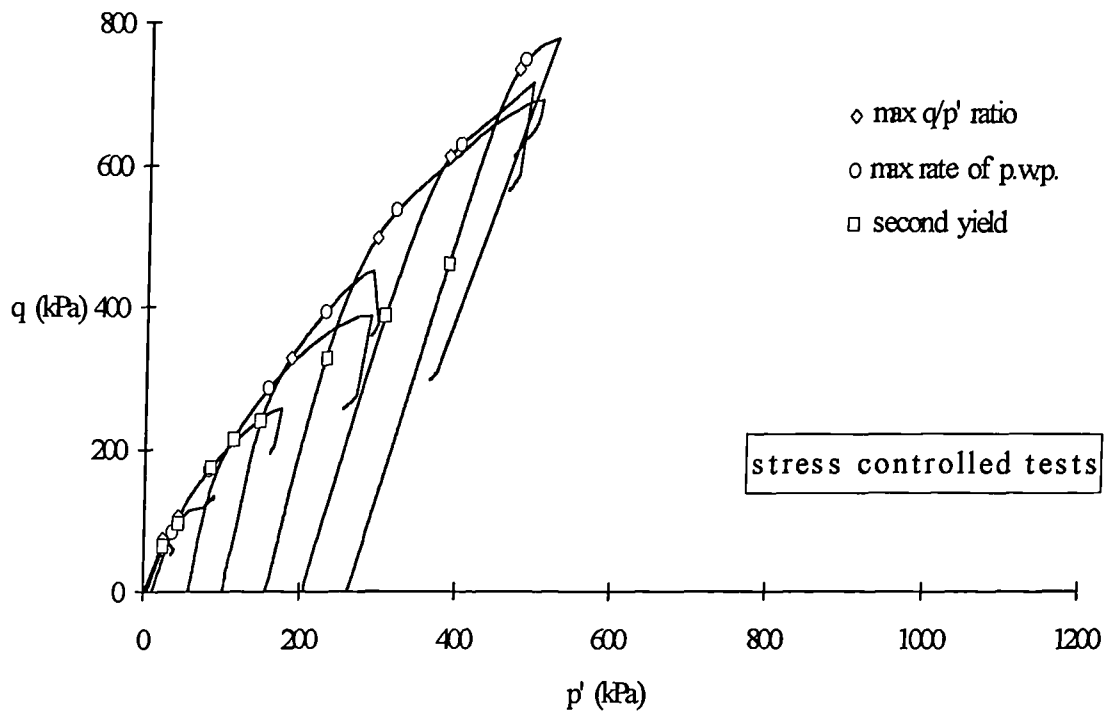
Fig. 5.6a   Stress paths showing second yield, max q/p' ratio and rate
of change of p.w.p. for the stress controlled tests
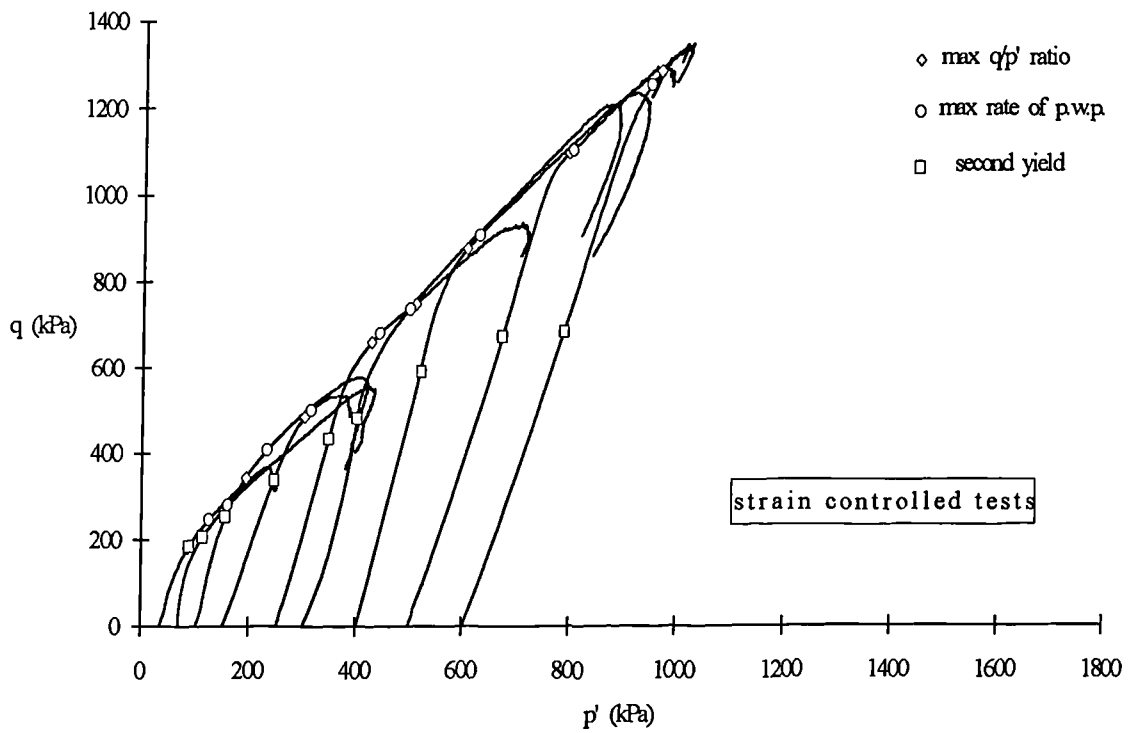
Fig. 5.6b   Stress paths showing second yield, max q/p' ratio and
rate of change of p.w.p. for the strain controlled tests
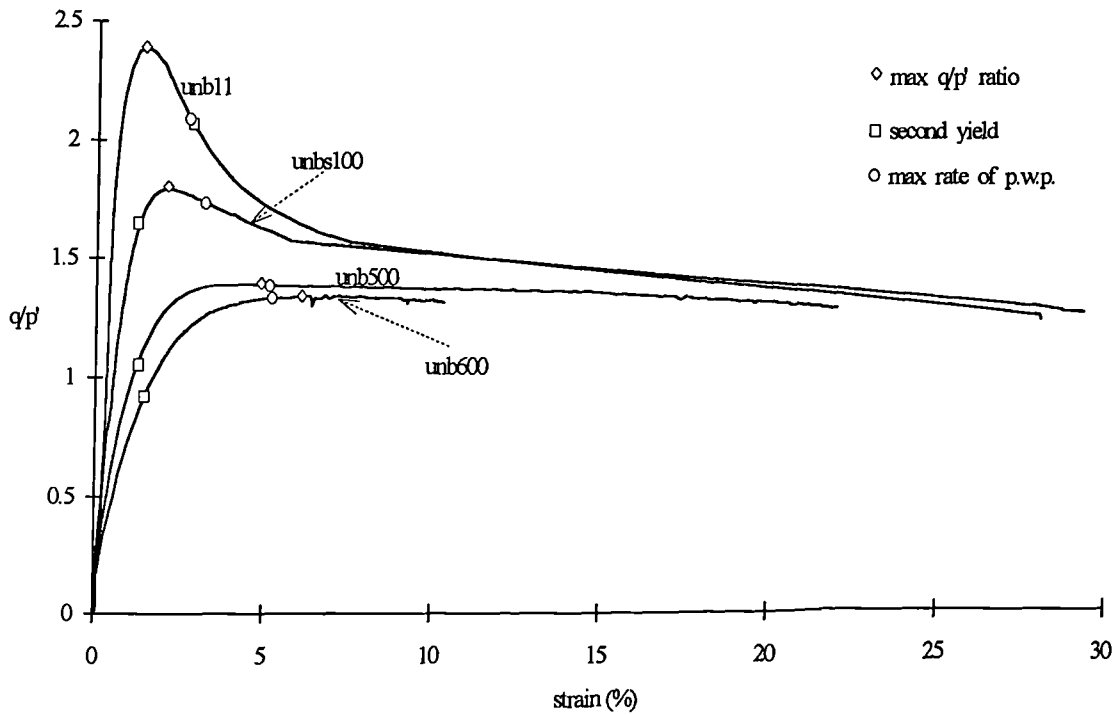
Fig. 5.7   Stress ratio versus axial strain for four tests sheared at different
confining stresses
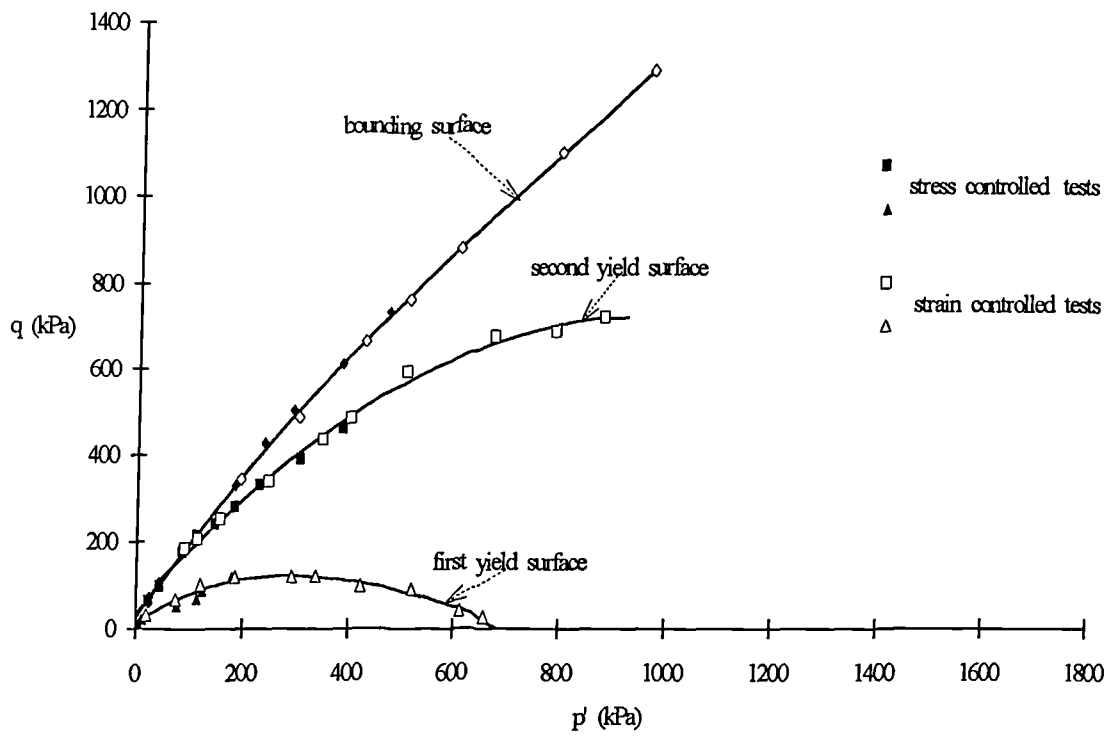
Fig. 5.8a Bounding surface and the two yield surfaces for
the bonded samples
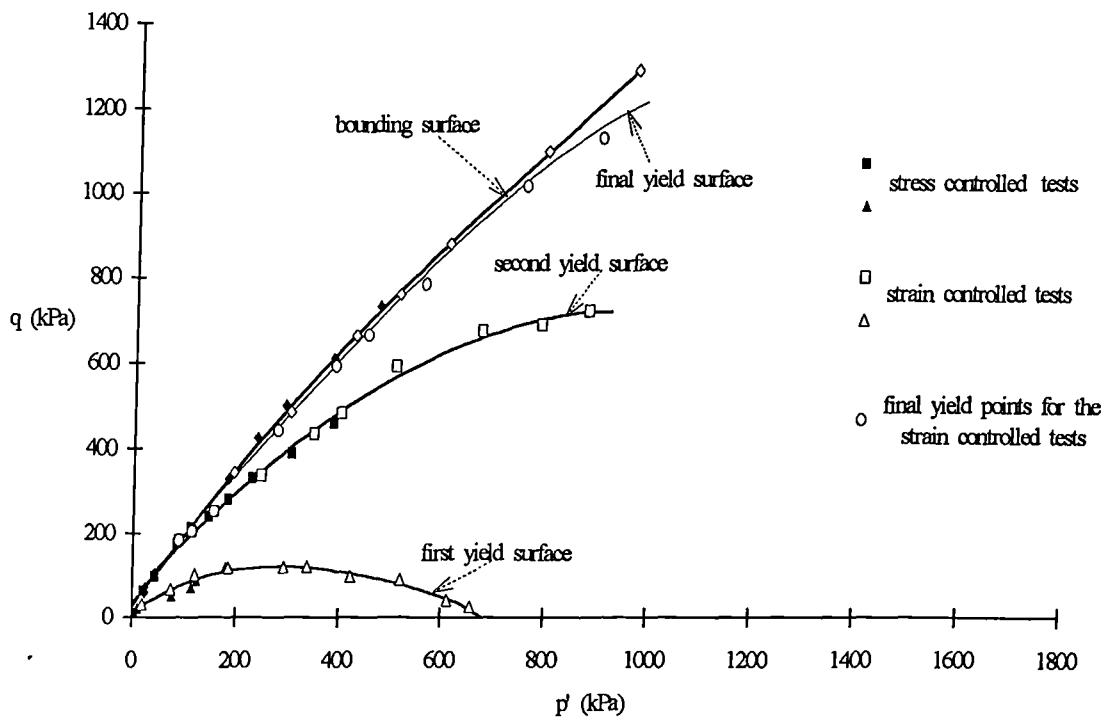
Fig. 5.8b Bounding surface and three yield surfaces for
the bonded samples

140
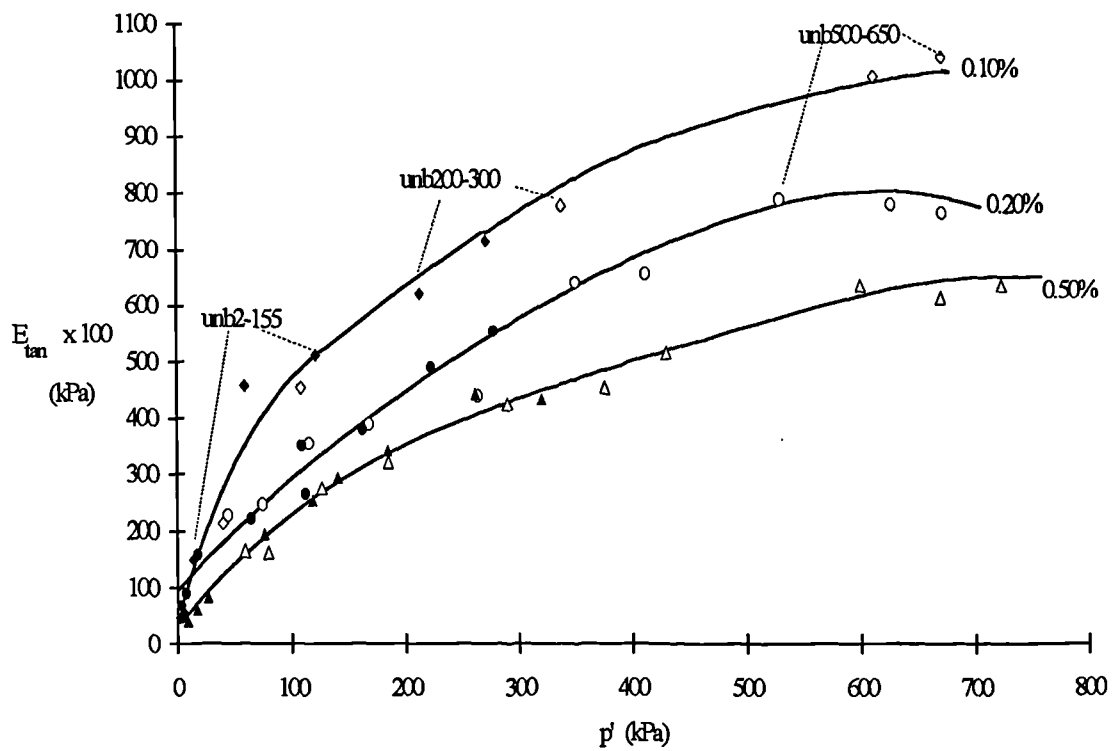
Fig. 5.9a Tangential stiffness versus p', for 0.1%, 0.2% and 0.5% of strain
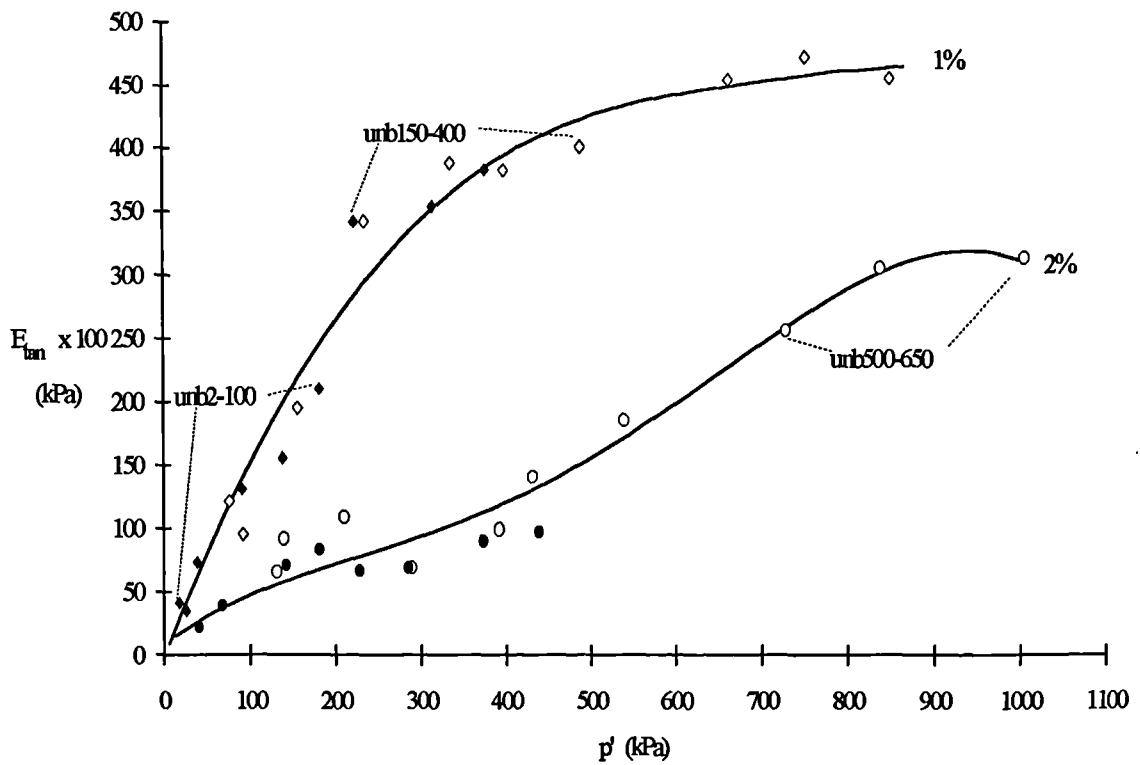
Fig. 5.9b Tangential stiffness versus p' for 1% and 2% of strain
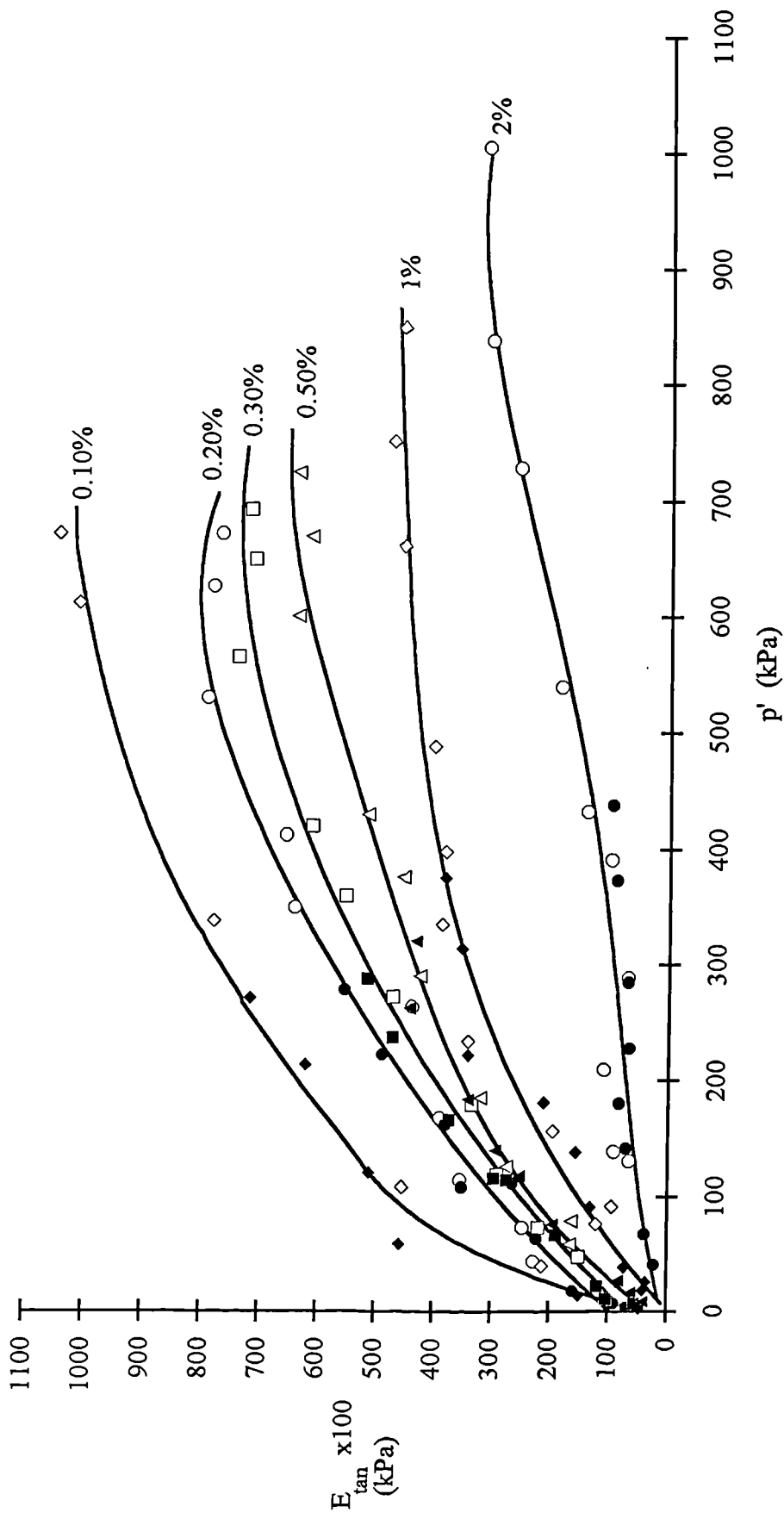
Fig. 5.9c Loss in tangential stiffness with the increase of axial strain for the bonded samples

142
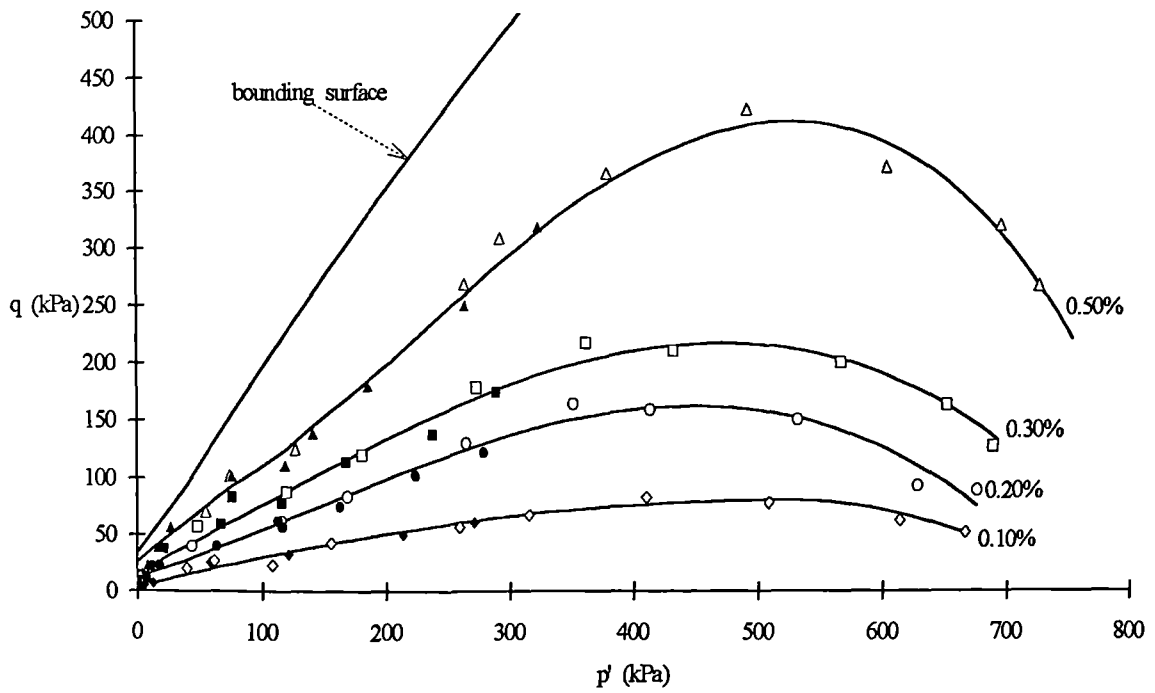
Fig. 5.10a Bounding surface and 0.1%-0.5% strain contours plotted in the stress space for the bonded samples
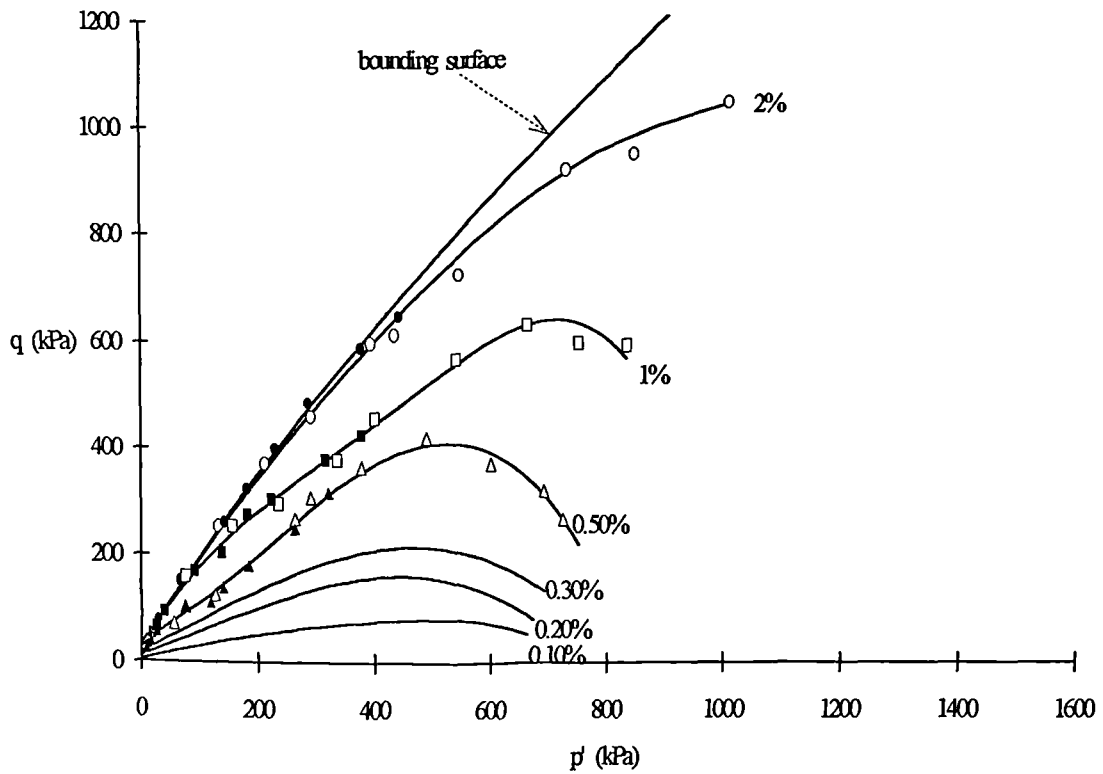
Fig. 5.10b Bounding surface and strain contours for the bonded soil

143
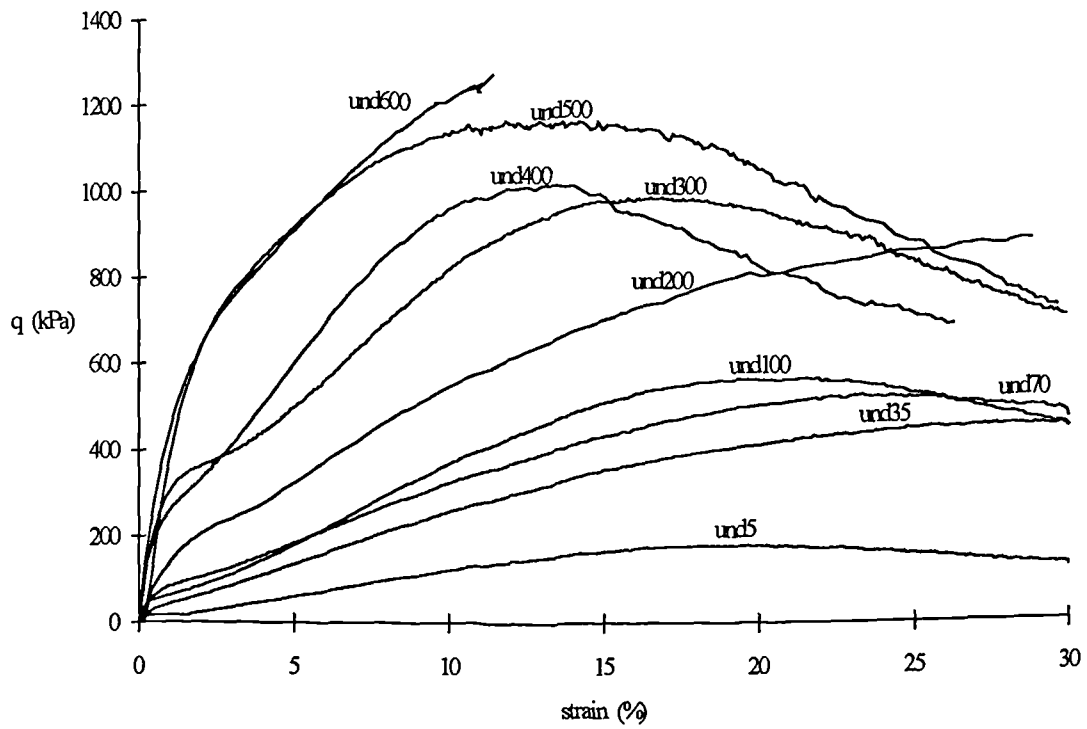
Fig. 5.11a   Stress-strain curves from the undrained triaxial tests
on the destructured soil
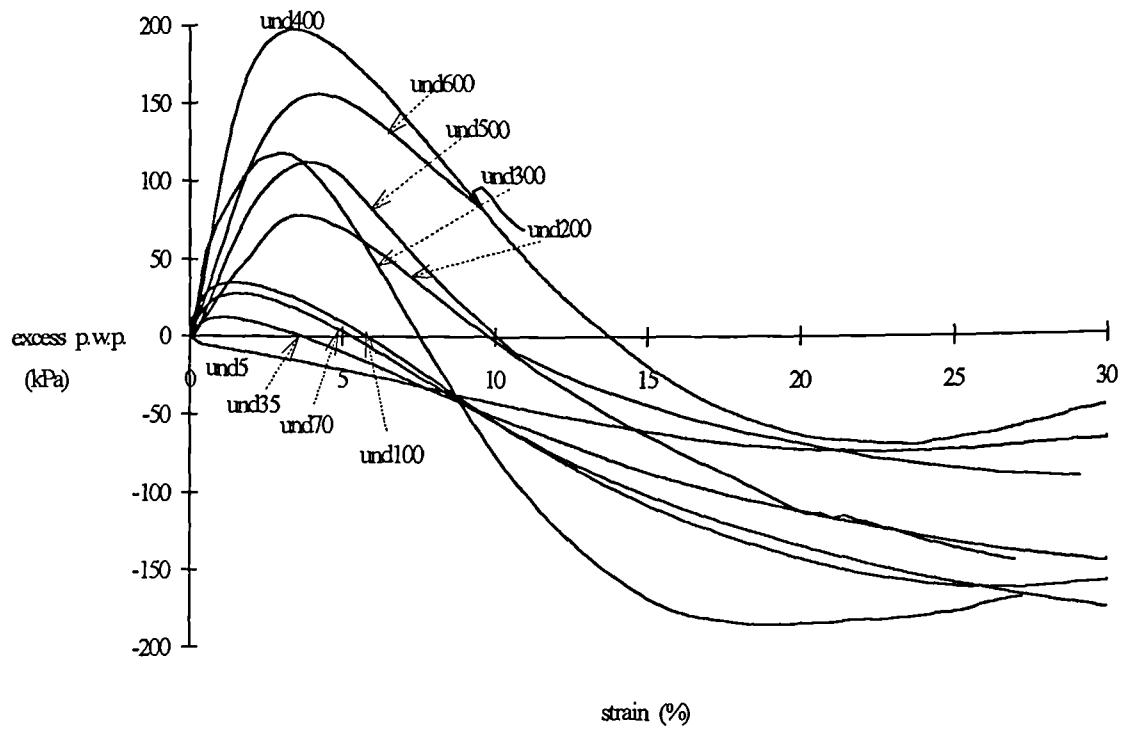
Fig. 5.11b   Excess pore water pressures versus axial strain
for the undrained tests

144
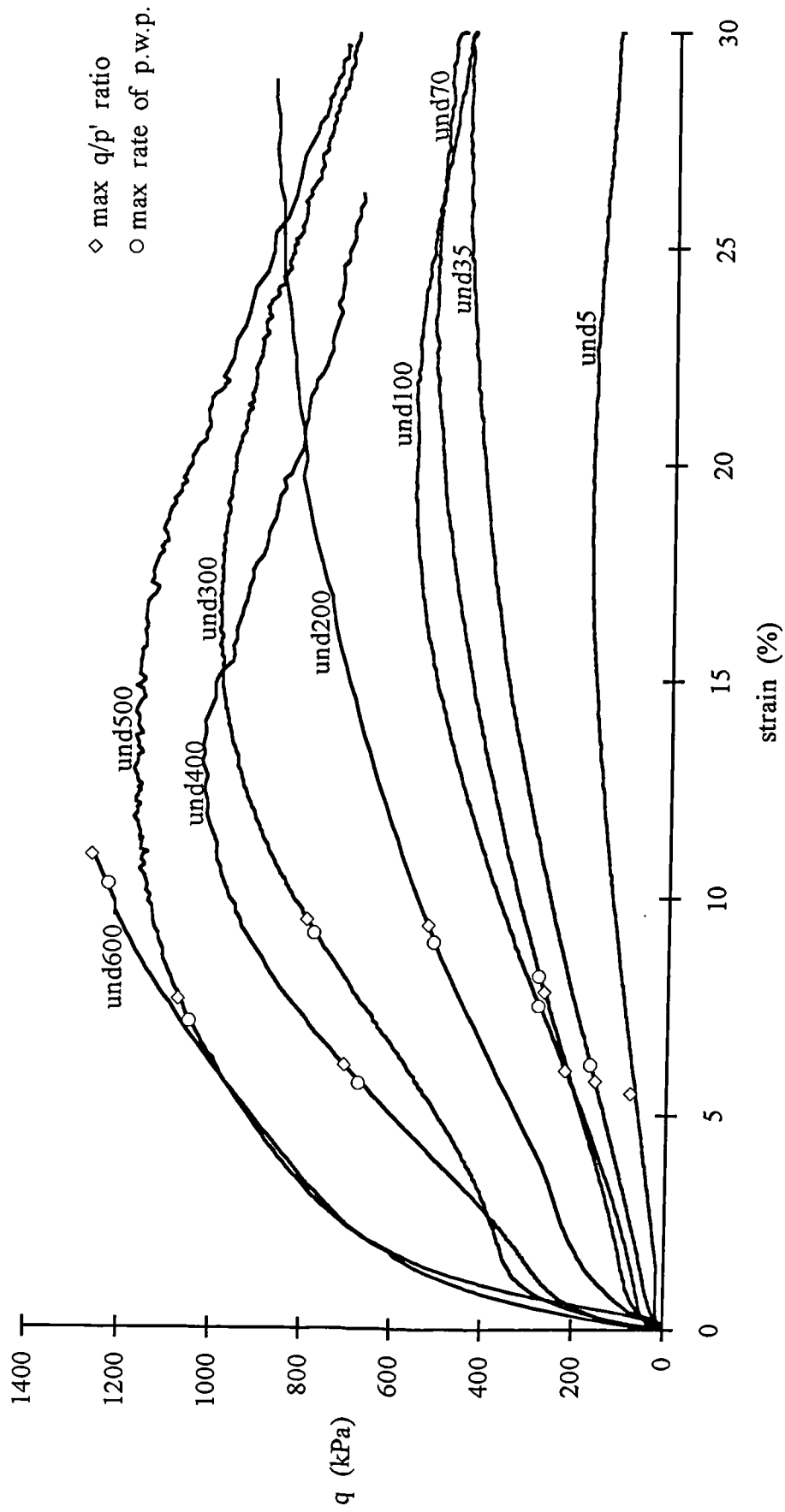
Fig. 5.12 Maximum q/p' ratio and maximum rate of p.w.p. for the destructured samples

145
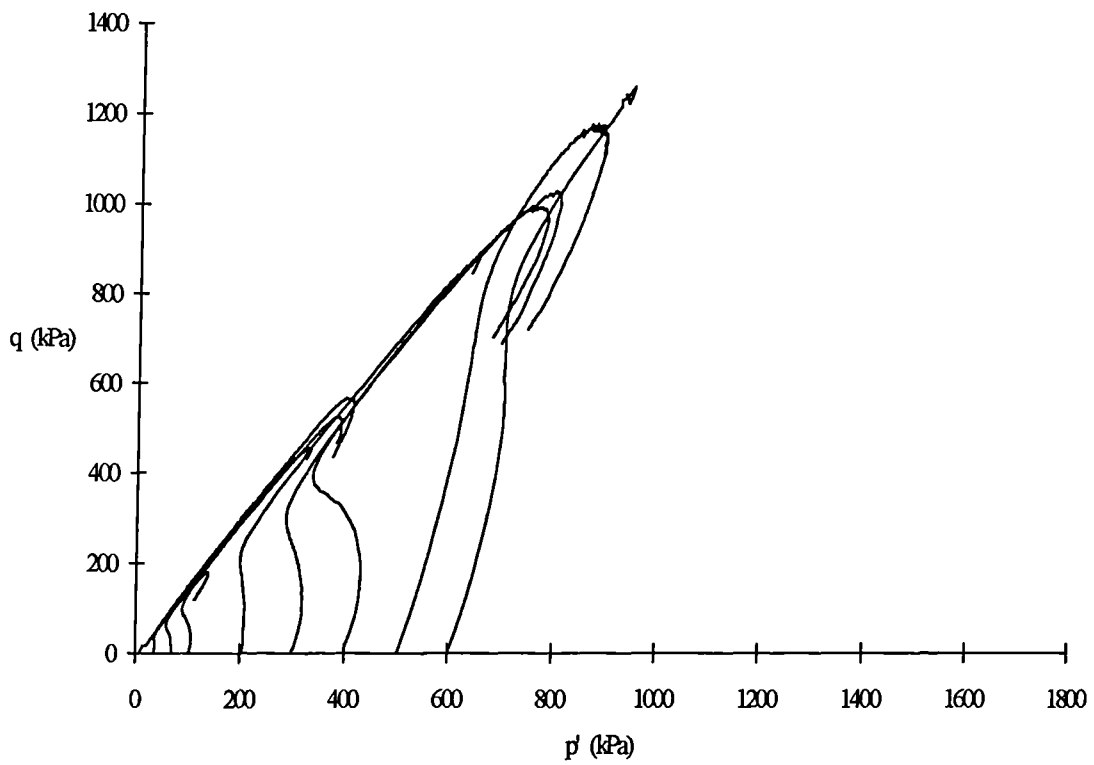
Fig. 5.13 Effective stress paths for the undrained triaxial tests
on the destructured soil
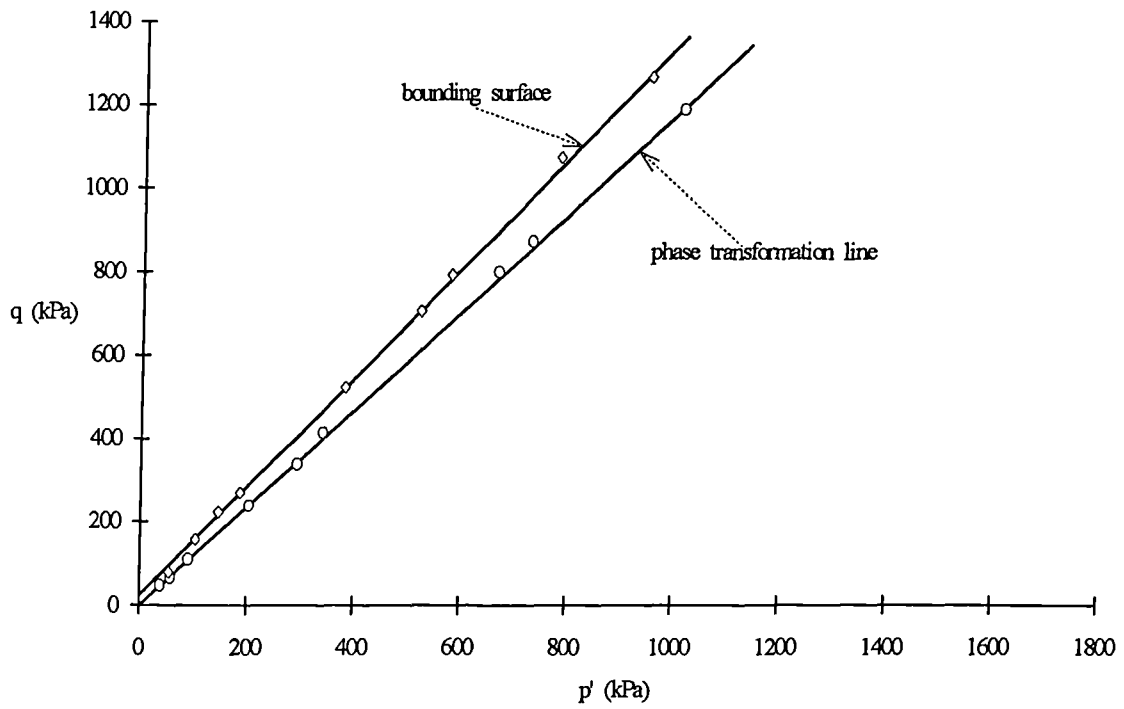
Fig. 5.14 Bounding surface and phase transformation line
for the destructured soil
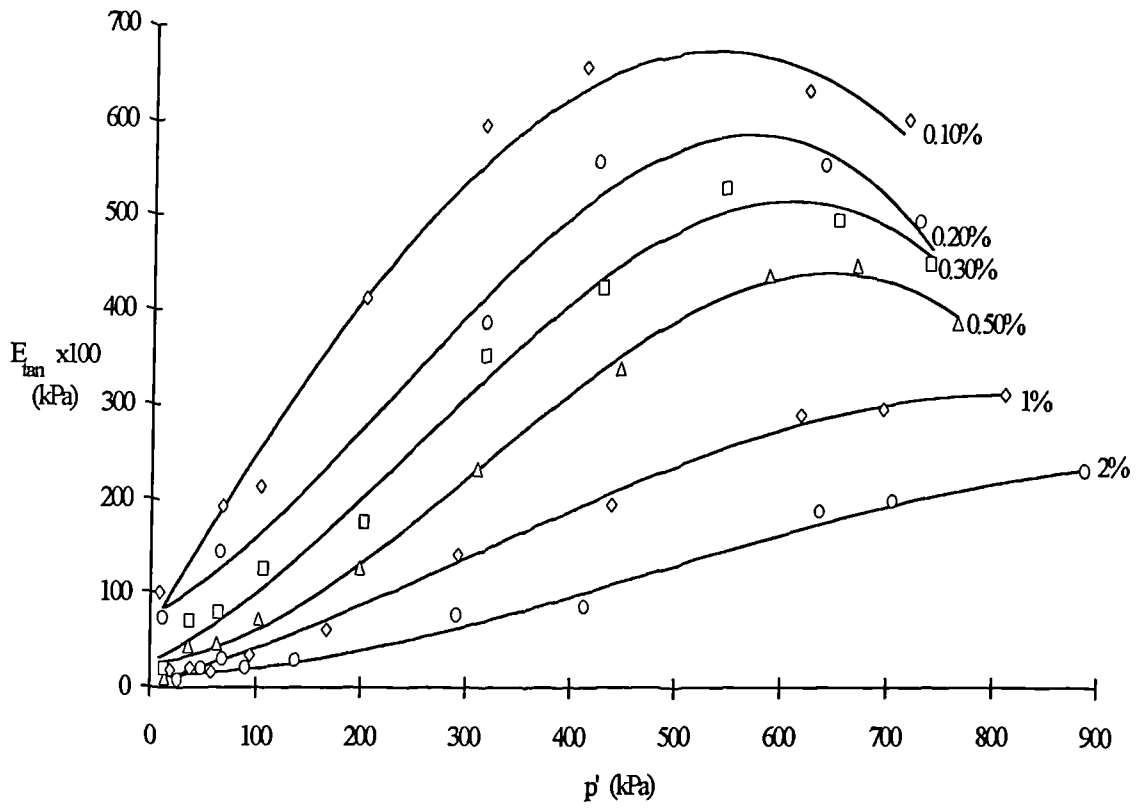
Fig. 5.15 Tangential stiffness versus p' for the destructured samples
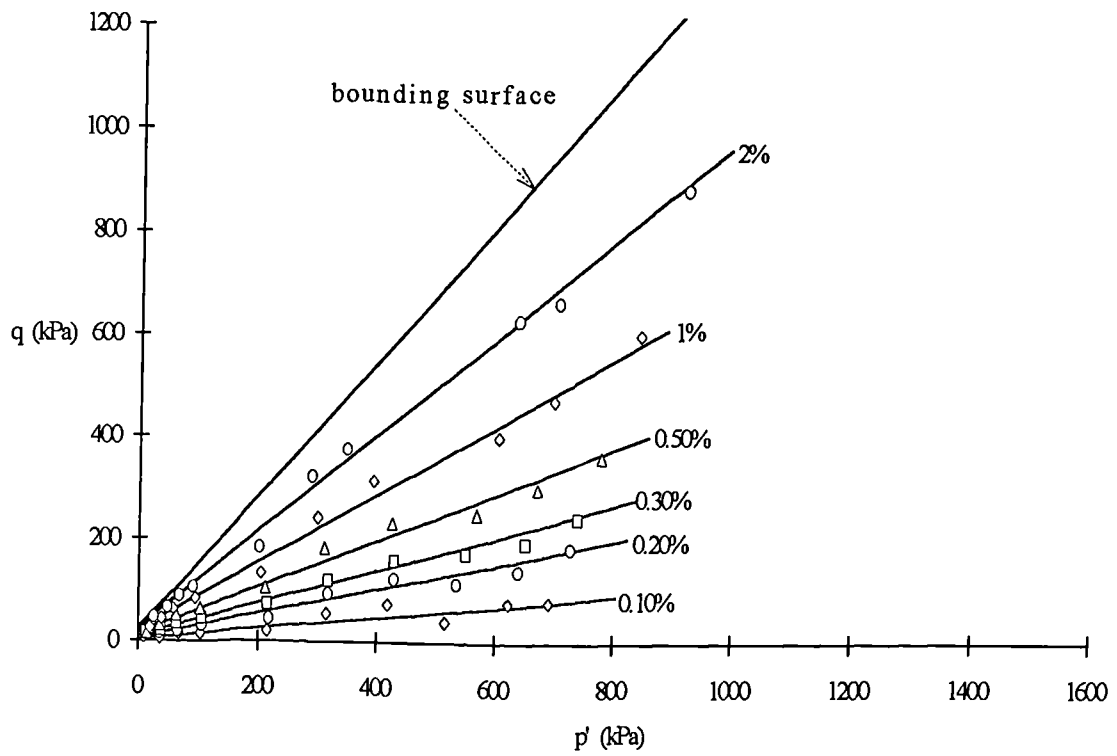
Fig. 5.16 Bounding surface and strain contours for the destructured samples

147
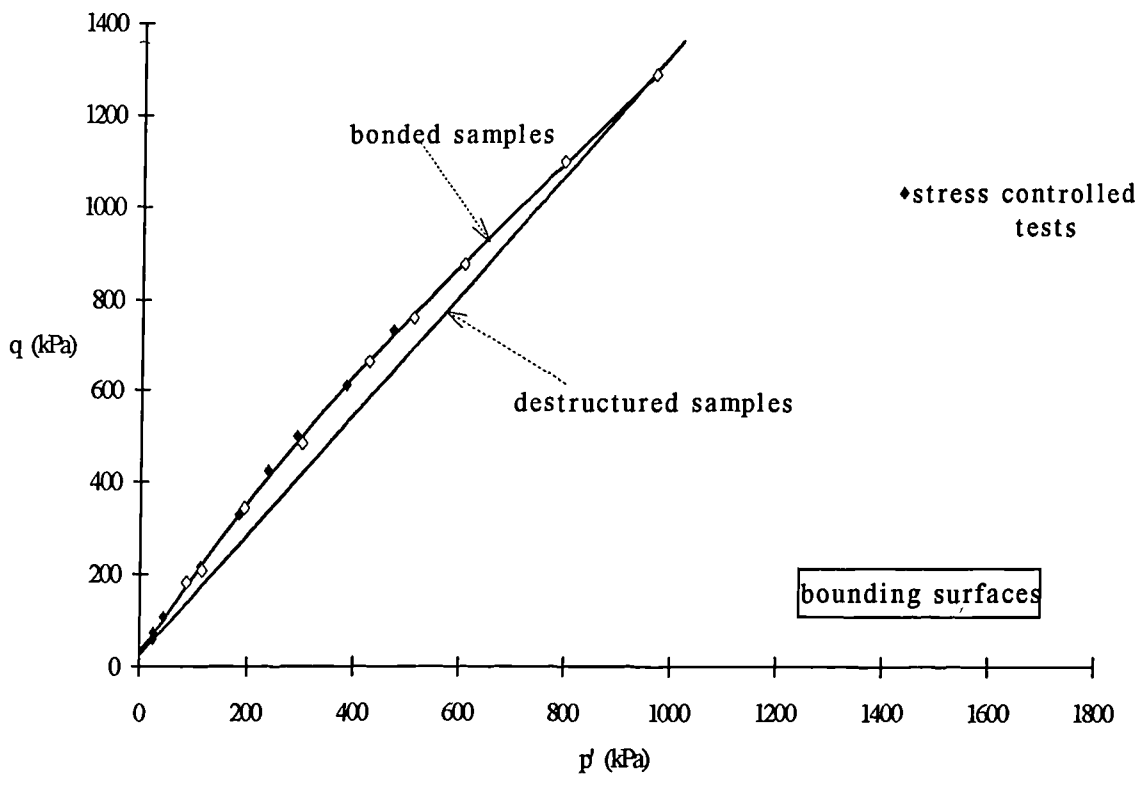
Fig. 5.17 Bounding surfaces for the bonded and the destructured samples
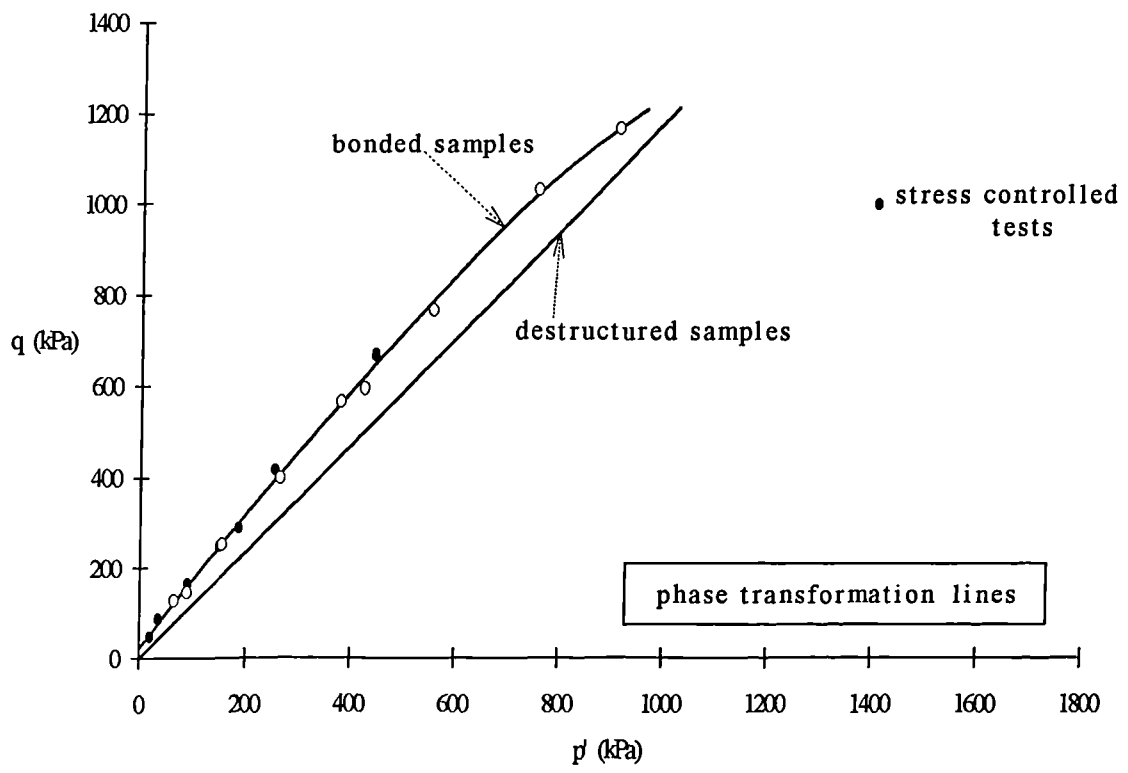
Fig. 5.18 Phase transformation lines for the two soils
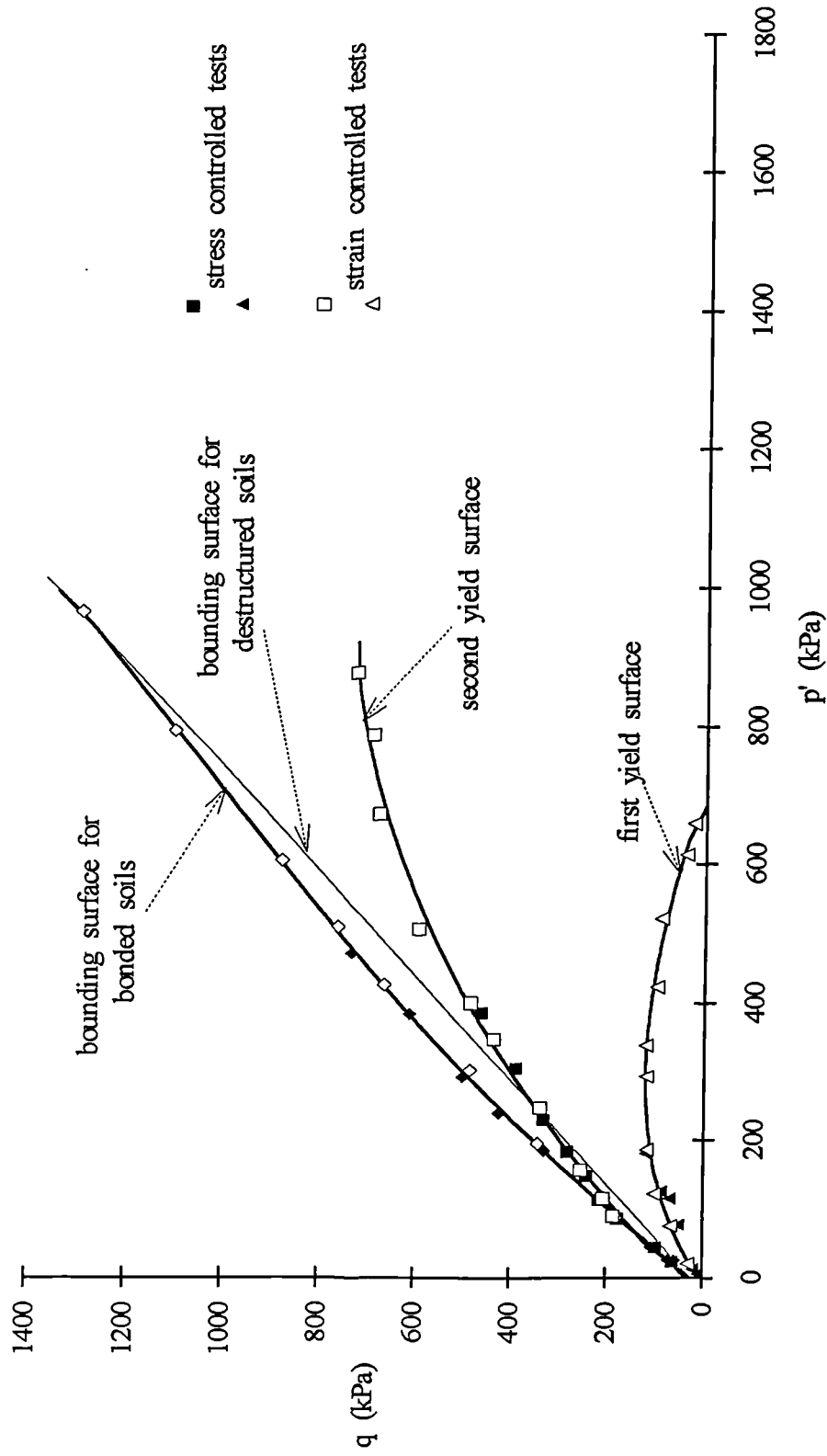
Fig. 5.19 First and second yield surfaces plotted with the bounding surfaces for the two soils after undrained triaxial tests
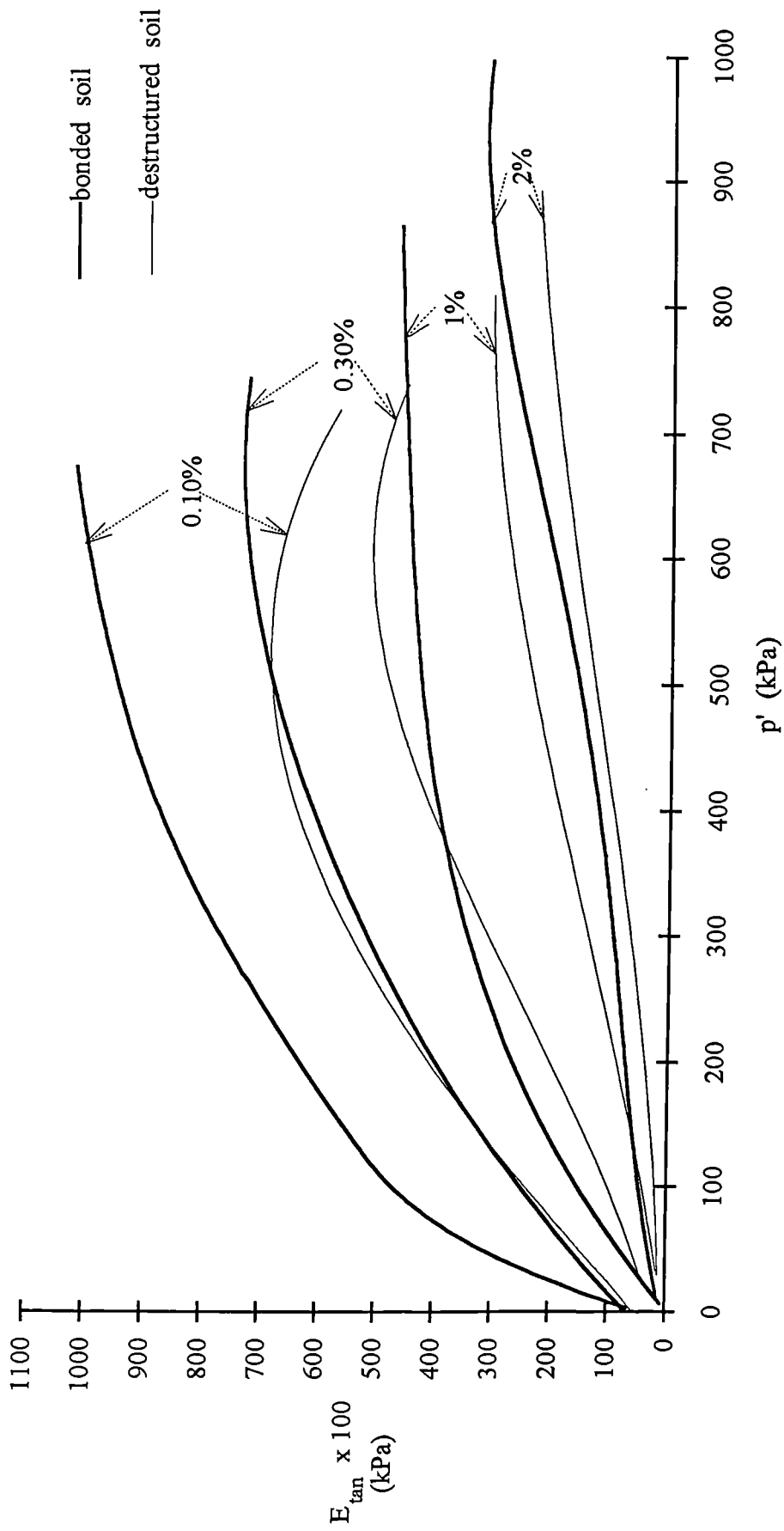
Fig. 5.20 Tangential stiffness versus p' for the two soils after undrained triaxial tests

150
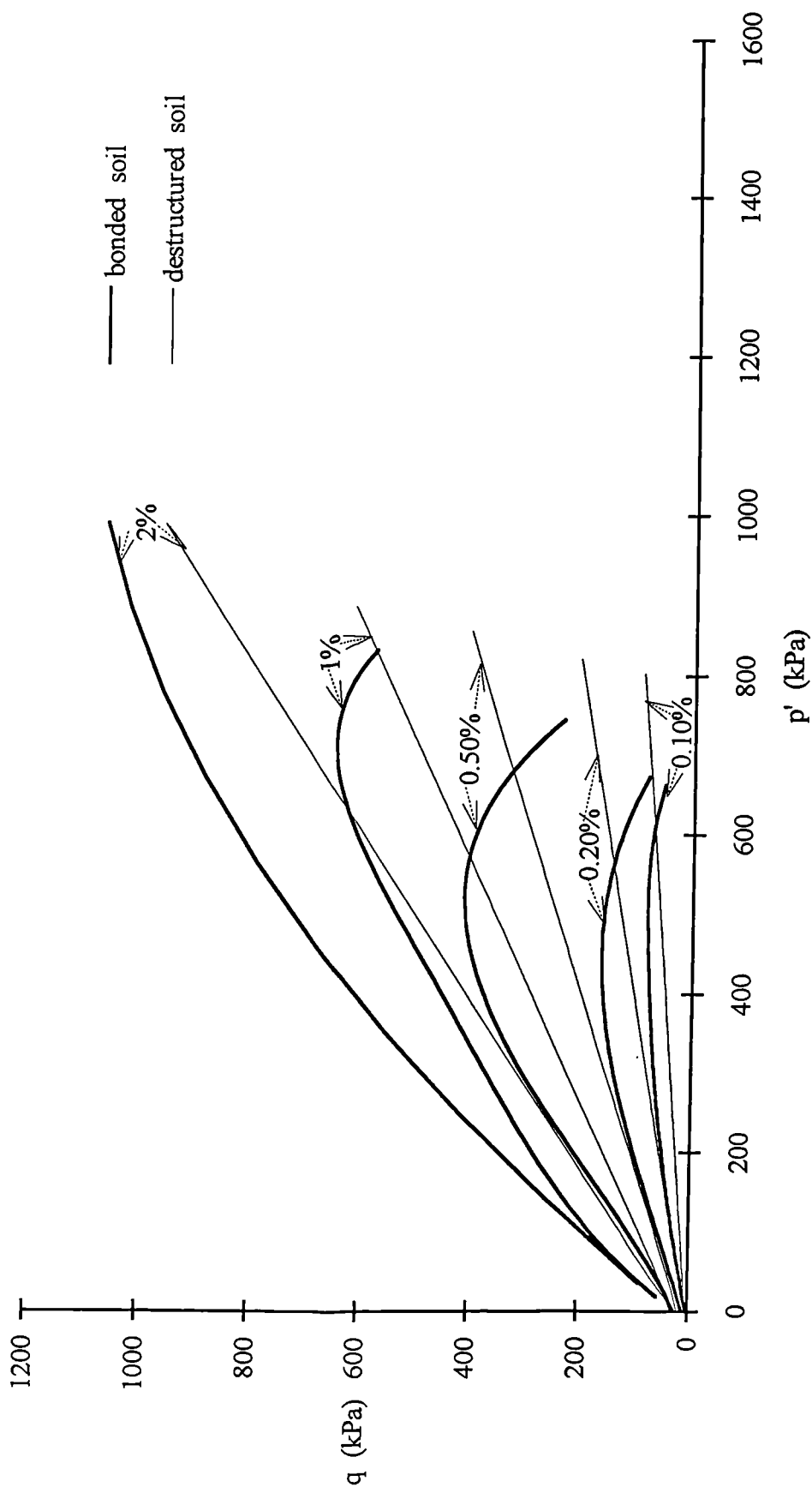
Fig. 5.21 Strain contours for the two soils plotted in the stress space

151
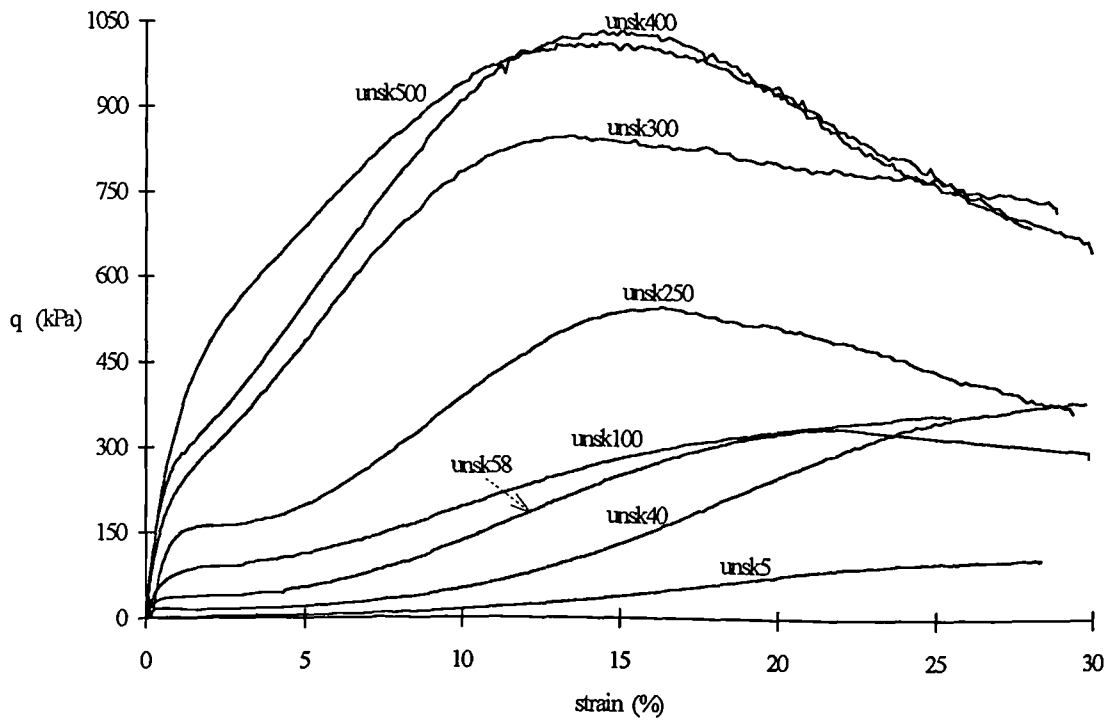
Fig. 5.22a Stress strain curves from the undrained triaxial tests
on the sand-kaolin samples
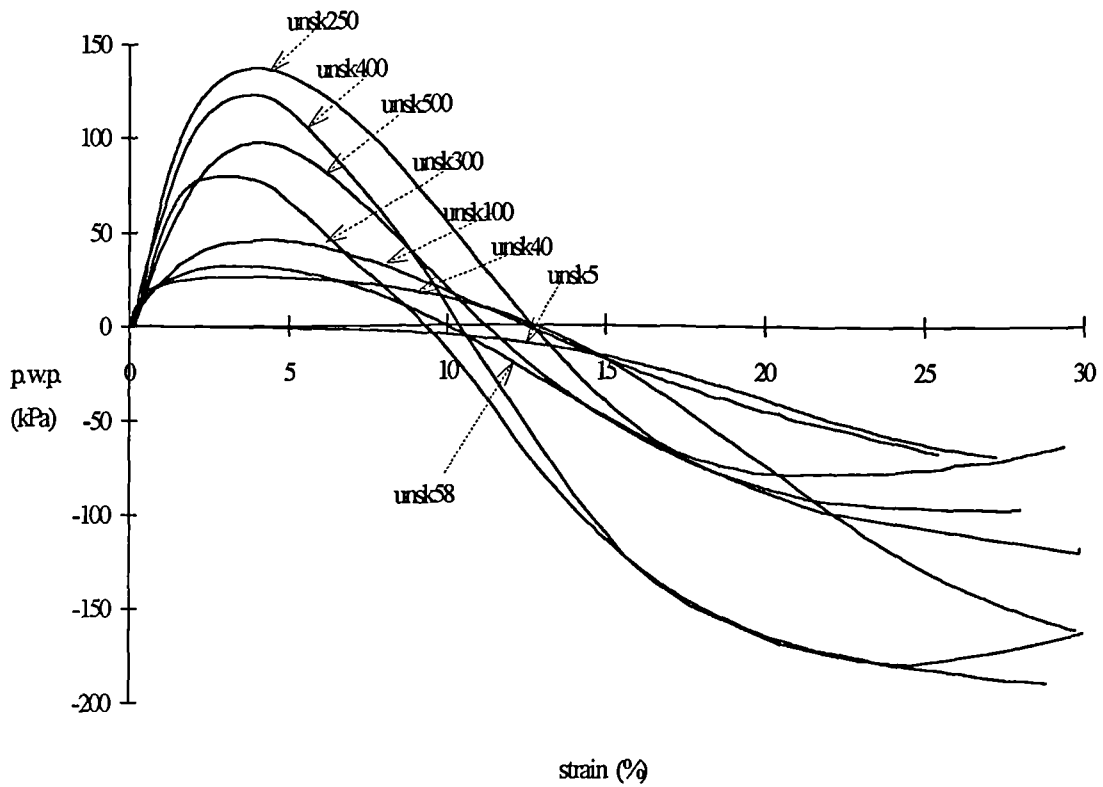
Fig. 5.22b Excess p.w.p. versus axial strain for the sand-kaolin samples
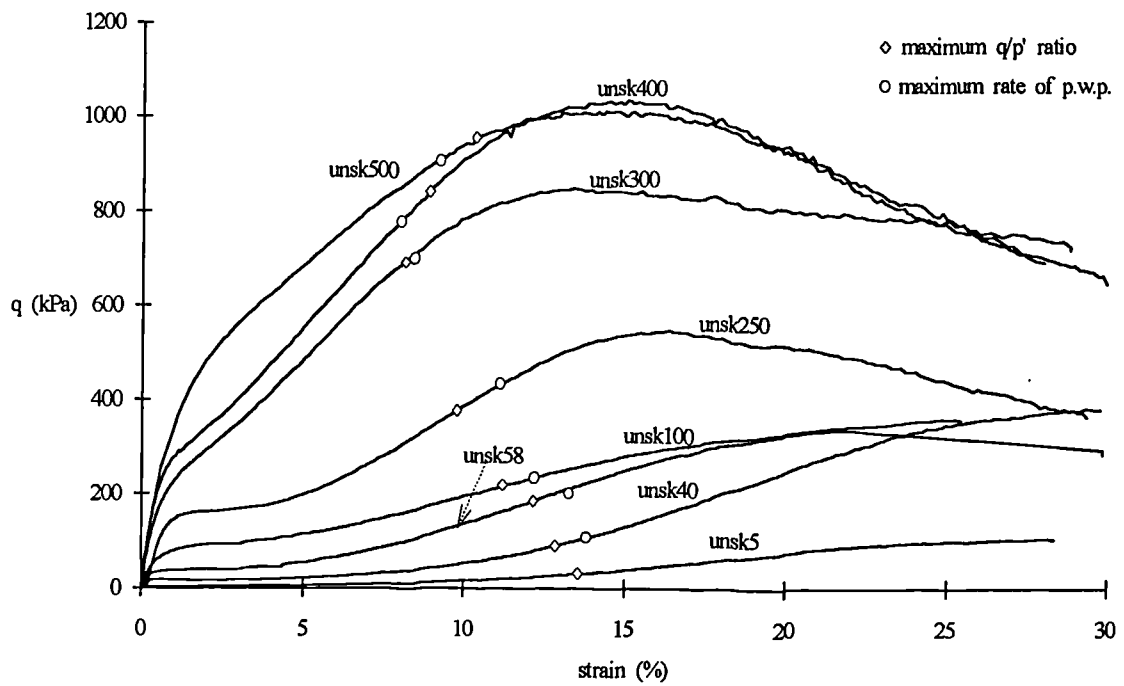
Fig. 5.23 Maximum q/p' ratio and rate of change of p.w.p. for
the sand-kaolin samples
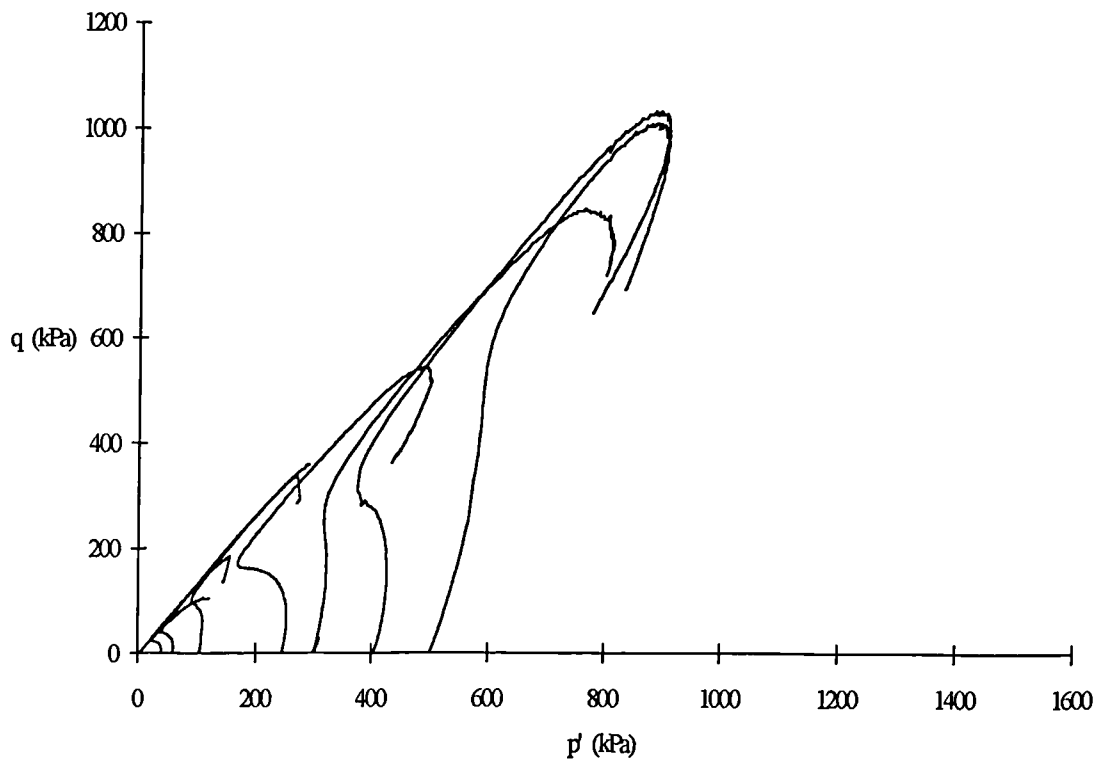
Fig. 5.24 Effective stress paths for the undrained triaxial tests
on the sand-kaolin samples
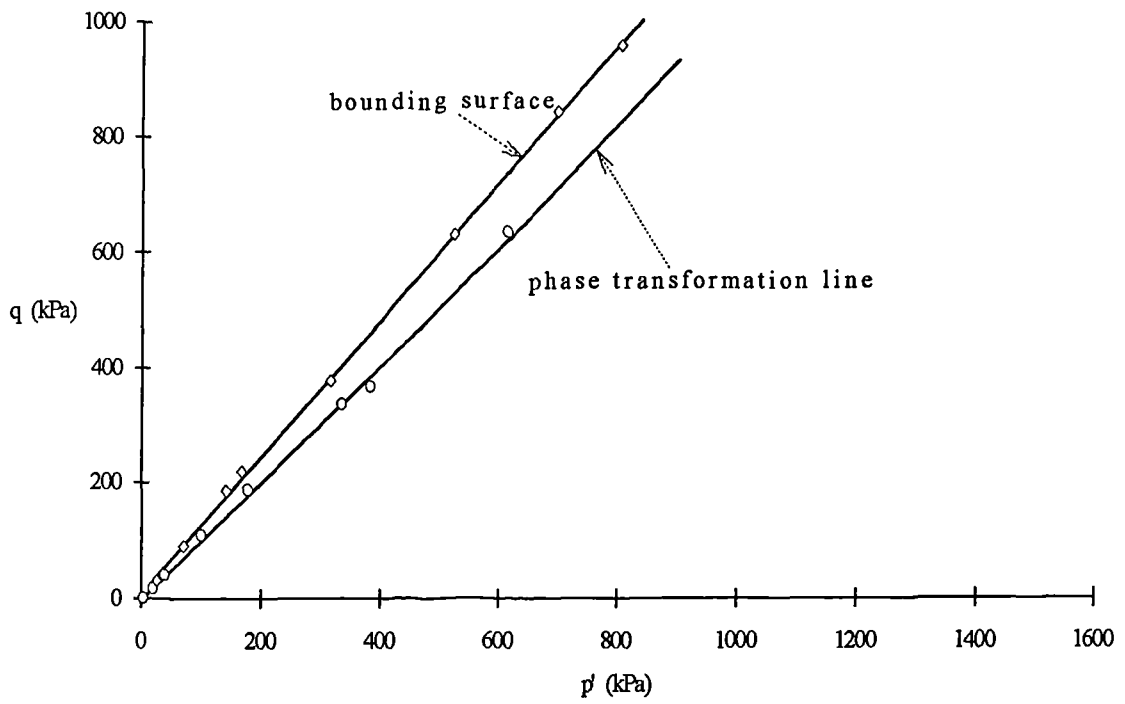
Fig. 5.25 Bounding surface and phase transformation line
for the sand-kaolin samples
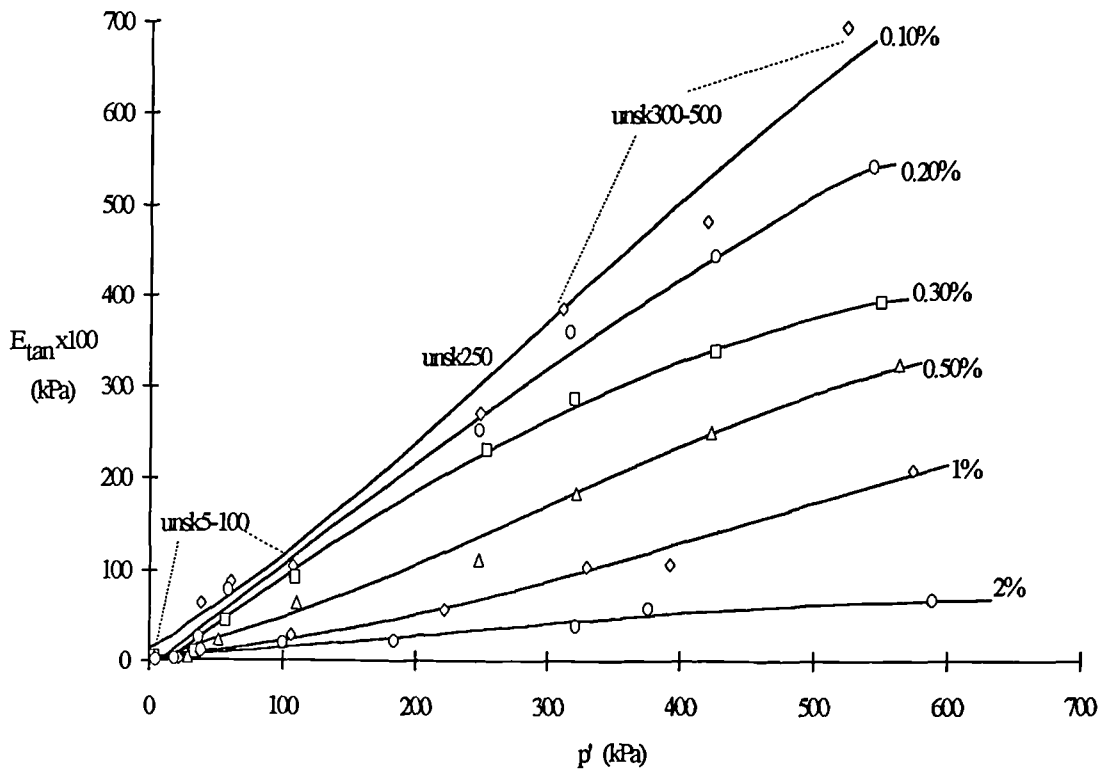
Fig. 5.26 Loss in tangential stiffness with the increase of axial strain
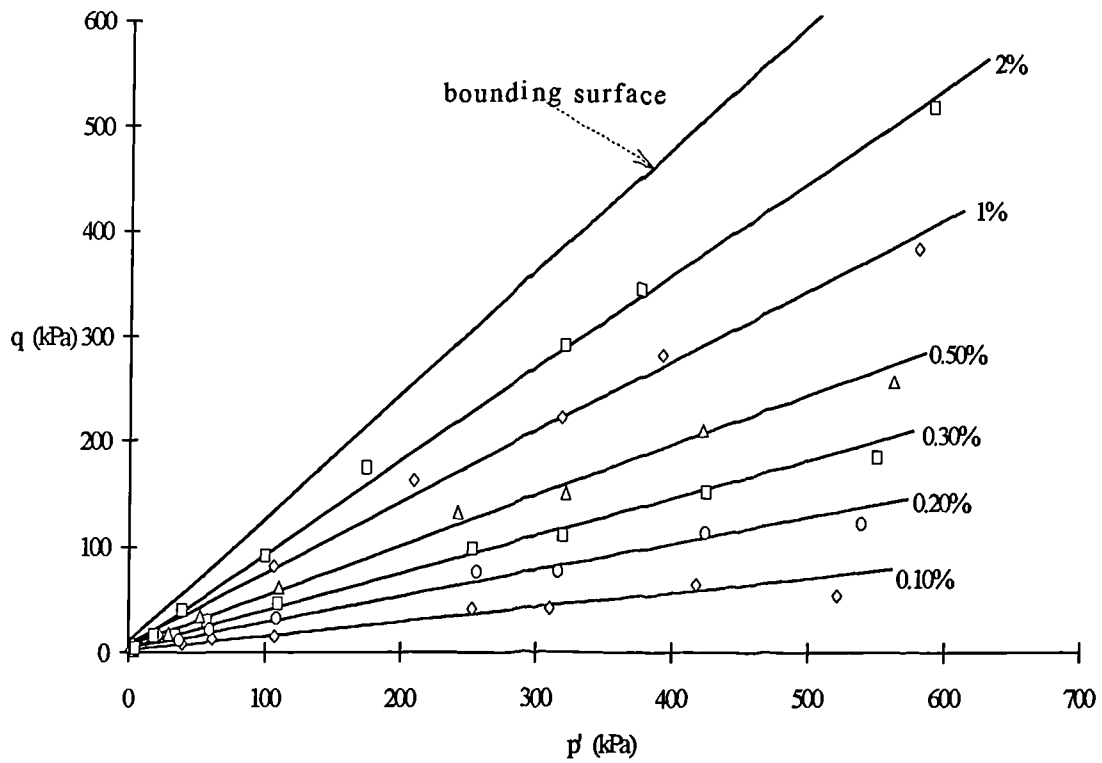
Fig. 5.27 Bounding surface and 0.1%-2% strain contours
for the sand-kaolin samples
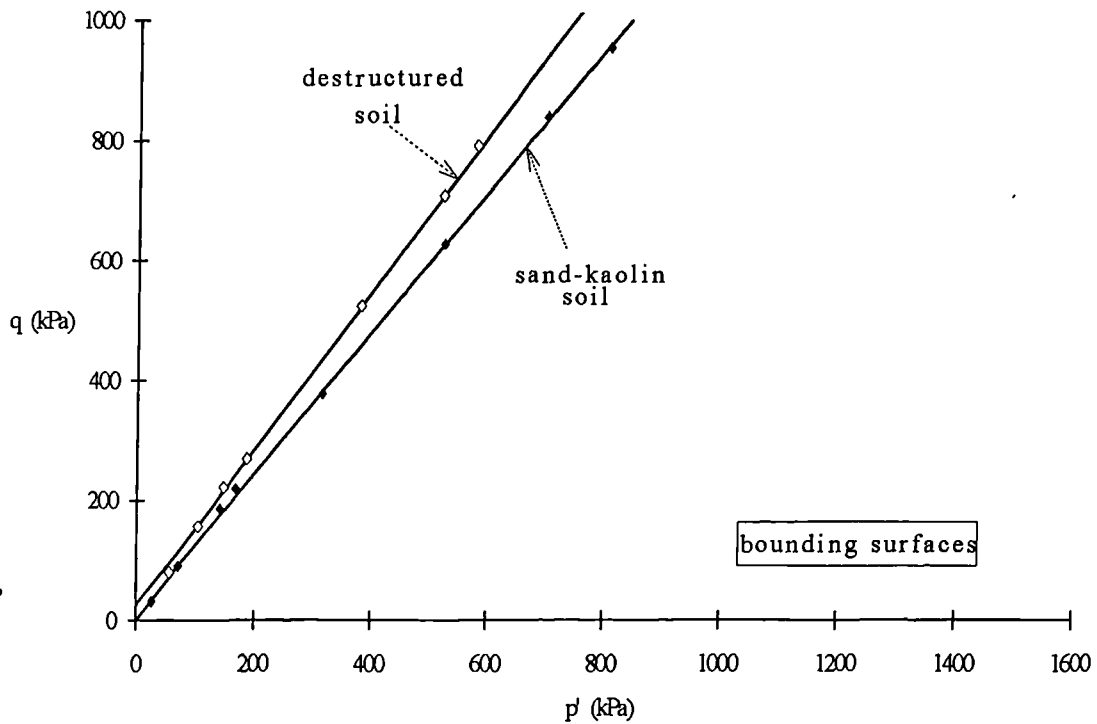
Fig. 5.28 Bounding surfaces for the destructured and the sand-kaolin samples
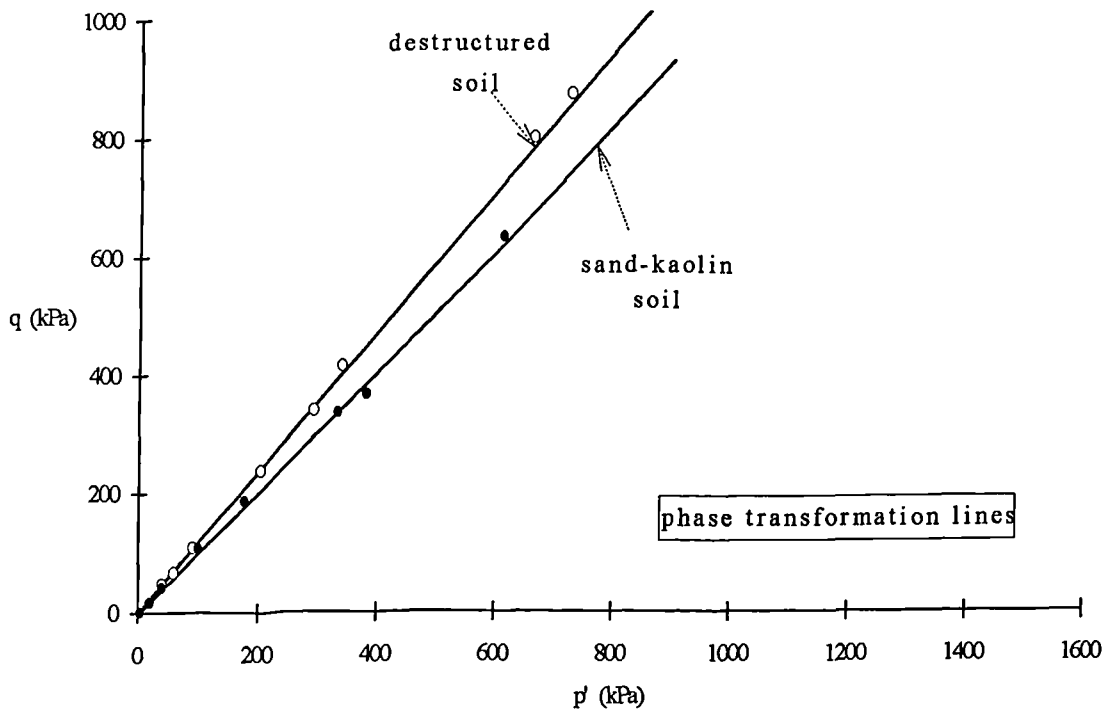
Fig. 5.29 Phase transformation lines for the destructured
and the sand-kaolin samples
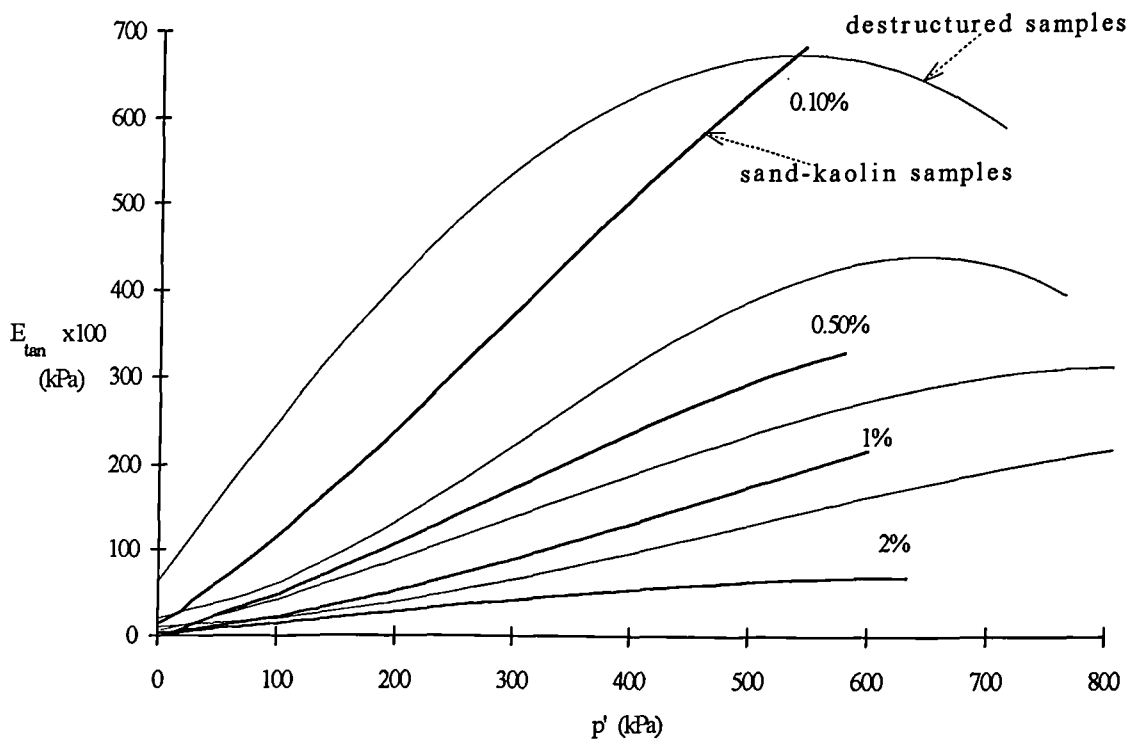
Fig. 5.30 Tangential stiffness versus p' for the two soils
for undrained tests
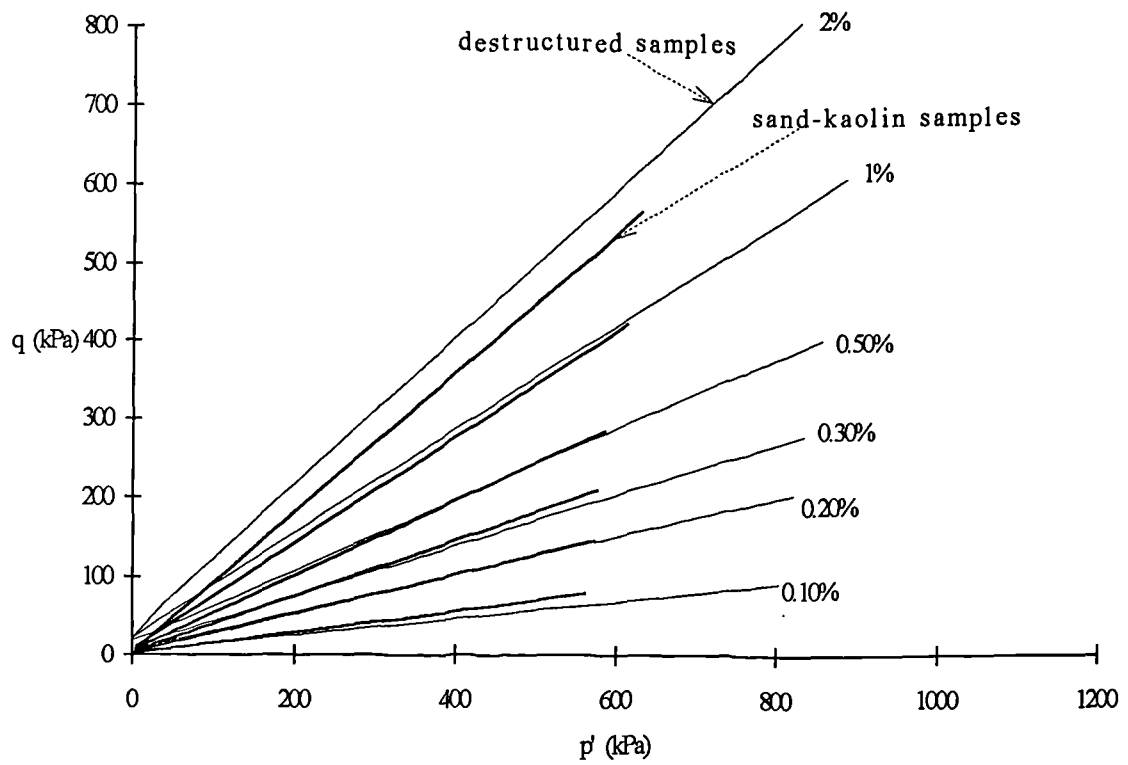
Fig. 5.31   Strain contours for the two soils plotted in the stress space
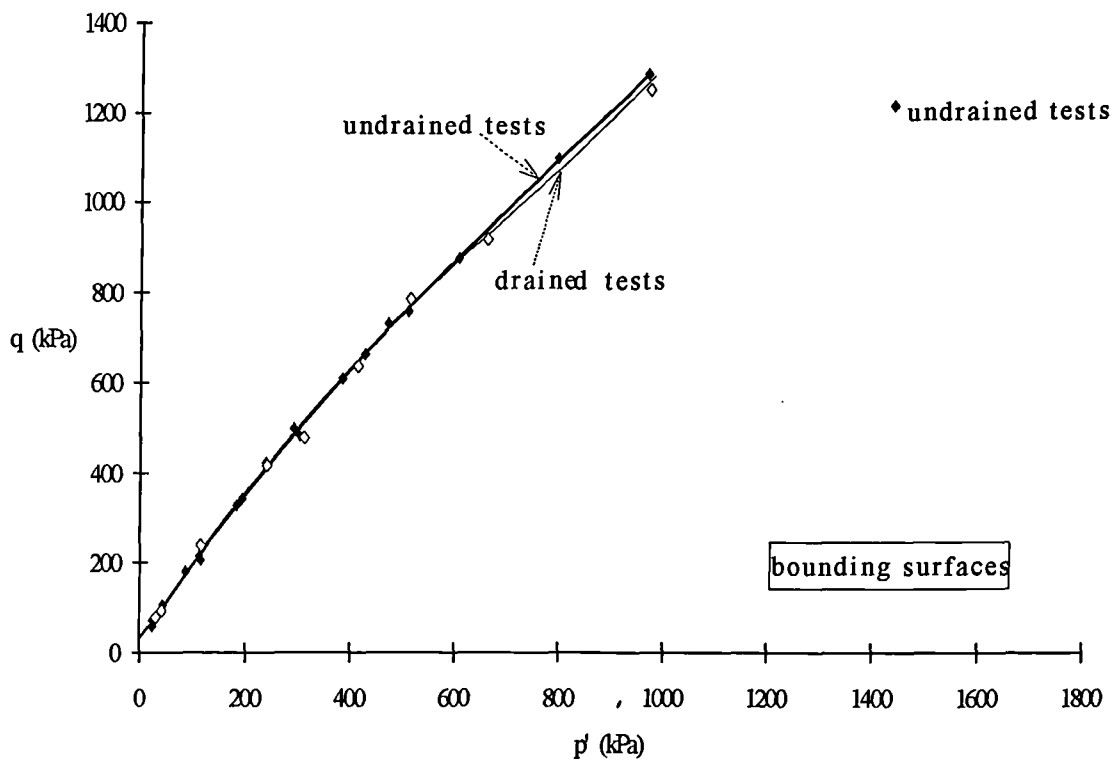
Fig. 5.32a   Bounding surfaces for the bonded soil for
undrained and drained triaxial tests

157
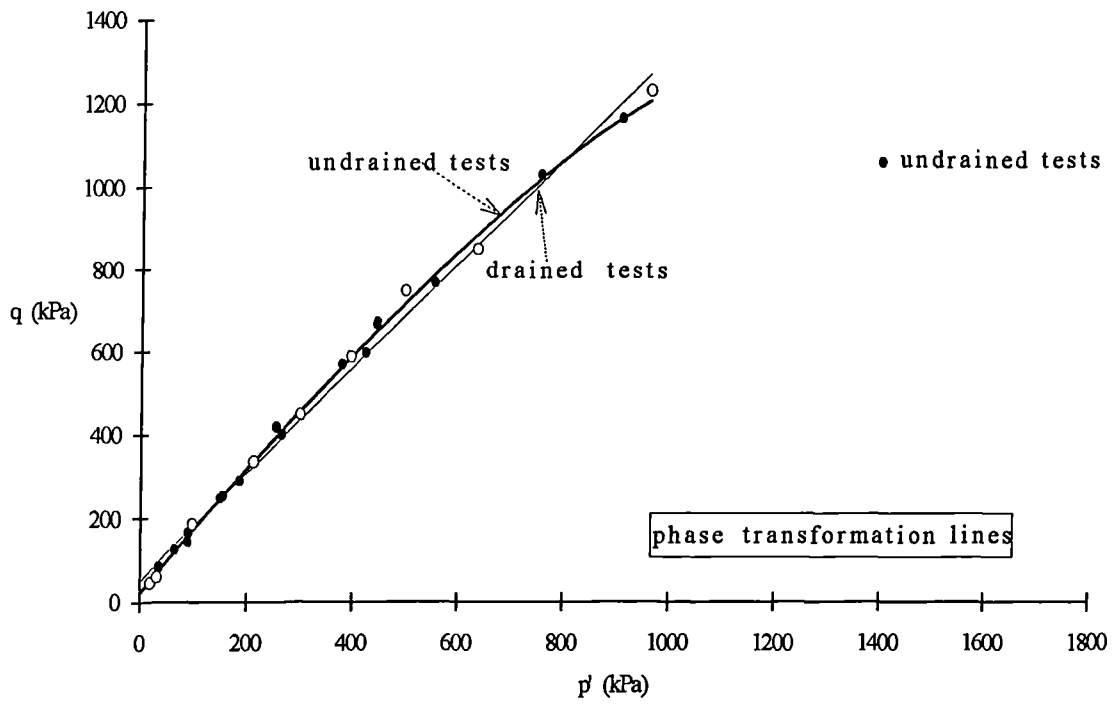
Fig. 5.32b Phase transformation lines for the bonded soil for
drained and undrained triaxial tests
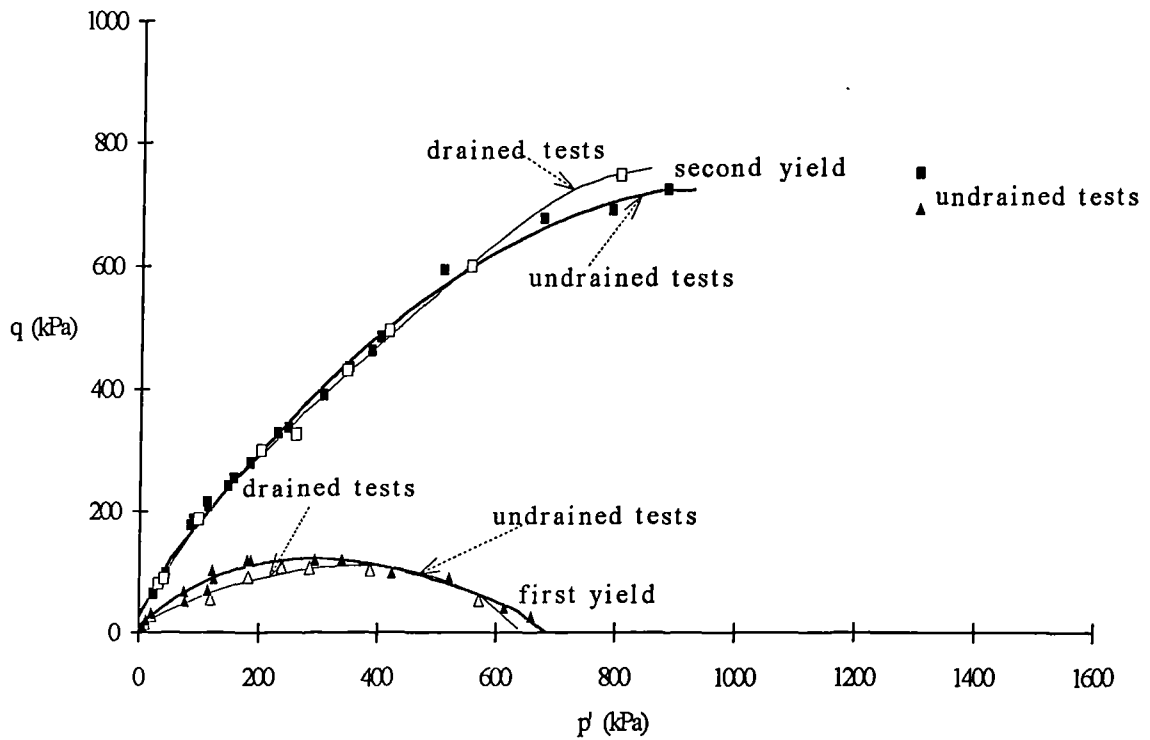
Fig. 5.33 Yield surfaces for the bonded soil for drained and
undrained triaxial tests

158
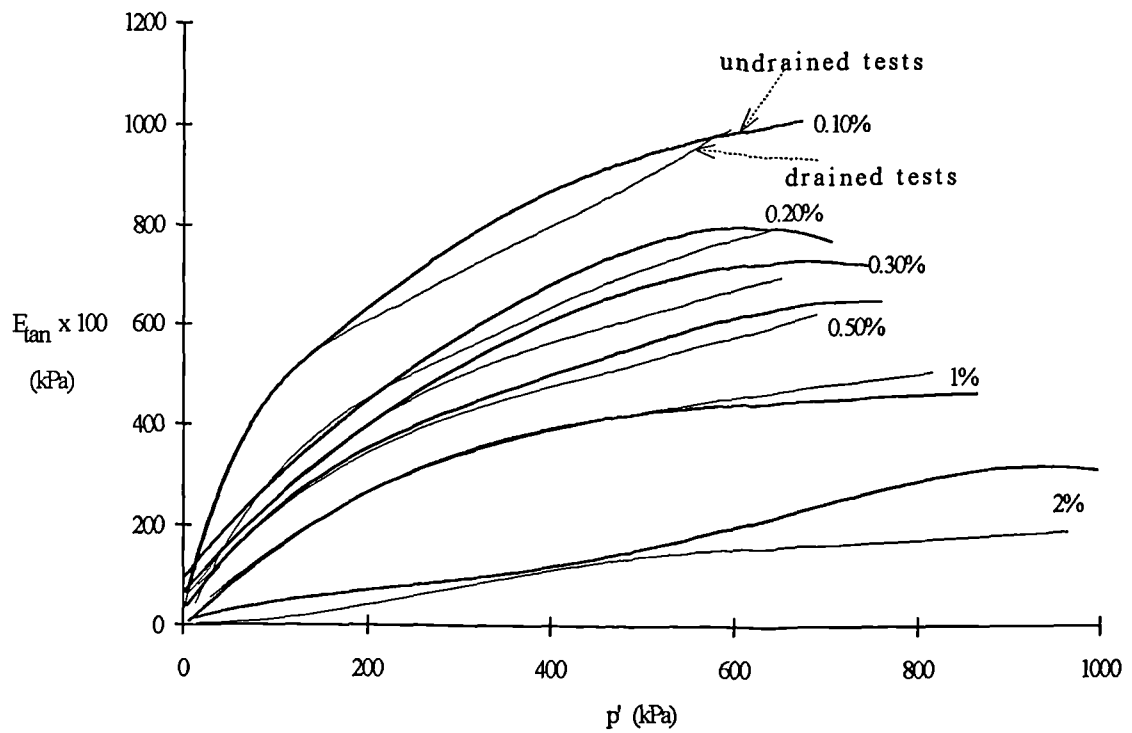
Fig. 5.34a Tangential stiffness versus p' for the bonded soil
for drained and undrained triaxial shearing
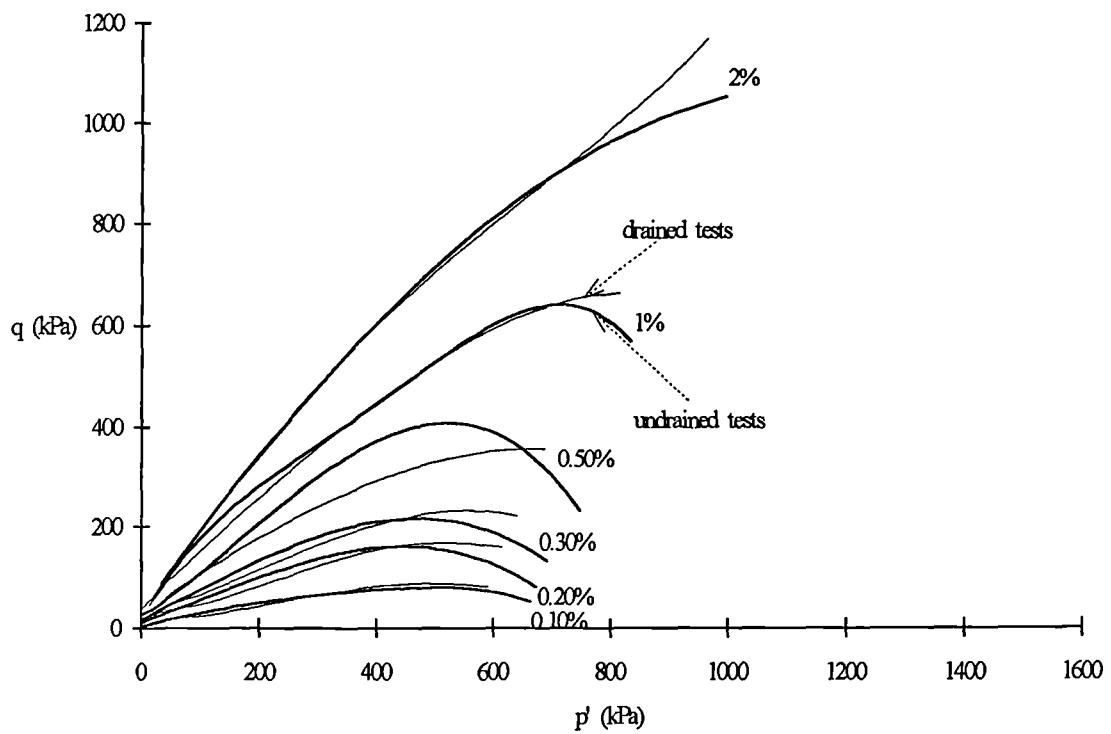
Fig. 5.34b Strain contours for the bonded soil for drained and
undrained triaxial tests

159
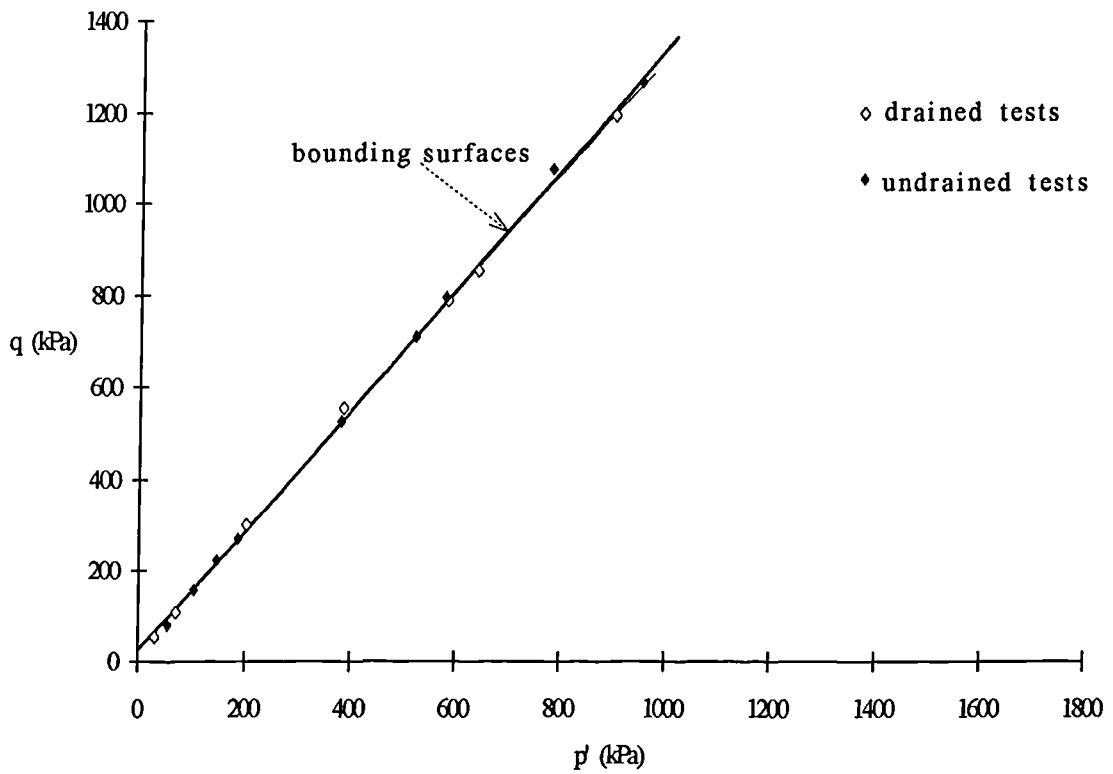
Fig. 5.35a Bounding surfaces for the destructured soil for
drained and undrained triaxial tests
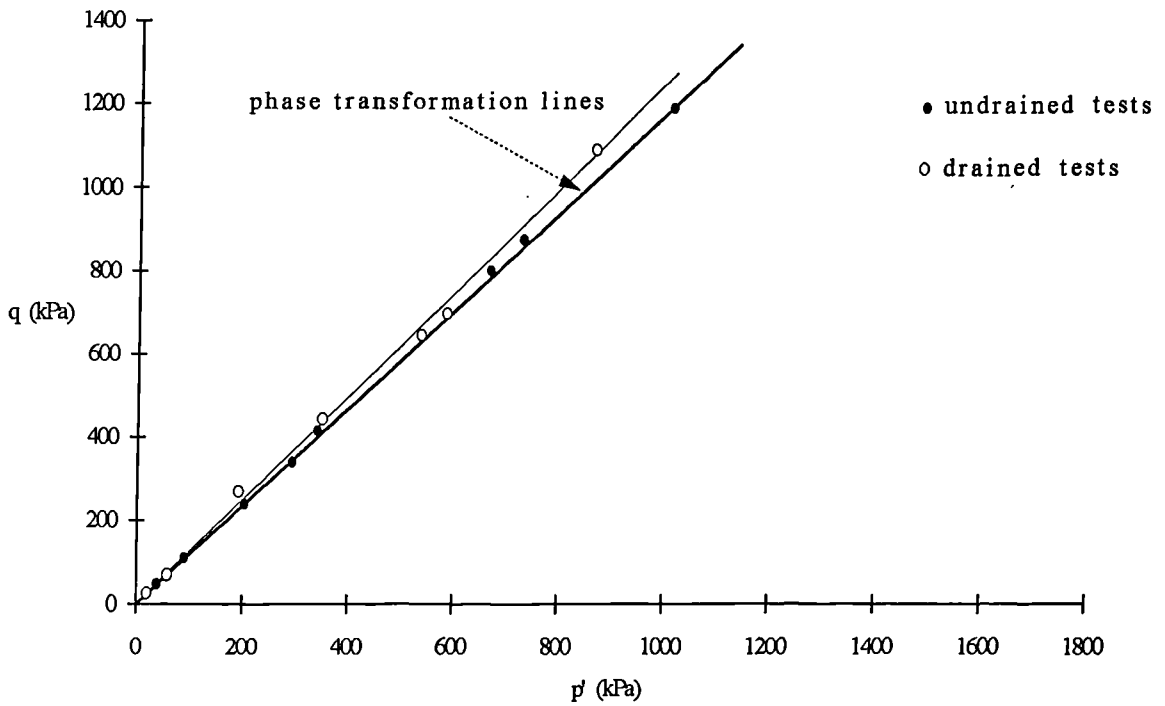
Fig. 5.35b Phase transformation lines for the destructured soil
for drained and undrained triaxial tests

160
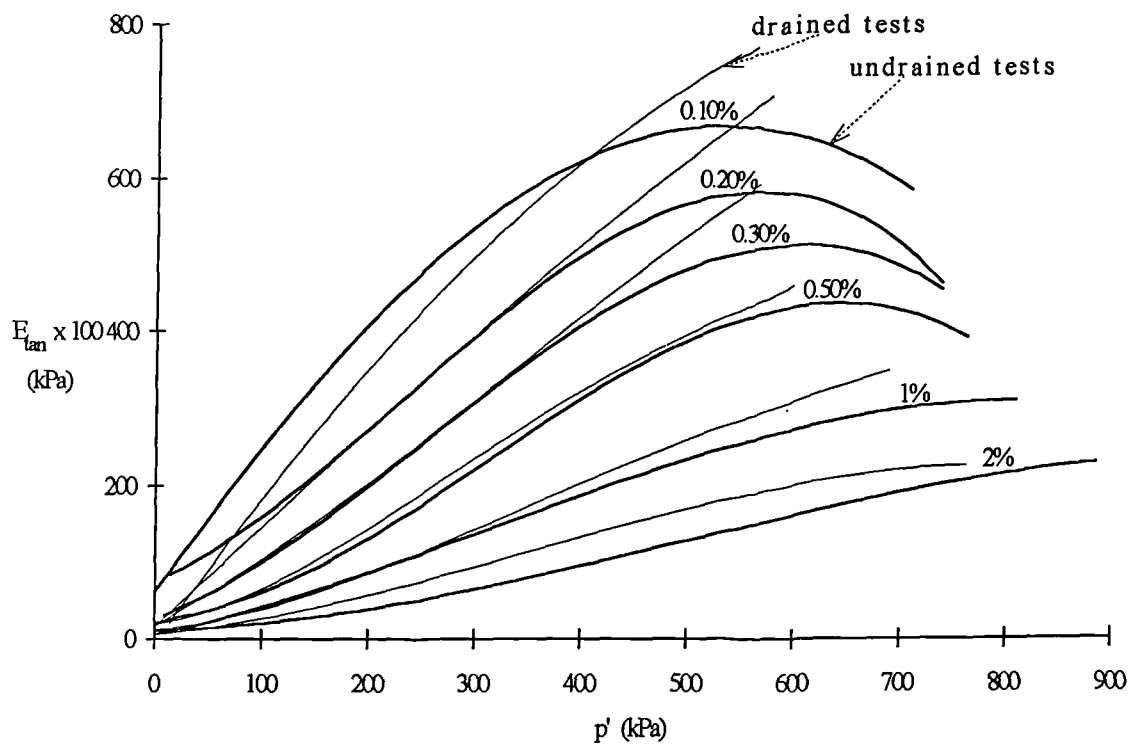
Fig. 5.36a   Tangential stiffness versus p' for the desrtuctured soil for
drained and undrained triaxial tests
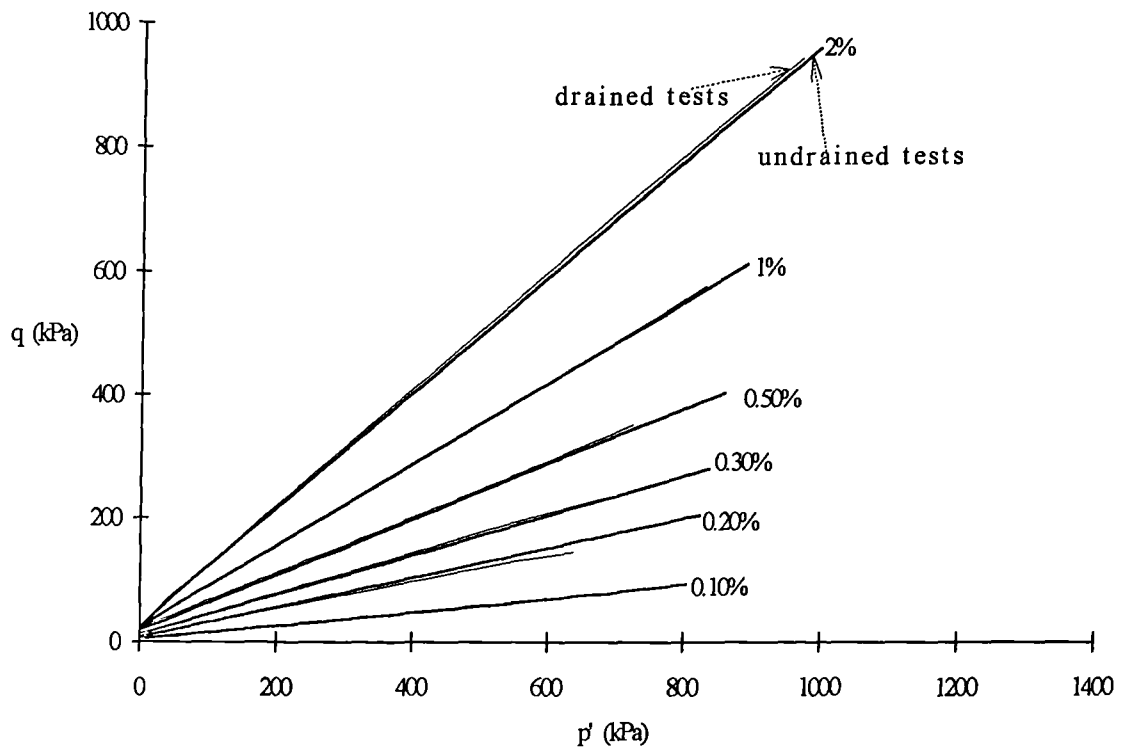
Fig. 5.36b   Strain contours for the destructured soil for
drained and undrained triaxial tests
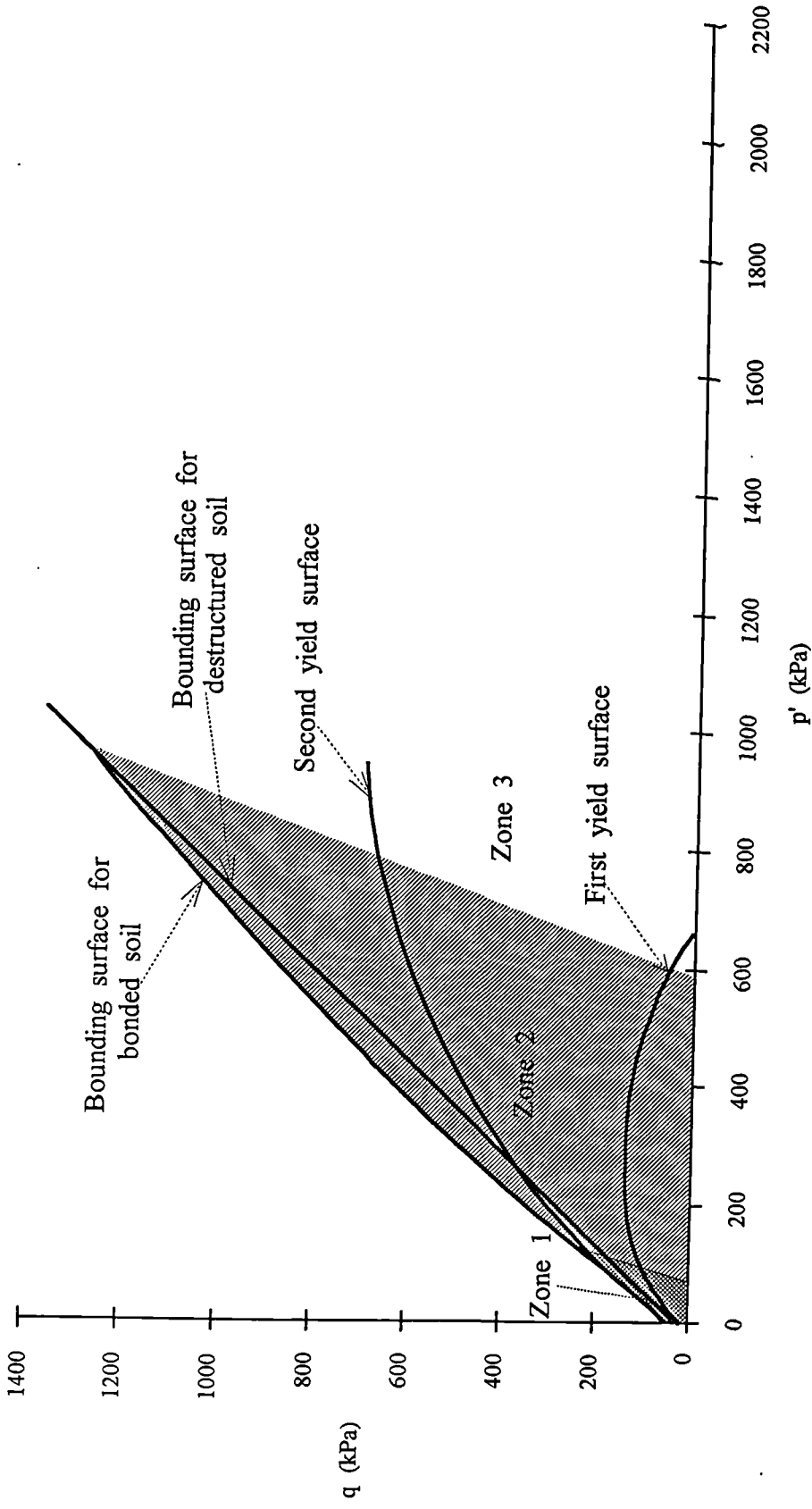
Fig. 5.37 Three zones of behaviour for the bonded soil

162
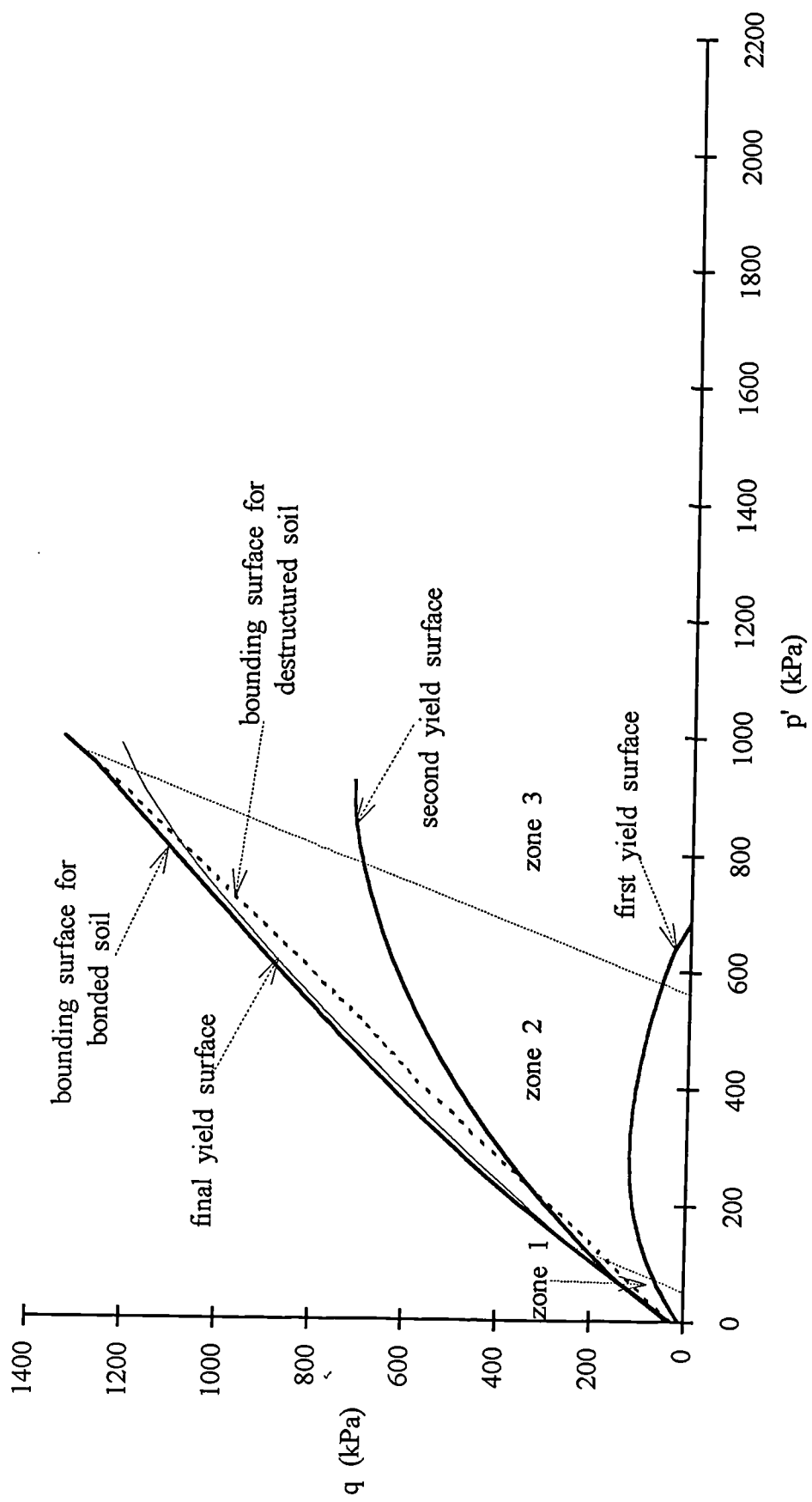
Fig. 5.38 Bounding surface and final and second yield surfaces plotted in the stress space for the bonded soil

CHAPTER 6   DRAINED PROBING TRIAXIAL TESTS

ON BONDED SOIL

6.1 INTRODUCTION

In this chapter the behaviour of the bonded soil is examined following drained triaxial stress paths which are different to the conventional constant σ_3' drained path. The paths which have been followed are constant mean stress (p') and constant σ_1'. Fig. 6.1 shows the different stress path directions followed. These have been carried out in order to probe the yield locus and investigate the effect of the stress path direction on the bounding surface.

The development of tangential stiffness and the position of the second yield defined from the two types of probing test are closely studied. The bounding surface that the soil reaches in the stress space, after following different stress path directions is also defined. The development of axial strain with respect to the stress paths, during the constant p' and constant σ_1' tests is examined and strain contours are plotted in the stress space.

Comparisons are also made between these results and those presented in the development of the general framework defined from the constant σ_3' drained and undrained tests. Differences in the soil's behaviour are observed, in respect of the development of tangential stiffness (E_{tan}), axial strain and the position of the second yield surface in the stress space. These differences relate to the rotation from the conventional constant σ_3' path in the stress space. Thus a more general picture is presented for the behaviour of the bonded soil, under shearing in different stress path directions.

6.2 CONSTANT MEAN EFFECTIVE STRESS DRAINED TRIAXIAL TESTS ON BONDED SOIL

The behaviour of the bonded soil under constant p' drained shearing is presented in this section. The development of the tangential stiffness and the position of the second yield are closely studied. The bounding surface and the second yield surface defined from the constant p' tests are plotted in the stress space. The development of axial strain with respect to the stress paths is also studied and strain contours defined from these tests are plotted in the stress space.

6.2.1 Testing details

A total of four constant p' drained tests were carried out on bonded samples. The samples were prepared at a void ratio of 0.6, as used for all previous tests described. The samples were first isotropically consolidated from 35 up to 500kPa and then sheared under constant p' drained conditions. Control of constant p' was achieved using the computer control system by defining a stage within which the mean effective stress was maintained constant with a tolerance of 0.5kPa (an example is given in fig. 3.9) and the deviatoric stress was increased at a constant rate of 50kPa/hr (the same as that used for the drained and the undrained tests on the bonded samples). Transducer readings were taken every 1 min up to 2% of strain and at higher strains every 5 mins. The name of the tests, the void ratio of the samples and the confining pressure at which consolidation took place prior to shearing are shown in table 6.1. The type of the sample is not included in the name of the test, as only bonded samples were tested under constant p' conditions. Thus for example, test cp'35 indicates a constant p' drained triaxial test that was carried out at $p'_o = 35$kPa.

6.2.2 Stress strain behaviour under constant p' drained conditions

The deviatoric stress-strain curves for all the samples are shown in fig. 6.2a. Smooth curves were achieved during shearing under constant p' conditions for all the tests. Test cp'35 reached a peak value of q at ε_a=0.8%, while the rest of the samples reached a peak value at $\varepsilon_a \cong 2\%$. At higher strains rapid strain softening followed for all the samples, with the formation of shear surfaces.

The volumetric strain versus axial strain curves are shown in fig. 6.2b. Except test cp'500 which showed compression at the beginning of shearing, followed by dilation at $\varepsilon_a>1\%$, the rest of the samples strongly dilated. The amount of dilation that the samples developed became less as confining pressure prior to shearing increased. Finally test cp'500 presented a small amount of compression at low strains. During a constant p' drained test σ_1' increased, while σ_3' decreased in order to keep p' constant. This has a direct effect on the development of radial strain, which shows high negative values (i.e. increase of sample diameter), and consequently affects the volumetric strains during shearing, producing greater dilation than for constant σ_3' paths.

The development of the tangential stiffness during shearing is plotted versus axial strain in fig. 6.3a and b for tests cp'35 and cp'500 respectively. According to the theory of elasticity (Wood, 1990), E_{tan} is defined by the following formula

$$E_{tan}=(\delta\sigma_1'-2\nu\delta\sigma_3')/\delta\varepsilon_a$$

where ν is Poisson's ratio. During a constant p' drained test, σ_3' has to decrease in order to maintain a constant value of p' and σ_1' increases simultaneously in order to increase the deviatoric stress. Therefore in order to define E_{tan} for a constant p' drained test, the $2\nu\delta\sigma_3'$ parameter has to be taken into account. This is different from a constant σ_3' drained test, where $\delta\sigma_3'$ equals zero. The Poisson's ratio is defined by $\nu=-\delta\varepsilon_r/\delta\varepsilon_a$, and thus the values of radial strain which had been calculated from the volumetric strains are accounted for in the final stiffness

values. The values of vstrain may not be precisely accurate due to membrane error effects and therefore the E_{tan} values are only used for a qualitative analysis of the test results.

In the first graph for test cp'35, (fig. 6.3a) an initial loss in E_{tan} occurs at $\varepsilon_a=0.074\%$, which possibly represents a first yield of the bonds, and a major loss occurs at $\varepsilon_a=0.55\%$ which represents the second yield. The sample sheared at a higher stress, $p_o'=500kPa$, also presents similar behaviour in fig. 6.3b. The first yield of the bonds is not so well defined, but the second yield at $\varepsilon_a=0.55\%$ is reasonably well defined. For the rest of the constant p' tests, the first yield of the bonds was not easily defined as it took place at very low values of strain. However the major loss in E_{tan} and consequently the second yield of the bonds was initiated at $0.5\%<\varepsilon_a<0.6\%$.

Comparisons between the last two figures and fig. 4.11, 4.12 and 4.13b presented in chapter 4, which show the position of the second yield for three conventional drained tests, show that the loss in E_{tan} in the latter was initiated at a higher strain percentage of about 0.5%-0.8%. The difference in the position of the second yield between the two types of tests can be accounted for by the different direction that the stress paths follow in the stress space. The high negative volumetric strains (dilation) that develop at the beginning of shearing in the constant p' tests, probably disrupt the bonds at lower axial strains.

The stress strain curves are presented again in fig. 6.4 and the positions at which the maximum q/p' ratio, the second yield and the maximum rate of dilation occurred are also marked. For test cp'35, second yield of the bonds occurred very close to the max q/p' ratio, which coincides with the max rate of dilation. Therefore, at that stress level the bonded structure of the soil almost entirely controls the soil's behaviour at failure, under drained shear. For $p_o'>35kPa$, the position of the second yield drops to lower deviatoric stresses, with respect to the

max q/p' ratio and the difference between the two increases with the increase of confining pressure. This suggests, that for higher stress levels the bonds are destroyed at lower deviatoric stresses and thus contribute less to the samples' max q/p' ratio. The max rate of dilation occurs after the max q/p' ratio for all the tests, but still very close to it.

6.2.3 Bounding and second yield surfaces for the constant p' tests

The stress paths for the constant p' tests are plotted in the stress space in fig. 6.5. The samples follow very precise constant p' stress paths, with only a 0.5kPa variation, which shows the high accuracy of the computer system in controlling an unconventional stress path.

The bounding and the second yield surfaces for the constant p' tests are plotted in the stress space in fig. 6.6. The position of the second yield for a drained test, cp'q430, sheared initially under constant p' conditions up to q=430kPa, is also marked on this graph in order to help clarify the position of the yield surface. A full description of the stress path followed by test cp'q430 is included in the next chapter.

The bounding surface and the second yield surface coincide for p'<50kPa (test cp'35). Thus, up to that stress the bonds almost entirely control the samples' behaviour and contribute to high stress ratio values. For p'>50kPa, the yield surface diverts from the bounding surface and the difference between the two increases with an increase of p'. At these higher stress levels the bonds start to be destroyed at lower deviatoric stresses and contribute less to the max q/p' ratios. Therefore the slope of the bounding surface drops to a lower value, for p'>100kPa.

6.2.4 Stiffness measurements at 0.1%-2% of strain

Tangential stiffness for all the constant p' drained tests is plotted in fig. 6.7 at different percentages of strain. There is a rapid increase in E_{tan} with p' for

p'<35kPa (test cp'35), for all the strain contours. For p'>35kPa, the slope of the curves for the 0.1%-0.5% contours gradually changes to lower values. For p'>450kPa, the contours show a tendency to level off almost parallel to the axis. There is an initial drop in stiffness after the 0.1% contour which probably coincides with the first yield of the bonds. For higher strains the loss from one contour to the other is quite small up to the 0.5% strain contour. After the 0.5% contour, second yield is initiated and the soil gradually looses a lot of the remaining stiffness up to 1% of strain. This loss is greater than that from 0.1% to 0.5% of strain. However, tests cp'250-500 still present stiffness values of higher than 15MPa even at 1% of strain. Finally at 2% of strain all the samples show very low stiffness values.

Strain contours for 0.1%-2% of strain and the bounding surface for the samples are plotted in the stress space in fig. 6.8. It can be seen that there is a rapid increase in q with an increase of p', for the 0.1%-0.5% strain contours up to p'<100kPa. For higher stresses the slope of the curves decreases to a lower value and the contours continue to increase in the stress space under almost a constant stress ratio. Tests cp'35-100 achieved their max q/p' ratio at ε_a<2% and therefore the 2% strain contour turns backwards for p'<100kPa and crosses the 1% contour. Tests cp'250 and cp'500 achieve max q/p' ratio at $\varepsilon_a \cong 2\%$ and thus the 2% contour is very close to the bounding surface.

It can also be seen, that the direction of the strain contours changes with the increase of strain percentage. For low axial strains where the behaviour of the soil is stiffer, the strain contours are closer to the isotropic axis. However after the second yield of the bonds initiated at 0.5% of strain, involving a major loss in E_{tan}, the contours change direction from the isotropic axis towards the bounding surface, in order to mirror more closely the shape of the latter.

6.3 CONSTANT AXIAL STRESS DRAINED TRIAXIAL TESTS
ON BONDED SOIL

The behaviour of the bonded soil under constant σ_1' drained triaxial tests is presented in this section. The development of E_{tan} and the position of the second yield during shearing is studied. The max q/p' ratios that the soil reached in the stress space and the second yield surface are also presented. The development of axial strain in respect of the stress paths is also studied and strain contours are plotted in the stress space.

6.3.1 Testing details

A total of five constant σ_1' drained tests were carried out on bonded samples. All samples had a void ratio of 0.6. The samples were first isotropically consolidated from 70 up to 525kPa and then sheared under constant σ_1' conditions. Control of the constant σ_1' stress condition was achieved by defining a stage where q was increasing at a constant rate of 50kPa/hr and σ_1' was maintained constant. In order to maintain σ_1' constant as q was increasing the system would decrease the cell pressure. Accordingly, the mean effective stress p' was also decreasing. Transducer readings were taken every 1 min initially and after 2% of strain every 5 mins. The name of the tests, the void ratio of the samples and the confining pressure at which consolidation took place prior to shear are shown in table 6.2. The name of the test indicates only the type of shearing and the confining pressure at which the sample was initially isotropically consolidated. Thus for example, test cs1'70 indicates a constant σ_1' drained triaxial test carried out at $p_0'=70$kPa.

6.3.2 Stress strain behaviour under constant σ_1' conditions

The deviatoric stress strain curves for all the samples are shown in fig. 6.9a. Smooth curves were achieved during shearing under constant σ_1' conditions from all the tests. Test cs1'200 stopped at $\varepsilon_a=4\%$ due to problems with the compressed air

supply to the system. However, at this strain level the major yield of the bonds and the maximum q/p' ratio of the sample had already occurred and thus it was decided to include this test in the presentation of the results. Tests $cs1'70$-200 reached a peak q value at $\varepsilon_a < 1\%$, while $cs1'300$ and $cs1'525$ reached peak at $\varepsilon_a > 1.3\%$. Rapid strain softening followed after failure for all the samples with the formation of shear surfaces.

The volumetric strain versus axial strain curves are plotted in fig. 6.9b. The samples showed dilation from the beginning of shearing, with the greatest value occurred for the sample sheared at the lowest consolidation pressure, test $cs1'70$. The amount of dilation measured in the samples during shearing decreases, as the confining pressure prior to shear increases; however tests $cs1'100$-525 develop similar negative volumetric strain values.

During a constant σ_1' test, q increases and σ_3' decreases in order to maintain σ_1' constant. This has a direct effect on the development of high negative radial strains (i.e. increase in sample diameter) at the beginning of shearing and consequently on the development of high negative volumetric strains. At the end of testing only $cs1'300$-525 reached an ultimate point of shearing under constant volume; however it is unlikely that critical state has been achieved, as q continues to decrease further with the increase of strain, for these tests.

The development of the tangential stiffness during shearing is plotted versus axial strain for tests $cs1'70$ and $cs1'525$ in fig. 6.10a, b respectively. Tangential stiffness during a constant σ_1' test is defined by the formula

$$E_{tan} = -2\nu\delta\sigma_3'/\delta\varepsilon_a$$

as $\delta\sigma_1'$ equals to zero. There is a major loss in E_{tan} for test $cs1'70$, initiated at $\varepsilon_a \cong 0.2\%$, which represents the second yield of the bonds. For test $cs1'525$ the loss

in E_{tan} is initiated at ε_a=0.25% of strain. It is not possible to observe a first loss in E_{tan}, which would represent the first yield of the bonds.

Second yield of the bonds for the rest of the constant σ_1' tests also occurred at 0.2%<ε_a<0.25% of strain. Comparisons between these test results and those for the constant p' and constant σ_3' drained tests, show a gradual drop in the value of strain at yield; $\varepsilon_a \cong 1\%$ in constant σ_3', $\varepsilon_a \cong 0.5\%$ in constant p' and $\varepsilon_a \cong 0.2\%$ in constant σ_1'. Therefore this suggests that following a stress path to the left of a constant σ_3' drained test in the stress space, directly influences the bonded structure of the soil, so that the second yield of its bonds occurs at lower percentages of axial strain.

The deviatoric stress versus axial strain curves are plotted again in fig. 6.11 and the positions at which the max q/p' ratio, second yield of the bonds and max rate of dilation occurred are also marked. For test cs1'70 the max q/p' ratio coincides with the max rate of dilation. For all the tests the difference between the position of the second yield and the max q/p' ratio increases with the increase of p_0' prior to shear. Therefore the bonds do not entirely control the samples' behaviour at failure for 70<p_0'<525. The max rate of dilation for tests cs1'100-525 always occurs after the second yield, but before the max q/p' ratio. This is different to the soil's behaviour under a constant σ_3' and a constant p' drained path and can only be accounted for by the different stress path direction during shearing.

6.3.3 Bounding and second yield surfaces for the constant σ_1' tests

The stress paths for the constant σ_1' drained tests are plotted in fig. 6.12. The samples follow very precise constant σ_1' drained paths in the stress space. After they reach the max q/p' ratios, they continue to shear under constant σ_1', but in the opposite direction (q decreasing).

172

The bounding surface and the second yield surface for the constant σ_1' tests are plotted in fig. 6.13. The second yield surface diverts from the bounding surface for the whole range of p'. The difference between the position of the two surfaces increases with the increase of p'. The destruction of the bonds under a constant σ_1' stress path occurs at very low axial strains, in comparison with those observed in a drained test (one sixth of the value) and this is reflected in the position of the second yield surface in the stress space. The bonded structure of the soil does not entirely control the soil's behaviour at failure for any specific stress level, as it gets destroyed at low q values. For p'>150kPa, the difference between the two surfaces increases and the slope of the bounding surface reduces.

6.3.4 Stiffness measurements at 0.1%-2% of strain

Tangential stiffness measurements for all the constant σ_1' drained tests are plotted versus p' at 0.1%-2% of strain, in fig. 6.14. The results for two more tests cs13'150-400 (sheared initially under constant σ_1' conditions) are also included in this graph. Full details of those tests are presented in chapter 7.

There is an immediate increase in stiffness with p' up to test cs1'300, for the 0.1%-0.5% contours. For p'>250kPa, the slope of the 0.1% curve decreases to a lower value and for p'>400kPa the curve levels off almost parallel to the p' axis. The slope of the rest of the contours increases for p'>150kPa and the 0.2%, 0.3% curves level off almost parallel to the p' axis for p'>250kPa. After 0.2% of strain, where the second yield of the bonds initiated, the soil gradually lost a lot of its stiffness with the increase of axial strain. At ε_a=0.5%, the samples up to p'<140kPa present very low values of stiffness in comparison with the rest of the samples sheared at higher stresses, which still show high values. At ε_a=1%, the samples have lost all of their remaining stiffness, which is substantially lower in comparison with that lost from 0.1% to 0.5% of strain.

The 0.1%-1% strain contours and the bounding surface defined from the constant σ_1' drained tests are plotted in fig. 6.15. As can be seen, there is an almost linear relationship for all the strain contours up to test cs1'200, while for higher stresses the slopes of the curves drop to lower values. The samples reach the bounding surface at $\varepsilon_a \cong 1\%$ except for test cs1'525. The stress points for $\varepsilon_a = 2\%$ are positioned at lower q values (i.e. during unloading), and are presented with an open circle for all the tests.

It can be seen that the direction of the strain contours changes with the increase of axial strain, for the whole range of p'. After the occurrence of the second yield of the bonds initiated at 0.2% of strain accompanied with the major loss in stiffness, the contours turn gradually towards the bounding surface for the whole range of p'.

6.4 COMPARISONS BETWEEN THE TEST RESULTS OBTAINED FROM THE THREE DIFFERENT TYPES OF DRAINED TESTS

In this section the effects that the direction of the stress path has on the soil's behaviour during shearing are closely studied. Initially, comparisons are presented between the E_{tan} values developed from the constant p', constant σ_1' and constant σ_3' tests, sheared at the same p_0'. The bounding surfaces that govern the behaviour of the bonded soil under the different stress paths and the relative positions of the yield surfaces defined in the stress space are clarified.

Comparisons between the development of the tangential stiffness at different strain percentages and the strain contours defined from the three different drained tests, are also presented. The differences observed in the behaviour of the bonded soil under shearing in different stress paths, are related to the rotation of the stress path direction to the left of the constant σ_3' drained path in the stress space. Final

174

remarks for the soil's behaviour under the constant p' and σ_1' paths are presented at the end of the chapter.

6.4.1 Tangential stiffness under different stress paths directions

Tangential stiffness for two sets of tests carried out under constant p' and constant σ_3' stress path directions, at the same p_0' values are presented first. E_{tan} for tests cp'35, db35 and cp'250, db250 is normalised with the current value of p' during shearing (not initial p') and is plotted versus axial strain in fig. 6.16a and b respectively.

Tangential stiffness for test cp'35 has higher values than those observed in test db35, up to ε_a=0.6% where yield of the bonds initiated. For ε_a>0.6%, E_{tan} for test cp'35 drops to a lower level than that which occurred for test db35, which continues to maintain an almost constant value up to the point at which second yield takes place at ε_a=1.3%.

A similar picture is presented in the second graph, where E_{tan} for test cp'250 shows higher values than test db250 up to ε_a=0.65%, where second yield of the bonds takes place in the constant p' test. For higher strains, E_{tan} for test db250 presents higher values than test cp'250 up to 1% of strain, where second yield of the bonds takes place. The behaviour of the bonded soil under these two different drained paths suggests, that a stress path to the left of the constant σ_3' path in the stress space causes higher values of stiffness to be developed from the soil than those observed in the conventional test. The constant p' stress path also influences the position of the second yield, with a loss in E_{tan} at lower values of axial strains than that which occurred in a constant σ_3' test.

Tangential stiffness for two sets of tests carried out under constant σ_1' and constant σ_3' drained paths, at similar p_0' values are presented in fig. 6.17a and b. In the

first graph E_{tan} is normalised with the current value of p' during shearing and plotted versus axial strain for test csl'300 and tests db250-350. Since no constant σ_3' test was carried out for p'=300kPa, the results for tests carried out at 250 and 350kPa are shown. As can be seen in fig. 6.17a, the results from the two tests followed similar curves.

Test csl'300 initially presents higher values of E_{tan} than the other two constant σ_3' tests. Second yield occurs at ε_a=0.2% and the sample continues to present higher values of stiffness than the other two tests, up to ε_a=0.6%. For ε_a>0.6%, the two constant σ_3' tests present higher E_{tan} values than the csl'300 test, up to 1% of strain, where second yield of the bonds occurred for both tests with a substantial loss in stiffness.

A similar picture is presented in the next figure, where E_{tan} is plotted for a constant σ_1' and a constant σ_3' test sheared at p_0'=525kPa and p_0'=550kPa respectively. Initially test csl'525 presents higher values than those developed during the db550 test, with second yield of the bonds occurred at ε_a=0.25%. For ε_a>0.8% the loss in E_{tan} for the constant σ_1' test is quite substantial and thus the constant σ_3' test presents higher stiffness values than the latter, up to the point that second yield occurred at ε_a=1.3%.

As can be seen from the last two figures the development of stiffness of the bonded soil during shearing, is affected by the stress path direction in the stress space. A constant σ_1' path positioned to the left of a constant σ_3' conventional drained test, influences the occurrence of the second yield of the soil, which takes place at very low axial strains. It also influences the development of the tangential stiffness, which shows higher values than those developed in the constant σ_3'.

The development of E_{tan} for three tests sheared under the three different stress path directions but at similar initial mean effective stresses, normalised with p', is plotted in fig. 6.18. The constant σ_1' test (cs1'525) presents initially higher E_{tan} values than the other two tests. Second yield occurs at ε_a=0.25% and the sample continues to present higher values of stiffness than the other tests, up to ε_a=0.7%. The constant p' test presents slightly higher E_{tan} values (although with some scatter) than the constant σ_3' test, db550, up to the point of yield at ε_a=0.55%. At higher strains, test db550 presents higher values of stiffness than the other two, up to ε_a=1.3% when second yield of the bonds occurs with an immediate loss in stiffness.

Therefore the stress path direction affects the development of the tangential stiffness during shearing and the occurrence of the second yield. A drained test following a stress path to the left of a constant σ_3' test produces higher values of E_{tan} than that presented from the latter. Accordingly the position of the second yield occurs at a lower strain level. The further the stress path is to the left the more it affects the higher values of E_{tan} and the occurrence of second yield at a lower strain level.

As was previously discussed, higher negative volumetric strains were initiated during shearing under the constant p' and σ_1' paths from the beginning of the tests, compared with a conventional drained test. These negative values very possibly account for the earlier destruction of the bonds, with the rotation of the stress path to the left side of the constant σ_3' path. It should also be noted, that the negative volumetric strains developed for the constant σ_1' tests at very low axial strains are larger than the values developed for the constant p' tests and thus this probably explains why second yield for these tests occurred at lower axial strains.

6.4.2 Bounding and second yield surfaces

The max q/p' ratios and the second yield points observed in the bonded soil, under a constant p' drained stress path are presented in fig. 6.19. The bounding surface and the second yield surface obtained from the constant σ_3' drained tests are also shown in this figure. The fact that the major loss in E_{tan} occurs at lower axial strain percentages in the constant p' tests (in comparison to that in the constant σ_3' tests), is reflected in the position of the second yield surface in the stress space, which occurs at lower q values than values defined from the constant σ_3' tests. As can be seen, the shape of the two yield surfaces is very similar but with an offset between them. There is a difference in q=50kPa between the two surfaces.

However, the difference in position of the yield surface does not affect the bounding surface that the samples reached in the stress space. There is generally good agreement between the results obtained for the max q/p' ratios, from the two different types of tests. The surface obtained from the constant p' drained tests is positioned at slightly lower stresses than that obtained from the constant σ_3' tests, but this is probably due the limited number of constant p' tests. Therefore, although the yield surface is affected by the path direction, a unique bounding surface appears to be independent of stress path direction.

The last graph is replotted in fig. 6.20 and the bounding surface for the destructured soil is also included for comparisons to be made between the two soils. The limits for the 3 zones defined for the bonded soil under constant σ_3' drained shearing are also presented (see section 5.8.2 and fig. 5.37). The yield surface in the constant p' tests diverts away from the bounding surface at an earlier point than that obtained from the constant σ_3' tests. Therefore the first zone (where the second yield surface coincides with the bounding surface) has substantially shrunk. This suggests that the different direction of the stress path in the constant

p' tests influences the size of the first zone where the bonds entirely control the soil's behaviour at failure, which is now defined up to $p_o' \cong 35kPa$.

In the second zone, the differences between the bounding surface and the yield surface defined from the constant p' tests, is larger than that shown between the two surfaces obtained from the constant σ_3' tests. However the lower position of the second yield surface does not affect the max q/p' ratios that the soil reached in the stress space, which are higher than that of the destructured soil in the first and the second zone. The max q/p' ratio values obtained from the two types of tests are very similar. However the lower values obtained for the constant p' tests for p'>250kPa, might indicate a tendency for the bounding surface to drop to lower stresses for p'>500kPa. Tests were no carried out at this stress level due to stress limitations of the system and thus the upper limit for the second zone, for constant p' tests is not defined.

The bounding and the second yield surfaces defined from the constant σ_1' and constant σ_3' tests are plotted in the stress space in fig. 6.21. There is a large difference between the positions of the two yield surfaces, with an initial value of q=100kPa which increases slightly with the increase of p'. Apparently, the loss in E_{tan} at very low strains during the constant σ_1' tests is reflected in the lower position of the yield surface in the stress space.

However, this lower position of the second yield surface does not affect the max q/p' ratio values that the samples reach in the stress space. These points define a bounding surface, which almost coincides with that defined from the constant σ_3' drained and undrained tests. There is only a very slight drop at p'=250kPa, for test csl'525.

The last graph is replotted in fig. 6.22 and the limits for the three zones defined from the constant σ_3' triaxial drained and the undrained tests are also included. In this graph the bounding surface for the destructured samples is also plotted, for

comparisons to be made between the different soils. The first zone (where the bonds entirely control the soil's behaviour at failure and the bounding surface coincides with the second yield surface) does not exists for the constant σ_1' tests, as the second yield surface diverts away from the bounding surface from the point of the origin. However the bonds still contribute to higher max q/p' values for the bonded soil, compared with those measured in the destructured soil.

In the second zone the yield surface defined from the constant σ_1' tests increases in the stress space almost parallel to the yield surface defined from the constant σ_3' tests. Even though the difference between the bounding surface and the yield surface has increased in this zone, the soil still presents higher max q/p' ratio values than the destructured soil, at the same stress level. However the drop in the max q/p' ratio, for $p'>250kPa$ might indicate a tendency of the bounding surface to turn closer to the bounding surface of the destructured soil at higher stresses. Tests were not carried out at a higher stress level, due to stress limitations of the system and thus the upper limit for this zone, where the bonds are destroyed and they do not contribute to higher max q/p' ratios (and thus the two bounding surfaces coincide) is not defined.

It can therefore be seen that the bounding surface is unique for the three stress path directions investigated. However, different second yield surfaces are observed. The unique bounding surface and the second yield surfaces defined by the different stress paths drained tests are plotted in fig. 6.23. As was previously discussed, the position of the second yield surface is influenced by the early loss in E_{tan} during the constant p' and constant σ_1' tests. Therefore the second yield surface defined from the constant p' tests falls below the constant σ_3' tests, as second yield for the constant p' tests takes place at $\varepsilon_a=0.55\%$. The second yield surface defined from the constant σ_1' tests is positioned at even lower q values, as second yield for these tests occurred at $\varepsilon_a\cong0.25\%$. The difference between this surface and that defined from the constant σ_3' tests is the largest.

Therefore the rotation of the stress path to the left of the conventional constant $\sigma_3{}'$ drained path, influences the position of the second yield surface in the stress space, at a lower stress level. A stress path even further to the left moves the position of the second yield surface to a lower stress level in the stress space. However the different positions of the yield surfaces did not affect the max q/p' ratios that the samples reach in the stress space, for $p'<400kPa$. A unique bounding surface governs the behaviour of the bonded soil, under the three different stress path drained tests.

6.4.3 Comparisons between the tangential stiffness measurements for the three types of test

The E_{tan} measurements at different percentages of strain for the constant $\sigma_3{}'$ and p' tests are plotted versus p', in fig. 6.24. Stiffnesses measured during the constant p' drained tests are higher than those defined from the constant $\sigma_3{}'$ drained tests up to 0.5% of strain and for the whole range of p'. There is a large drop in E_{tan} after the 0.1% of strain for both the constant p' and constant $\sigma_3{}'$ tests, which coincides with the first yield of the bonds. Second yield for the constant p' drained tests is initiated at 0.5% of strain and thus at 1% of strain the values of stiffness for these tests are substantially lower than those observed for the constant $\sigma_3{}'$ tests at the same strain level, as second yield of the bonds has not yet taken place for the latter. At 2% of strain, second yield of the bonds has already occurred for the constant $\sigma_3{}'$ drained tests and the results from the two types of tests are similar.

In fig. 6.25, E_{tan} is plotted versus p' for the three different types of drained tests. The samples sheared under the constant $\sigma_1{}'$ path present much higher stiffness values than any other stress path at 0.1% of strain and for the whole range of p'. At this strain level the constant p' tests present slightly higher values than those from the constant $\sigma_3{}'$ tests. At 0.5% of strain, the samples sheared under the constant $\sigma_1{}'$ path have lost a substantial amount of their stiffness, as second yield

of the bonds had already occurred at $\varepsilon_a \cong 0.25\%$. Thus up to $p'<140kPa$ they present lower E_{tan} values than those observed from the other two types of tests, while for $p'>140kPa$ the samples still present higher values of stiffness than those observed from the other two types of tests, carried out at the same stress level. However at 0.5% of strain the samples sheared following a constant p' path, still present higher values than those observed from the constant σ_3' tests.

At 1% of strain, the samples sheared under the constant σ_3' path present higher values of stiffness than the other two types of tests. The samples sheared under the constant σ_1' path have lost virtually all of their stiffness and E_{tan} from the constant p' tests has substantially decreased, as second yield of the bonds has already occurred at $\varepsilon_a \cong 0.55\%$. Finally at 2% of strain, the samples sheared following the constant σ_3' path present very low values of stiffness, as second yield has already occurred at lower strains and values become similar to those observed in the constant p' tests at the same strain level.

Therefore as it was previously discussed, the rotation of the stress path direction to the left of a conventional constant σ_3' path directly influences the development of E_{tan} during shearing, with higher values of stiffness presented from the σ_1' tests than any other test. The constant p' tests presented slightly higher E_{tan} values than those observed by the constant σ_3' tests and substantially lower than those from the constant σ_1' tests. However, because the position of the second yield is also affected by the rotation of the stress path direction and occurs at lower strains, E_{tan} in the constant σ_1' tests decreases earlier (at lower strains) than the other tests. Thus only the constant σ_3' tests presented higher stiffness values than the other two types of tests at $\varepsilon_a \cong 1\%$, as this is prior to second yield of the bonds for this stress path direction.

6.4.4 Strain contours for the three different types of drained test

The 0.1%-2% strain contours defined from the three different types of test are plotted in the stress space in fig. 6.26. Except for the contours at 0.1% of strain, the rest of the contours at specific strain percentages follow the same pattern of behaviour. The strain contours for the constant σ_3' tests are positioned at lower q values in the stress space than the contours defined from the constant p' and the constant σ_1' tests, for the whole range of p'. All the contours defined from the constant p' tests are positioned closer to the constant σ_3' contours, for almost the whole range of stresses. Before the second yield of the bonds the contours are closer to the p' axis. However after the second yield takes place, for the constant σ_1' at $\varepsilon_a \cong 0.25\%$, for the constant p' at $\varepsilon_a \cong 0.55\%$ and for the constant σ_3' at $\varepsilon_a \cong 1\%$, the contours change direction towards the bounding surface.

Therefore the different stress paths directions followed in the drained tests affected the development of axial strain with respect to the stress paths. A drained test following a stress path to the left of the constant σ_3' tests influences the development of axial strain in the stress space with less strain developing for a given deviatoric stress. A stress path even further to the left, moves the position of the strain contours to a higher stress level in the stress space. Thus as can be seen in fig. 6.26 and 6.15, the samples from the constant σ_1' tests approach the bounding surface at a lower strain level ($\varepsilon_a \cong 1\%$), than that developed during the constant p' and the constant σ_3' tests. However it should be noted that the stress path direction followed under a constant σ_1' test is a major change in stress path direction in comparison with that followed under a constant σ_3' test and involves a decrease in mean effective stress.

6.4.5 Rotation of the stress path direction in the stress space

From the results previously presented there is evidence that the rotation of the stress path direction to the left of a conventional constant σ_3' drained test, directly

influences the soil's behaviour in respect of the development of E_{tan} during shearing, the position of the second yield of the bonds and the development of axial strain with respect to the stress paths.

A first rotation of the stress path to the left of the constant σ_3' path, to a constant p' drained path, caused an increase in E_{tan} compared with that presented from the constant σ_3' tests. Second yield of the bonds is initiated at a lower percentage of axial strain. This is reflected to the position of the second yield surface in the stress space, which occurs at lower q values than those defined from the constant σ_3' tests. Accordingly, for the same deviatoric stress level less axial strain is developed compared to that observed during the constant σ_3' tests.

A further rotation of the stress path to the left, to a constant σ_1' path, caused a further increase in the E_{tan} values and a further decrease in the value of axial strain at which second yield of the bonds takes place. Thus the second yield surface has a lower position in the stress space. Furthermore for the same deviatoric stress level, less axial strain is developed from the samples sheared under the constant σ_1' path. Generally a more significant change is observed in the rotation of stress path direction from constant p' to constant σ_1', than that seen in rotating from constant σ_3' to constant p'.

6.4.6 Yield of the bonded structure

The change of the position of the second yield surface with the rotation of the stress path direction indicates an anisotropic destruction of the bonded structure of the soil, when shearing along different stress paths in the stress space. However the structure of the bonded soil can not account for that; Maccarini (1987), and Bressani (1990), both underline the fact that the initial structure of the soil before shearing is quite isotropic. Furthermore Bressani (1990), presented microphotographs of bonded soil sheared under a conventional drained path, up to 2% and 20% of

axial strain. The sample sheared up to 2% of strain presented a fairly uniform and isotropic structure with some of the bond bridges between the sand grains broken. However no particular orientation of the particles was observed, even though second yield had already occurred. Only the sample tested up to 20% of axial strain showed a matrix of sand particles and broken fired kaolin.

Therefore the earlier loss in E_{tan} observed with the rotation of the stress path direction is probably due to the development of high negative volumetric and radial strains, induced by the stress path followed in the stress space. During the constant p' and constant σ_1' tests, σ_3' decreases with time in order to keep constant the desired stress path. This decrease in σ_3' initiated high negative radial and volumetric strains from the beginning of shearing, which therefore initiated an earlier destruction of the bonded structure compared with that observed in a constant σ_3' test. However due to possible membrane error effects, the values of the volumetric and radial strains can only be used for a qualitative study.

Therefore the second yield surfaces defined from the constant σ_3' and the constant σ_1' drained paths define two limiting yield surfaces in the stress space. Thus a sample sheared along a constant stress path between the constant σ_1' and the constant σ_3' paths will yield at a point between the two yield surfaces defined in fig. 6.23. Furthermore the position of yield under different stress path directions also depends on the initial p_0' at which the soil was consolidated before shearing. In fig. 6.27 the three yield surfaces are plotted in the stress space and yield loci, defined for different p_0' are also presented. Thus for example, a sample consolidated at $p_0'=300kPa$ and sheared under different stress path directions between the limiting σ_1' and σ_3' paths, will yield on this surface defined for $p_0'=300kPa$. It is interesting to see that the yield loci increase in shape with the increase of p' and that indicates that yield is stress level dependent and not dependent on the bond strength alone.

6.4.7 Final remarks

In this chapter the behaviour of the bonded soil was studied under probing triaxial drained tests. The soil under the constant p' and constant σ_1' tests presented max q/p' ratios similar to that observed under the conventional drained tests (fig. 6.19 and 6.21). However the rotation of the stress path direction to the left of the constant σ_3' path strongly influenced the second yield of the bonds, which occurred at lower axial strains than those observed under the constant σ_3' path. The greater the degree of rotation of the stress path direction the lower the axial strain at yield.

Three yield surfaces were defined in the stress space, each of which corresponds to the stress path direction followed (fig. 6.23). The anisotropic breakdown of the bonds is suggested to be due to the development of higher negative volumetric and radial strains in the probing tests, compared to those developed in the conventional drained tests. Yield was also found to be stress level dependent and yield surfaces for specific p_0' were plotted in the stress space (fig. 6.27).

The rotation of the stress path direction also influenced the development of E_{tan}, producing higher values than those observed from the conventional drained tests (fig. 6.25), up to the point of yield when a loss in E_{tan} was initiated for all the tests. The development of axial strain with respect to the stress paths was also affected and less strain was developed for a given deviatoric stress. The strain decreased to lower values with the increase of the degree of rotation to the left of the constant σ_3' path (fig. 6.26).

Test	Initial void ratio e_0	Consolidation pressure (kPa)
cp'35	0.597	35
cp'100	0.600	100
cp'250	0.598	250
cp'500	0.601	500

Table 6.1 Details for the constant p' drained triaxial tests on bonded samples

Test	Initial void ratio e_0	Consolidation pressure (kPa)
cs1'70	0.601	70
cs1'100	0.597	100
cs1'200	0.603	200
cs1'300	0.600	300
cs1'525	0.599	525

Table 6.2 Details for the constant σ_1' drained triaxial tests on bonded samples
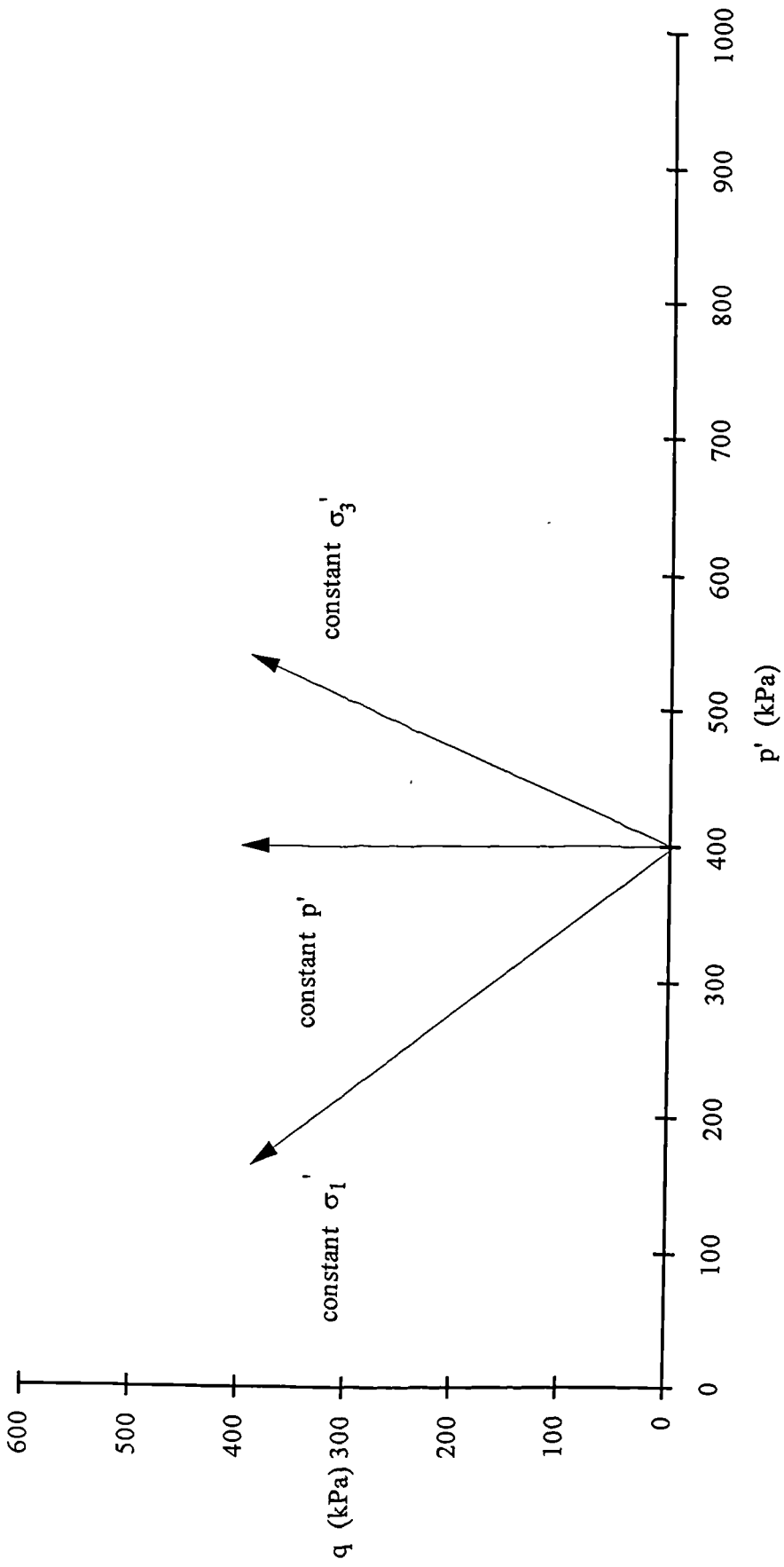
Fig. 6.1 Triaxial drained probing tests on bonded soil
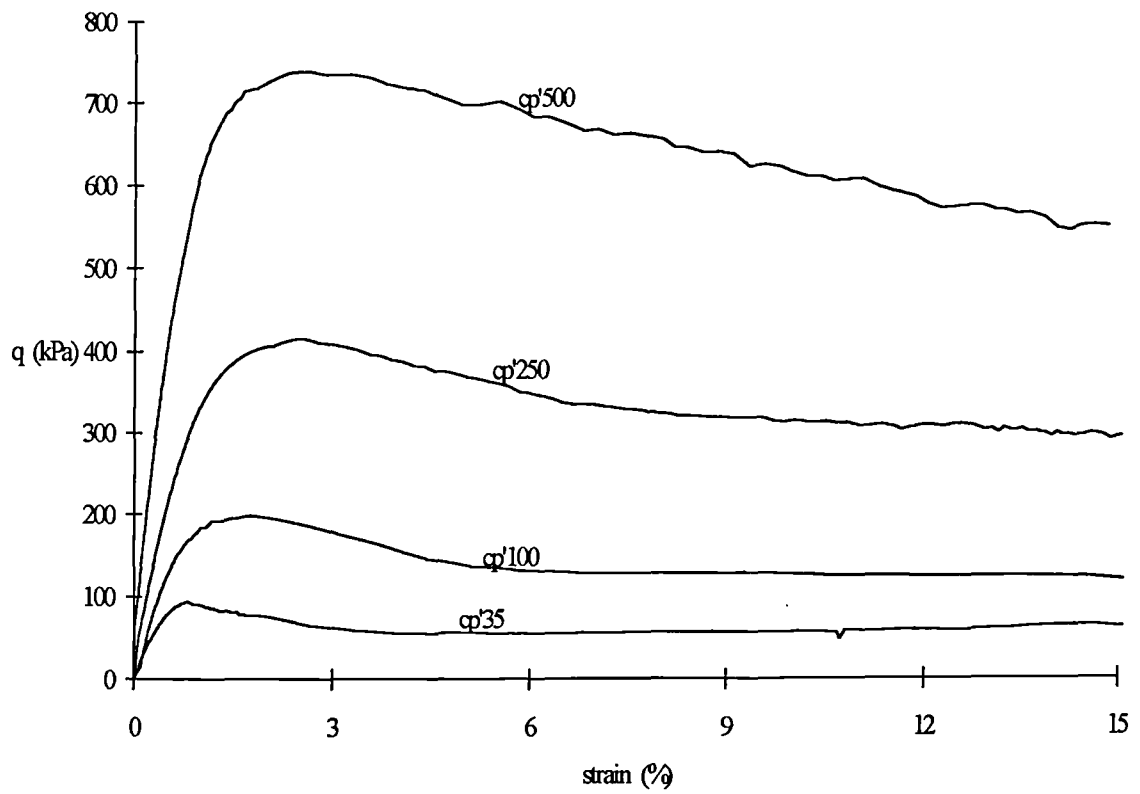
Fig. 6.2a Stress strain curves for the triaxial constant p' drained tests
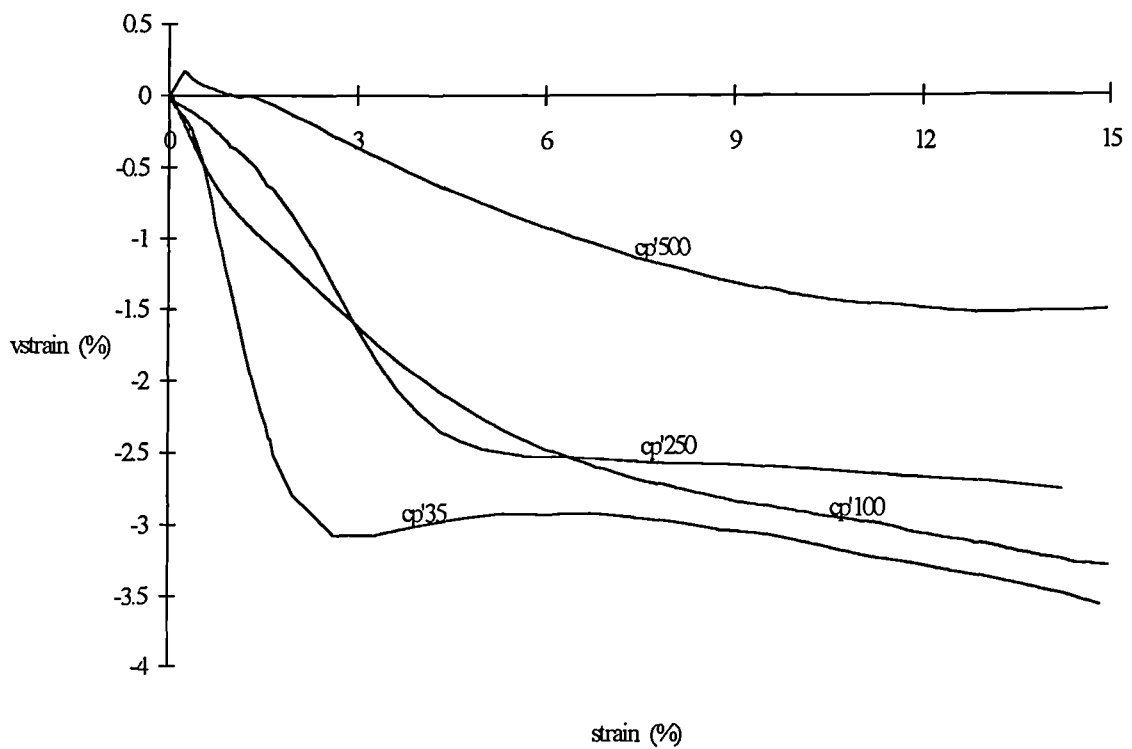
Fig. 6.2b Volumetric strain versus axial strain for the constant p' tests

189
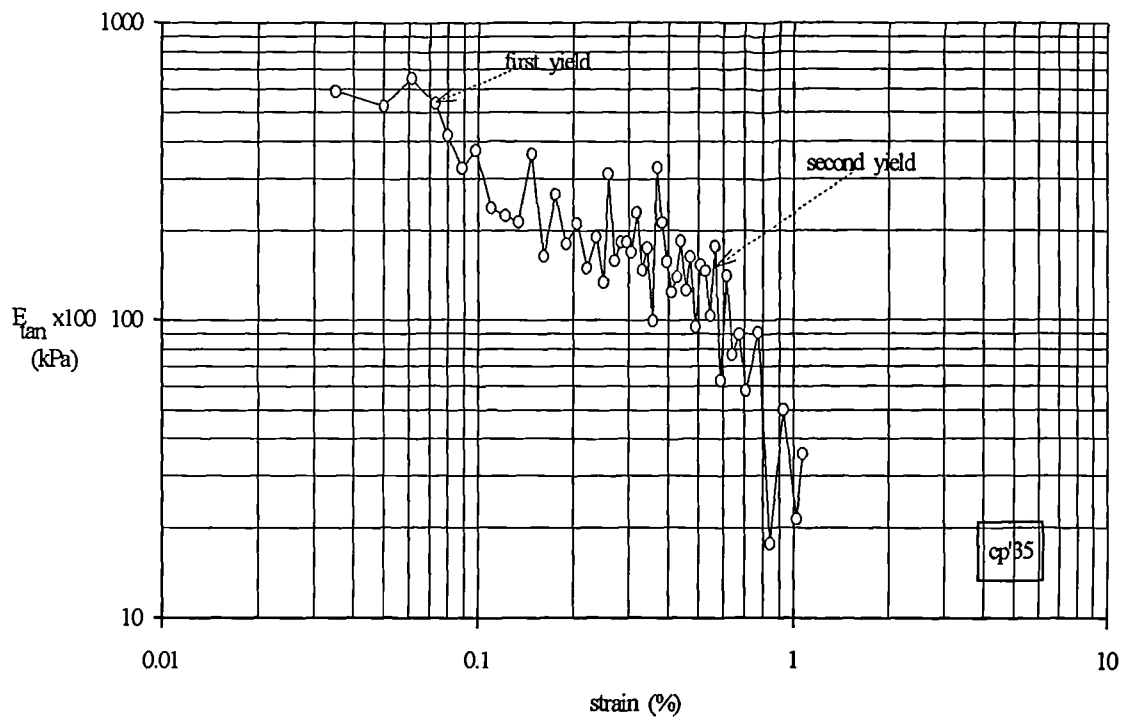
Fig. 6.3a Tangential stiffness during shearing for test cp'35
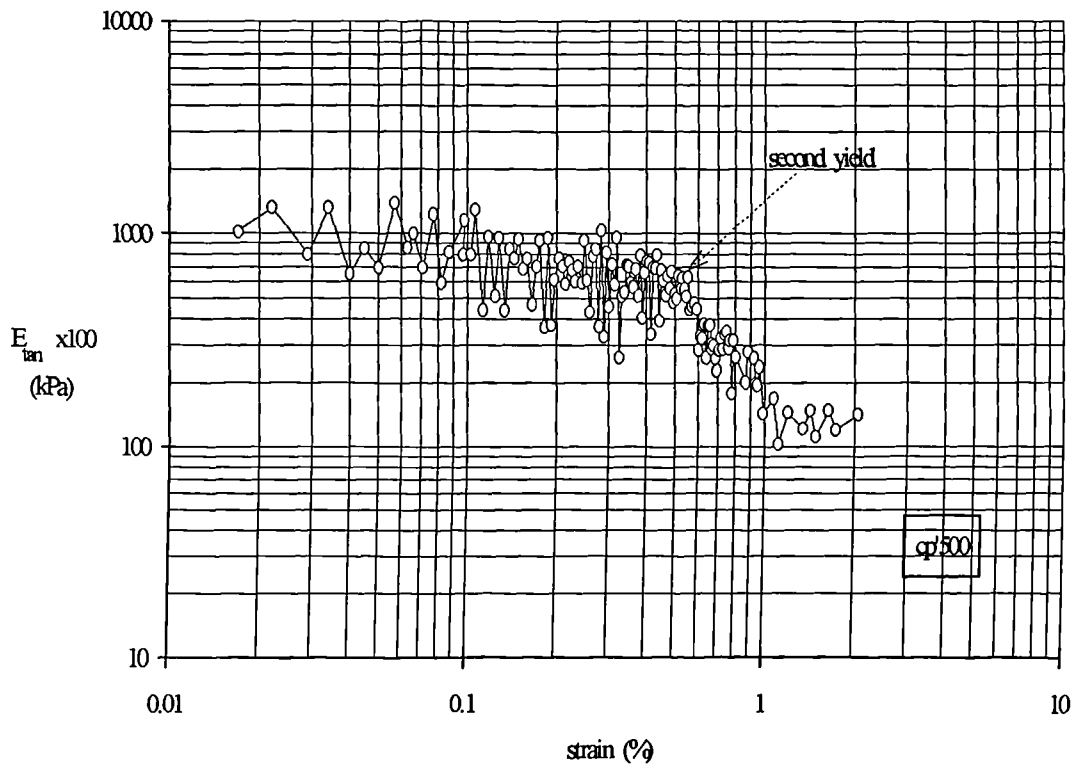
Fig. 6.3b Tangential stiffness during shearing for test cp'500
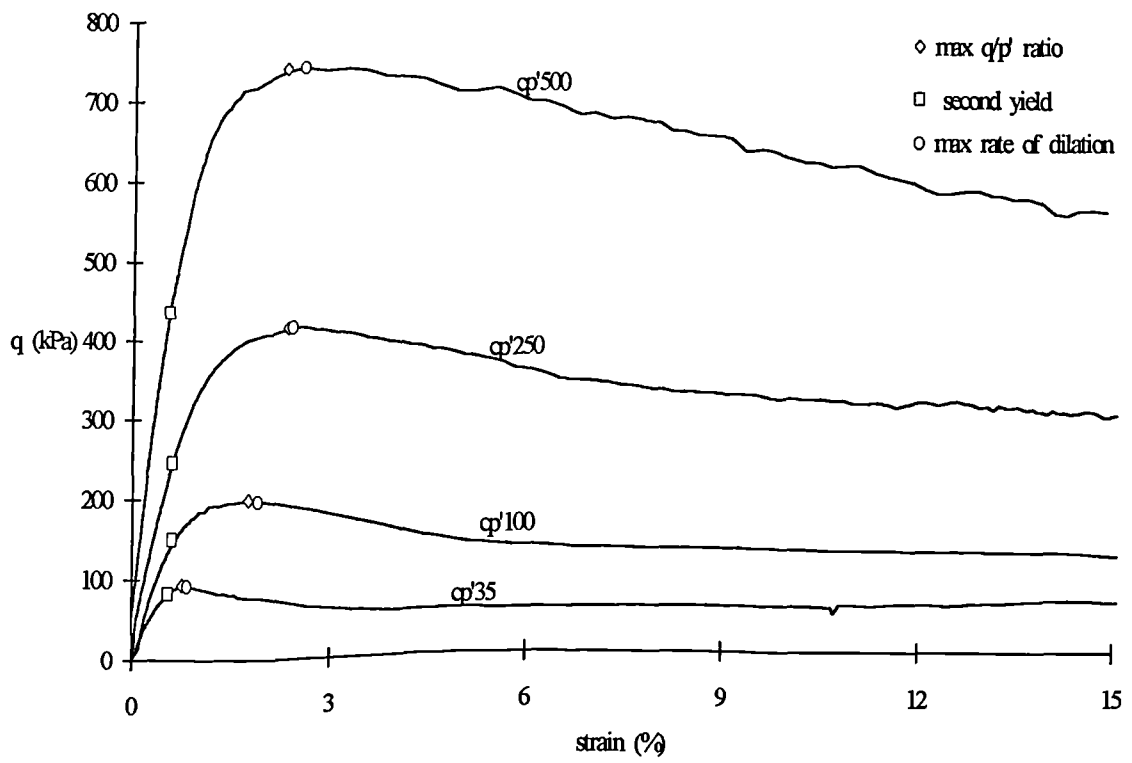
Fig. 6.4 Max q/p' ratio, second yield and max rate of dilation
for the constant p' tests
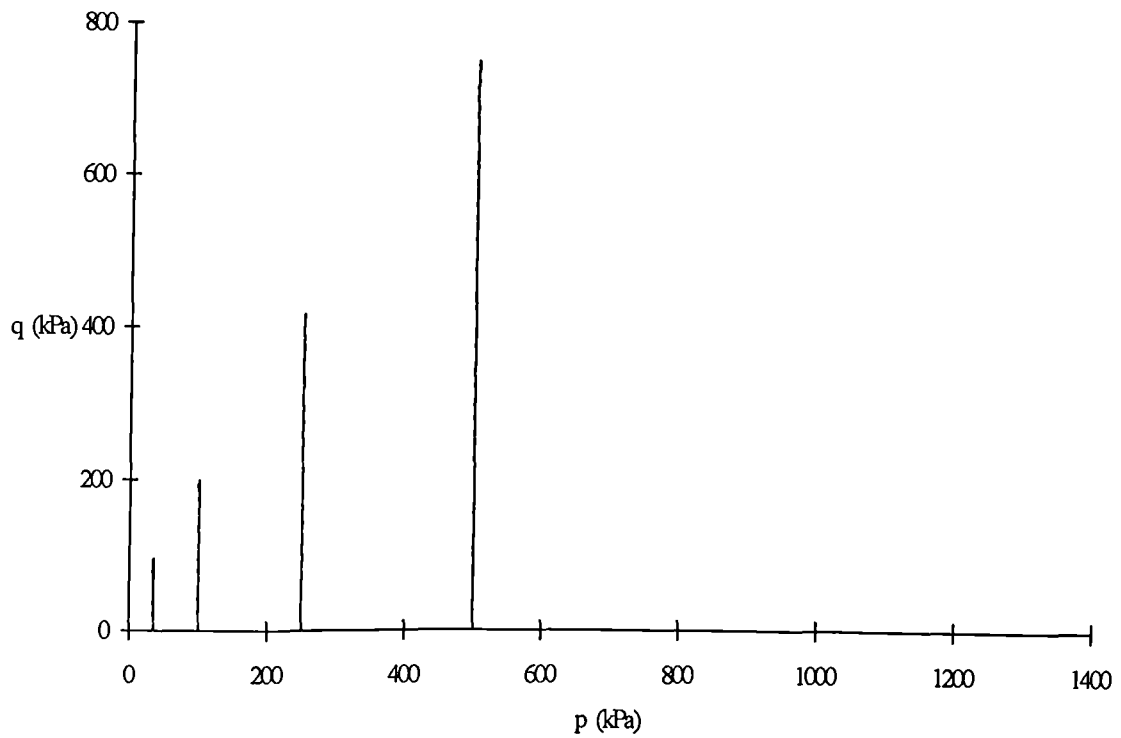
Fig. 6.5 Stress paths for the constant p' drained tests

191
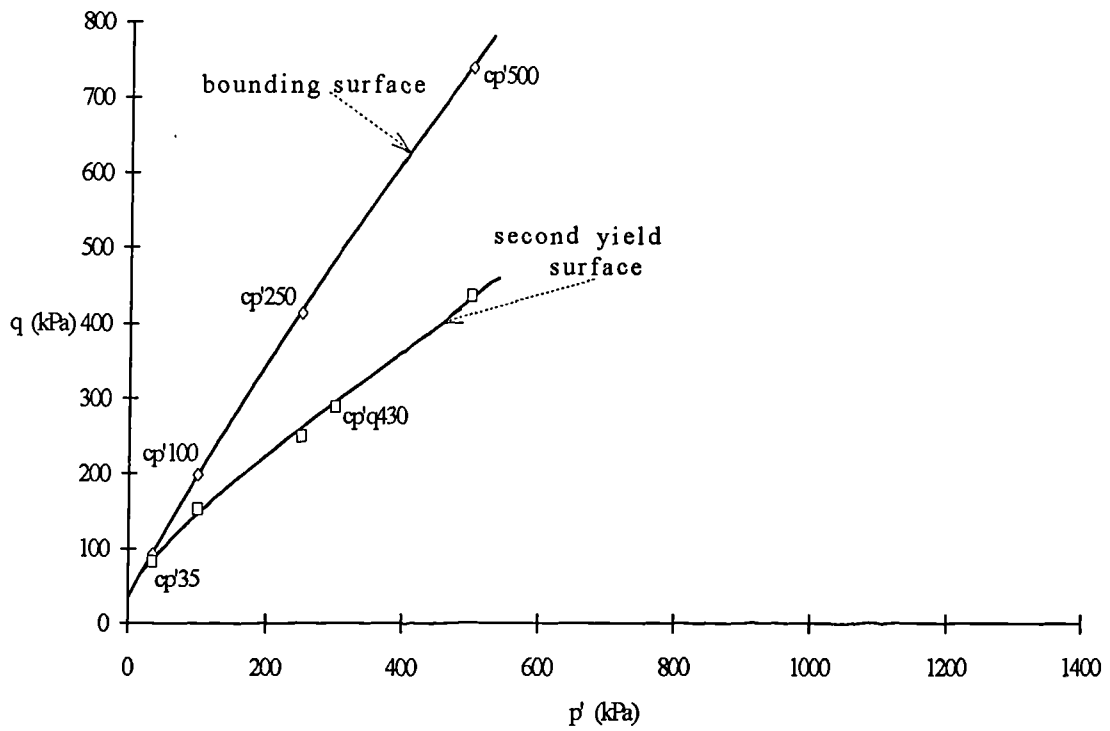
Fig. 6.6 Bounding and second yield surfaces plotted for the constant p' tests
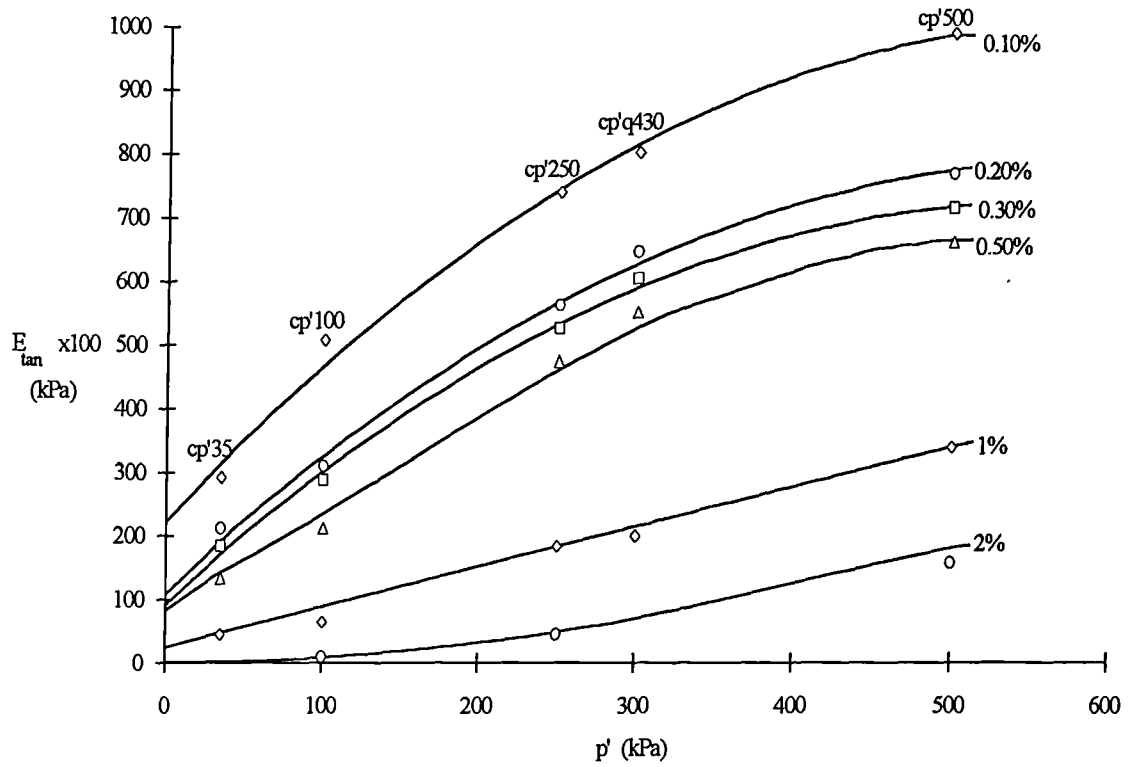
Fig. 6.7 Tangential stiffness plotted versus p' for the constant p' tests
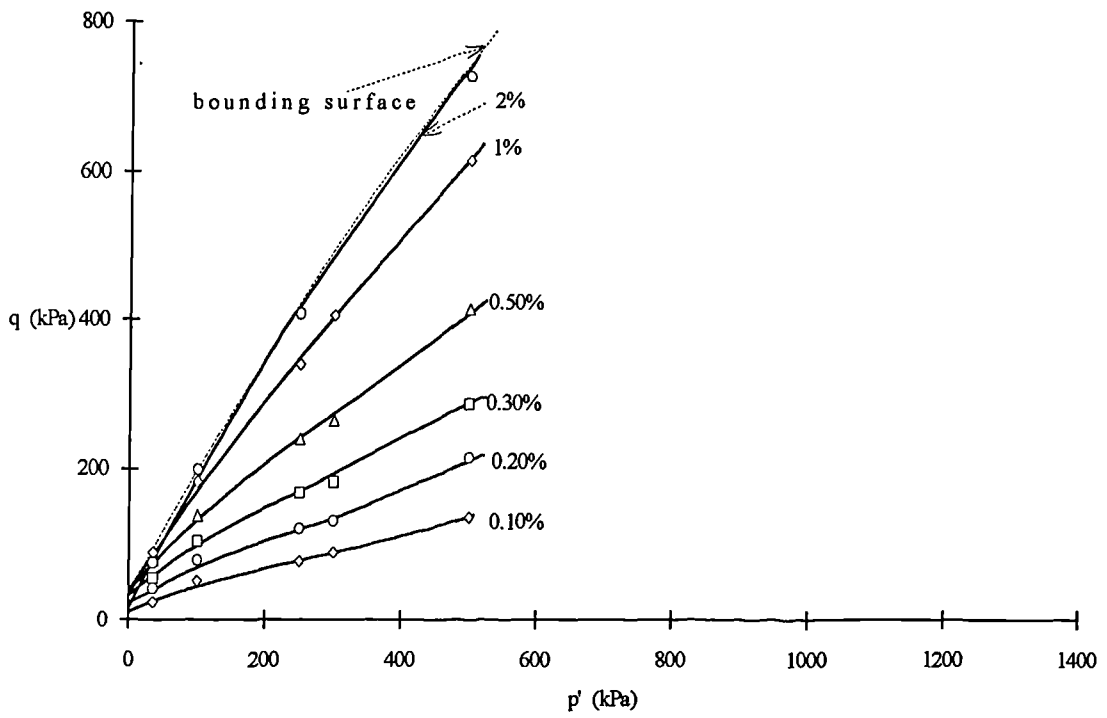
Fig. 6.8 Strain contours and bounding surface for the constant p' drained tests
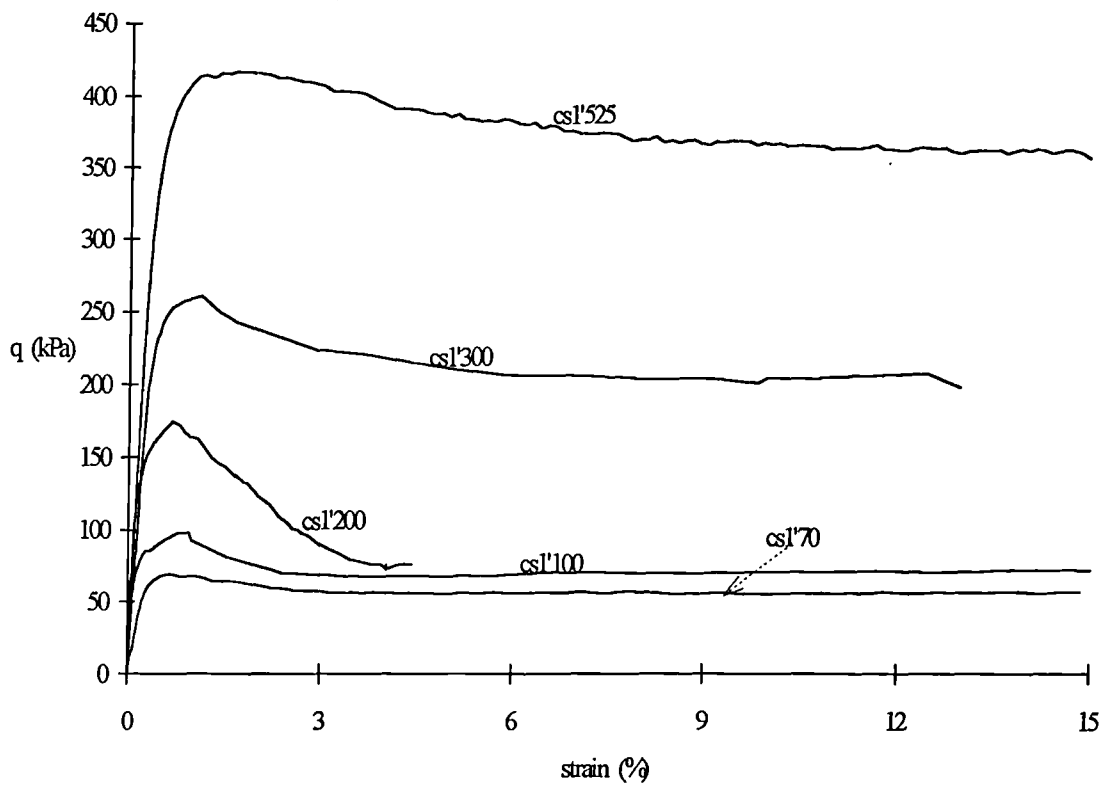
Fig. 6.9a Stress-strain curves for the constant σ_1' drained tests

193
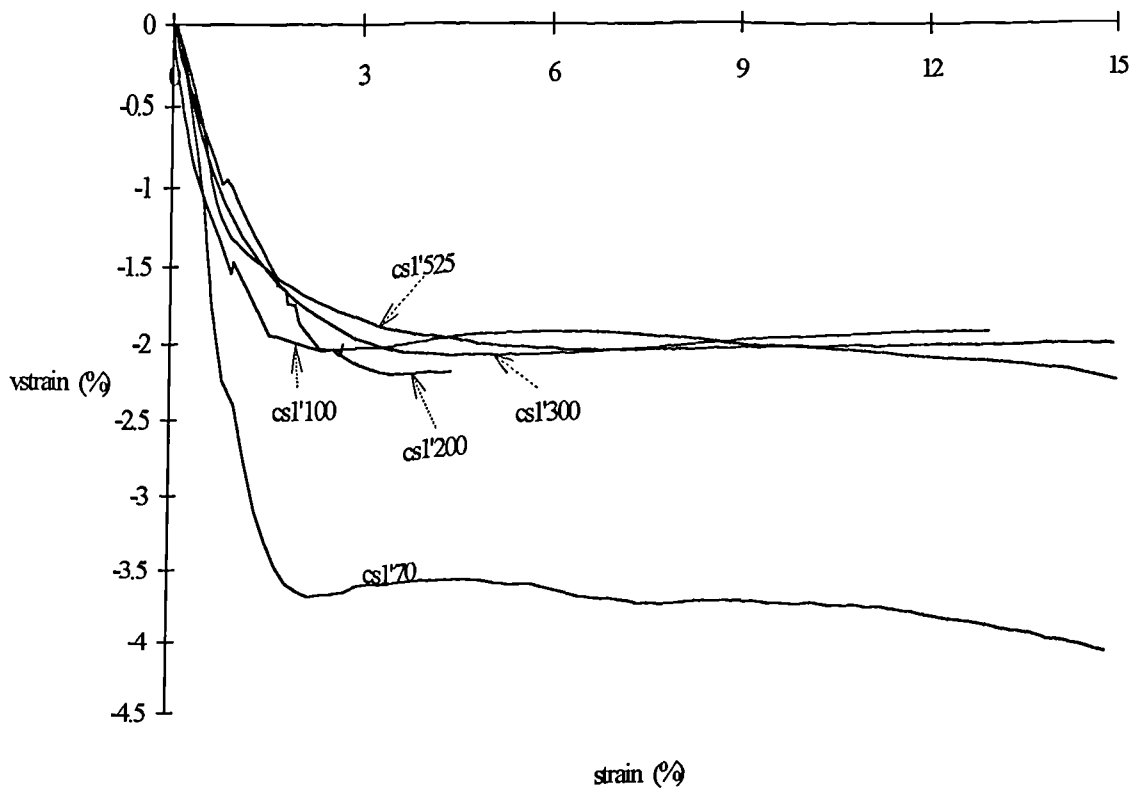
Fig. 6.9b Volumetric strain versus axial strain for the constant σ_1' tests
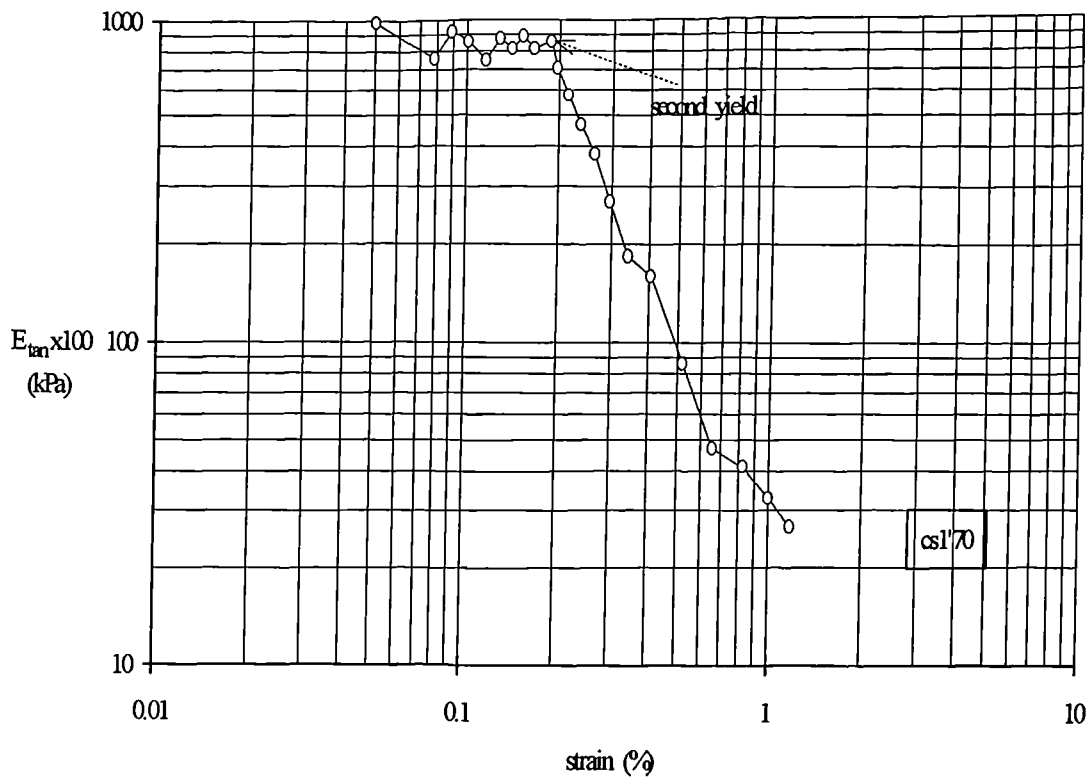
Fig. 6.10a Tangential stiffness during shearing for test csl'70
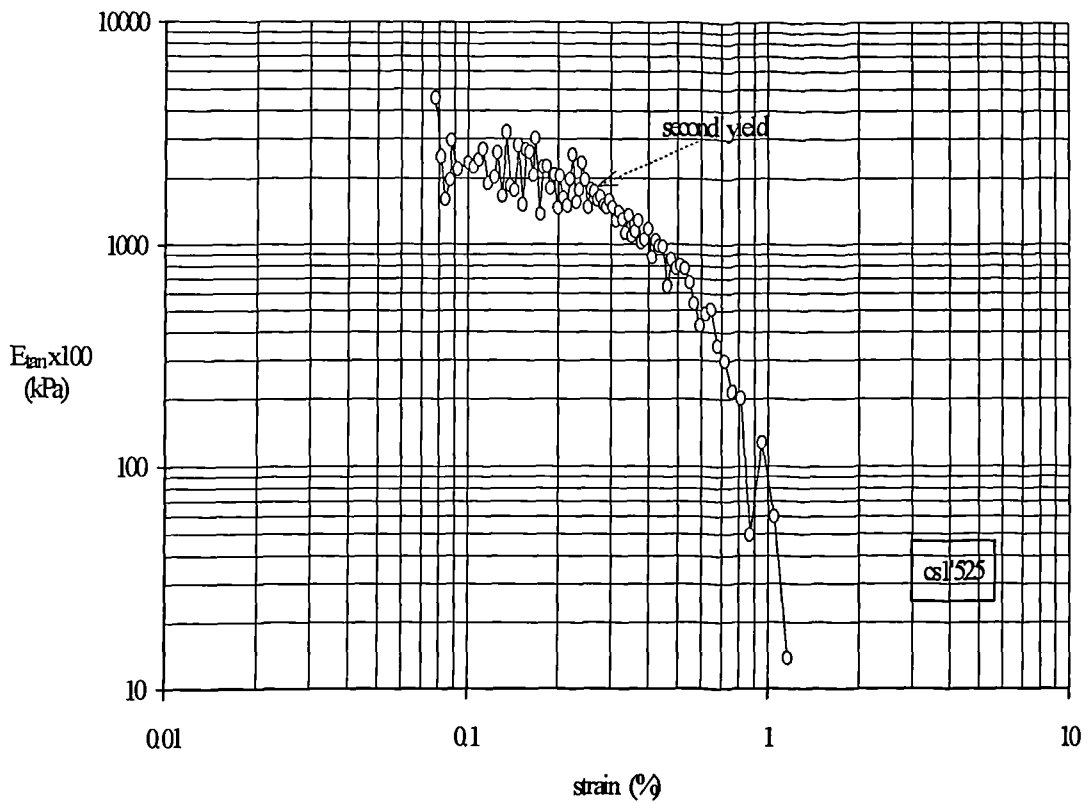
Fig. 6.10b   Tangential stiffness during shearing for test cs1'525
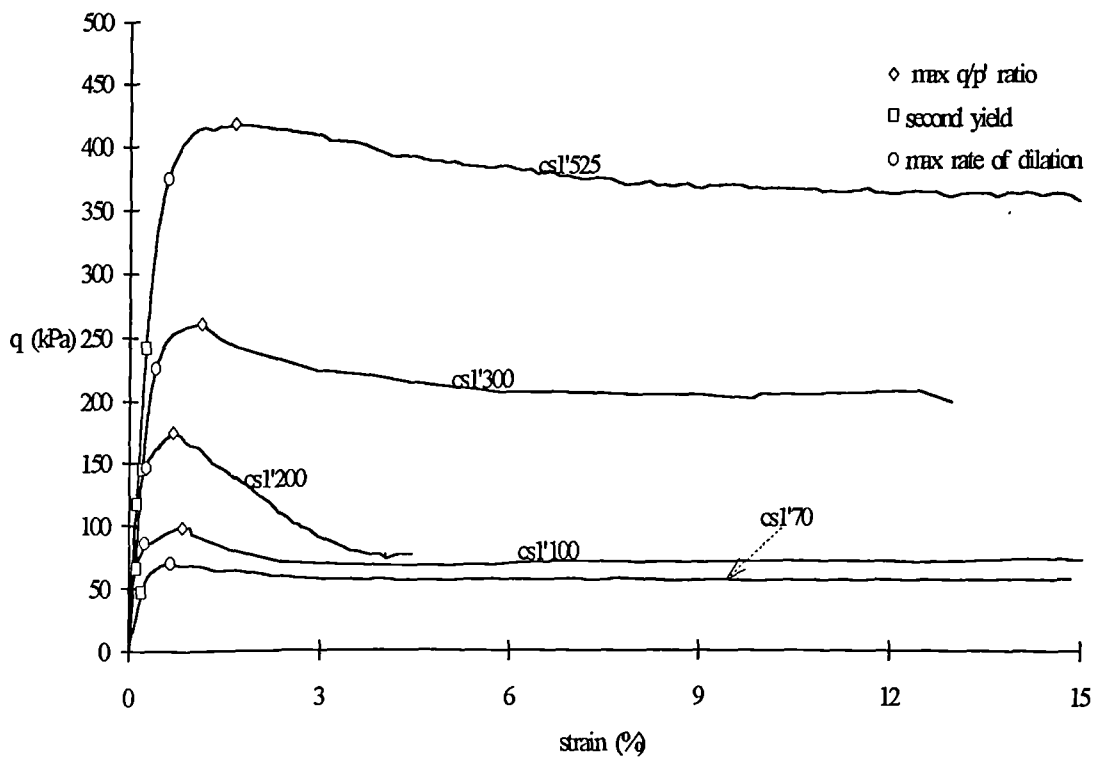
Fig. 6.11   Max q/p' ratio, second yield and max rate of dilation
for the constant σ_1' tests

195
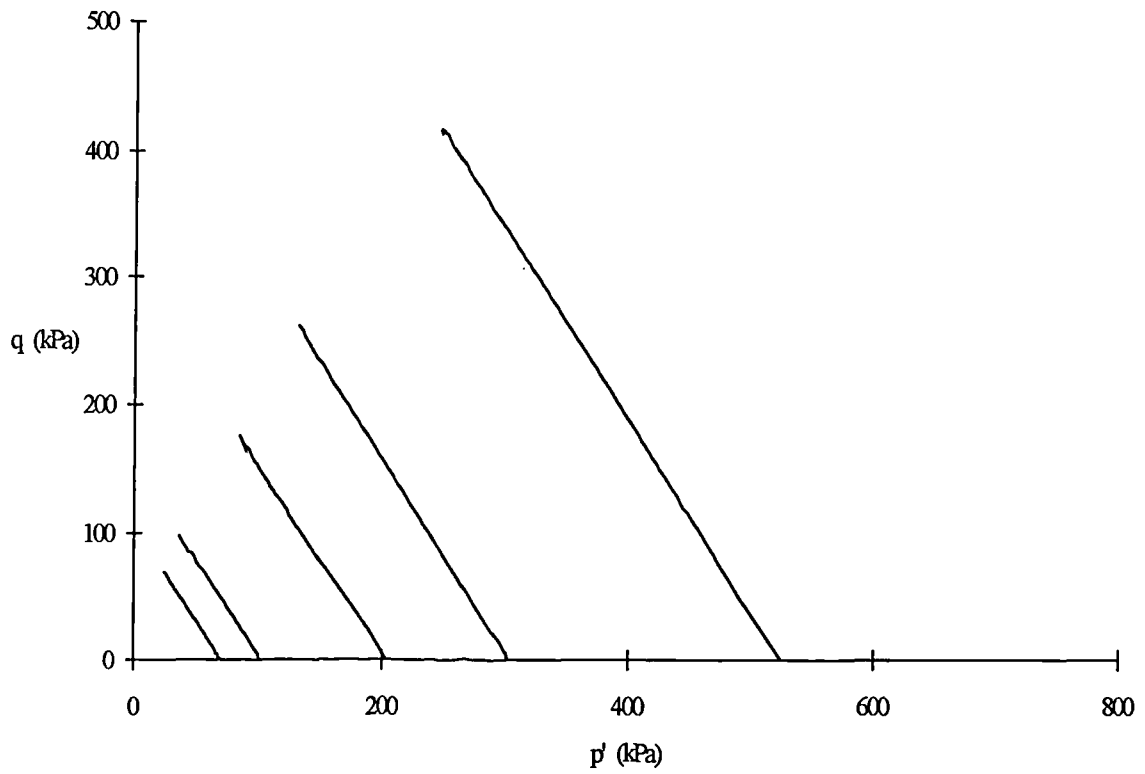
Fig. 6.12 Stress paths for the constant σ_1' triaxial drained tests
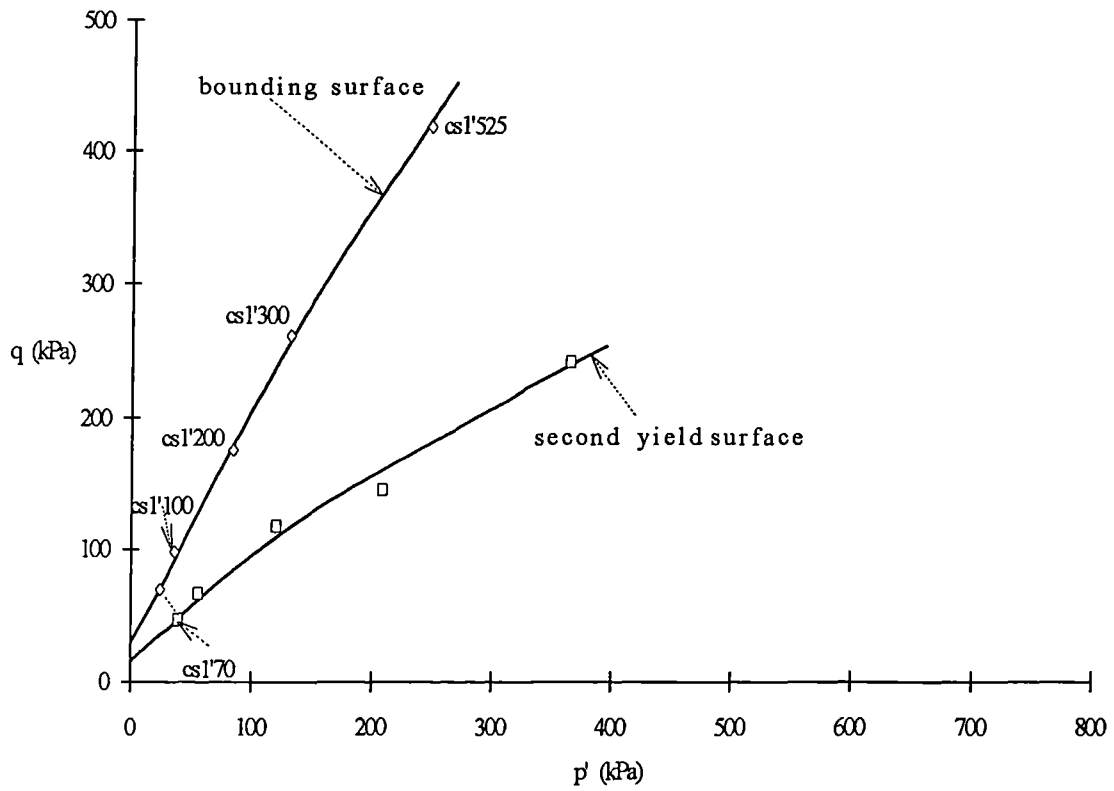
Fig. 6.13 Bounding and second yield surfaces plotted for the constant σ_1' tests

196
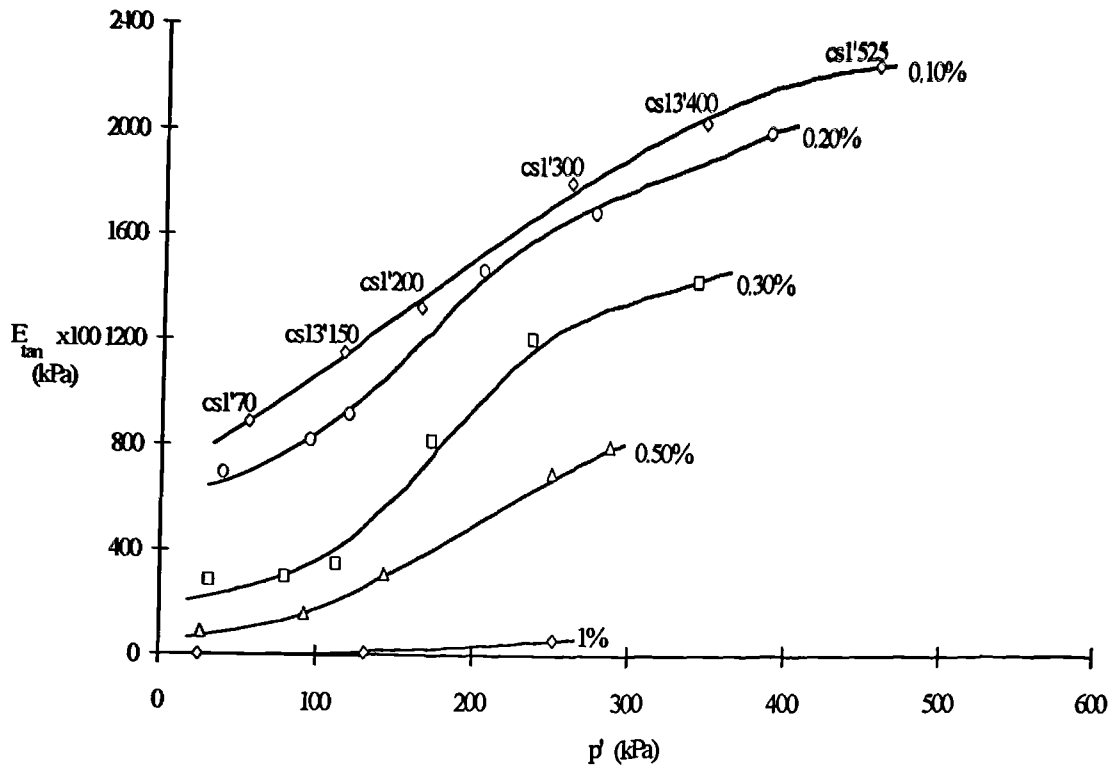
Fig. 6.14 Tangential stiffness plotted versus p' for the constant σ_1' tests
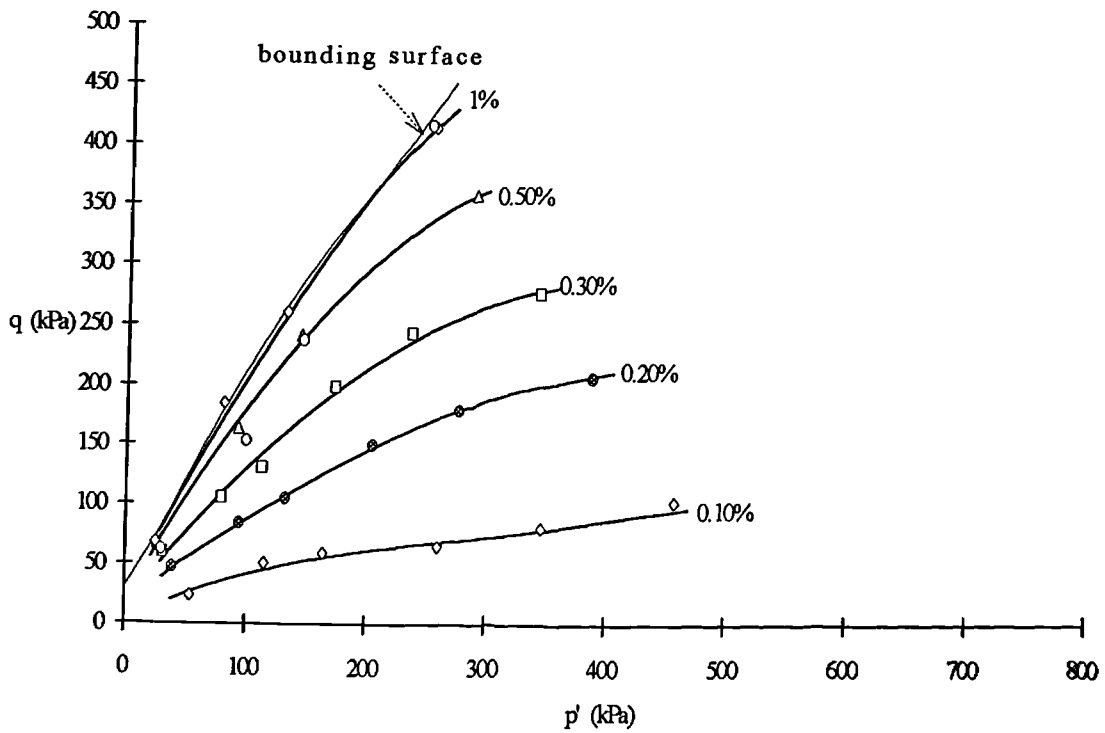
Fig. 6.15 Bounding surface and strain contours for the constant σ_1' tests
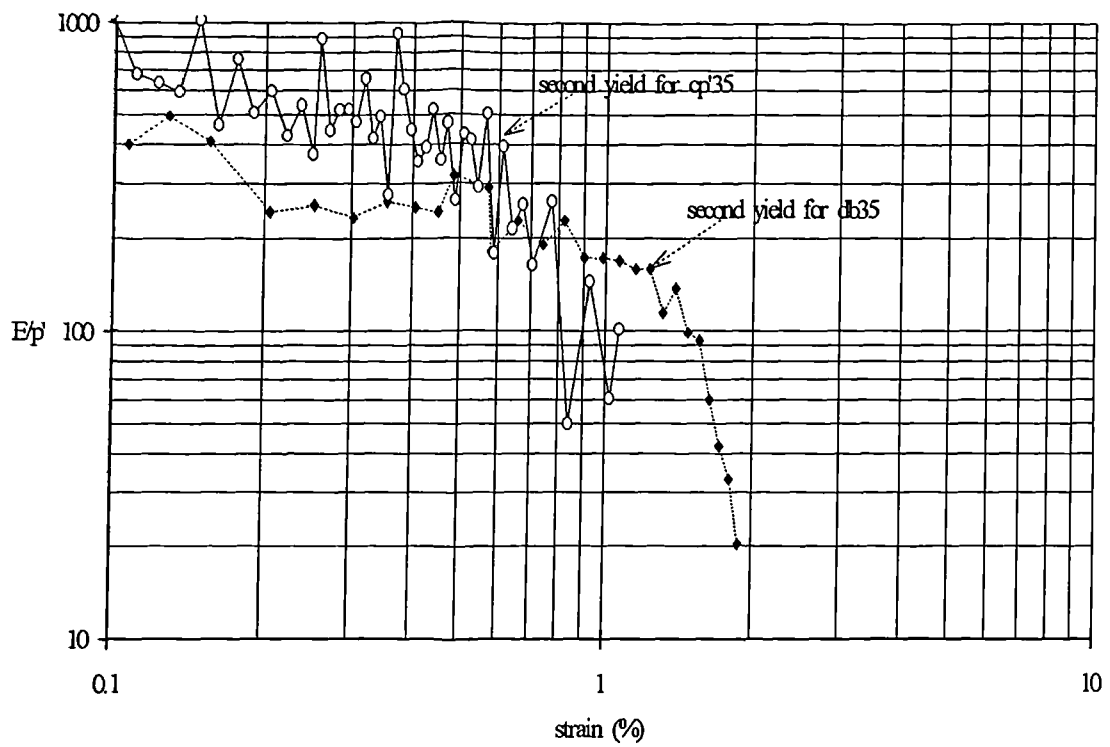
Fig. 6.16a   Second yield for a constant p' and a constant σ_3' test
sheared at p_o'=35kPa
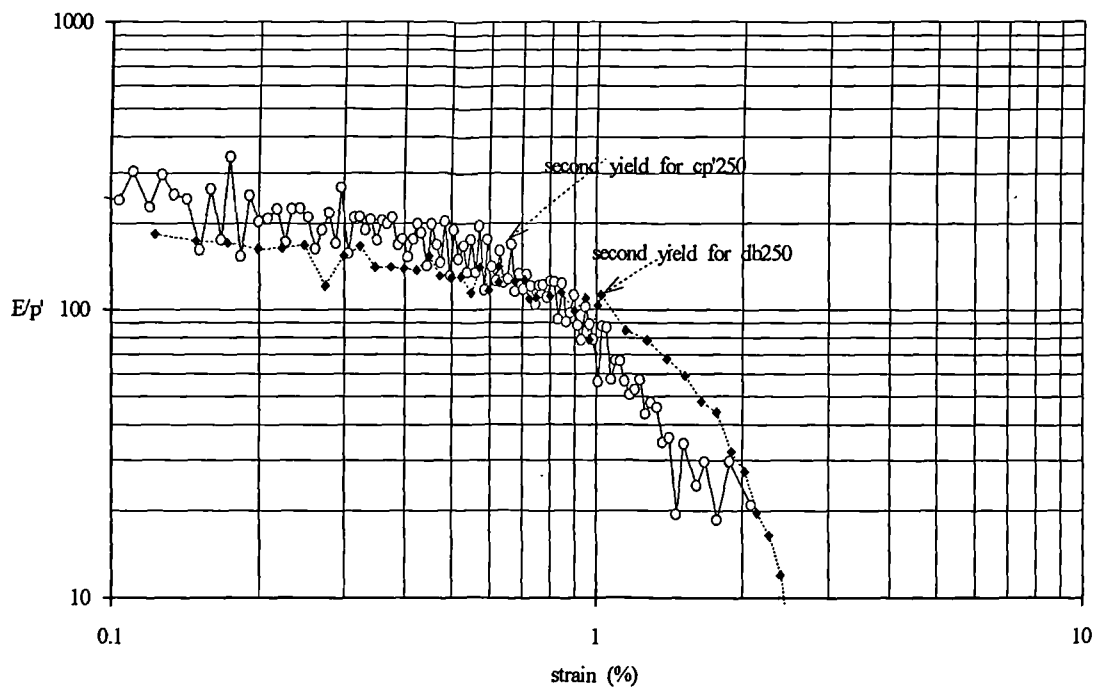
Fig. 6.16b   Second yield for a constant p' and a constant σ_3' test
sheared at p_o'=250kPa
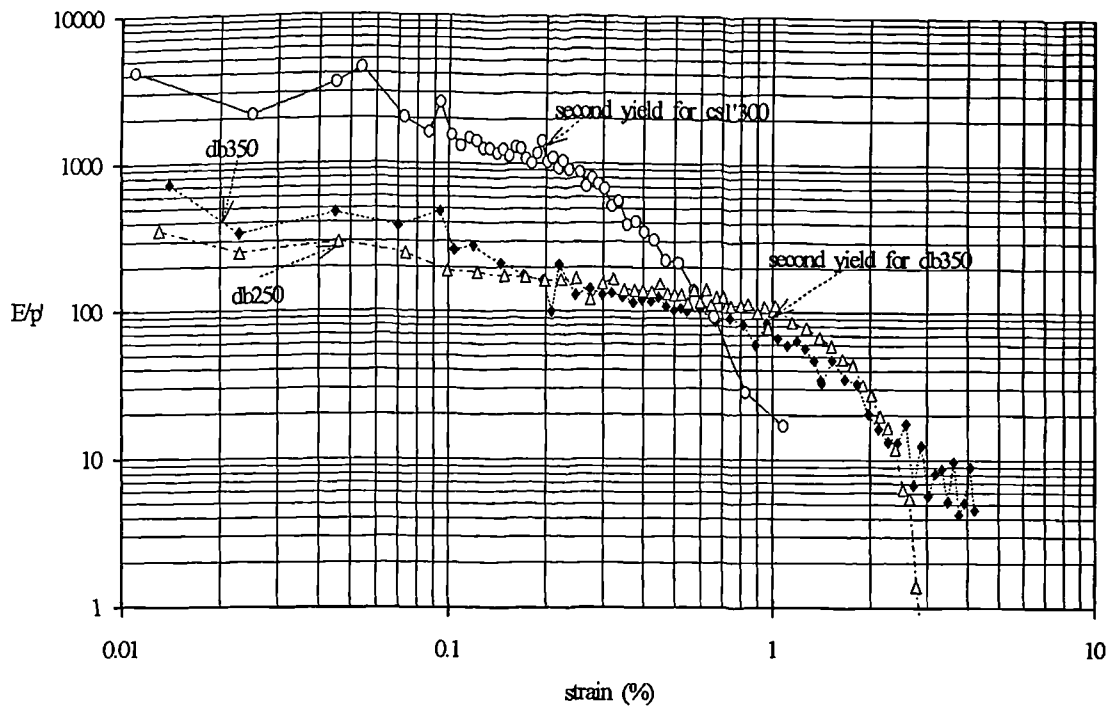
Fig. 6.17a Second yield for a constant σ_1' and two constant σ_3' triaxial drained tests sheared at similar p_0'
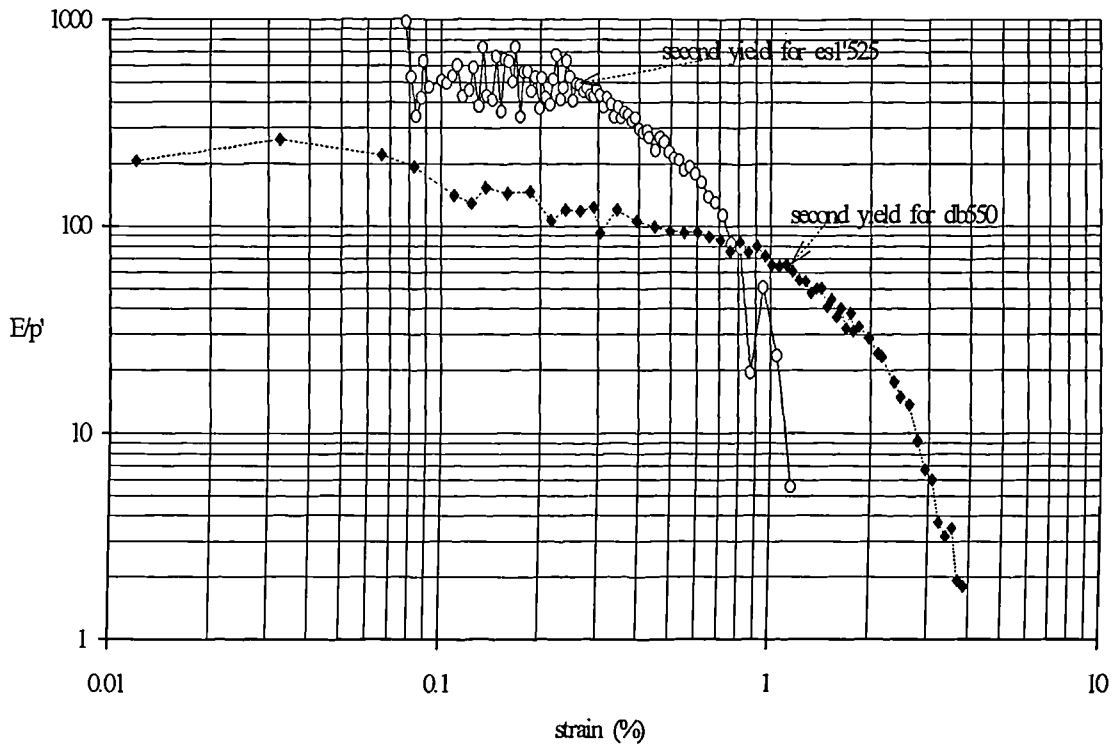
Fig. 6.17b Second yield for a constant σ_1' and a constant σ_3' test sheared at similar p_0'
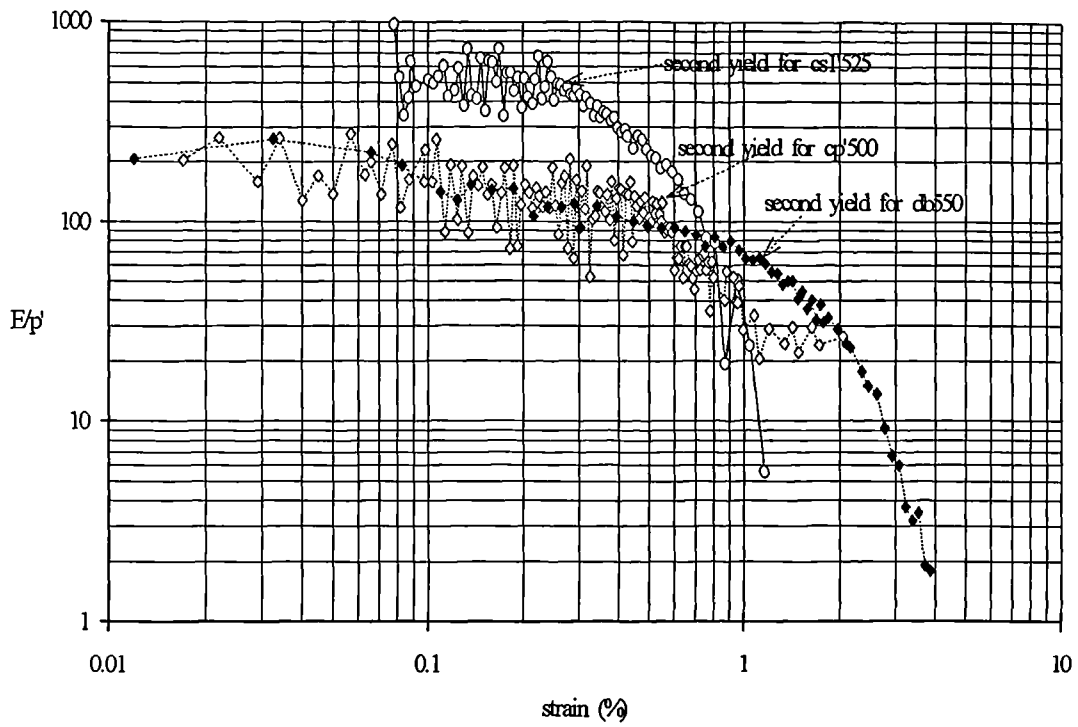
Fig. 6.18 Second yield for a constant σ_1', a constant p' and
a constant σ_3' triaxial drained test sheared at similar p_0'
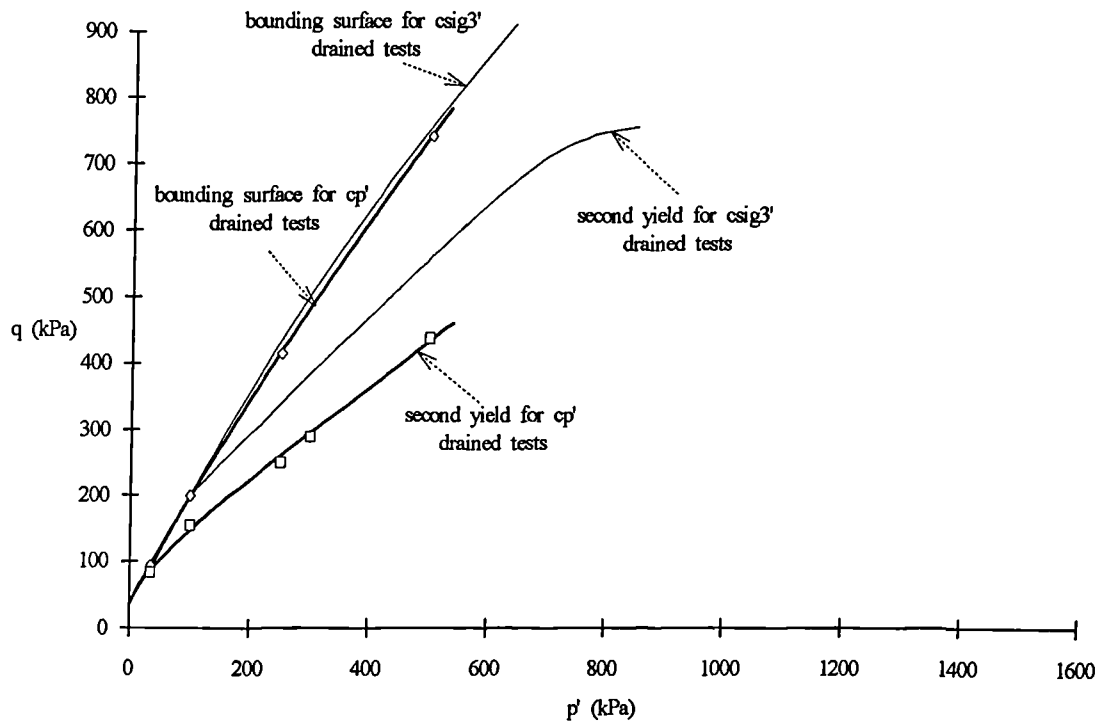
Fig. 6.19 Bounding and second yield surfaces after constant p'
and constant σ_3' tests
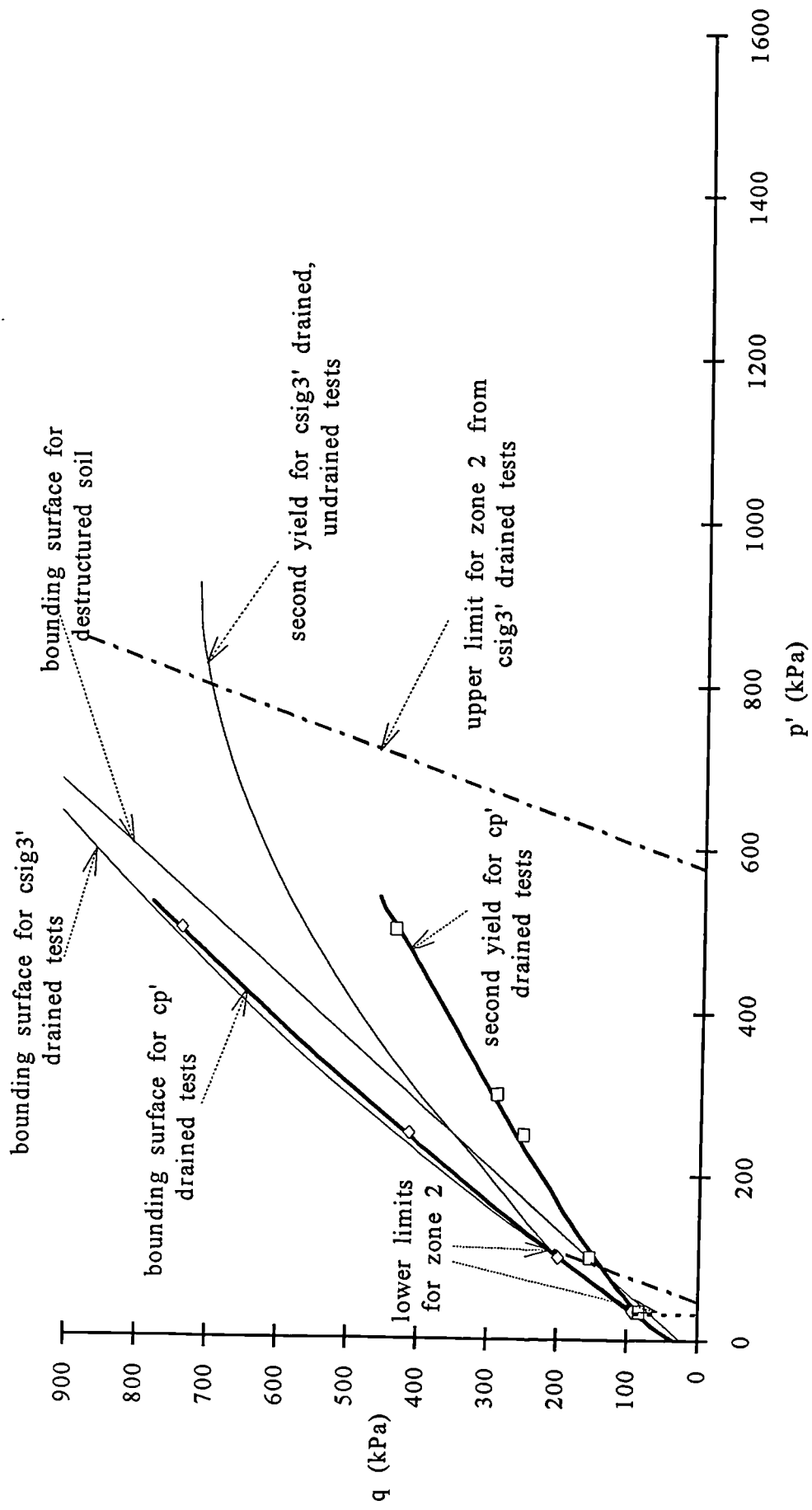
Fig. 6.20 First and second zones of behaviour for the bonded soil for the constant p′ and constant $\sigma_3′$ tests

201
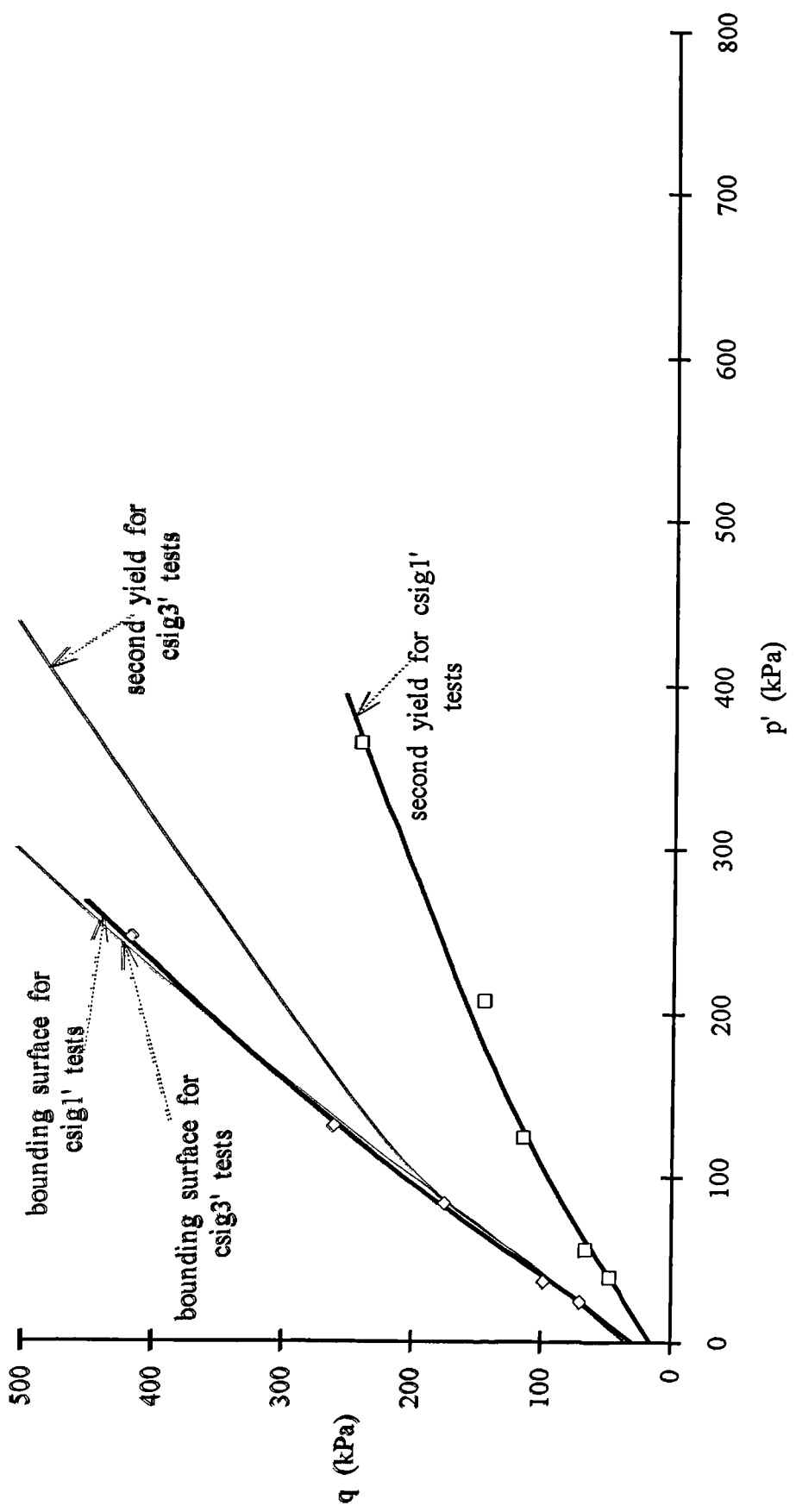
Fig. 6.21 Bounding and second yield surfaces after constant σ_1' and constant σ_3' tests

202
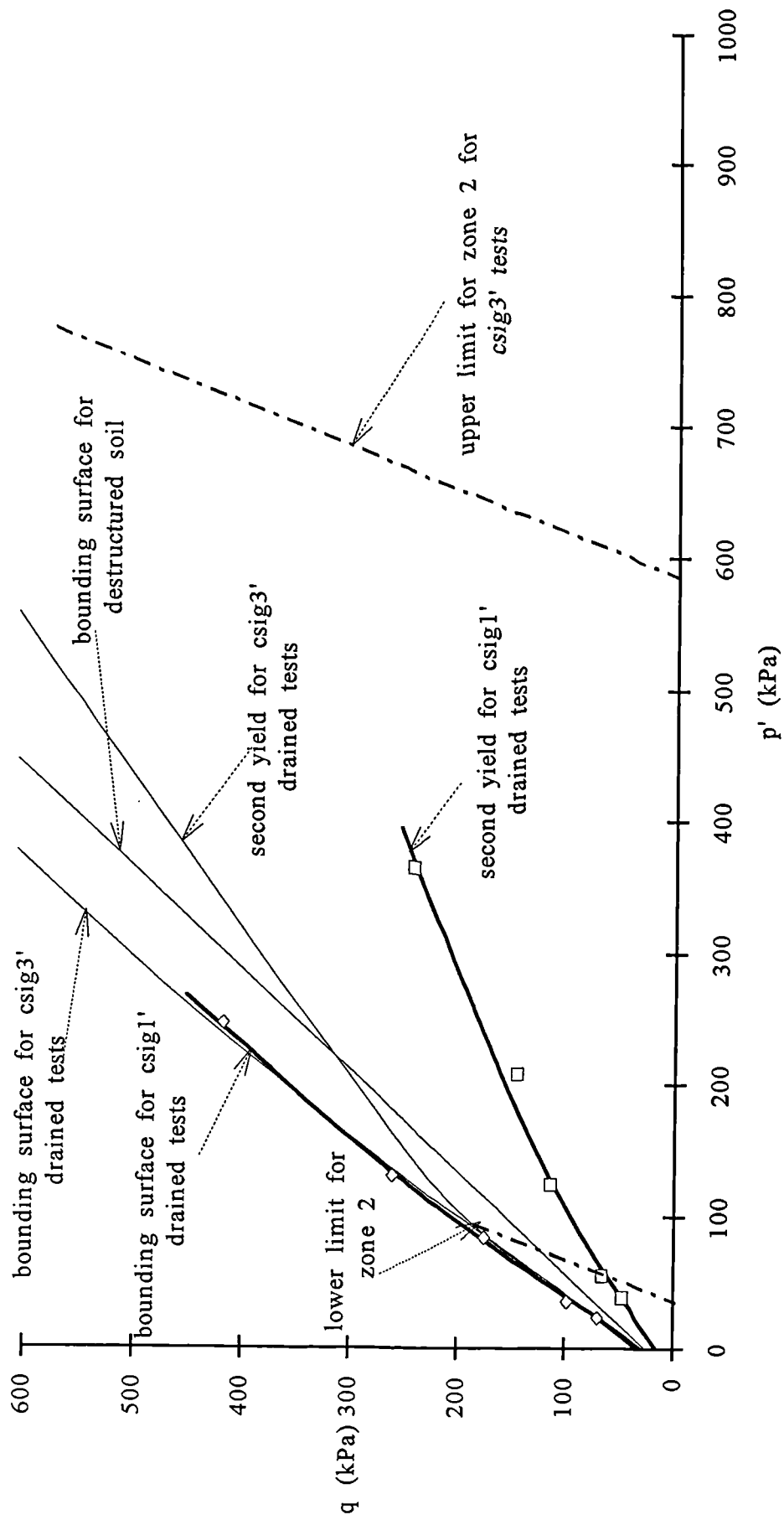
Fig. 6.22 First and second zones of behaviour for the bonded soil for the constant σ_1' and constant σ_3' triaxial drained tests

203
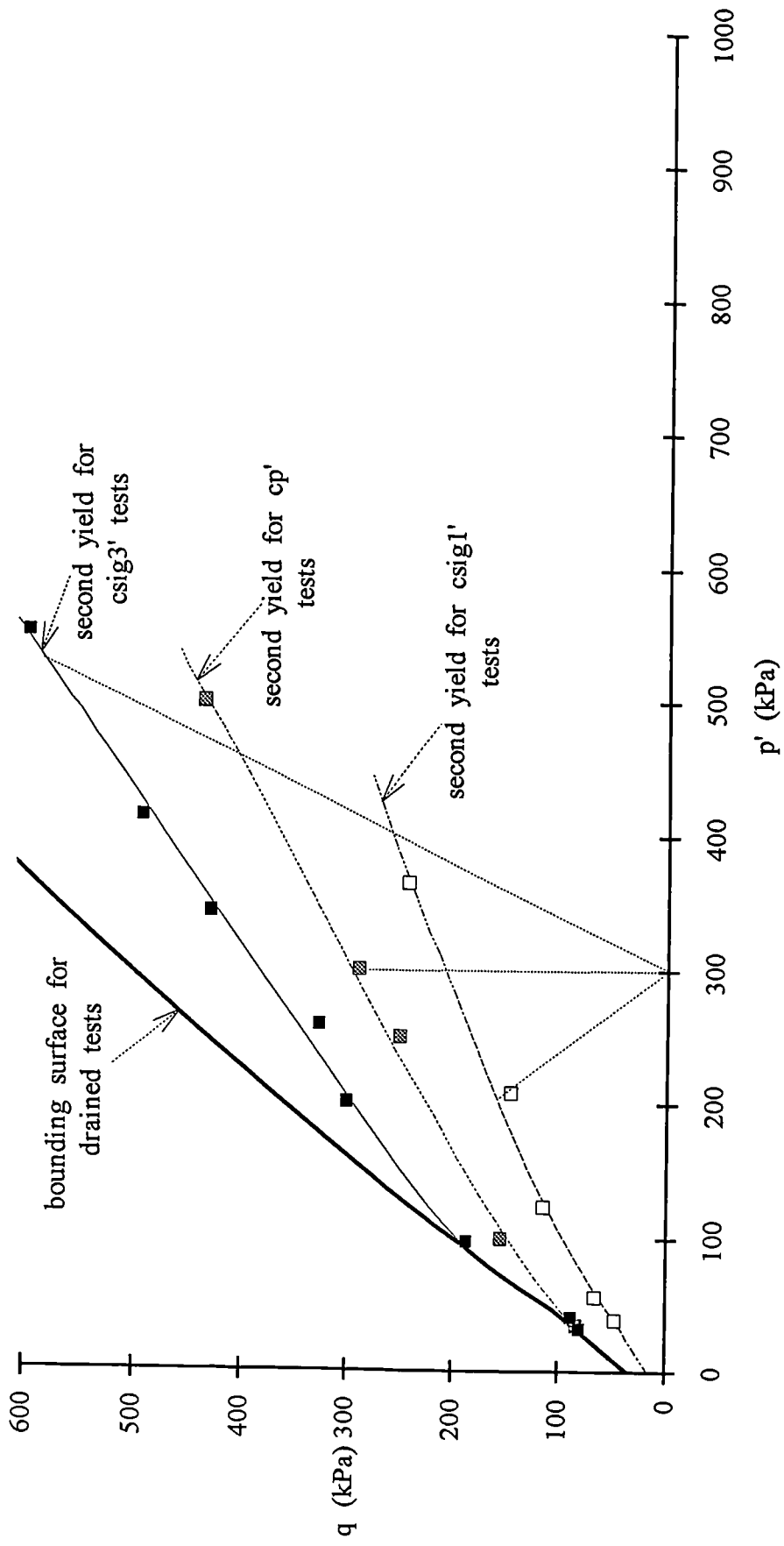
Fig. 6.23 Bounding surface and second yield surfaces for the constant σ_1', constant p' and constant σ_3' triaxial drained tests

204
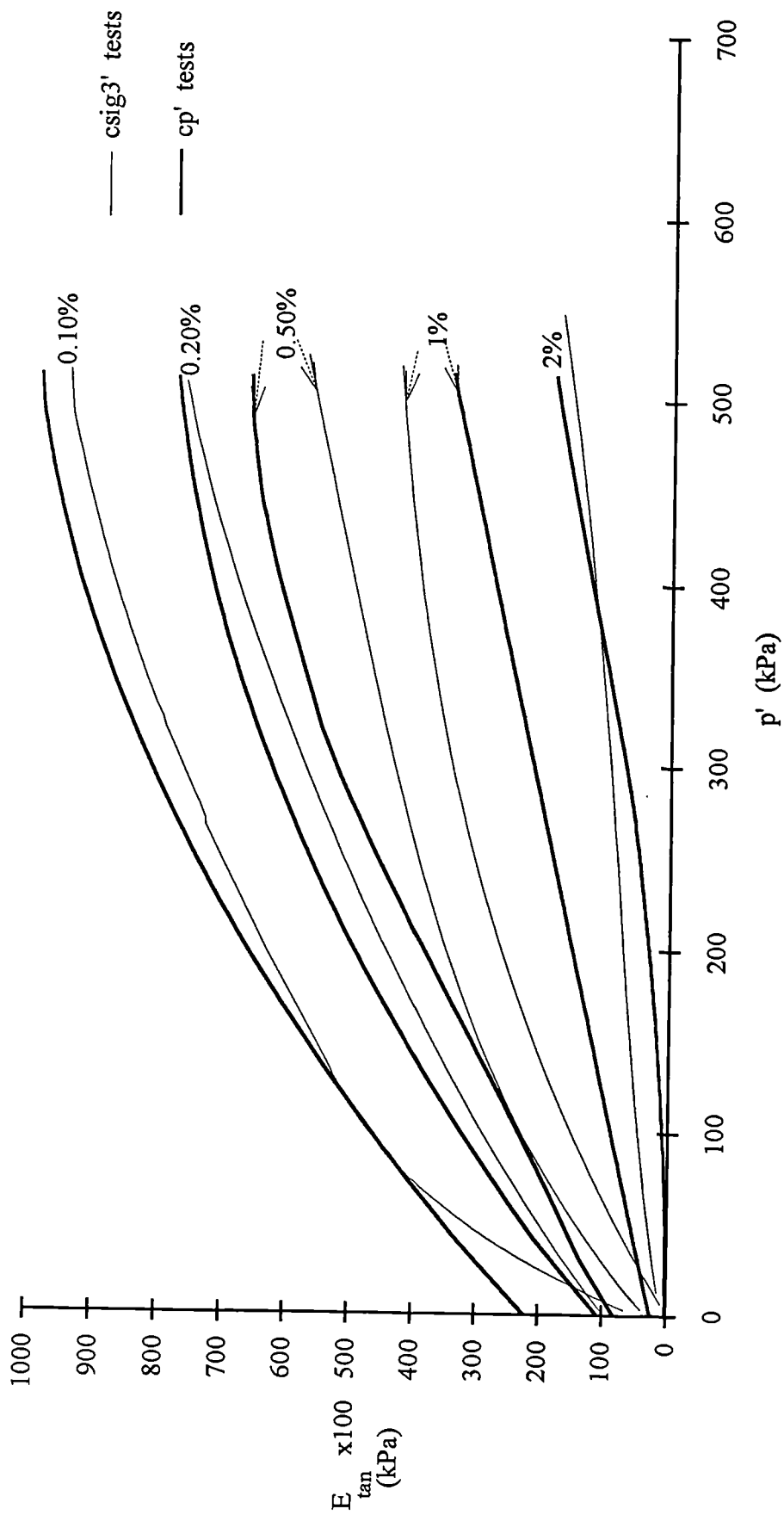
Fig. 6.24 Tangential stiffness versus p' for the constant p' and constant σ_3' drained tests

205
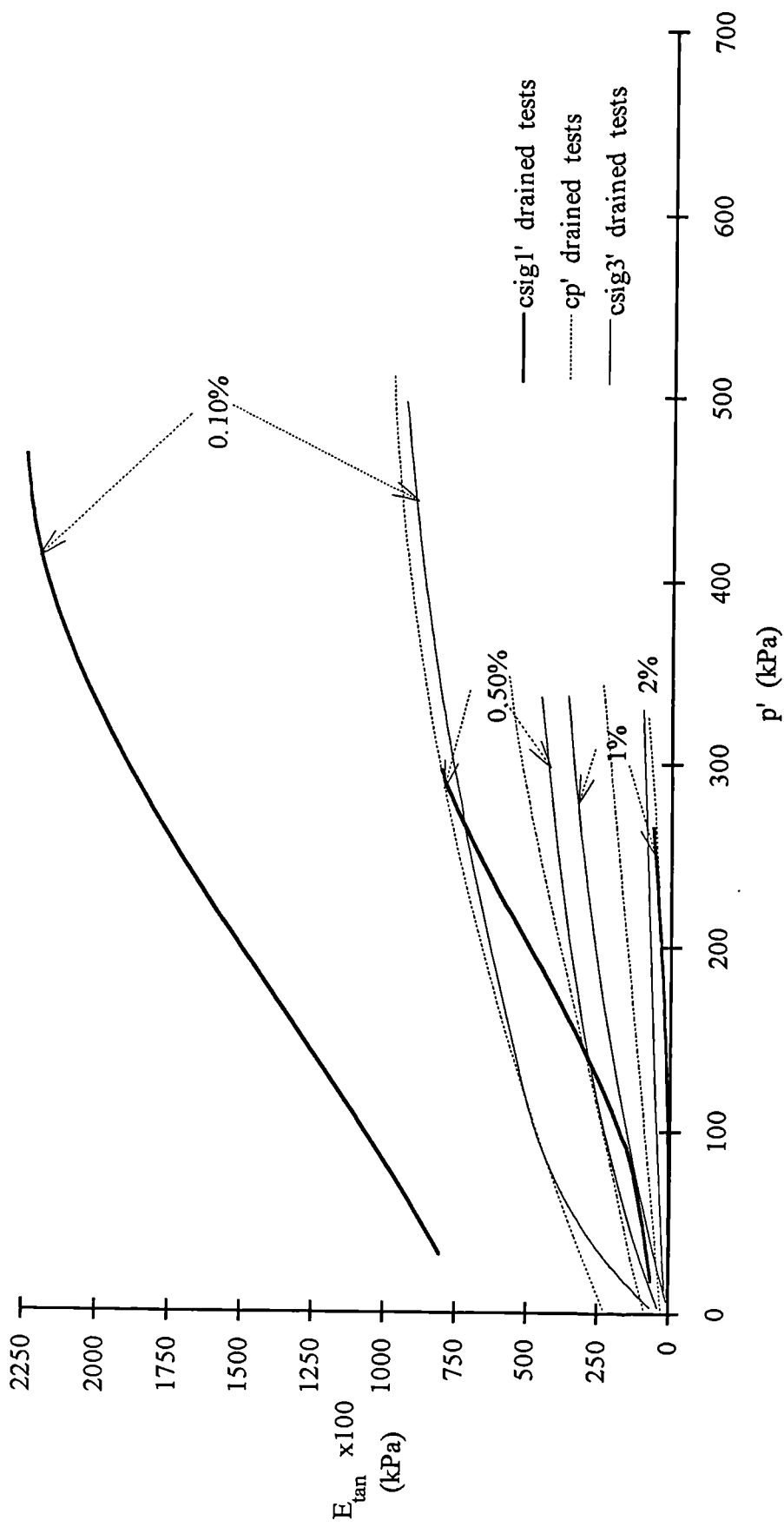
Fig. 6.25 Tangential stiffness versus p' for the constant σ_1', constant p' and constant σ_3' triaxial drained tests

206
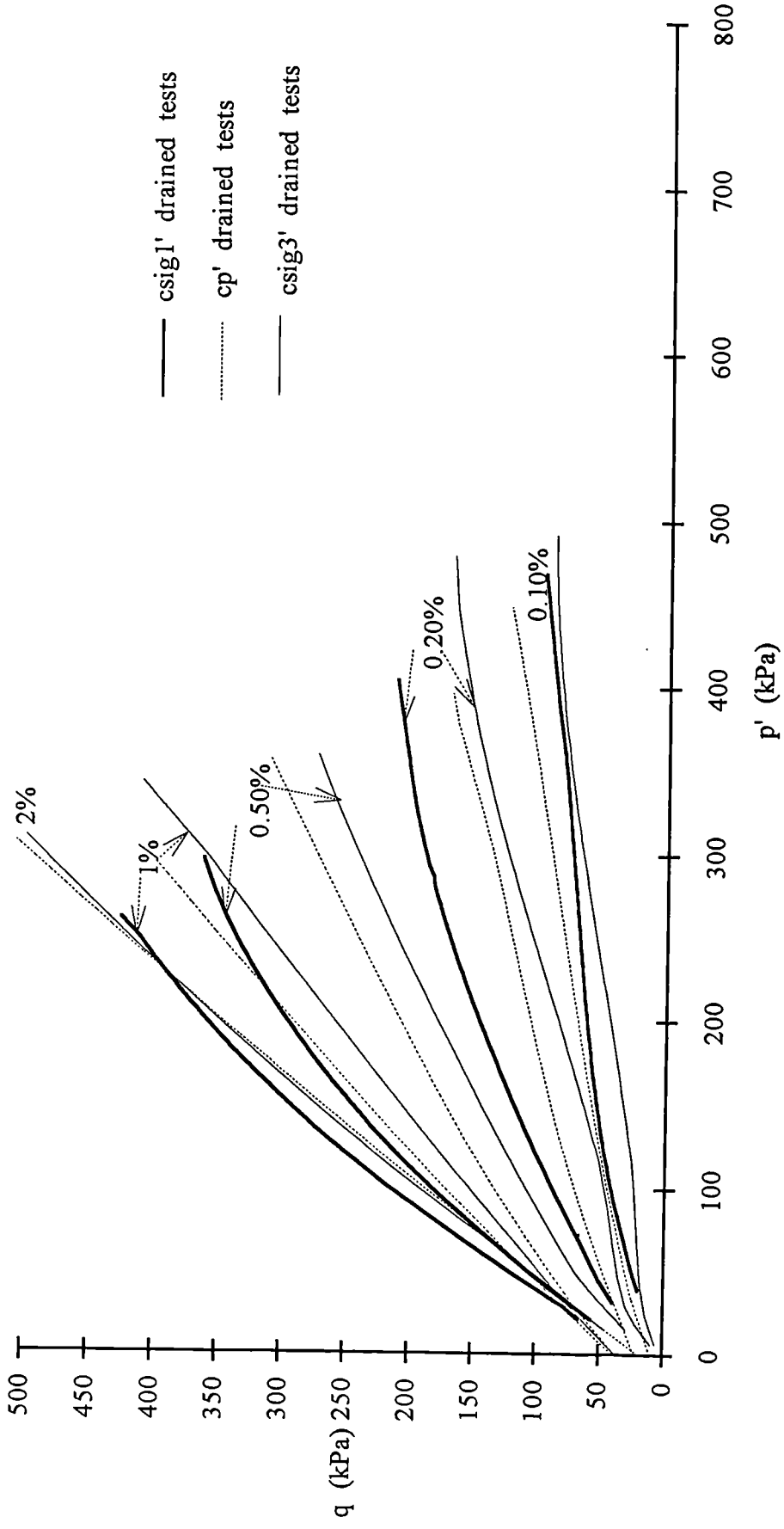
Fig. 6.26 Strain contours for the constant σ_1', constant p' and constant σ_3' drained triaxial tests

207
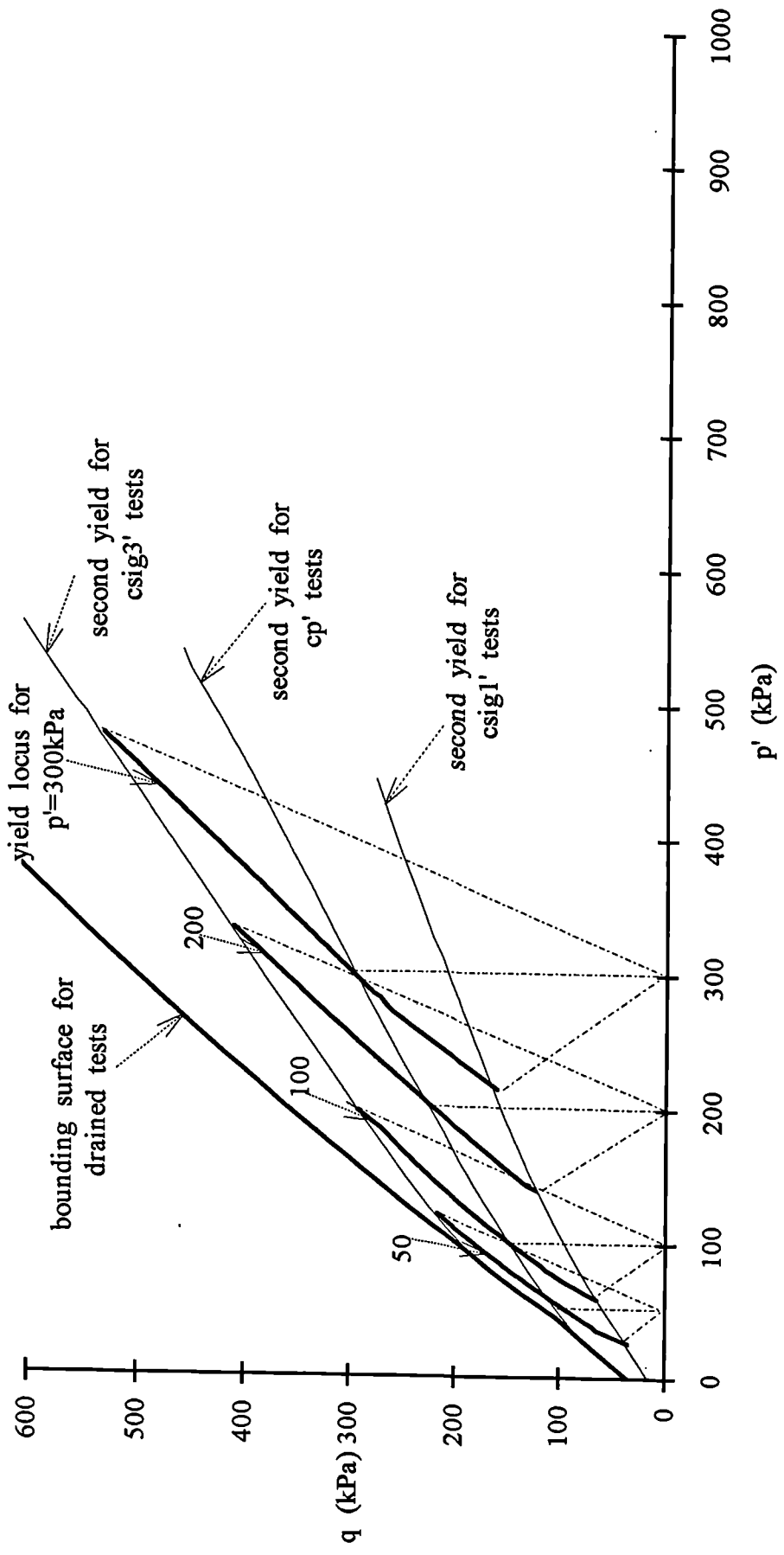
Fig. 6.27 Yield surfaces for different confining pressures

208

CHAPTER 7   DRAINED PROBING TRIAXIAL TESTS ON BONDED SOIL WITH CHANGES IN STRESS PATH DIRECTIONS DURING SHEAR

7.1 INTRODUCTION

In this chapter the behaviour of the bonded soil is studied under drained shearing when changes in stress path direction are introduced during shear. Initially the behaviour of the soil is examined for samples which start by following a constant p' path and then the stress path direction is changed to a constant q path. The development of tangential stiffness under the different stress paths and the max q/p' ratios that the soil can sustain in the stress space are closely studied.

The behaviour of the soil is also examined when subjected to clockwise changes in the stress path directions during shear. Constant σ_1' paths were followed initially before a change to constant σ_3' or constant p' shearing paths, at different stress levels. The development of E_{tan} under the different stress path directions is presented and comparisons are also made with stiffness values developed from samples sheared along the same stress paths, but without a shearing history which involves a change of direction. Yield of the bonds is examined for each individual stress path followed in the stress space. The limiting stress ratios that the soil sustained in the stress space are also examined. Finally a framework is presented that clarifies the influences of the different shearing paths on the soil's behaviour.

7.2 DRAINED TRIAXIAL TESTS ON BONDED SOIL WITH A CHANGE FROM CONSTANT P' TO CONSTANT Q STRESS PATH

The behaviour of the bonded soil sheared initially under constant p' conditions and afterwards along a constant q path, is examined in this section. The stress strain

behaviour, the development of stiffness and the max q/p' ratios that the samples sustained in the stress space are closely studied. Comparisons are also made with previous test results presented by Bressani (1990).

7.2.1 Testing details

A total of three drained tests with a change from a constant p' path to a constant q stress path were carried out on bonded samples. The samples were first isotropically consolidated to p_o'=300kPa and then sheared initially under constant p' drained conditions. A change of shearing direction onto a constant q path was introduced at q=70kPa for the first test, at q=270kPa for the second and 430kPa for the third test. Thus the soil's behaviour is examined under the change of the path direction, before and after the occurrence of the second yield during the constant p' path (fig. 6.6).

Control of the constant q path was achieved by defining a stage, where q was maintained constant and p' was set to decrease at a constant rate of stress of 50kPa/hr. The same stress rate was also used (rate of change of q), for the first part of shearing, under constant p' conditions. The names of the tests, the void ratio of the samples and the deviatoric stress at which shearing changed onto the constant q path, are shown in table 7.1. The name of each test presents the method of shearing control and also the value of q at which the stress path changed direction. The value of p_o' prior to shear is not included because all the samples were consolidated at the same p_o'=300kPa. Thus test cp'q270 indicates a bonded sample that was sheared initially along a constant p' drained path, which changed direction at q=270kPa and followed a constant q path.

7.2.2 Stress strain behaviour and stress paths for the three constant p'-q tests

The deviatoric stress versus axial strain curves for the three tests are plotted in fig. 7.1a and the stress paths are presented in the stress space in fig. 7.1b. It can

be seen from these figures that although the computer control system was set to maintain a constant q path, once failure was reached it was not able to do so. The value of q therefore drops. Since p' continues to decrease, a path is followed which drops down towards the origin.

It can be seen in fig. 7.1a, that the three samples generated very low percentages of axial strain during the second part of shearing under constant q conditions. Test cp'q70, at the lowest deviator stress shows very little axial strain even though it follows the longest constant q path. Test cp'q270 shows a little more strain. Highest values of axial strain are observed in test cp'q430, that was sheared at the higher q value.

In fig. 7.2 the stress paths are plotted in the stress space and the bounding surface for both the bonded soil and the destructured soil, defined from previous drained and undrained tests, are also presented. As can be seen, test cp'q70 reached a max q/p' ratio very close to the bounding surface and test cp'q270 apparently at a slightly higher stress. However test cp'q430, sheared at a higher q value than the other two constant q tests presented a lower max stress ratio in the stress space. This suggests that a change in the stress path direction in a triaxial drained test at high deviatoric stresses, might have an effect on the max q/p' ratio that the soil can sustain in the stress space.

7.2.3 Test cp'q70 carried out under a low constant q stress

The results for test cp'q70 carried out under a low q value, are studied in this section. As can be seen in fig. 7.2, the sample at the beginning of the second part of shearing has the greatest distance to the bounding surface compared to the other two samples. The constant q path is an unloading path (in terms of mean stress) and this clearly influences the low axial strain developed during the second part of shearing.

The sample generated $\varepsilon_a = 0.448\%$, during the first part of shearing following the constant p' path. However with the change in the stress path direction, the axial

strain initially decreased to ε_a=0.421%, as p' decreased to 90kPa. With a further decrease of p' the sample generated a small percentage of axial strain. Axial strain started to increase substantially as the stress path approaches the bounding surface of the bonded soil. However as can be seen in fig. 7.1, only when the sample reached its maximum q/p' value in the stress space the increase in axial strain accelerated. At the end of shearing the sample developed ε_a=2.5% .

The volumetric strain versus axial strain for the three tests is plotted in fig. 7.3. Test cp'q70 showed initially low values of compression, followed by dilation after the point of change in the shearing path direction. High values of dilation were developed, as the stress path approached the bounding surface.

In order to investigate whether the samples' bonded structure was totally destroyed, the sample was reconsolidated to p'_o=35kPa and sheared again under constant σ_3' conditions. During reconsolidation the sample developed another ε_a=2.5%, and during shearing showed compression up to ε_a=12%, before reaching a max q/p' ratio. As can be seen in fig. 7.2, the sample failed very close to the bounding surface defined for the destructured soil and this suggests that the bonded structure has been almost entirely destroyed during the first part of shearing. Otherwise the soil would have crossed the bounding surface for the destructured soil.

The development of stiffness for test cp'q70 is normalised with the current value of p' and plotted versus axial strain, in a log-log graph in fig. 7.4a. As can be seen, the initial decrease in axial strain during the constant q path and the slight increase afterwards has influenced the development of stiffness at this strain level, which becomes very high. However as the stress path was approaching the bounding surface the axial strain started to increase substantially and this is reflected to the stiffness values, which now start to decrease. When the soil reached its max q/p' ratio at ε_a=0.667%, it had lost all of its stiffness. Therefore yield of the bonds

took place very close to the max q/p' ratio, or actually coincided with the latter. The sample, when sheared again under the constant σ_3' path, again presented some stiffness, which however decreased rapidly with the increase of axial strain.

7.2.4 Test cp'q270 carried out under an intermediate constant value of q

In this section the results for test cp'q270 are examined. During the first part of shearing under the constant p' path the sample generated a small amount of axial strain ε_a=0.542%. As can be seen in fig. 7.3, the sample showed very low values of compression at this strain level. With the change in the stress path direction the sample showed initially a slight increase of axial strain and started to dilate. For a decrease in p' to 160kPa, only a 0.1% increase in axial strain was observed. However axial strain increases further as p' drops below 160kPa and accelerated as the stress path approached the bounding surface of the bonded soil. The sample reached its max q/p' ratio at ε_a=1.14%, followed by rapid strain softening with the initiation of shear surfaces. The negative volumetric strain (dilation) accelerated as the stress path approaches the origin at ε_a>8.5% (fig. 7.3).

In fig. 7.4b the development of stiffness is normalised with p' and plotted versus axial strain for test cp'q270. An immediate increase in E_{tan} occurred with the change in stress path direction, as the rate of the development of axial strain was quite small. However for ε_a>0.65%, a loss in E_{tan} takes place that indicates a major destruction of the bonds at this stress level. When the sample reached the max q/p' ratio at ε_a=1.14%, it had lost almost all of its stiffness.

7.2.5 Test cp'q430 carried out under a higher constant q stress

In this section, the results for test cp'q430 are discussed. The sample during the first part of shearing along the constant p' path, generated 1% of axial strain. Up to this point it showed low values of compression, followed by a gradual change in behaviour to dilation with the change of the stress path direction (fig. 7.3). During

the second part of shearing, the sample immediately developed high values of axial strain up to the point of the max q/p' ratio, followed by rapid strain softening at higher strains (fig. 7.1a). As the stress path was approaching the origin, the negative volumetric strains strongly accelerated.

As can be seen in fig. 7.2, the stress path has already passed the bounding surface for the destructured soil following the constant p' path and is positioned closer to the bounding surface for the bonded soil, than any other previous constant p'-q test. However the sample sustained a lower max q/p' ratio in the stress space than that previously defined from the drained and undrained tests, carried out at the same stress level.

It is interesting to see that the sample after it has reached the max q/p' ratio, followed a stress path very close to the bounding surface of the destructured soil, for p'<350 and ε_a>5%. This suggests that the structure of the soil at this strain level, is probably very similar to that of the destructured material.

The tangential stiffness developed during shearing is normalised with p' and is plotted versus axial strain in fig. 7.4c. As was expected a first loss in E_{tan} took place at ε_a=0.5%, at a similar strain level to that at which second yield occurred for the constant p' tests presented in the previous chapter. However with the change in the stress path direction a small increase in stiffness is observed, followed by a second loss at ε_a=1.2%. At the point of max q/p' ratio at ε_a=1.77%, the sample has lost all of its stiffness.

7.2.6 General remarks about the soil's behaviour and discussion of test results presented by Bressani (1990)

The stress paths for tests cp'q70-430 are plotted in fig. 7.5 and the second yield surface defined from the constant p' tests is also included. As can be seen, the change in the path direction for tests cp'q70-270 took place at lower deviator

stresses than the second yield surface for the constant p' tests, and thus no major loss in E_{tan} had occurred for these samples. However the change in the stress path direction for test cp'q430 took place after the stress path had crossed the second yield surface in the stress space, which was accompanied with a major loss in E_{tan}.

As was discussed in the previous chapter (section 6.4.2), the major loss in E_{tan} for the constant p' tests at $\varepsilon_a \cong 0.55\%$ did not have any influence on the max q/p' ratio that the soil sustained in the stress space. Test cp'q270 with a change in the stress path direction before any loss in E_{tan} presented a max q/p' ratio similar to those previously defined. However test cp'q430, with a change in the stress path direction after the occurrence of a major loss in E_{tan} did show a lower max q/p' ratio. This suggests that the change in the stress path direction can influence the max q/p' ratio that the soil is able to sustain in the stress space. However this is only true when the change takes place after the soil has yielded, due to its previous shearing path history. When a change in the stress path direction takes place before yield the max q/p' ratio is unaffected by the previous shearing path history of the soil.

Bressani (1990), presented test results for three bonded samples sheared initially under constant σ_3' conditions and afterwards under constant q conditions. The results for two tests are presented in fig. 7.6a. The samples were formed by a similar method to that used in this study and the proportions of the dry weights were 13% of kaolin, 57% of sand and 30% fired kaolin 'sand'. Previous research by Maccarini (1987), showed that including fired kaolin up to 30% of dry weight did not affect the yield stress of the samples and thus comparisons can be made with results from tests carried out on bonded soil without kaolin 'sand'. The samples used in this study had a void ratio, $e_0 = 0.6$, while these presented by Bressani had a void ratio, $e_0 = 1.5$.

As can be seen, the two samples sustained higher stress ratios in the stress space that those defined after constant σ_3' drained and undrained tests carried out on the same

soil (shown by $\varphi'=34°$ line). It should be noted though that the samples were quite loose and the tests were carried out at very low confining pressures (s'<100kPa).

The stress path of another sample with a void ratio $e_0=1.1$, sheared initially along a constant σ_3' path and afterwards along a constant q path is presented in fig. 7.6b. This sample reached the same peak strength line defined from constant σ_3' drained tests on bonded samples with the same void ratio. However as can be seen, this soil was sheared at a higher p_0' than the previous two samples ($p_0'=600$kPa).

Bressani (1990), underlined the important role that density plays in the soil's behaviour when sheared under different stress paths. The two samples with lower density sheared under constant σ_3' and constant q conditions sustained higher q/p' ratios in the stress space than those reached by the sample with higher density. This is in good agreement with the test results presented in this work for denser samples sheared under constant p' and constant q paths. However there is evidence from this study, that the behaviour of the soil sheared under different stress paths is also influenced by the stress level at which the second part of shearing takes place, which is directly related to the initial loss in E_{tan} that takes place during the first part of shearing. The different stress levels at which shearing took place might also have influenced the soil's behaviour in the tests presented by Bressani. Therefore, in order to investigate the behaviour of the soil under different stress path directions, further tests were carried out on bonded soil at different stress levels and following different stress paths.

7.3 PROBING DRAINED TRIAXIAL TESTS WITH A CHANGE FROM CONSTANT σ_1' TO CONSTANT σ_3' OR CONSTANT P'

The behaviour of the bonded soil sheared initially under constant σ_1' conditions and then following constant σ_3' or constant p' paths is examined in this section. The

stress strain behaviour and the development of stiffness during shearing is closely studied. Comparisons are also made with previous results from constant σ_3' and constant p' tests sheared at similar stress levels. The effects that the different shearing paths have on the max q/p' ratios that the soil sustained in the stress space, are closely studied. Finally, a framework is presented for the behaviour of the bonded soil sheared under different stress paths.

7.3.1 Testing details

A total of seven drained triaxial tests were carried on bonded samples. The samples were first isotropically consolidated to different confining pressures and then sheared initially along a constant σ_1' path. Shearing for six of the tests changed to a constant σ_3' path after the development of low percentages of axial strain (0.2%-0.45%). One test that was initially carried out under a constant σ_1' path changed to a constant p' drained path, at $\varepsilon_a > 0.25\%$. Control of shearing under the different stress paths took place under a constant rate of deviator stress of 50kPa/hr. Transducer readings were taken every 3 mins at the beginning of the test and every 6 mins, at axial strains higher than 2%.

The name of each test, the void ratio of the samples, the confining pressure that they were consolidated to prior to shearing and the value of q at which the stress path changed direction are shown in table 7.2. The name of each test indicates the stress paths followed during shearing and the initial consolidation pressure. Thus for example test cs13'150, indicates a sample consolidated at p_0'=150kPa, sheared initially under a constant σ_1' path and changed onto a constant σ_3' path; test cs1p'300 changed onto a constant p' path. Tests cs13'L70 and cs13'H70 were both carried out at the same p_0'=70kPa, but the change in the path direction for the first (cs13'L70) took place at lower q value (q=33kPa) than that for the latter at q=48kPa.

7.3.2 Stress paths and stress strain behaviour for the seven samples

The stress paths for the seven tests are plotted in the stress space in fig. 7.7a. The samples were sheared initially under a constant σ_1' path, followed by a change in direction at higher stresses. In order to examine the behaviour of the bonded soil under different stress paths, the change in the path direction was initiated at different stress levels for each test.

The deviatoric stress-strain curves for all the samples are plotted in fig. 7.7b. Smooth curves were followed during shearing along the different stress paths. The samples showed brittle behaviour, followed by rapid strain softening with the initiation of shear surfaces. As can be seen in fig. 7.7a, tests cs13'L70 and cs13'150 followed stress paths which come together in the stress space and the samples reached the same maximum value of q. The same occurs for tests cs13'300 and cs1p'300.

The deviatoric stress-strain curves are plotted again in fig. 7.8a, and the volumetric strains versus axial strain are plotted for all the tests in fig. 7.8b. The points of change in the path direction and the points at which the samples reach the max q/p' ratio are also included on the two figures. As can be seen, at the beginning of shearing the samples developed negative volumetric strains (dilation), followed by a change to compressive behaviour after the change in the path direction. This is more apparent for samples sheared at low confining pressures and followed a constant σ_1' path up to low q values (tests cs13'L70-H70). After the initial change of behaviour during the constant σ_3' shearing path, all the samples start to dilate again at higher strains; when they reached the max q/p' ratios at $\varepsilon_a < 2\%$, high rates of dilation followed.

It can be seen in the last figure that the change of the stress path direction during shearing strongly affects the development of volumetric strains; even though close

comparisons between the tests results can not be made, a very similar pattern of behaviour is presented by all the samples.

7.3.3 Tangential stiffness during shearing under different stress paths

In this section the development of E_{tan} during shearing is studied for all the samples. E_{tan} is normalised with the current value of p' and plotted versus axial strain in log-log graphs. Comparisons are also made with results from constant σ_3' or constant p' tests sheared at similar stress levels. A small key graph is presented on each figure which shows the stress paths followed in the stress space, for the different tests under consideration.

7.3.3.1 Tests cs13'L70-cs13'H70

Tangential stiffness for tests cs13'L70-H70 is plotted versus axial strain in fig. 7.9a. The development of E/p' for test cs1'70, is also included in this graph, for comparisons to be made between the different tests.

As can be seen, test cs13'L70 presents initially high stiffness values, similar to those presented by test cs1'70. With the change in the path direction a rapid loss in E/p' occurs at $\varepsilon_a > 0.074\%$. The loss in stiffness is quite similar to that presented by test cs1'70, but takes place at a lower strain percentage. A difference in behaviour is presented at higher strains, as the constant σ_1' test showed a further decrease in E/p' with the increase of strain, while test cs13'L70 presented almost constant values of E/p' for $\varepsilon_a > 0.4\%$. However for $\varepsilon_a > 1.35\%$ a second drop in E/p' takes place for cs13'L70.

Test cs13'H70 also shows similar initial stiffness values to the two other tests when it followed the constant σ_1' path. The change of the shearing path direction for this test took place at a higher strain than that for test cs13'L70 ($\varepsilon_a = 0.171\%$), followed by an immediate loss in E/p', which is however more rapid than that presented by test cs13'L70. The change of the path direction was also very close to the position

219

at which second yield of the bonds occurred for test cs1'70. At higher strains test cs13'H70 presents similar behaviour to cs13'L70 and the sample showed almost constant values of stiffness for $\varepsilon_a > 0.3\%$. This is very different to cs1'70, which showed a further decrease in E/p' with the increase of axial strain. A second drop in E/p' occurred at $\varepsilon_a = 0.98\%$, very close to the point that a similar drop in E/p' occurred for test cs13'L70.

Therefore it can be seen in the last graph that the behaviour of the bonded soil sheared in the cs13'70 tests is strongly influenced by the change in the stress path direction during shearing. The development of stiffness during the second part of the tests, changes from that of a typical constant σ_1' test. Since the path changes to a constant σ_3' path it is interesting to compare the results with other constant σ_3' test results. Therefore, E/p' for tests cs13'L70-H70 is replotted in fig. 7.9b and the development of stiffness for a constant σ_3' test, db35, is also included on the same graph. As can be seen in the key graph, test db35 had followed almost the same stress path as test cs13'L70, during the second part of shearing.

During the first part of shearing, tests cs13'L70-H70 presented higher E/p' values than those after test db35 (similar to those for the equivalent test cs1'70). The major loss of stiffness for a constant σ_1' test is expected to take place at $\varepsilon_a \cong 0.2\%$, as it was demonstrated in the previous chapter. However the samples in tests cs13'L70-H70 have lost much of their stiffness at the point of change of the shearing path direction, which took place at $\varepsilon_a < 0.2\%$. After this initial loss in E/p', the samples presented similar values of stiffness to those of test db35. For $\varepsilon_a > 0.2\%$ the samples maintained constant E/p' values and presented a second drop at higher strains, which is very close to the point at which second yield of the bonds took place for test db35.

This suggests, that the development of stiffness during the second part of shearing, in the constant σ_1' - constant σ_3' tests is strongly influenced by the change in the shearing path. During the second part of shearing, E/p' presents similar values with those developed during a constant σ_3' test carried out at the same stress level. However, despite the initial drop in E/p' during the constant σ_1' path, the samples presented a second drop in stiffness at higher strains, very similar to that which occurred during the constant σ_3' test.

7.3.3.2 Test cs13'150

The development of E/p' for test cs13'150 is plotted versus axial strain in fig. 7.10a and results for test db35 are also included. During the second part of shearing, test cs13'150 follows a stress path very close to that of test db35. As can be seen, initially the two samples presented similar E/p' values, with slightly higher values for test cs13'150. A first drop in E/p' is initiated for the latter test at ε_a=0.2% (similar with that at the constant σ_1' tests) and stiffness continues to decrease up to ε_a=0.32%, the point of change in the stress path direction. During the second part of shearing E/p' continued to decrease with the increase of axial strain, but with a lower slope up to ε_a=0.8%, where a second drop in E/p' took place.

In fig. 7.10b the results for tests cs13'L70-H70-150 are plotted. Test cs13'L70 which followed a very close stress path to test cs13'150 presented constant values of stiffness up to the point of the second drop. Similar behaviour is also presented by test cs13'H70. The only difference between the three tests is that the shearing path for the two cs13'70 tests changed direction before the major yield of the bonds takes place under the constant σ_1' path at ε_a=0.2%, while for test cs13'150 the path changed direction well after the initial loss in E/p' took place.

This suggests, that the development of stiffness is not only affected by the change in the stress path direction but is also influenced by the stress level at which this

change takes place. It can also be seen, that test cs13'150 presented a second drop in E/p' at ε_a=0.7%, lower than that for db35, while test cs13'H70 showed a second drop in E/p' at similar strain level to db35 (fig. 7.9b).

7.3.3.3 Test cs13'300

The development of stiffness for test cs13'300, carried out at higher stresses is presented in fig. 7.11 and the results for tests db35 and db100 are also included. As can be seen in the key graph, the stress path for test db100 is positioned closer to test cs13'300, but the results for test db35 are also included for comparisons to be made between the different tests. Tests db35 and db100 have generally similar E/p' values; test db35 has slightly higher values for ε_a>0.7% and second yield of the bonds occurred at a higher strain level than that for test db100.

Initially, test cs13'300 presented higher E/p' values than the other two constant σ_3' tests. A first drop in E/p' occurred at ε_a=0.21%, at a similar axial strain at which second yield occurred for the constant σ_1' tests (see section 6.3.2, fig. 6.10a and b), and stiffness continued to decrease up to ε_a=0.42%, the point of change in the stress path direction. During the second part of shearing the sample presented constant E/p' values, with the increase of axial strain up to ε_a=0.7%, where a second drop in E/p' took place. However there is a difference between the E/p' values for the three tests at ε_a>0.4%, which increases further when the second drop in stiffness takes place for test cs13'300.

Test cs13'300 presents a similar pattern of behaviour with the previous cs13' tests. However the difference between the E/p' values for test cs13'300 and the two constant σ_3' tests during the second part of shearing is higher than any other set of tests (fig. 7.9b, 7.10a). Test cs13'300 was carried out at a higher p_0', than the previous tests and also the change of the path direction took place at a higher percentage of axial strain. Therefore it is very likely that the development of E/p' is

affected by the higher stress level at which shearing took place and also by the higher strain level at which the stress path changed direction.

7.3.3.4 Test cs1p'300

The development of E/p' for test cs1p'300 is plotted versus axial strain in fig. 7.12. The development of E/p' for tests cp'100 and cp'250 is also included in the same graph, for comparisons to be made between the different tests. The tangential stiffness values for the two constant p' tests are very similar throughout the whole range of axial strain and therefore this suggests that a test carried out under a constant p' path at $p'_0 = 191$kPa will develop E/p' values close to those presented from tests cp'100-250.

At very low axial strains, test cs1p'300 presented higher values of stiffness than the other two tests up to $\varepsilon_a = 0.19\%$, where a first drop in E/p' takes place. The stress path direction was changed at $\varepsilon_a = 0.25\%$ and shearing continued under a constant p' path. As can be seen, during the second part of shearing the sample presented almost constant values of E/p', followed by a second drop at $\varepsilon_a = 0.55\%$. The values of E/p' are very close to those presented by the constant p' tests and the point of the second drop in E/p' is at the same strain level as the point at which second yield of the bonds occurred in the latter tests.

The results from the last test confirm again that the development of stiffness is influenced by the different stress path directions. However the constant p' path is positioned closer to the constant σ_1' path (in terms of the angle between the paths), than the constant σ_3' path and that might have influenced the development of E/p'. Thus it produces less difference between the E/p' values for the change from constant σ_1' to constant p' than those presented in fig. 7.11 for the change to constant σ_3'. In addition the change of the path direction for test cs1p'300 took

place at ε_a=0.25%, while for test cs13'300 it took place at ε_a=0.42%. This might have influenced the development of E/p' for the latter test.

7.3.3.5 Test cs13'400

The development of E/p' for test cs13'400 is plotted versus axial strain in fig. 7.13, and the results for test db150 that followed a close stress path in the stress space, are also included. Transducer readings for test cs13'400 were only taken every 4 mins and thus a limited number of data points are presented. However a clear pattern of behaviour is presented, similar to that showed by the previous constant σ_1'- constant σ_3' tests. At the beginning of shearing, test cs13'400 presented higher values of E/p' than test db150. A first drop in E/p' takes place at ε_a=0.19% and stiffness decreases further, up to the point of the change in the stress path direction. During the second part of shearing the sample presented almost constant values of E/p' with the increase of axial strain up to ε_a=1%, where the second drop in E/p' took place. The stiffness values are substantially lower than those presented by test db150, but the second drop in E/p' took place at the same axial strain as second yield of the bonds occurred for the latter test.

7.3.3.6 Test cs13'600

The development of E/p' for test cs13'600 is presented in fig. 7.14, and the results for test db200 are also included for comparison to be made between the different tests. As can be seen, test cs13'600 presents initially higher E/p' values than the constant σ_3' test. At ε_a=0.23%, a first loss in E/p' is initiated, with stiffness decreasing rapidly with the increase of strain up to ε_a=0.51%, where the shearing path changed direction. During the second part of shearing, the sample presented almost constant values of stiffness with the increase of axial strain. The values of E/p' at this strain level are lower than those presented by test db150 and the second drop in E/p' took place at a lower percentage of axial strain, than the occurrence of the second yield for the latter test.

7.3.4 Discussion

A similar pattern of behaviour is presented from all the samples in which the stress path direction changes during shear. The development of E/p' is influenced by the change in the stress path direction. The samples present a small decrease in stiffness after the change in direction, followed by a second major drop at higher strains.

Initially the development of stiffness in a constant σ_1'- constant σ_3' test is the same as that in a constant σ_1' test. All the tests except cs13'L70-H70 pass through yield before the stress path direction is changed. During the second part of shearing, the samples develop E/p' values below those presented during a constant σ_3' test carried out at the same stress level. A second drop in E/p' then occurs, generally at a lower axial strain than that at which second yield takes place in the constant σ_3' test. Similar behaviour is also shown by the sample sheared along the constant σ_1'- constant p' path. Again stiffness during the constant σ_1' path mirrors other tests following this path and yield occurs before the change in the stress path direction takes place. After the point of change in direction, the E/p' values mirror those from equivalent constant p' tests and a second drop in E/p' takes place at a similar strain percentage as second yield occurred for the latter tests. Tests cs13'L70-H70 did not yield prior of the change in the stress path direction and they presented similar values of E/p' with the corresponded constant σ_3' tests. The rest of the constant σ_1'- constant σ_3' tests which passed through yield after the change in direction presented lower values of stiffness than the corresponded constant σ_3' tests.

As was previously discussed in chapters 4 and 6, second yield of the bonded structure is associated with the initiation of a major loss in tangential stiffness. The rotation of stress path to the left of the constant σ_3' path influenced the occurrence of the second yield due to the anisotropic nature of the breakdown of the bonds. Second yield of the bonds, for a sample sheared under a constant σ_1' path takes place at $\varepsilon_a \cong 0.2\%$, under a constant p' path at $\varepsilon_a \cong 0.55\%$, and under a constant

$\sigma_3{'}$ path at $\varepsilon_a \cong 1\%$. However when shearing the bonded soil under two different stress paths, two major drops in E/p' occurred, each associated with the segment of the stress paths followed. Therefore these drops in stiffness represent two major breakdowns of the bonded structure at different stress levels.

Shearing a sample under a constant $\sigma_1{'}$ path, a first drop in E/p' occurs at low strains which indicates a major destruction of the bonds and also a substantial decrease of the bond strength at this stress level. If a change in the stress path direction takes place at a strain level where the soil has not yet lost all of its stiffness, a second drop in E/p' occurs at higher strains and is associated with the stress path which is being followed. After the second drop in E/p', the bonded structure of the sample is probably very much broken down and the bond strength is at very low levels. Therefore it is possible that these two major decreases in bond strength during shearing under different stress paths might have an effect on the maximum stress ratios that the soil sustains in the stress space. A further discussion about the max q/p' ratios that the soil presented after the constant $\sigma_1{'}$- constant $\sigma_3{'}$ tests, follows in the next section.

7.3.5 Bounding surface and stress paths plotted in the stress space

The bounding surface for the bonded and the destructured soil defined after triaxial drained and undrained tests and the stress paths for the constant $\sigma_1{'}$- constant $\sigma_3{'}$ and p' tests are plotted in the stress space in fig. 7.15. As can be seen, the samples sheared at low confining pressures reached the bounding surface for p'<120kPa, while the rest of the samples sheared at higher stresses sustained lower max q/p' ratios which are closer to those defined for the destructured soil.

This suggests that the change in the stress path direction during shearing, has strongly influenced the behaviour of the bonded soil. The two major decreases of the soil's bond strength during shearing probably accounts for the lower stress ratios

226

that the soil presents in the stress space. However the soil's behaviour proved to be more complicated, as high max q/p' ratios were reached for $p'<120kPa$, the same as those defined from all the previous drained and undrained tests.

7.3.6 First and second loss in E_{tan} presented in the stress space

In fig. 7.16, the points of the two major drops in E/p' during the constant σ_1'- constant σ_3' and p' tests are plotted in the stress space and the bounding and the yield surfaces defined from the constant σ_3', constant p', and constant σ_1' tests are also included. As was expected, the first drop in E/p' is governed by the yield surface defined from the constant σ_1' tests. The surface is extended to higher p' values than that previously defined in fig. 6.23, in order to compare the sample's behaviour sheared in test cs13'600. However the second drop in E/p', for all the samples sheared under the constant σ_1'- constant σ_3' and the constant σ_1'- constant p' paths, is positioned in the stress space very close to the yield surfaces defined for the constant σ_3' and the constant p' tests respectively. Therefore this suggests that a bonded sample sheared under different stress paths, yields under each individual shearing path that is followed in the stress space.

Thus the behaviour of the bonded soil sheared under the constant σ_1'- constant σ_3' and constant σ_1'- constant p' paths, in respect of the major losses in tangential stiffness, is governed by the three yield surfaces. However as was previously discussed in chapters 4 and 5, the max q/p' ratios that the bonded soil sustains, depend on the relative position of the major yield of the bonds in the stress space. Three main zones for the soil's behaviour during shearing under the constant σ_3' path were identified and were associated with the occurrence of the second yield (fig. 5.37). Two zones of behaviour were defined for shearing the soil under the constant p' path (fig. 6.20), and only one zone was defined for shearing under the constant σ_1' path (fig. 6.22).

The stress paths for the constant σ_1'- constant σ_3' and constant σ_1'- constant p' tests, the bounding surface for the bonded and the destructured soil and the yield surfaces defined from the constant σ_3' and the constant p' tests are plotted in fig. 7.17. The boundary between zones 1 and 2 defined from the constant σ_3' and constant p' tests is also included. The samples sheared under constant σ_1'- constant σ_3' paths sustained the same q/p' ratios as the drained constant σ_3', constant p' and constant σ_1' tests for p'<120kPa. This stress level coincides with the position of the upper limit of the first zone defined from the constant σ_3' tests, in the stress space.

Test cs13'150, carried out initially under a constant σ_1' path and afterwards under a constant σ_3' path in the first zone showed two major drops in E/p' which are governed by the corresponding yield surfaces in the stress space. After the second major yield of the bonds, the sample continues shearing at slightly higher stresses and reached the bounding surface previously defined. Tests cs13'300-400-600 sheared in the second zone, showed two major yields under the two different stress path directions and continued shearing at higher stresses. The samples sheared in this zone were somehow unable to sustain limiting q/p' ratios as high as those reached after the constant σ_3' tests, carried out at the same stress level. Similar behaviour is presented by test cs1p'300, sheared in the second zone of behaviour defined by the constant p' tests. After the two major drops in E/p', the sample reached a lower max q/p' ratio than those defined from the latter tests carried out in the same zone.

The difference in behaviour of a sample sheared under a constant σ_3' path compared to that sheared initially under a constant σ_1' path and afterwards under a constant σ_3' path is due to the substantial decrease of the bond strength during the first part of shearing. However the decrease in the bond strength becomes very important for the soil's behaviour, only when shearing takes place in the second zone of behaviour, where lower max q/p' ratios are reached. As was previously

discussed, samples sheared in the first zone showed stiffness values during the second part of shearing which are very close to those presented from test db35 (tests cs13'L70-H70, fig. 7.9b) or slightly lower (test cs13'150, fig. 7.10a). The rest of the samples sheared in the second zone developed substantially lower E/p' values than those presented from the corresponding constant σ_3' tests during the second part of shearing (fig. 7.11, 7.13, 7.14). Therefore that indicates a higher degree of destruction of the bonded structure for the samples sheared under the constant σ_1'- constant σ_3' paths, than those sheared under the constant σ_3' path, at the stress level of the yield surface defined for the constant σ_3' shearing path in the stress space.

However the behaviour of a bonded sample at failure, sheared in the second zone under a constant σ_3' path is not entirely controlled by its bonded structure, as yield of the bonds has occurred before reaching the bounding surface. This is reflected in the lower slope of the bounding surface at this stress level. Inherently, the second zone is a transitional zone of behaviour for the soil sheared under a constant σ_3' path, as major yield takes place at lower stresses than the max q/p' ratio. Also when shearing takes place close to the upper limit of this zone, the behaviour of the bonded soil becomes similar to that of the destructured material. Therefore this suggests that the higher destruction of the bonded structure for the samples sheared under constant σ_1'- constant σ_3' paths within the second zone, influences the behaviour of the soil with a direct result of lower max q/p' ratios being sustained in the stress space. As can be seen in fig. 7.17, the decrease in the stress ratios presented in the second zone, increases with the increase of p'.

Similar behaviour is also presented from the sample sheared along the constant σ_1'- constant p' path. The test was carried out in the second zone of behaviour defined from the constant p' drained tests and the sample sustained a lower max q/p' ratio than that defined from the constant σ_3' and constant p' tests. However the sample presented similar E/p' values with the corresponded constant p' tests during

the second part of shearing. This suggests that the high E/p' difference between the constant σ_1'- constant σ_3' tests and the corresponding constant σ_3' tests previously presented, is probably related to the greater degree of rotation between the positions of the stress paths followed in the stress space in these tests, than the constant σ_1'- constant p' and the constant p' tests. The constant path σ_1' is positioned closer to the constant p' path in the stress space than the constant σ_3' path and that has a different influence on the development of the corresponded E/p', when a change in the shearing path direction takes place.

7.3.7 Framework for the behaviour of the bonded soil sheared under different stress paths

The behaviour of the bonded soil in respect of the position of yield and the max q/p' ratios that the soil sustains is strongly influenced by the different shearing paths. Yield of the bonded structure of the soil occurs under each stress path direction followed in the stress space. Furthermore, the position of yield is independent of the previous shearing path history of the soil and occurs at certain q and p' stresses which are related to the corresponded yield surface defined for the current shearing path direction. However, yield of the soil's bonded structure has only been examined for clockwise changes of the stress path direction.

Bonded samples sheared under the constant σ_1'- constant σ_3' paths within the first zone of behaviour, sustained the same max q/p' ratios as samples without any previous shearing path history. However, when shearing took place in the second zone, the samples presented lower max q/p' ratios than those observed in constant σ_3' tests carried out at the same stress level. The greater loss in E/p' with the corresponding decrease of the bond strength during the first part of shearing is accounted for by the lower max q/p' ratios that the soil can sustain in this transitional zone of behaviour.

The bounding surface defined by the constant σ_1'- constant σ_3' and constant σ_1'- constant p' tests is shown in fig. 7.18. For p'<120kPa, the bounding surface coincides with that defined for the constant σ_3' tests. However for higher stresses the two surfaces diverge and the difference between the two increases with the increase of p'. For p'>500kPa, the bounding surface defined from samples without a previous shearing history turns closer to that defined for the destructured soil, sheared at the same stress level. Therefore, it is very likely that the bounding surface for the samples sheared under constant σ_1'- constant σ_3' paths, will turn down and meet the bounding surface of the destructured soil at this stress level.

It should also be noted, that the new bounding surface governs the behaviour of samples that were sheared under the constant σ_1'- constant σ_3' paths, when a change of the shearing path direction took place after the occurrence of a major loss in E/p', during the first part of shearing. However, if the change of the stress path direction takes place before any substantial loss in E/p', the behaviour of the soil will probably be similar to that without a previous shearing history. This might also explain the behaviour of the soil sheared in tests cp'q270-430 (fig. 7.19), which presented different max q/p' ratios in the stress space, due to the different positions of the change in the stress path direction during shearing. It can also be seen in fig. 7.19, that test cp'q430 presented a higher max q/p' ratio than those presented from the constant σ_1'- constant σ_3' and constant σ_1'- constant p' tests carried out in the second zone of behaviour and therefore this suggests that the bonded structure of the soil is probably destroyed differently under a constant q path, than under the constant σ_1'- constant σ_3' and constant σ_1'- constant p' paths.

Generally the behaviour of the bonded soil sheared initially along the constant σ_1' path and afterwards along a constant p' or constant σ_3' path, depends on two factors. First, it depends to the initial shearing path and up to what degree E/p' has decreased at the point of change of the path direction. Second, it depends on the

231

stress level at which the second part of shearing takes place. This also determines the particular zone of behaviour that corresponds to the current shearing path. However when the change of the path direction takes place after the occurrence of the loss in E/p', the zone of behaviour in which the second part of shearing takes place plays a tremendous role in determining the further behaviour of the soil. The constant σ_1' path sets a limit in the stress space for the stress paths followed to the left side of the constant σ_3' path, as a first zone of behaviour does not exist for this shearing path.

In this work the behaviour of the bonded soil was studied under clockwise changes of the stress path directions in the stress space. However the major yield of the bonds under the constant σ_1' path takes place at lower stresses than that under the constant σ_3' path and therefore is very likely that the soil's behaviour under anti-clockwise changes of the stress path direction will depend more on the stress level at which this change takes place, prior to or after the occurrence of a major yield, and less on the zone of behaviour in which shearing takes place.

The behaviour of the samples in test cp'q270-430 sheared initially under a constant p' path and afterwards under the limiting constant q path at the same zone of behaviour (zone 2), partially confirms the previous idea. The sample in test cp'q430 is sheared along the constant q path after the occurrence of a major loss in E/p' and it sustained a lower max q/p' ratio in the stress space than those presented from tests cp'q70-270, in which the change of the path direction took place before any loss in E/p'.

7.3.8 Final remarks

In this chapter the behaviour of the bonded soil was examined under drained shearing with clockwise changes in the stress path directions (fig. 7.7a). A sample which has yielded following one stress path direction will yield again if the stress

path direction is changed. Yield occurs at a stress level which corresponds to the yield surface defined for the current shearing path direction (fig. 7.16).

The max q/p' ratios that the soil sustains when following two different shearing paths were influenced by the decrease of the bond strength due to two major losses in E/p'. Furthermore the limiting stress ratios depended on the zone of behaviour in which the shearing path changed direction and also to what extent stiffness has decreased under the initial shearing path. The soil reached high max q/p' ratios when the change in the shearing path took place in the first zone of behaviour, defined for shearing under the latter path (fig. 7.17). At this stress level a unique bounding surface defined from the constant σ_3', p', σ_1' drained and the undrained tests governs the soil's behaviour.

When the change in the path direction took place in the second transitional zone of behaviour, the soil reached lower max q/p' ratios than those defined from the drained and undrained tests, and closer to those sustained by the destructured soil sheared at the same stress level (fig. 7.17). Therefore the soil's behaviour under shearing with changes in the stress path directions is not governed by a unique bounding surface for the whole range of p' examined (fig. 7.18).

Samples sheared under anticlockwise changes in stress path directions, indicated that the zone in which the second part of shearing takes place (zone 1 or 2) probably has less influence on the soil's behaviour, in respect of the max q/p' ratios sustained in the stress space. In this case, the stress level at which the shearing path changes direction, prior to or after the major loss in E_{tan} due to the previous shearing history, is more important (see fig. 7.19).

Test	Initial void ratio e_0	Change of path direction q (kPa)
cp'q70	0.598	70
cp'q270	0.602	270
cp'q430	0.601	430

Table 7.1 Details for the constant p' and q triaxial drained tests on bonded samples

Test	Initial void ratio e_0	Consolidation pressure (kPa)	Change of path direction q (kPa)
cs13'L70	0.597	70	33
cs13'H70	0.600	70	48
cs13'150	0.601	150	112
cs13'300	0.598	300	218
cs1p'300	0.599	300	166
cs13'400	0.601	400	276
cs13'600	0.597	600	392

Table 7.2 Details for the constant σ_1' and σ_3' triaxial drained tests on bonded samples

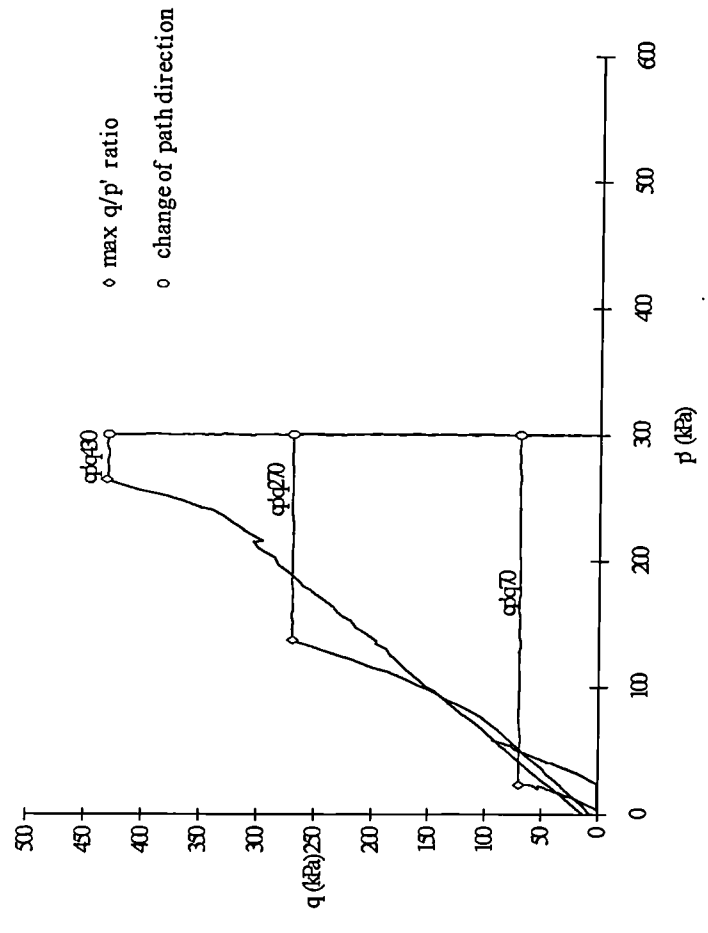Fig. 7.1b Stress paths for the three constant p'-q
triaxial drained tests

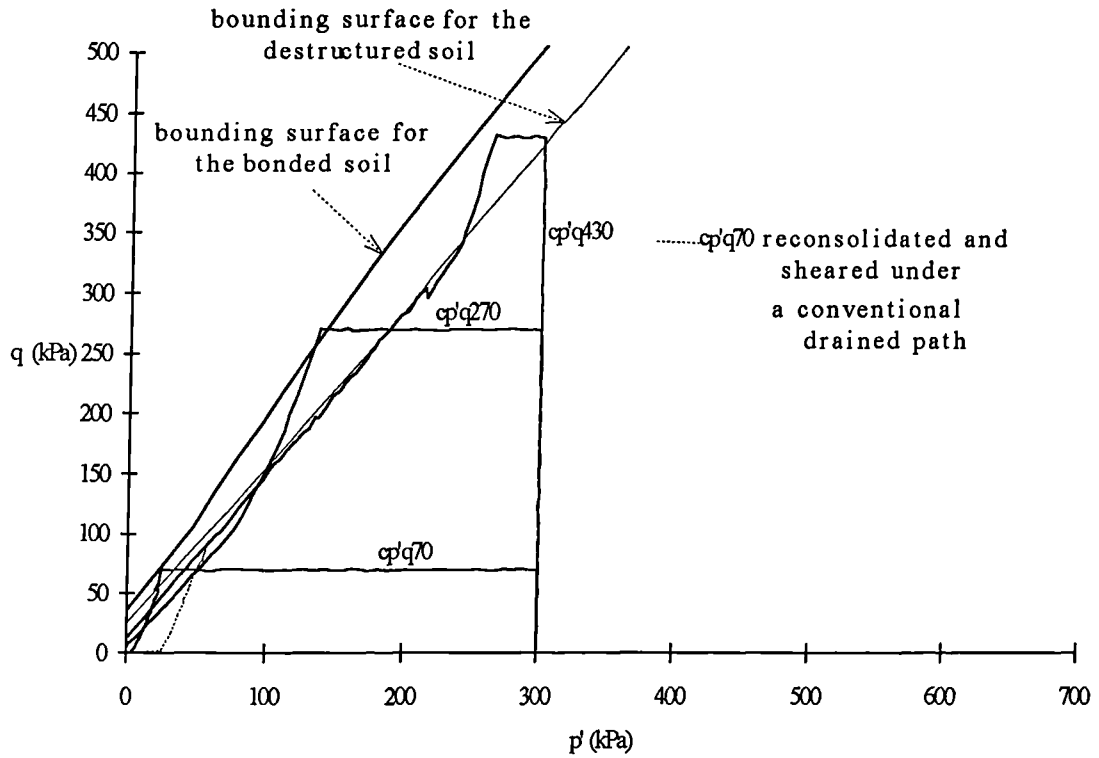Fig. 7.1a Stress strain curves for the three
constant p'-q tests

235

Fig. 7.2 Bounding surfaces for the bonded and the destructured soil and stress paths for the constant p'-q tests plotted in the stress space
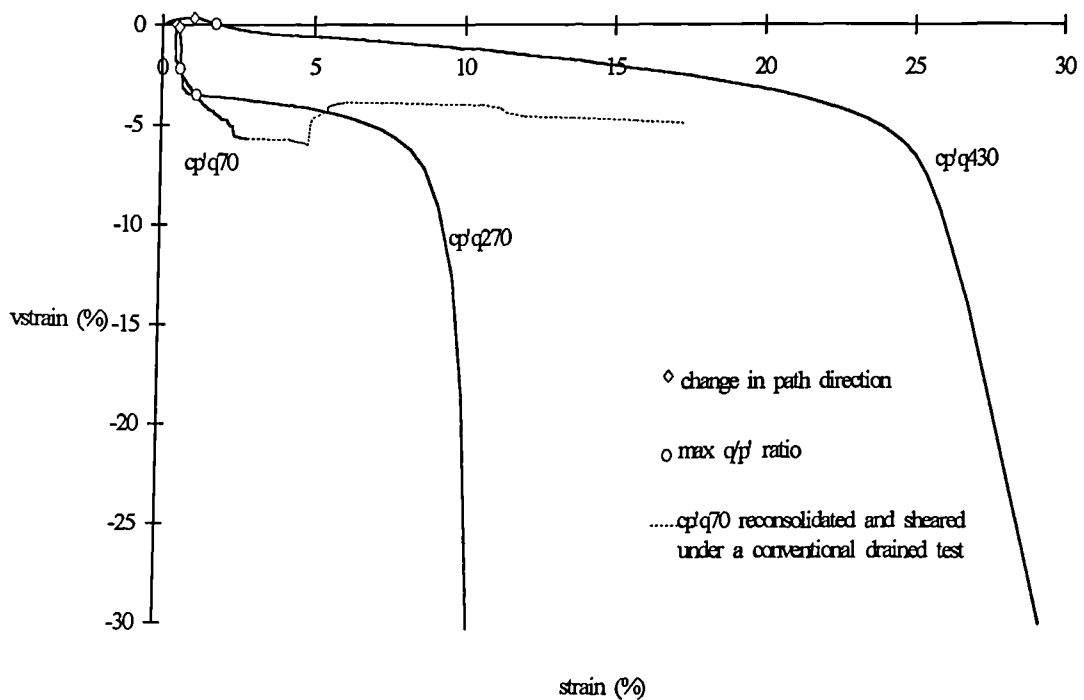

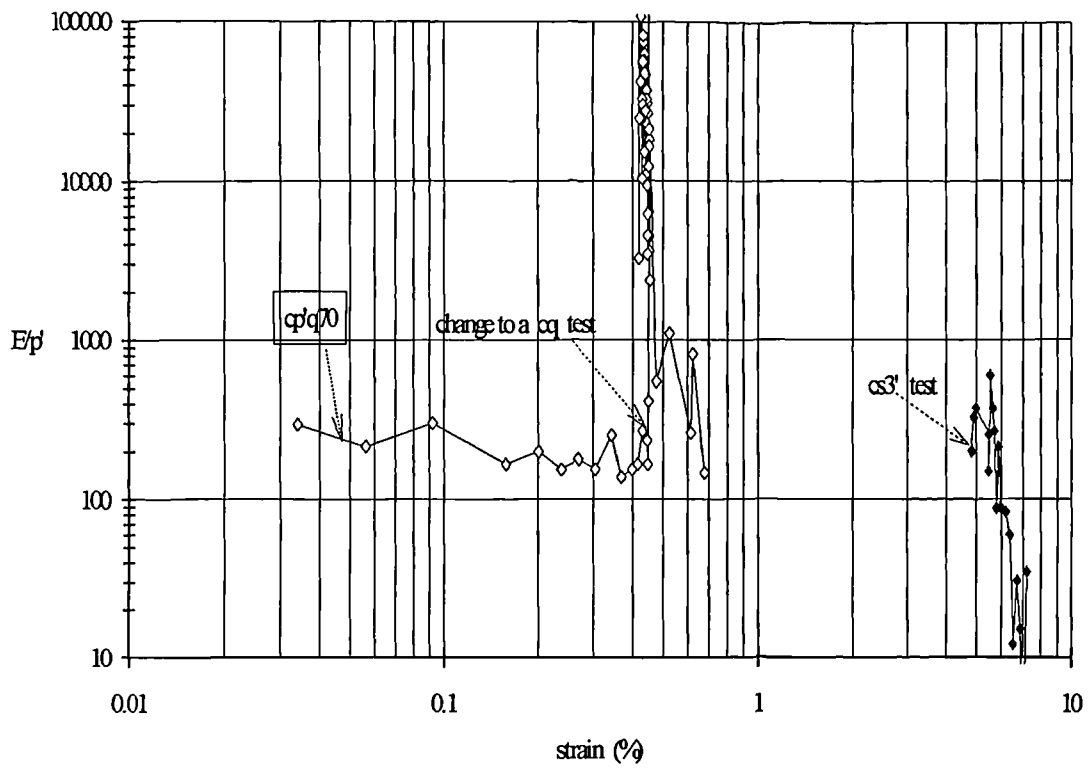Fig. 7.3 Volumetric strain versus axial strain for the constant p'-q triaxial tests

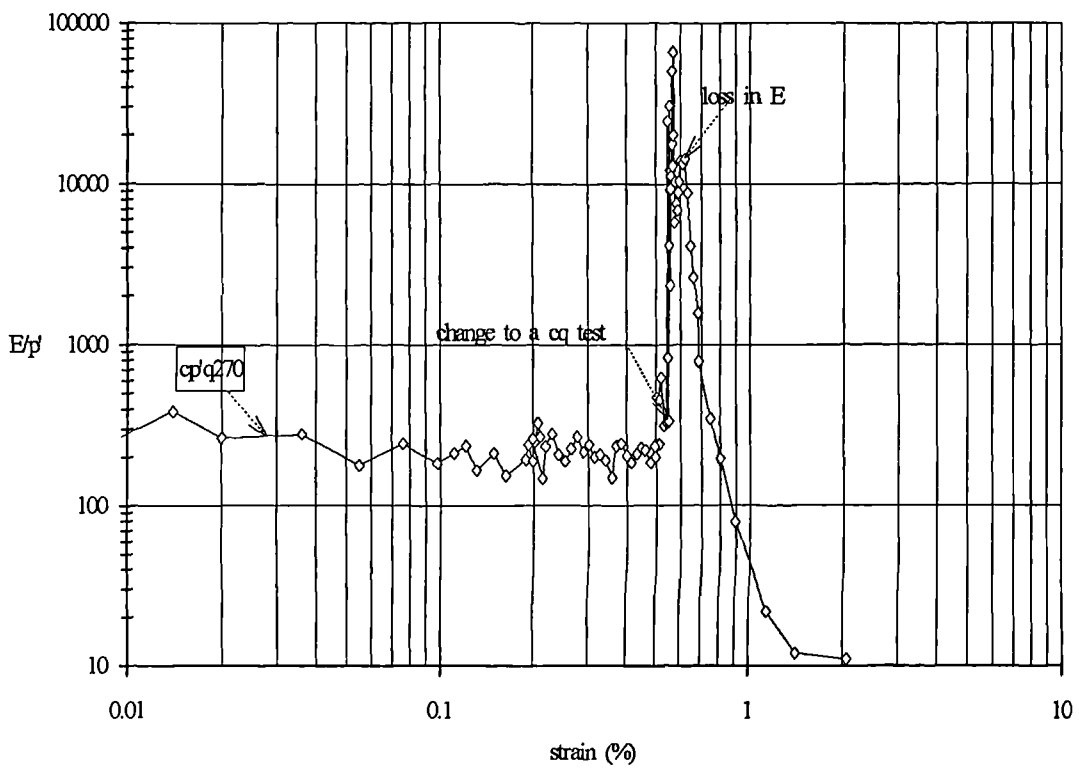Fig. 7.4a Tangential stiffness versus axial strain for test cp'q70

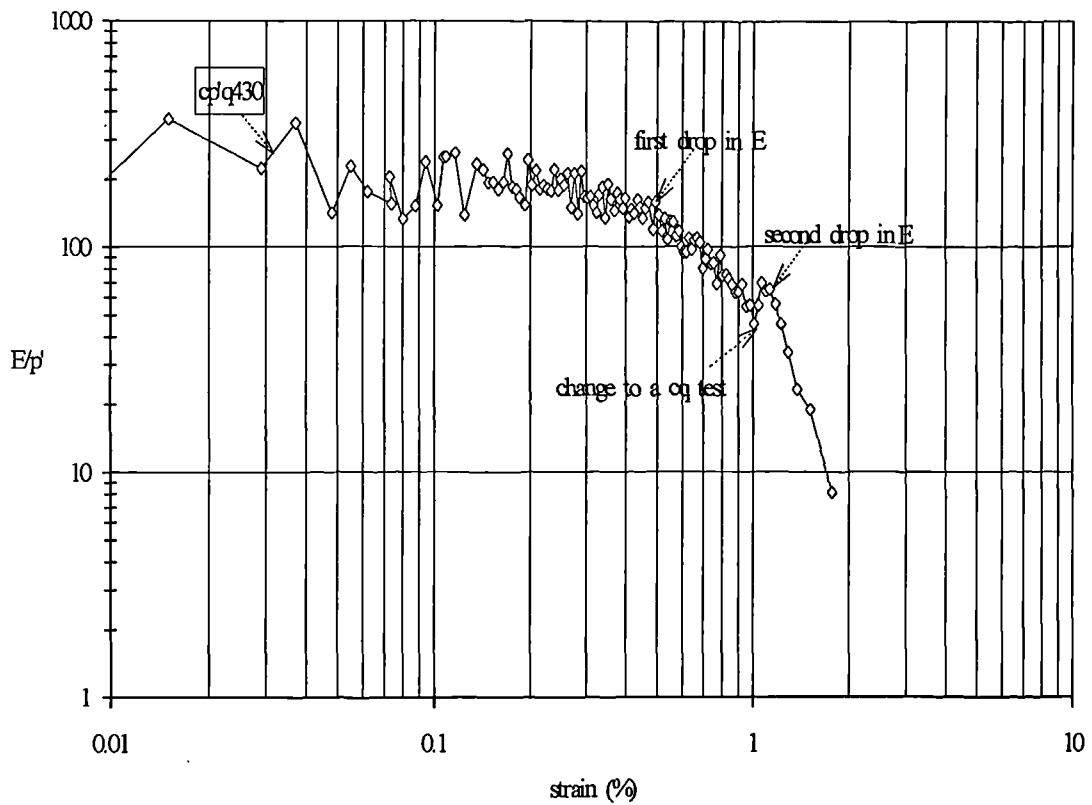Fig. 7.4b Tangential stiffness versus axial strain for test cp'q270

237

Fig. 7.4c Tangential stiffness versus axial strain for test cp'q430
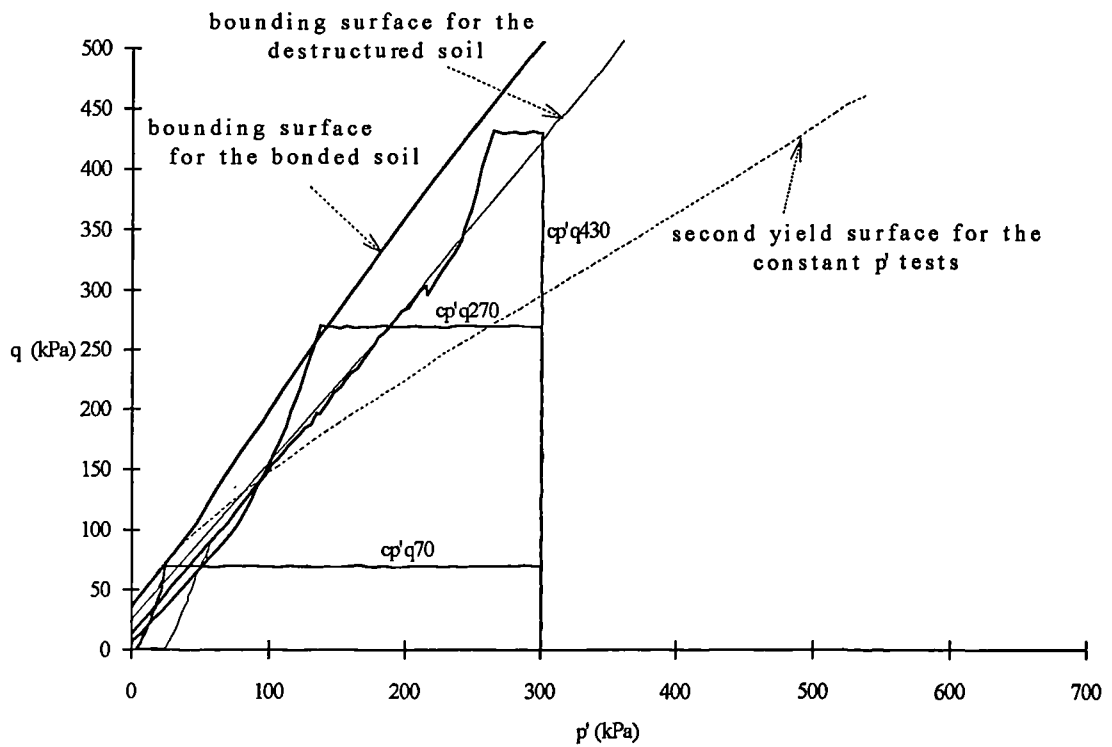

Fig. 7.5 Bounding surface and second yield surface defined
from the constant p' drained tests
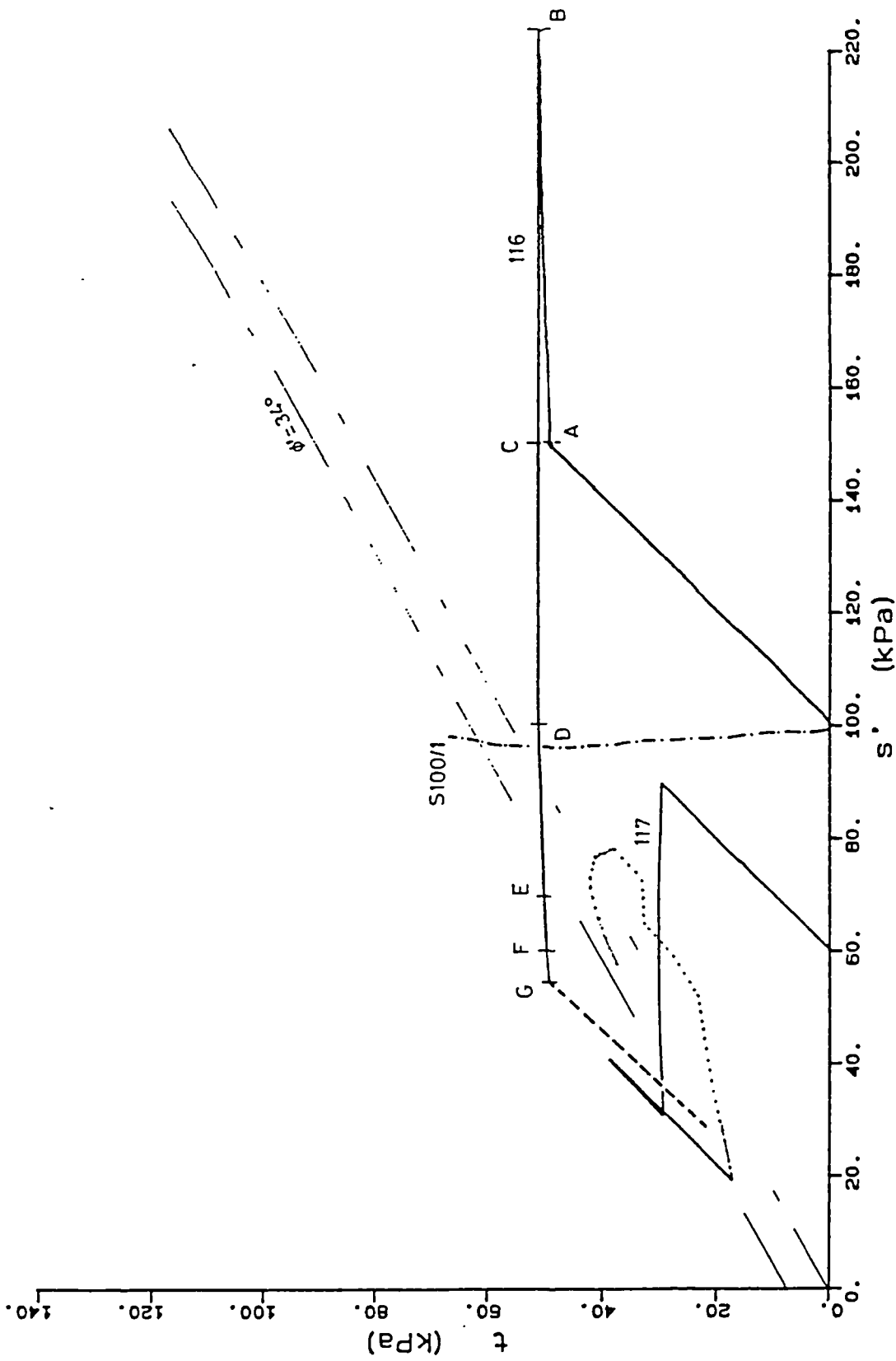
Fig. 7.6a Stress paths for two triaxial drained constant σ_3'-q tests (soil with $e_0=1.5$), after Bressani (1990)

239
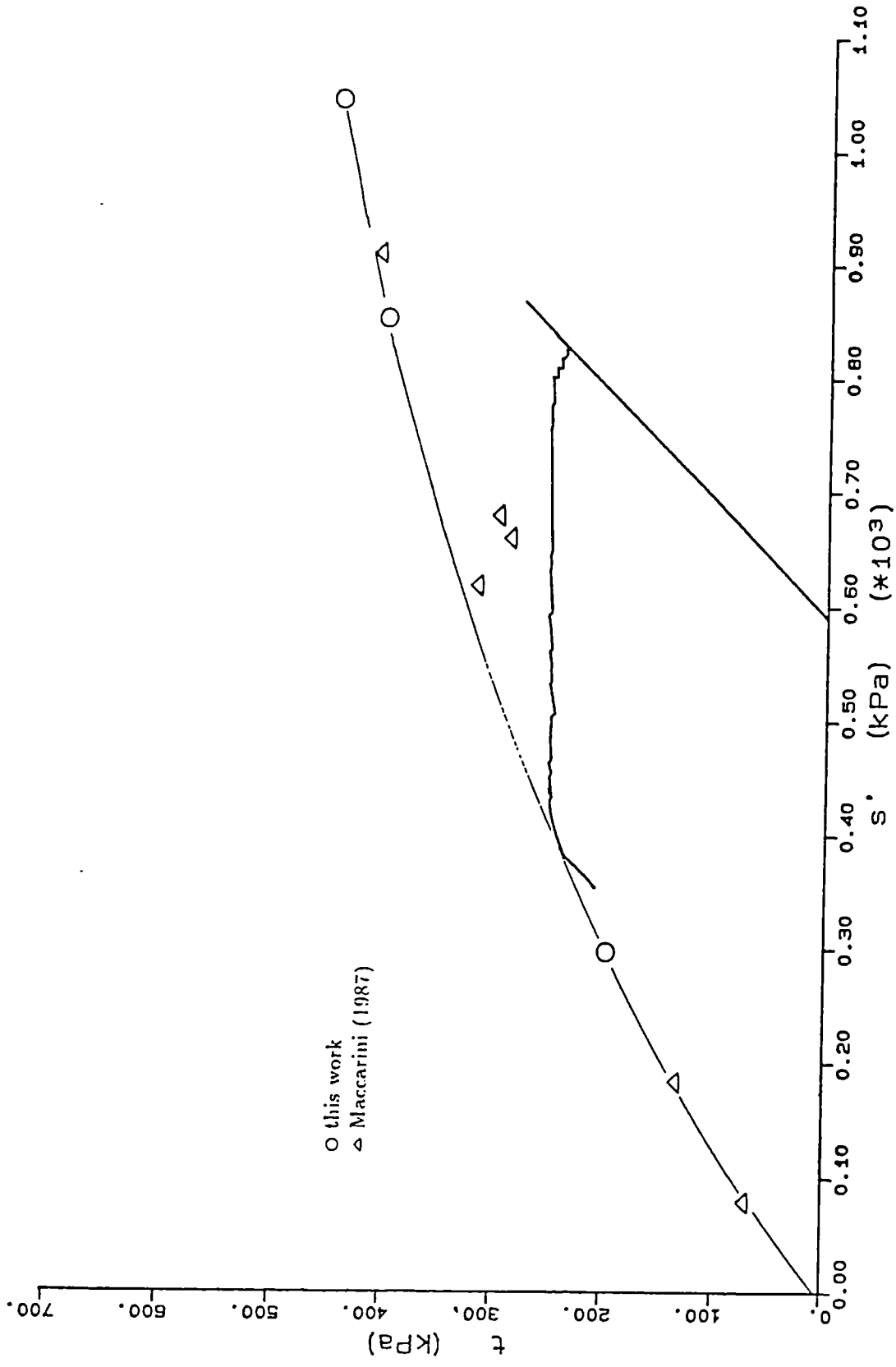
Fig. 7.6b Stress path for a triaxial constant σ_3'-q test (soil with e_o=1.1), after Bressani (1990)

240
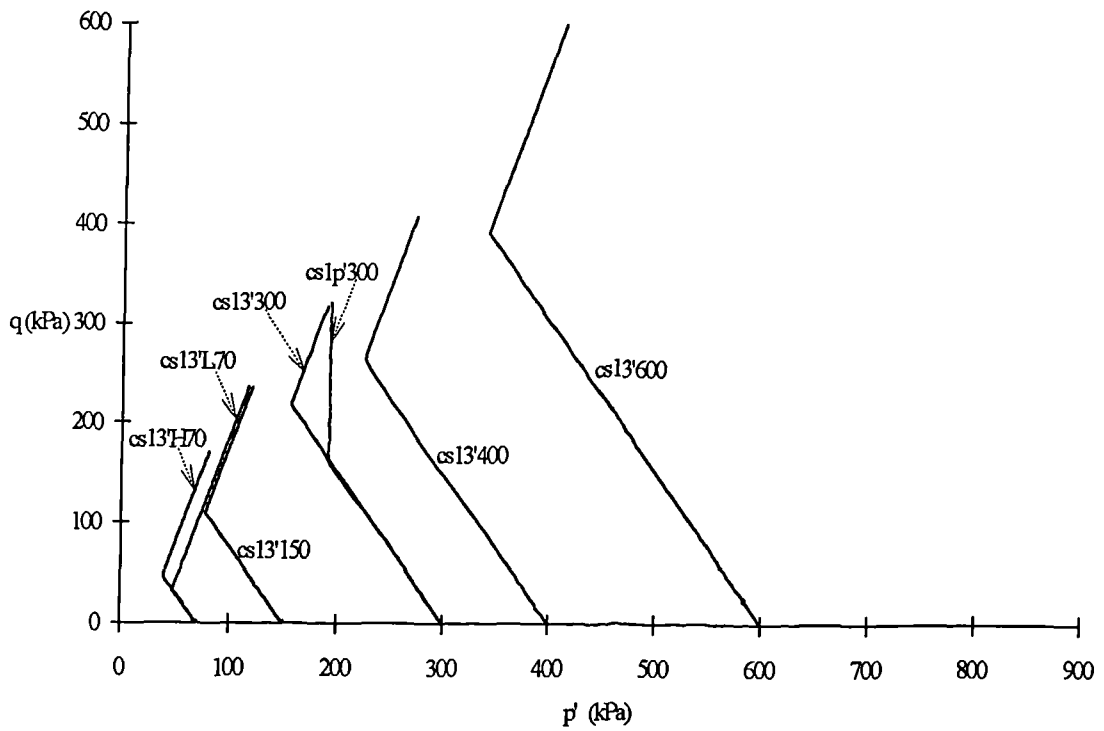
Fig. 7.7a Stress paths for the constant σ_1'- constant σ_3' and p' tests plotted in the stress space
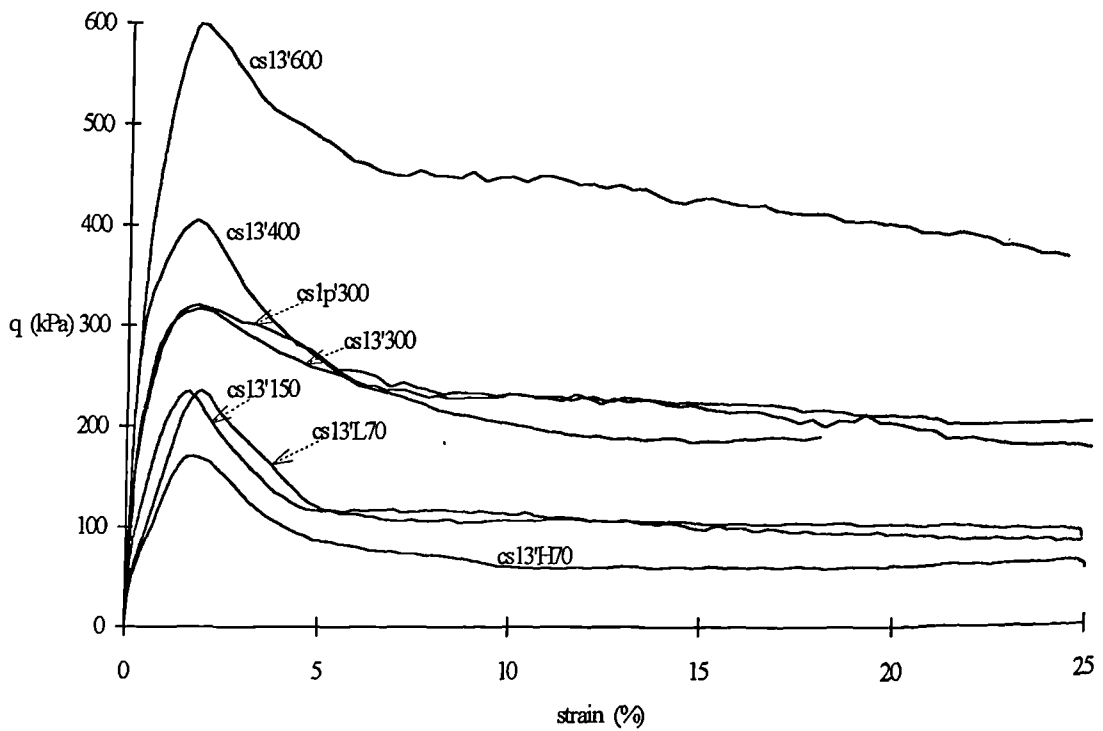
Fig. 7.7b Deviatoric stress versus axial strain for the constant σ_1'- constant σ_3' and p' tests
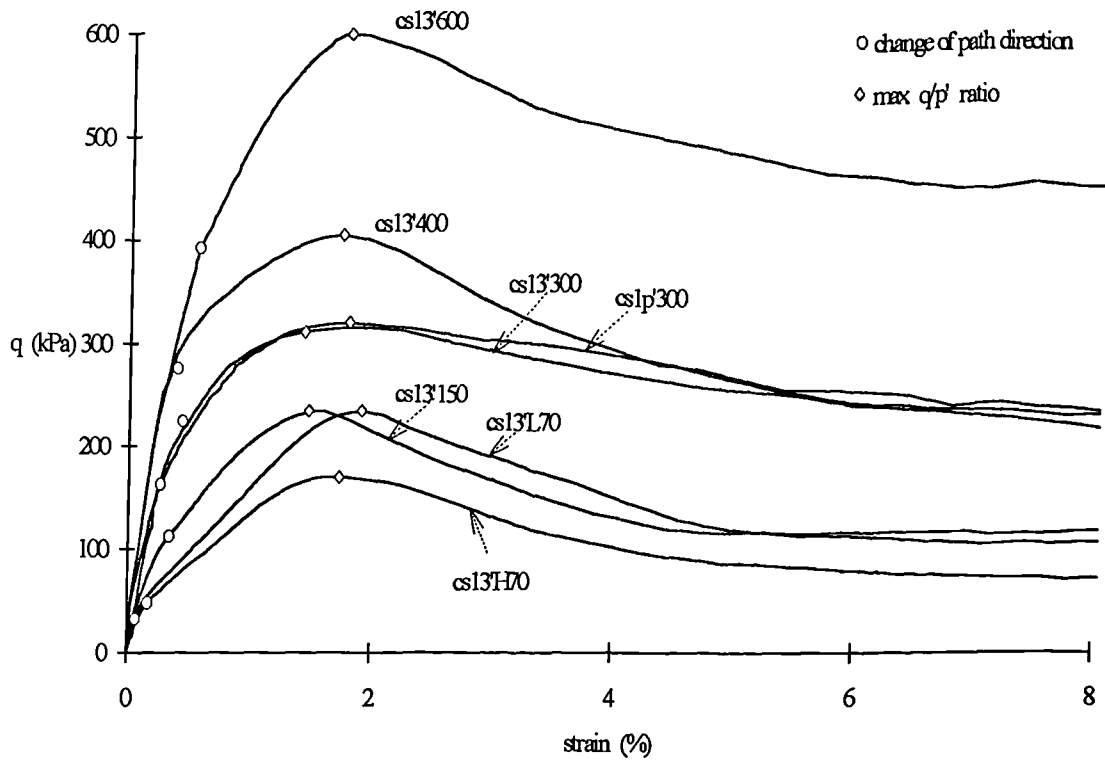
Fig. 7.8a Stress strain curves and points of change of path direction and max q/p' ratios
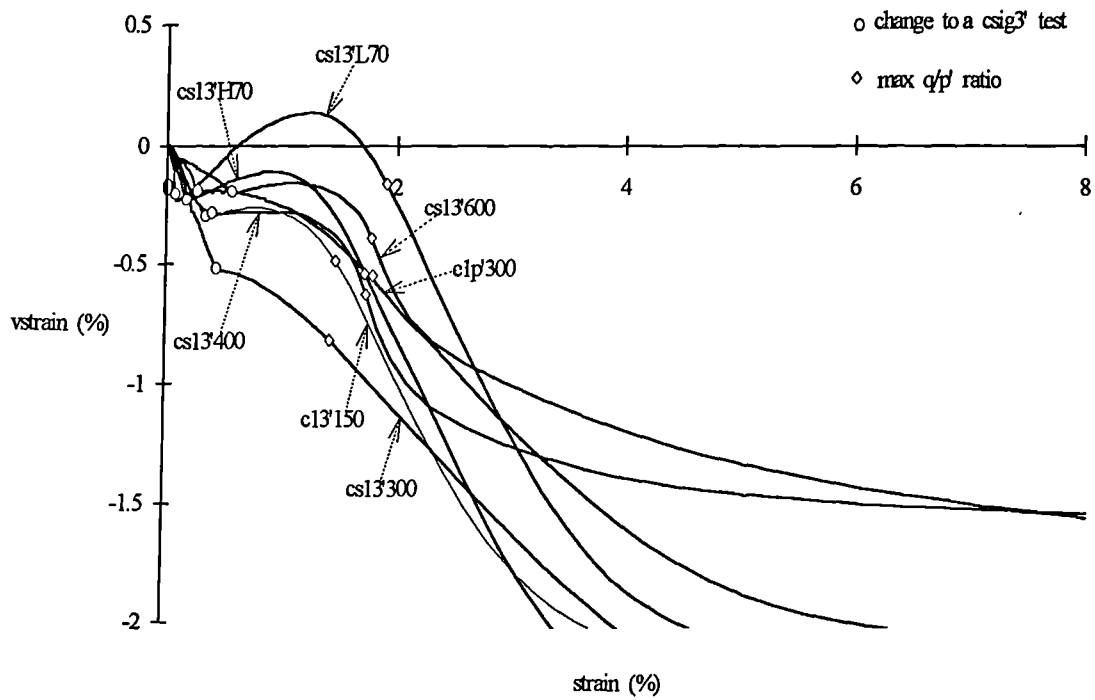
Fig. 7.8b Vstrains versus axial strain for the constant σ_1'- constant σ_3' and p' tests
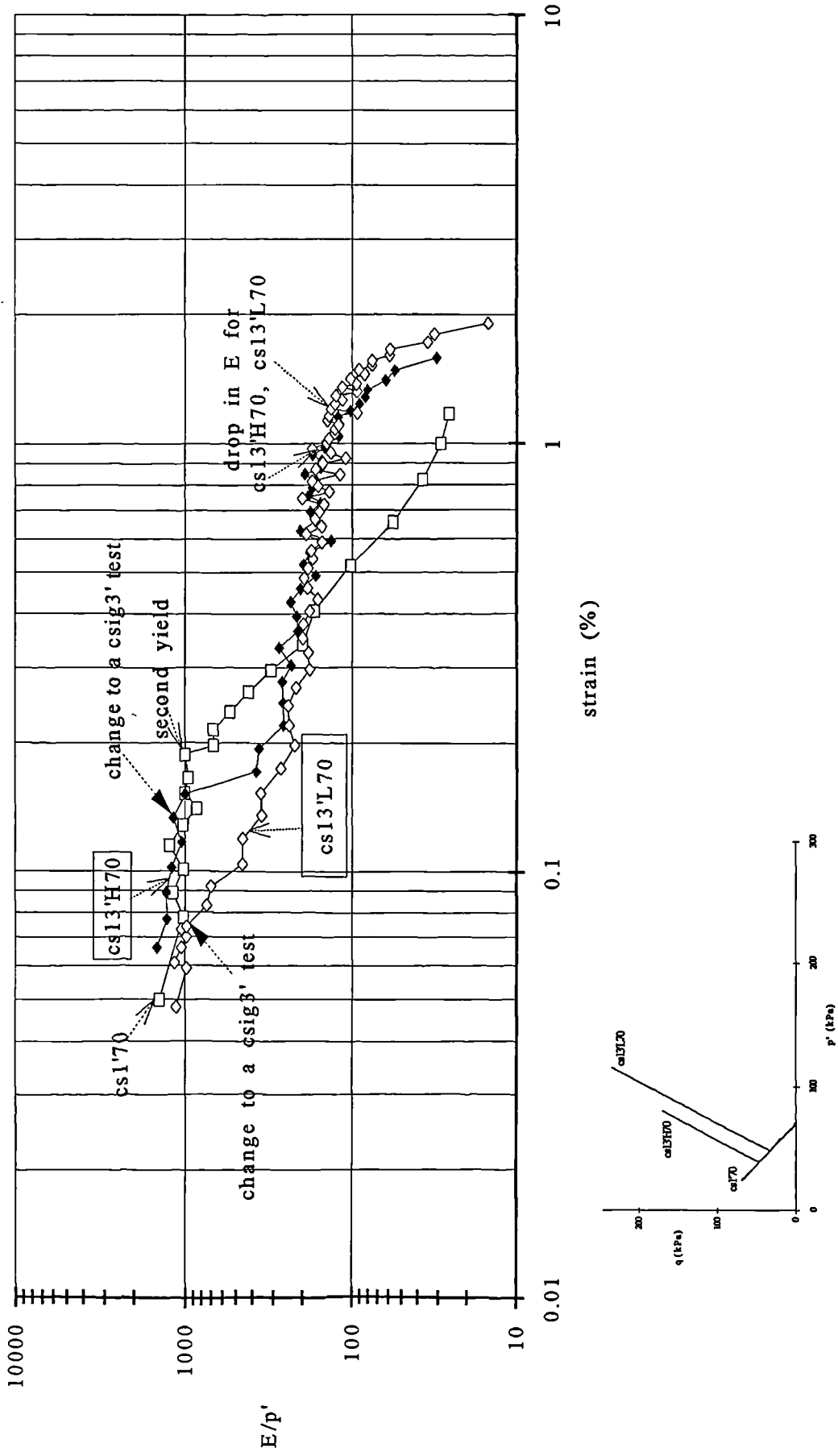
Fig. 7.9a Normalised tangential stiffness versus axial strain for tests cs13L70-H70 and csl'70

243
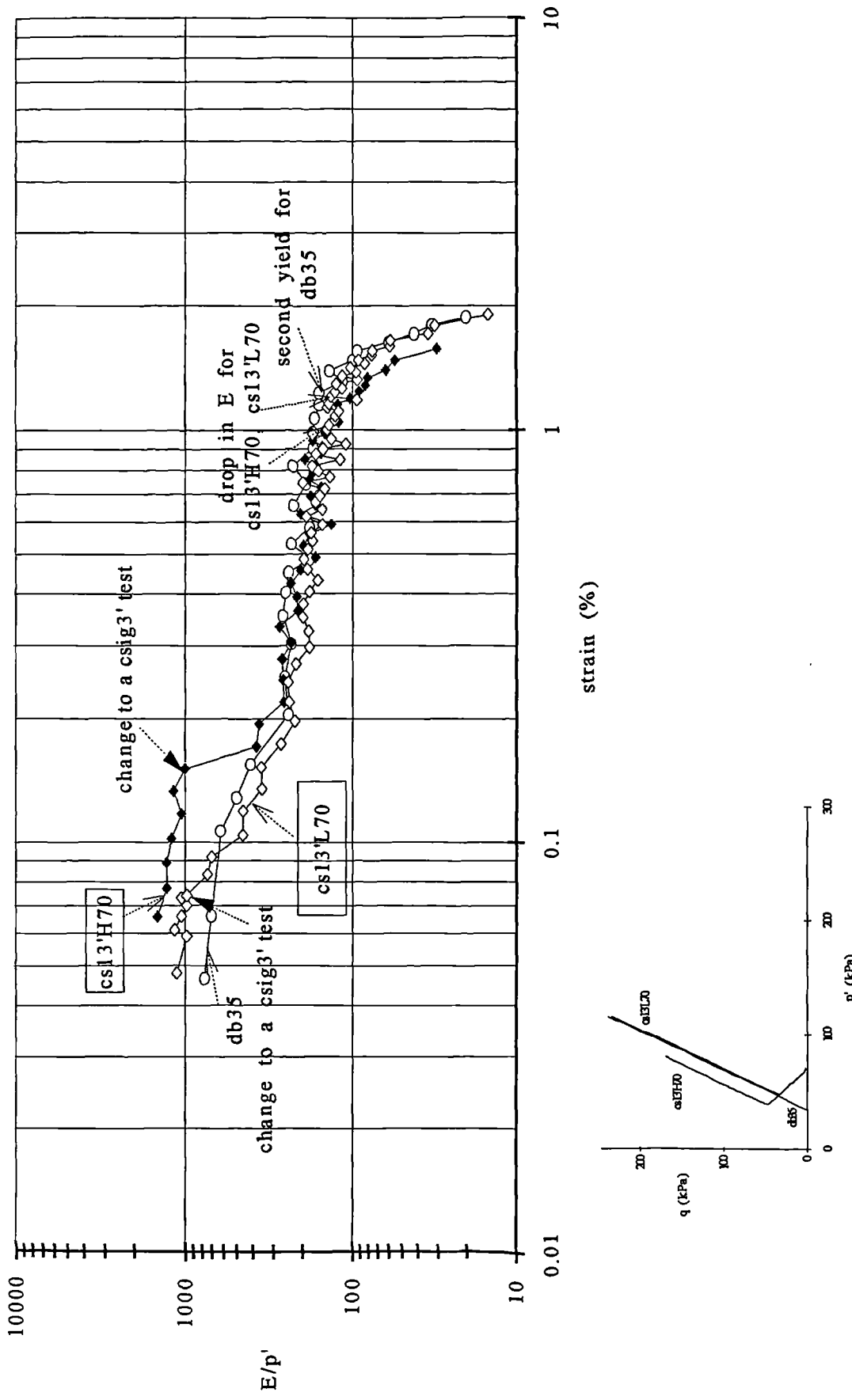
Fig. 7.9b Normalised tangential stiffness versus axial strain for tests cs13L70-H70 and db35

244
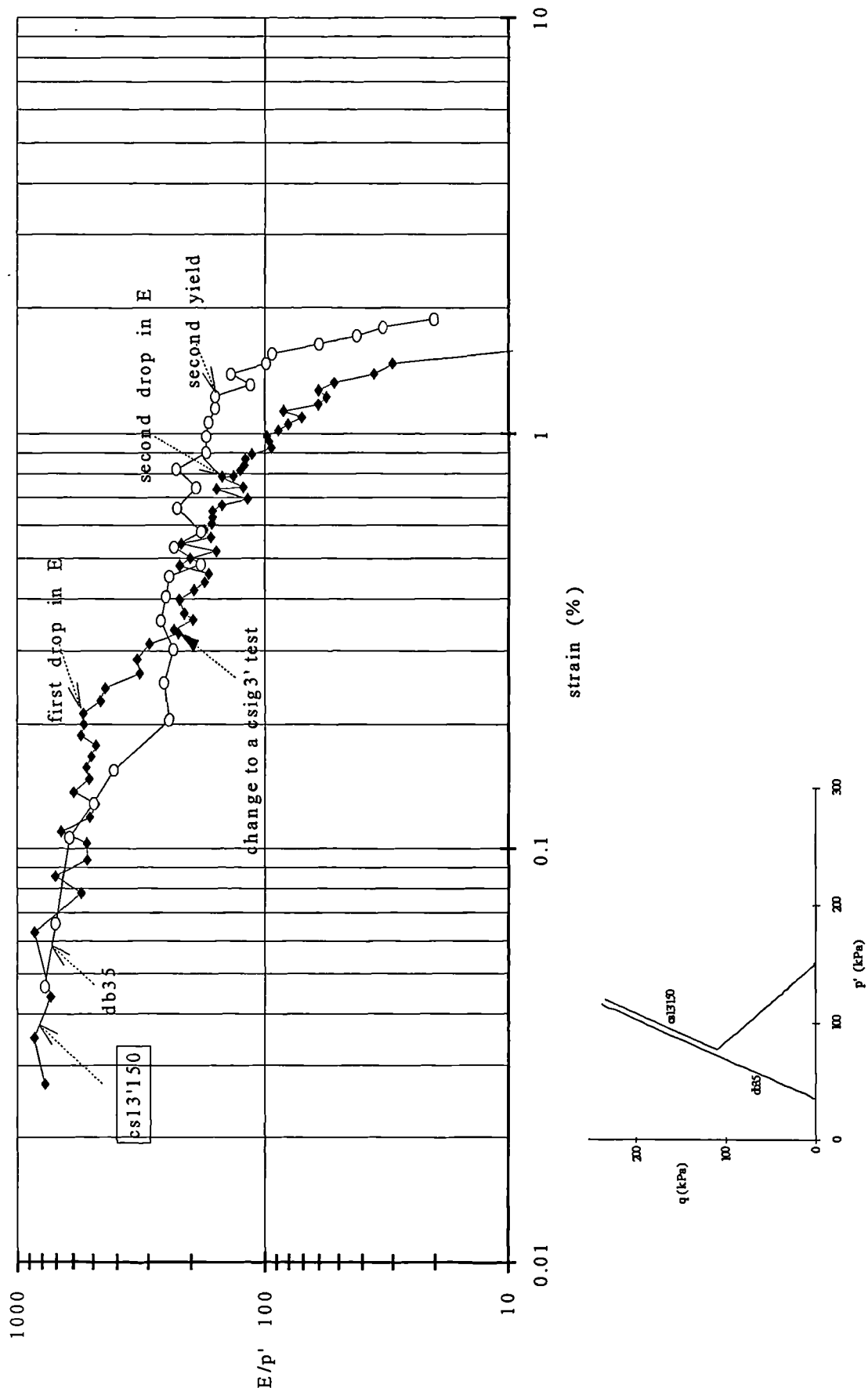
Fig. 7.10a Normalised tangential stiffness versus axial strain for tests cs13′150 and db35

245
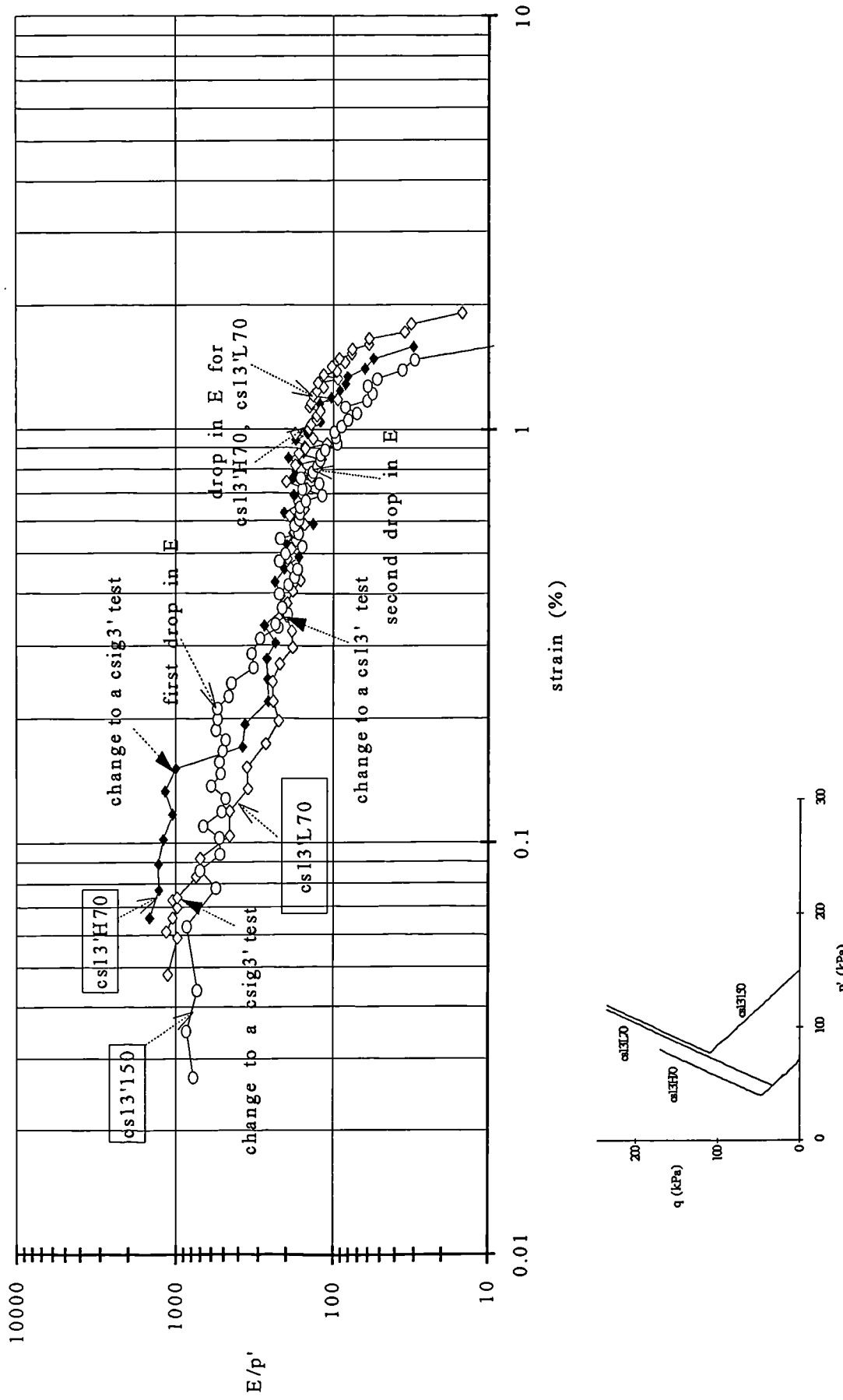
Fig. 7.10b Normalised tangential stiffness versus axial strain for tests cs13'L70-H70 and cs13'150

246
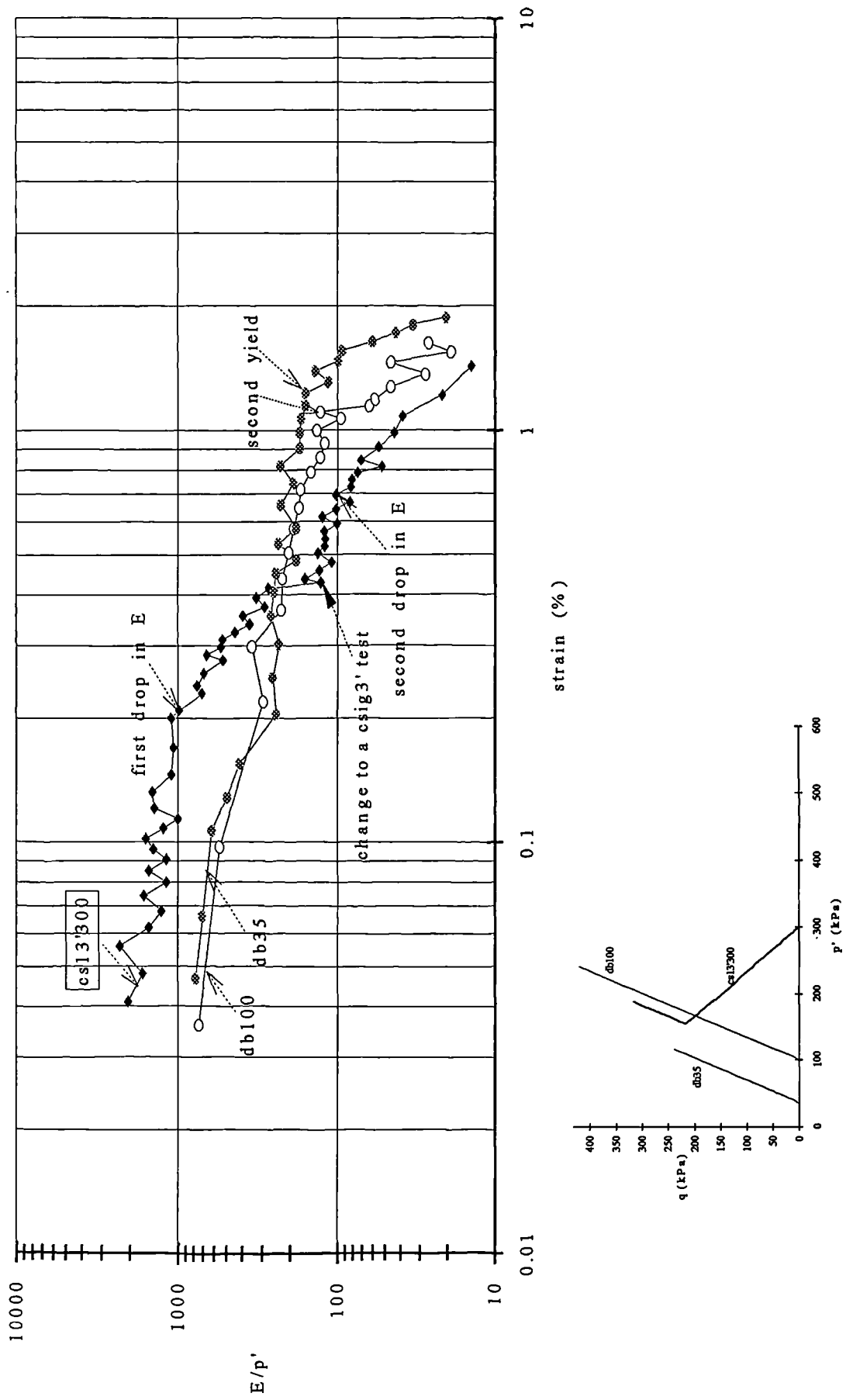
Fig. 7.11 Normalised tangential stiffness versus axial strain for tests cs13'300 and db35-100

247
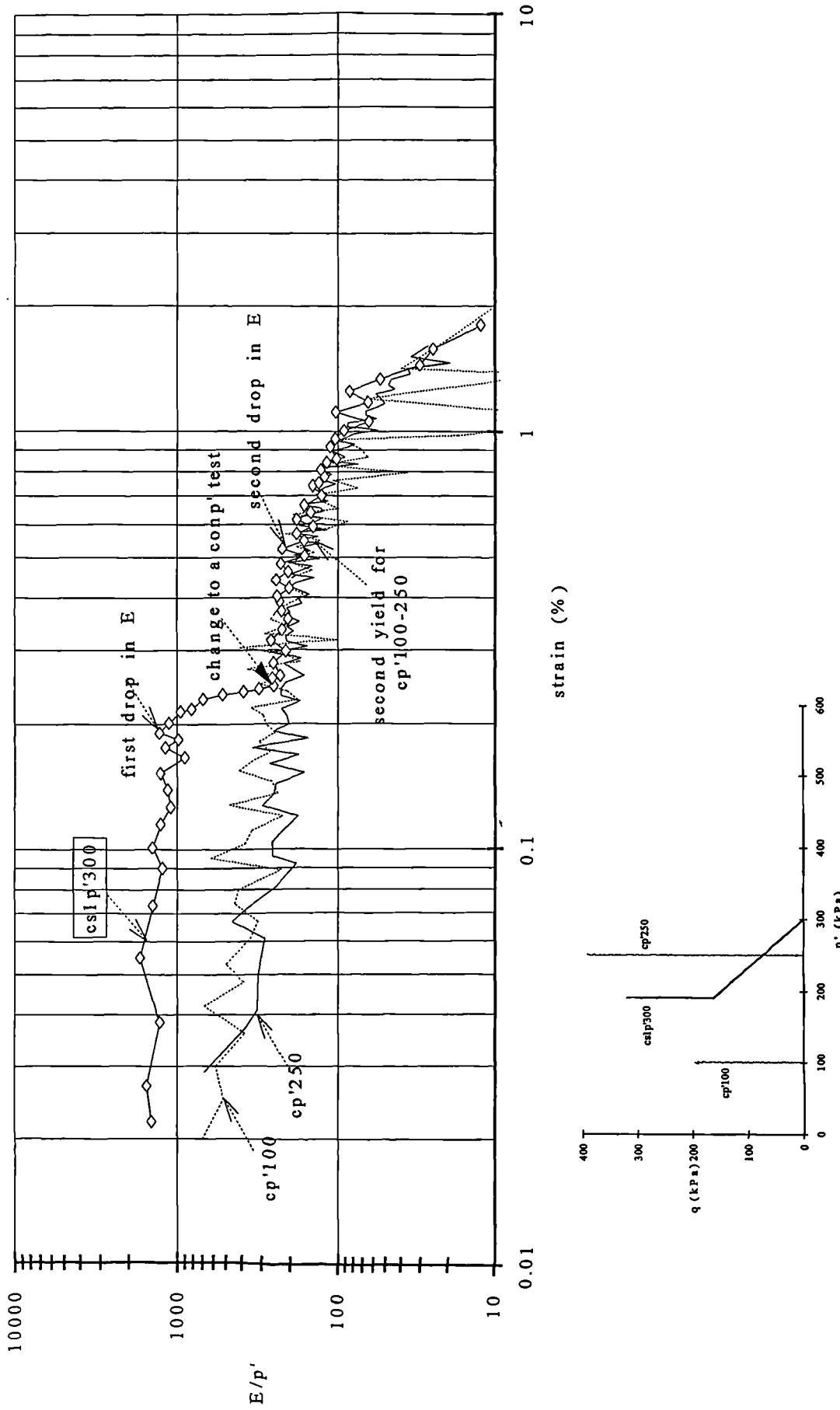
Fig. 7.12 Normalised tangential stiffness versus axial strain for tests cslp'300 and cp'100-250

248
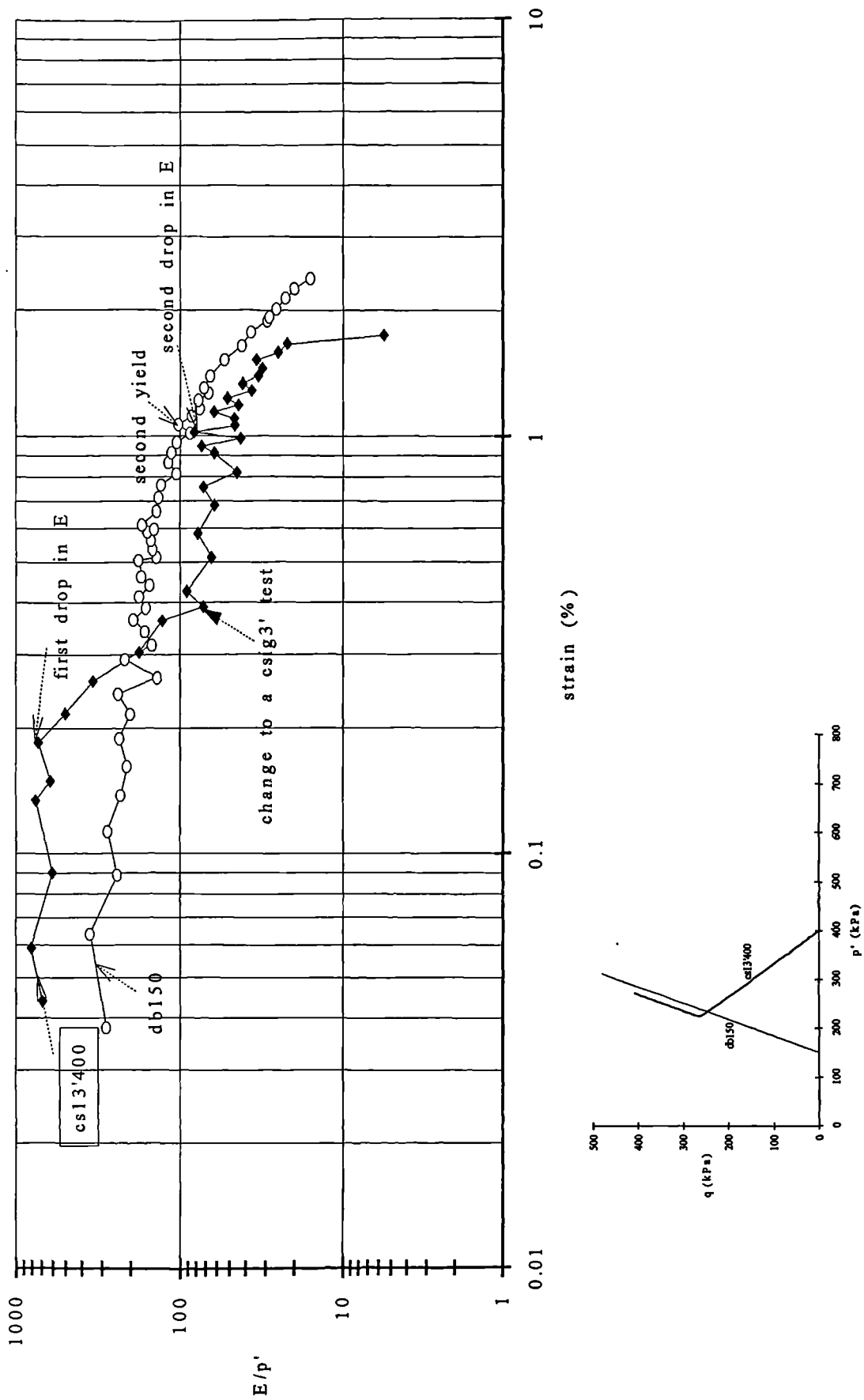
Fig. 7.13 Normalised tangential stiffness versus axial strain for tests cs13'400 and db150

249
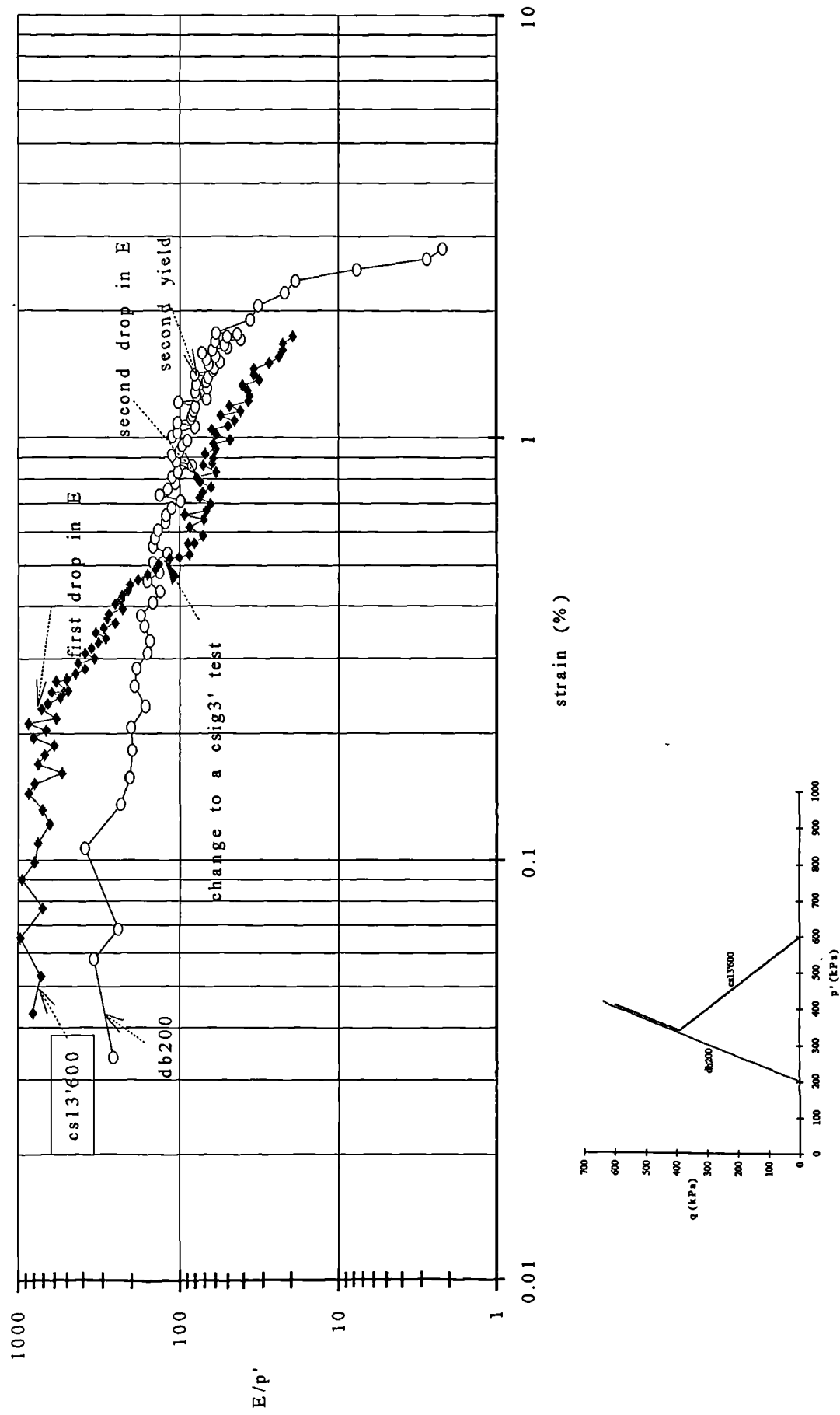
Fig. 7.14 Normalised tangential stiffness versus axial strain for tests cs13'600 and db200

250
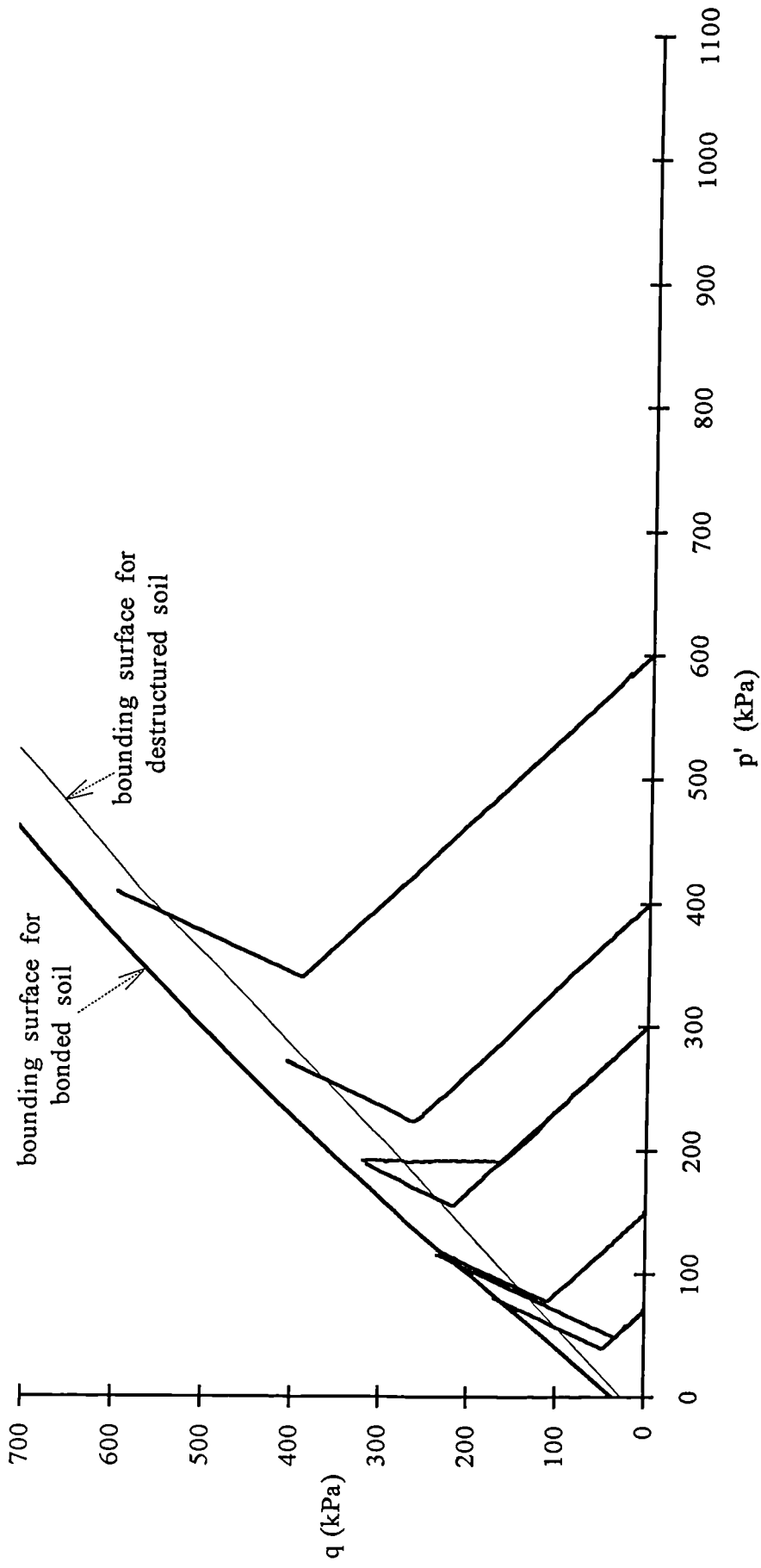
Fig. 7.15 Stress paths for the constant σ_1' constant σ_3' and p' tests and bounding surfaces for the bonded and the destructured soil defined from constant σ_3' tests

251
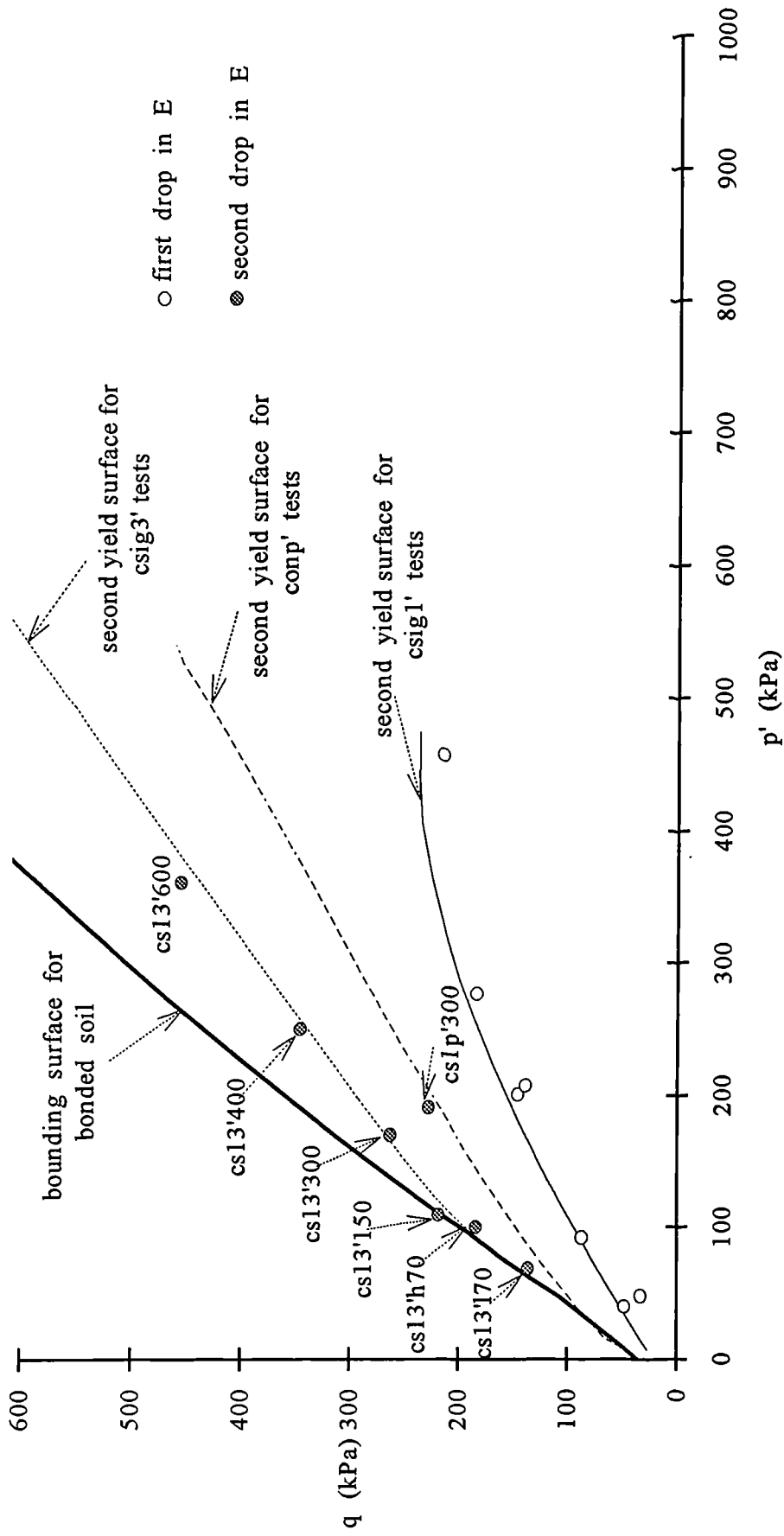
Fig. 7.16 First and second drop in E_{tan} for the constant σ_1'- constant σ_3' tests plotted in the stress space

252
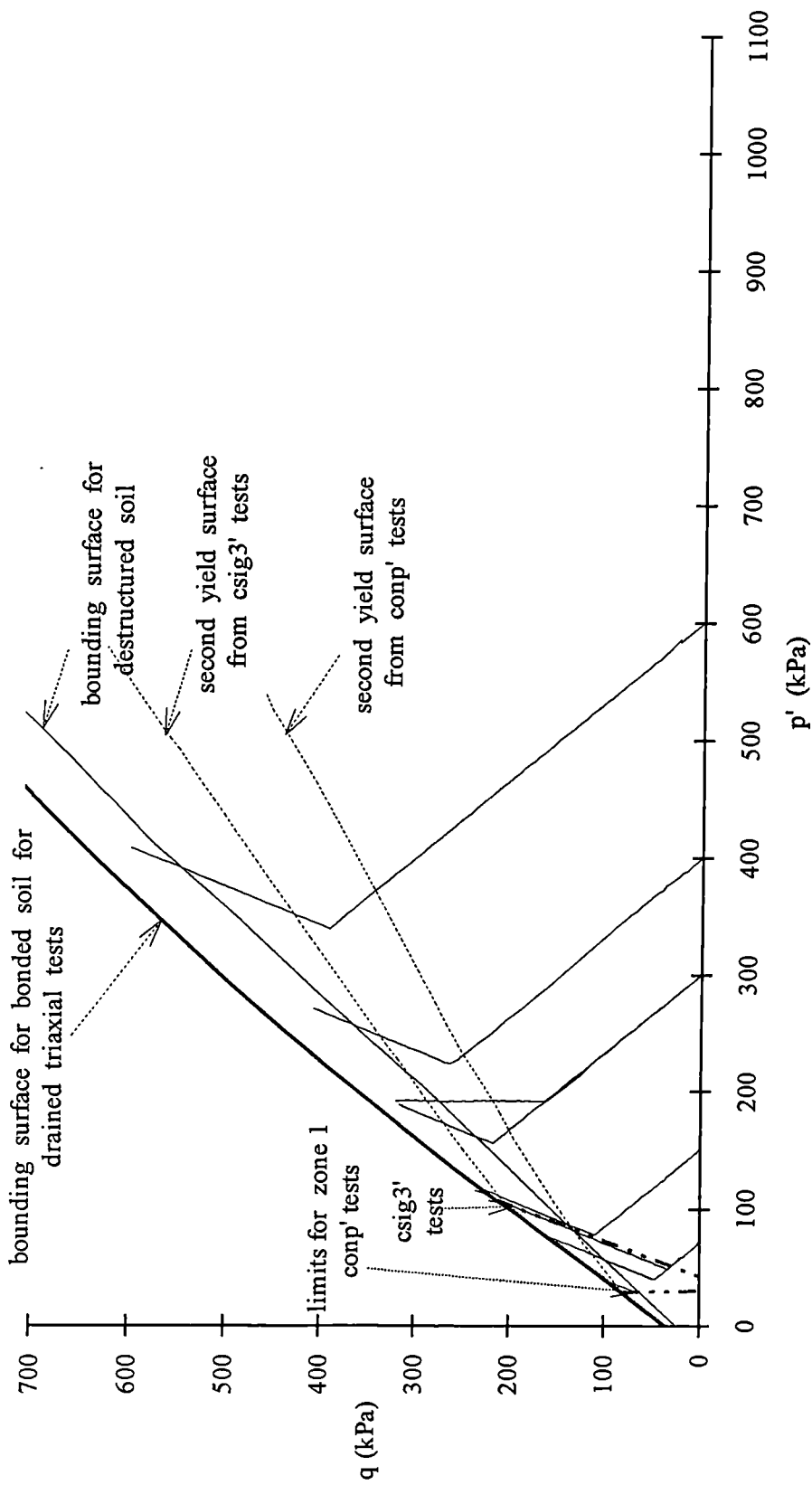
Fig. 7.17 Stress paths for the constant σ_1'- constant σ_3' tests and bounding and yield surfaces defined from the constant σ_1' and constant σ_3' tests plotted in the stress space

253
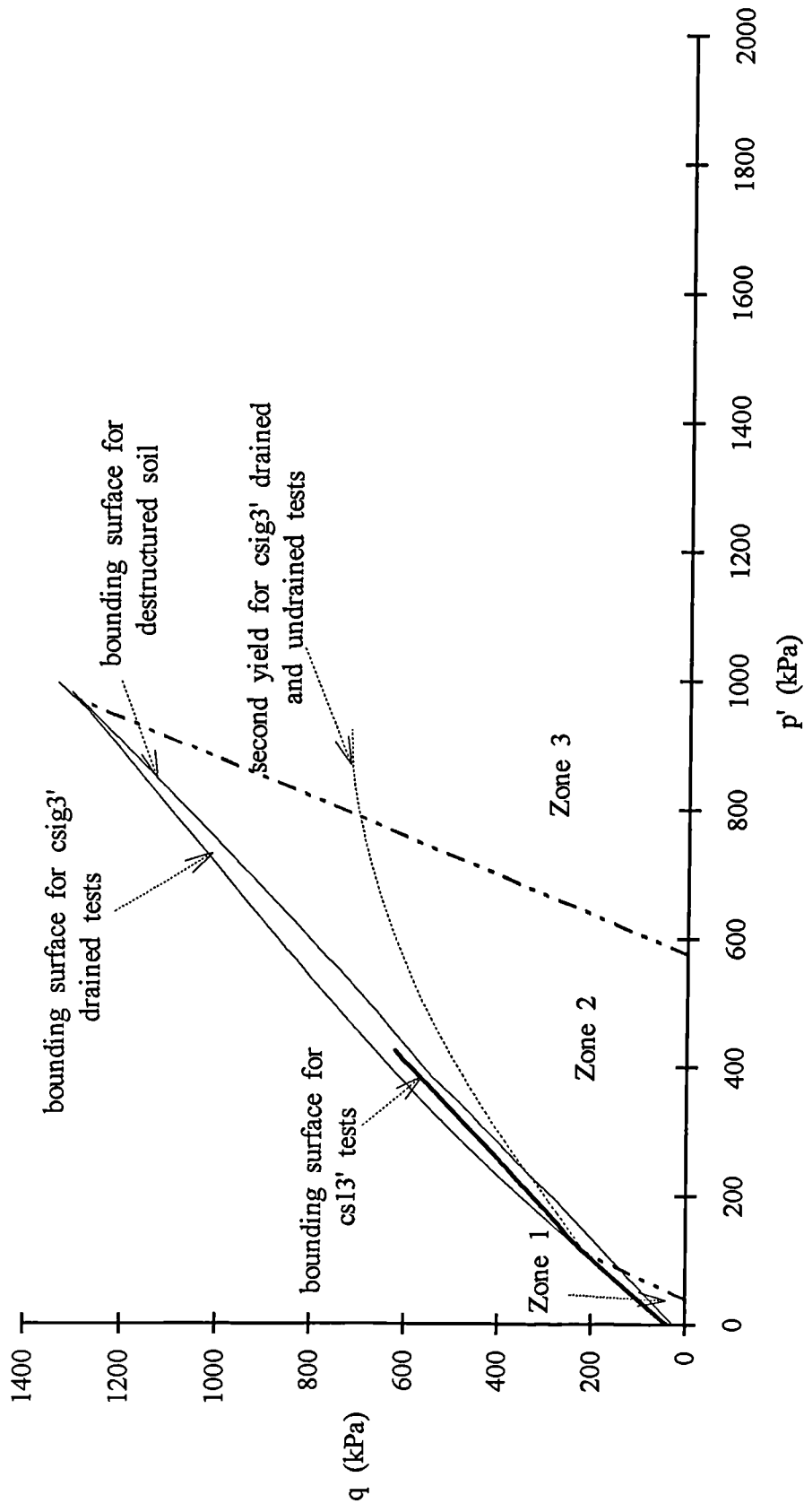
Fig. 7.18 Bounding surface defined from the constant σ_1'- constant σ_3' tests and the three zones of behaviour for shearing under the constant σ_3' path plotted in the stress space

254
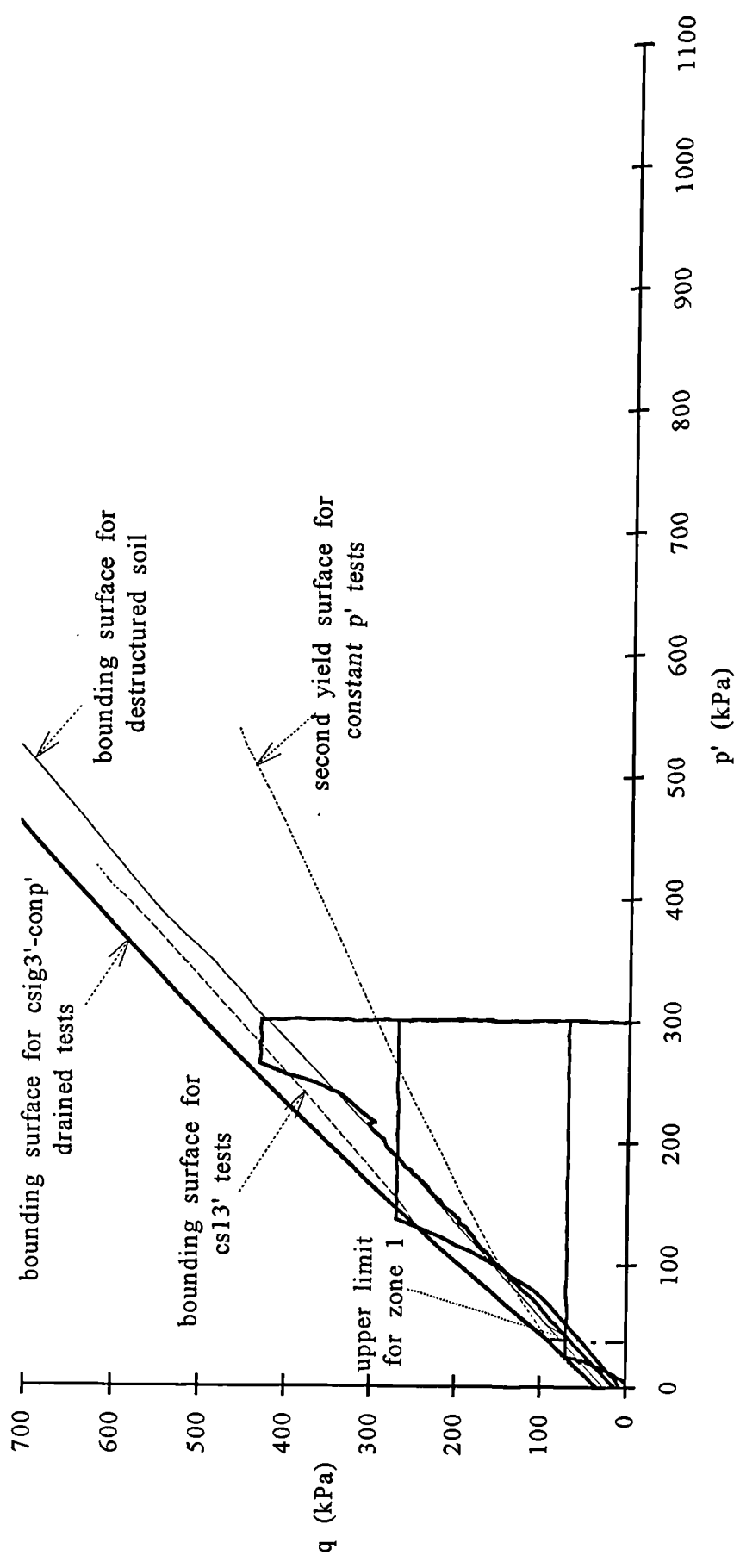
Fig. 7.19 Stress paths for the constant σ_1'- constant σ_3' tests and bounding surface defined after the constant σ_1'- constant σ_3' tests plotted in the stress space

255

CHAPTER 8   CONCLUSIONS

8.1 INTRODUCTION

In this chapter conclusions are presented for the more important findings of this study. Some suggestions for further research on the behaviour of the artificially bonded soil are presented at the end of the chapter.

8.2 CONCLUSIONS

The behaviour of the artificially bonded soil under drained and undrained shear in triaxial compression was found to be strongly affected by its bonded structure. The bonded soil sustained higher max q/p' ratios than the destructured material for mean stresses up to 800kPa. The generation of volumetric strains and pore water pressures was also influenced and the phase transformation line for the bonded soil is positioned at higher stress levels compared to that of the destructured soil. The bonded structure of the soil influenced the development of axial strains and tangential stiffness and higher stiffness values were observed compared to those of the destructured material.

The bonds yielded gradually during shearing as axial strain increased and two yield surfaces could be defined in the stress space. The second yield represents a major loss of stiffness and has greater significance than the first yield. A final yield condition could also be defined at a strain level where the soil has lost all of its stiffness, as a result of the breakdown of the bonds. Yielding of the bonds has a direct influence to the shape of the bounding surface of the bonded soil. As p' increases the slope of the bounding surface decreases gradually and turns closer to

that of the destructured soil, as the bonds are destroyed and contribute less to the limiting stress ratio which the soil can sustain.

The behaviour of the bonded soil in conventional drained and undrained tests is governed by three main zones of behaviour which are stress level dependent. In the first zone (for p'<115kPa) the bonds entirely control the soil's behaviour up to failure, as the second yield occurs at the same stress level as the bounding surface. Thus the soil sustained higher limiting stress ratios than the destructured soil sheared at the same stress level. The development of the initial tangential stiffness and the strain contours in this zone present a linear relationship with p'.

In the second zone (for 115<p'<800kPa), the bonds only partially control the soil's behaviour as yield occurs before failure is reached and they contribute less to the limiting stress ratios which can be sustained. The slope of the bounding surface is directly affected and decreases to a lower level. However, due to some post yield influence of the bonds the soil can still sustain higher maximum q/p' ratios than that of the destructured soil. Nevertheless, as p' increases, the gradual destruction of the bonds causes the difference between the bounding surface and the second yield surface gradually to increase and the difference between the two bounding surfaces to decrease. In this zone the slopes of the tangential stiffness curves and the strain contours, with respect to p', decrease to lower levels.

In the third zone (for p'>800kPa), the soil's behaviour at failure is not affected by the bonds. Yielding of the bonds at lower deviator stresses does not allow high max q/p' ratios to be reached and the bounding surface of the bonded soil coincides with that of the destructured soil. Tangential stiffness in this zone is almost constant irrespective of the stress level and the strain contours change direction and turn down towards the isotropic axis.

The method of controlling shearing (stress or strain controlled tests) did not affect the behaviour of the bonded and destructured soil. Both drained and undrained tests showed a consistent pattern of behaviour.

Differences were observed between the test results for the destructured soil and sand/kaolin mixtures, which had the same initial grading as material used to produce the bonded samples, but which had not been subjected to the firing process. The maximum q/p' ratios, phase transformation line, tangential stiffness development and strain contours all showed differences. This highlights the importance of using a destructured soil with the same nature and grading as the bonded soil in order to study the effects of bonding on the soil's behaviour.

Anticlockwise rotation of the stress path direction to the left of the conventional drained path (constant p' and constant σ_1' tests) influenced the soil's behaviour. Second yield occurred at lower axial strains than those observed in the conventional drained tests. The greater the degree of rotation of the stress path direction the lower the axial strain at yield. Different yield loci were observed for each stress path direction. The anisotropic nature of the breakage of the bonds under the probing drained tests is thought to be due to differences in development of radial and volumetric strains. Higher negative radial and volumetric strains (dilation) were observed from the beginning of shearing in the constant p' and constant σ_1' tests, compared with the conventional drained tests.

Although the position of the second yield surface is affected by the stress path direction, the limiting stress ratios that the soil could sustain in the stress space were unaffected, for the stress levels at which tests were carried out. A unique bounding surface governs the soil's behaviour for all the stress paths followed in this study. However, the rotation of the shearing path direction influenced the position of the upper limit of the first zone of behaviour. The first zone (where the

bonds entirely control the soil's behaviour at failure) does not exist for the highest degree of rotation (the constant σ_1' path).

The development of tangential stiffness under the probing tests was influenced by the rotation of the shearing path direction. Higher values were observed in the samples sheared under the constant σ_1' path than under the other two path directions, up to the point of the second yield. The strain contours were also affected.

Clockwise changes in the stress path directions during drained shearing strongly influenced the behaviour of the bonded soil. Even after yield had occurred when following one stress path direction, a further yield could be observed if the stress path direction was changed. Yield occurred at a stress level that corresponded to a yield surface defined for the current shearing path direction.

The limiting stress ratios that the soil sustained in the stress space depended more on the zone of behaviour that the shearing path changed direction and less on the stress level at which this change took place, prior to or after the major loss in E_{tan} along the initial shearing path. The one condition when the bounding surface of the bonded soil was affected was when a change in stress path direction occurred within zone 2. In this case, the limiting stress ratios were found to fall below the unique bounding surface for the bonded soil, but still above the bounding surface for the destructured soil defined by tests in which no change in stress path direction had been followed.

The position of the final yield surface (where the soil has lost all stiffness) under drained and undrained shearing could be defined close to the bounding surface. This yield condition could not be used to define the second zone of behaviour. However the ability to identify this zone is quite important as it is a transitional zone of

behaviour, where the post yield influence of the bonded structure allows the soil to sustain higher max q/p' ratios than those of the destructured soil. Furthermore, in this zone, when drained tests were carried out with changes in the stress path directions, the soil presented lower maximum q/p' ratios than those sustained under conventional drained tests. Therefore determination of the second yield of the bonds from the loss in tangential stiffness was found to be more important than the final yield and essential for a better understanding of the soil's behaviour, as it clarifies this transitional zone of behaviour.

This work has developed a consistent framework which explains the behaviour of an artificial weakly bonded soil. It significantly extends previous approaches to bonded soils' behaviour by considering a range of different stress path directions. The model can also be used to describe the behaviour of natural structured soils, using only a small number of tests to characterise the natural soil.

8.3 FURTHER RESEARCH

With the completion of this study a number of points which deserve further investigation can be identified. It would be interesting to define the position of the second yield loci for $p'>800$kPa and to investigate the soil's behaviour with respect to the development of tangential stiffness and axial strain in the third zone following conventional drained shearing.

The lower limit of the second zone of behaviour for constant p' and constant σ_1' shearing paths was seen to move to lower stress levels than that defined for conventional drained shearing. It would be very interesting to investigate if the position of the upper limit also changes due to the rotation of the stress path direction. The transitional zone of behaviour was shown to be quite unstable when

shearing with changes in the stress path directions. Therefore it is important to define the limits of this zone.

Shearing of the bonded soil under clockwise changes of the stress path directions showed that the soil's behaviour mainly depends on the zone of behaviour in which the second part of shearing takes place. However, an indication is also given from this study that under anticlockwise changes of the shearing path, the stress level at which the path changes direction (before or after the occurrence of the major yield under the initial shearing path) is probably more important. The zone of behaviour in which the second part of shearing continues, might play a secondary role and thus a different framework may apply. However this needs further investigation, before final conclusions could be drawn.

This study was carried out using external measurements of strain which are, of course, influenced by measurement errors. The consistency of the results obtained show that comparisons between tests using external measurements are valid. However, use of internal, sample mounted strain measuring devices would allow truer values of stiffness to be obtained.

REFERENCES

Allman, M. A. and Atkinson, J. H. (1992). *Mechanical properties of reconstituted Bothkennar soil.* Geotechnique 42, No. 2, pp 289-301.

Anagnostopoulos, A., Kalteziotis, N., Tsiambaos, G. K. and Kavvadas M. (1991). *Geotechnical properties of the Corinth Canal marls.* Geotechnical and Geological Engineering, 9, pp 1-26.

Atkinson, J. H. and Bransby, P. L. (1978). *The mechanics of soils.* London: McGraw-Hill.

Atkinson, J. H. (1993). *An introduction to the mechanics of soils and foundations.* London: McGraw-Hill.

Bishop, A. W. and Wesley, L. D. (1974). *A hydraulic triaxial apparatus for controlled stress path testing.* Geotechnique 25, No. 4, pp 657-670.

Bressani, L. A. (1990). *Experimental properties of bonded soils.* PhD thesis, University of London.

Bressani, L. A. (1993). *The secant stiffness behaviour of Corinth marl.* Proceedings of the International Symposium on the Geotechnical Engineering of Hard Soils-Soft Rocks, Athens, Vol 1, pp 391-396.

Clayton, C. R. I., Hight, D. W. and Hopper, R. J. (1992). *Progressive destructuring of Bothkennar clay : Implications for sampling and reconsolidation procedures.* Geotechnique 42, No. 2, pp 219-239.

Clough, G. W., Sitar, N., Bachus, R. C. and Rad, N. S. (1981). *Cemented sands under static loading.* Journal of the Geotechnical Engineering Division, ASCE, June, pp 799-817.

Coop, M. R. and Atkinson, J. H. (1993). *The mechanics of cemented carbonate sands.* Geotechnique 43, No. 1, pp 53-67.

Cuccovillo, T. and Coop, M. R. (1993). *The influence of bond strength on the mechanics of carbonate soft rocks.* Proceedings of an International Symposium on the Geotechnical Engineering of Hard Soils-Soft Rocks, Athens, Vol 1, pp 447-456.

Georgiannou, V. N. (1988). *The behaviour of clayey sands under monotonic and cyclic loading.* PhD thesis, University of London.

Georgiannou, V. N, Burland, J. B. and Hight, D. W. (1990). *The undrained behaviour of clayey sands in triaxial extension and compression.* Geotechnique 40, No. 3, pp 431-450.

Head, K. H. (1980). *Manual of soil laboratory testing.* London: Pentech Press, 1.

Hight, D. W., Bond, A. J. and Legge, J. D. (1992a). *Characterisation of the Bothkennar clay : An overview.* Geotechnique 42, No 2, pp 303-347.

Huang, J. T and Airey, D. W. (1991). *Manufacture and index testing of an artificially cemented soil.* Ninth Asian Regional Conference On Soil Mechanics and Foundation Engineering, Vol 1, pp 143-146.

Kavvadas, M., Anagnostopoulos, A., Leonardos, M. and Karras, B. (1993). *Mechanical properties of Ptolemais lignite.* Proceedings of an International Symposium on the Geotechnical Engineering of Hard Soils-Soft Rocks, Athens, Vol 1, pp 585-592.

Leddra, M. J., Jones, M. E. and Goldsmith, A. S. (1990). *Compaction and shear deformation of a weakly-cemented, high porosity sedimentary rock.* Conference on The Engineering Geology of Weak Rock, Leeds, pp 45-54.

Leroueil, S. and Vaughan P. R. (1990). *The general and congruent effects of structure in natural soils and weak rocks.* Geotechnique 40, No. 3, pp, 467-488.

Leroueil, S., Magnan, J-P, Tavenas, F. (1990). *Embankments on soft clays.* England: Ellis Horwood Limited.

Little, J. A and Hataf N. (1990). *Some monotonic and cyclic properties of weathered undisturbed and reconstituted Keuper Marl.* Conference on The Engineering Geology of Weak Rock, Leeds, pp 55-64.

Loe, N. M., Leddra, M. J. and Jones, M. E. (1992). *Strain states during stress path testing of the chalk.* Rock Mechanics, pp 927-936.

Maccarini, M. (1987). *Laboratory studies of a weakly bonded artificial soil.* PhD thesis, University of London.

Maccarini, M. (1993). *A comparison of direct shear box tests with triaxial compression tests for a residual soil.* Geotechnical and Geological Engineering, 11, pp 69-80.

Malandraki, V. and Toll D. G. (1994). *Yielding of a weakly bonded artificial soil.* International Symposium On Pre-Failure Deformation Characteristics Of Geomaterials.

Petley, D., Leddra, M., Jones, M., Kageson-Loe, N., Fan, C., and Stafford, C. (1993). *Deformation and fabric changes in weak fine-grained rocks during high pressure consolidation and shear.* Proceedings of an International Symposium on the Geotechnical Engineering of Hard Soils-Soft Rocks, Athens, Vol 1, pp 737-744.

Rampello, S. Georgiannou, V. N, Viggiani, G. (1993). *Strength and dilatancy of natural and reconstituted samples of two overconsolidated clays.* Proceedings of an International Symposium on the Geotechnical Engineering of Hard Soils-Soft Rocks, Athens, Vol 1, pp 761-768.

Sangrey, D. A. (1972). *Naturally cemented sensitive soils.* Geotechnique 22, No 1, pp 139-152.

Saxena, S. K. and Lastrico, R. M (1978). *Static properties of lightly cemented sand.* Journal of the Geotechnical Engineering Division, ASCE, December, pp 1449-1464.

Schofield, A. N. and Wroth, C. P. (1968). *Critical state soil mechanics.* London: McGraw-Hill.

Smith, P. R., Jardine, R. J. and Hight, D. W. (1992). *On the yielding of the Bothkennar clay.* Geotechnique 42, No. 2, pp 257-274.

Sitar, N. (1979). *Behaviour of slopes in weakly cemented soils under static and dynamic loading.* PhD thesis. University of California Berkley.

Taylor, D. W. (1948). *Fundamental of soil mechanics.* New York: John Wiley.

Toll, D. G. (1993). *A computer control system for stress path triaxial testing.* 5th International Conference on Civil and Structural Engineering Computing, Edinburgh, pp 107-113.

Toll, D. G. and Malandraki V. (1993). *Triaxial testing of a weakly bonded soil.* Proceedings of an International Symposium on the Geotechnical Engineering of Hard Soils-Soft Rocks, Athens, Vol 1, pp 817-824.

Vargas, H. (1953). *Some engineering properties of residual clay soils occurring in southern Brazil.* Proceedings of the 3rd International Conference in Soil Mechanics and Foundation Engineering, Switzerland, vol. 1, pp 84-90.

Vaughan, P. R. and Kwan, C. W. (1984). *Weathering structure and in situ stress in residual soil.* Geotechnique 34, No 1, pp 43-59.

Vaughan, P. R. (1985). *Mechanical and hydraulic properties of in situ residual soils*-general report. Proc. 1st International Conference in Geomechanics in Tropical Lateritic and Saprolitic Soils. Brasilia, Vol 3, pp 231-263.

Vaughan, P. R. (1988). *Characterising the mechanical properties of the in-situ residual soil.* Proceedings of the 2th International Conference on Geomechanics in Tropical Soils. Singapore, Vol 2, pp 469-487.

Vaughan, P. R., Maccarini, M. and Mokhtar, S. M. (1988). *Indexing the engineering properties of residual soil.* Quarterly Journal of Engineering Geology, Vol 21, pp 61-84.

Wood, D. M (1990). *Soil behaviour and critical state soil mechanics.* New York: Cambridge University Press.